# Characterisation of the transcriptional response to cytokine induced polarisation in human $CD4^+$ T cells and monocyte derived macrophages

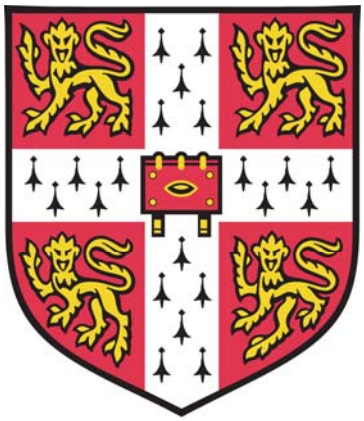


Eddie Cano Gámez

Wellcome Trust Sanger Institute

University of Cambridge
Trinity Hall

This dissertation is submitted for the degree of Master in Philosophy in Biological Science

August, 2017

# Abstract

The immune system is composed of plastic cell populations which are capable of acquiring specialized functions upon cytokine stimulation. This phenomenon, known as cytokine induced cell polarisation, generates different effector states within cell types, and has been associated to autoimmune inflammation. In this study, we characterised the transcriptional response of different cell types to polarisation with cytokines linked to autoimmunity.

First, we isolated human naive $CD4^+$ T cells and monocytes from peripheral blood of two healthy individuals. Next, we polarised the cells with different cytokine combinations linked to autoimmunity and performed low coverage RNA-seq of 26 different conditions: ten $CD4^+$ T cell samples activated with anti CD3/CD28 antibodies and polarised with cytokines (Th0, Th1, Th2, Th17, iTreg, IL-10, IL-21, IL-27, IFN-β, and TNF-α) at two different time points, and six monocyte polarisations (M0, M1, M2, IL-23, IL-26, and TNF-α). In order to study differences between stimulation in the presence or absence of cytokines, we performed differential gene expression analysis. Furthermore, for selected conditions we also characterised the whole proteome. Together, these data were used to identify genes and pathways involved in cytokine induced cell polarisation.

This study generated a valuable resource for future investigation of gene expression in immune cells. Furthermore, our results confirmed that the response to type I interferons is reduced upon Th2 cell differentiation, and revealed that downregulation of genes in the phosphatidylinositol-3-kinase (PI3K) pathway may be involved in the differentiation of Th17 and iTreg cells. Finally, using a gene co-expression network analysis, we also identified transcription factors which coordinate the response to cytokine induced polarisation in $CD4^+$ T cells and macrophages such as IRF8, IRF9, and Sox4.

# Declaration of originality

I hereby declare that this dissertation is the result of my own work and includes nothing which is the outcome of work done in collaboration except where specifically indicated in the text and in the initial collaboration note. It is not substantially the same as any that I have submitted for, or is being concurrently submitted for a degree or other qualification at the University of Cambridge or any other University or similar institution. I further state that no part of my dissertation has already been or is being concurrently submitted for any such degree, diploma or other qualification. Finally, I hereby declare that my dissertation does not exceed the word limit prescribed in the Special Regulations of the MPhil examination for which I am a candidate (This thesis consists of 19,393 words, exclusive of abstract, tables, references and appendix).

Date: _____

Signature: _____

# Collaboration note

The work described in this dissertation was carried out by myself and members of the Immune Genomics Group at The Wellcome Trust Sanger Institute, Cambridge, and is part of a study designed by Gosia Trynka and Blagoje Soskic. I performed the cell isolation, and stimulation experiments in collaboration with Blagoje Soskic and Marta Baldrighi. These experiments included cell culture, flow cytometry, RNA isolation and quantification. Blagoje Soskic performed the Immunophenotyping of monocyte derived macrophages. In addition, library preparation and RNA-sequencing were carried out by the Sequencing facility at The Sanger Institute, while protein isolation, mass spectrometry, and peptide quantification analysis were performed by Theodoros Romeliotis and the Proteomics facility at The Sanger Institute, in collaboration with Marta Baldrighi. Fluorescence activated cell sorting was carried out by the cytometry facility at The Sanger Institute. I performed all the RNA-sequencing data analysis, including read mapping, differential gene expression, functional annotation, and gene co-expression network analysis. This project is done in collaboration with the public-private initiative for drug discovery Open Targets, and consequently the pharmaceutical firms GSK and Biogen were also involved in the study design.

# Acknowledgments

“I am grateful to intelligent people. That doesn’t mean educated. That doesn’t mean intellectual. I mean really intelligent”, said American poet Maya Angelou. I am grateful to all the intelligent people I found myself surrounded with during this year. Firstly, I want to thank my supervisor Dr Gosia Trynka for accepting in her lab a student with virtually no experience in the field and who travelled 8600 kilometres with a suitcase full of dreams. Thank you for your incisive feedback and for providing an environment where I can wake up every day to do world leading science. Furthermore, I want to thank people at The Sanger Institute for introducing me to completely new ways of approaching biology and tackling issues which were unsolvable only a few years ago. I am particularly grateful to Blagoje Soskic, who has been my immunology mentor and who introduced me to the red queen paradox, the promiscuity of T cells, the danger model and all sorts of fascinating ideas. I also want to thank all members of the Immune Genomics group who were always willing to help me when I was lost, Dr Daniel Gaffney and Dr Matthias Zilbauer for providing feedback on this project, and everyone listed in the collaboration note for making this work possible. Moreover, I am also grateful to Rosana Pelayo and her laboratory in Mexico City for letting me do cell culture for the first time during my undergraduate studies. Lastly, I am grateful to all the professors who made me fall in love with science: Jacqueline Oliva who first taught me immunology, Carlos Prado who showed me mathematics can describe anything, Juan Bravo who let me design and experiment for the first time, and Eric Lander who taught me molecular biology via his online videos without ever meeting me.

I am most grateful to my family for their unconditional support. To my sister Tábata Cano, who discussed science with me over dinner for years before I even started University, and who eventually took me to Cambridge. I cannot thank my mum and my dad enough. They believed in me even at moments when I couldn’t believe in myself. Thank you for making me who I am today: you are Maya Angelou’s really intelligent people. I am also grateful to my extended family, specially to my grandmother.

Last, I thank the Gates Cambridge trust and community not only for funding my studies (twice), but also for caring for each and every student they have and for building a unique space where we can find a home. Special thanks go to all the people who helped me endure the long Cambridge winter and the emotional challenges of this degree. Particularly to Alex Kong for showing me what kindness is about, and to Noor Shahzad and Francesca Brown, who fed me books and lines of poetry when I was about to starve.

# Table of contents

# 1. Introduction

The immune system is able to constantly face a wide variety of infections. Moreover, diverse pathogens pose different challenges for which the immune system needs to elicit targeted responses. One of the mechanisms for tailoring the immune response to different threats is cytokine induced cell polarisation (1). This process is mediated by proteins which act as messengers between immune cells, and is key for the response of cells to environmental cues. Moreover, cytokine induced polarisation is also involved in driving pathological responses to self-antigens that lead to autoimmunity (2).

In this chapter I summarise our current understanding of cytokine induced cell polarisation, focusing on two cell types which have been associated to autoimmune disease: $CD4^+$ T cells and macrophages, (3, 4). Next, I describe the role of cytokine induced polarisation in autoimmunity. Finally, I state the aims and experimental design of the present study.

## 1.1 Cytokine induced polarisation of $CD4^+$ T cells

### 1.1.1 $CD4^+$ T cells are key players of the adaptive immune response

T cells are a subtype of lymphocyte that coordinates multiple aspects of the immune response (1). The stimuli that trigger T cell responses occur in secondary lymphoid organs, where professional antigen presenting cells (APC) such as macrophages and dendritic cells (DCs) present peptides to T cells (5). For successful activation T cells need to receive two signals from APCs. The first signal is triggered when T cell receptor (TCR) recognizes antigen presented in the context of major histocompatibility complex (MHC) molecules. In addition, APCs provide a second signal known as costimulation via interaction of the receptor CD28 on the surface of T cells with CD80 and CD86 molecules expressed on the surface of APCs (6-8). Following stimulation, T cells undergo clonal expansion and acquire specialized functions (1).

$CD4^+$ T cells are sometimes referred to as T “helper” (Th) cells due to their role in recruiting and modifying the function of other cell types (1, 9). For example, $CD4^+$ T cells can instruct class switching of B cells, specifying which type of antibody should be secreted (10). Moreover, $CD4^+$ T cells can also provide “help” to macrophages by promoting phagocytosis (11). These aspects of $CD4^+$ T cell function are mediated by cytokines, proteins which bind

to receptors in the surface of target cells and modify gene expression via transcription factors (TFs) such as signal transducers and activators of transcription (STATs) (12).

### 1.1.2 Cytokines guide the differentiation of $CD4^+$ T cells

Multiple subsets of $CD4^+$ T cells are generated in response to infection, each of them with different cytokine secretion profiles and in charge of providing a specific type of "help" (13). The specialization of $CD4^+$ T cells into subsets is itself guided by cytokines present in the microenvironment during and after T cell activation and is referred to as cytokine induced T cell polarisation (13). Polarisation of $CD4^+$ T cells to different subsets with specialised functions was first described in 1986 by Mosmann et al. who reported the existence of two types of $CD4^+$ T cells with characteristic cytokine secretion profiles (14). These cells were named Th1 and Th2, and were defined by their secretion of IFN-γ but not IL-4, and IL-4 but not IFN-γ, respectively (15, 16). Several other studies expanded upon these observations to include IL-10, IL-5, and IL-13, which are also secreted by Th2 cells (17). Th1 cells were found to also secrete IL-2 and GM-CSF (14). Despite their initial description in cell lines, Th1 and Th2 cells were later identified *in vivo* in mouse models of infection (18, 19) and equivalent cell populations have been described in humans (20, 21). *In vitro*, these cell types can be induced by $CD4^+$ T cell activation in the presence of IL-12 or IL-4, respectively (22-24). This paradigm has been extended to include Th17 cells, characterised by secretion of IL-17 but not IL-4 or IFN-γ, and which arise as an independent lineage upon $CD4^+$ T cell activation in the presence of TGF-β, IL-1β and IL-23 (25-27). Furthermore, induced regulatory T (iTreg) cells develop upon T cell activation in the presence of TGF-β (28). More recently, Th9 and Th22 cells have also been described as subsets that secrete IL-9 and IL-22 respectively, though their phenotypic stability is still debated (29, 30). The total number of T cell subsets thus remains unclear and continues to be an area of debate.

$CD4^+$ T cell polarisation is also affected by the intensity of TCR signalling (31). This was first suggested by *in vitro* stimulation of mouse $CD4^+$ T cells, which showed that polarisation efficiency is proportional to stimulation time (32). Further experiments in mice showed that strong TCR stimulation, as measured by $Ca^{2+}$ flux, generally enhances Th1 polarisation, while Th2 polarisation is favoured by weak stimulation (33). However, it remains unclear whether other lineages could also fit in this model. A study of human $CD4^+$ T cell stimulation with different strengths of TCR signalling suggested that Th17 differentiation is favoured by low intensity stimulation (34). It has even been proposed that signalling strength might be

more important than the cytokine milieu in determining T cell fate, since some degree of differentiation is achieved even upon cytokine blockade (33). Nonetheless, this hypothesis needs further validation.

The current paradigm proposes that polarisation of $CD4^+$ T cells is a differentiation processes which generates stable cell lineages (13). T cell polarisation is triggered by the expression of specific TFs called “master regulators”, which are able to modify the chromatin landscape of activated T cells (13). T-bet and GATA-3 regulate Th1 and Th2 differentiation, respectively (35, 36), while Th17 differentiation is controlled by RORγ (37). PU.1 and the aryl hydrocarbon receptor (AHR) have been proposed as master regulators of the Th9 and Th22 lineages respectively (30, 38). Moreover, TGF- β induces iTreg differentiation, most likely mediated by upregulation of the TF FoxP3 (39, 40). However, recent evidence from epigenetic studies suggests that to carry out their function these master regulators need other TFs such as STATs, which modify the chromatin landscape and create active enhancers (41, 42). This suggests that T cell polarisation is coordinated by a complex network of TFs rather than a single master regulator. Moreover, direct interaction of TFs is also involved in fate determination. For example Th1 cells express GATA-3, but here the TF is unable to bind its target genes because of direct interaction with T-bet (43). Consequently, chromatin remodelling and TF networks play a major role in determining $CD4^+$ T cell fate.

### 1.1.3 DCs polarise $CD4^+$ T cells to different phenotypes in response to different pathogens

T cell polarisation states have a functional role in the immune response to infection, with each subset responding more efficiently against a specific type of pathogen (44). Th1 cells, for example, arise in response to viruses and intracellular bacteria and are able to enhance the phagocytic capacity of macrophages via secretion of IFN-γ (11). Conversely, Th2 cells enhance the mobilization of eosinophils and generate alternatively activated macrophages which clear helminths and other multicellular organisms (45). Th17 cells, on the other hand, interact with neutrophils in the immune response to extracellular bacteria via secretion of IL-17 (46, 47). Thus, T cell polarisation is a tightly controlled developmental process dependent on the pathogenic challenge. Cytokines that guide $CD4^+$ T cell differentiation are secreted by DCs, which were previously exposed to specific pathogen in the tissues and subsequently migrated to the lymph nodes (48, 49). For example, in response to stimulation with lipopolysaccharide (LPS), a component of the outer membrane of gram negative bacteria,

DCs secrete IL-12 which promotes Th1 differentiation (50). Nematode infections cause DCs to secrete high levels of IL-4, promoting Th2 responses (51).

Interestingly, it has been demonstrated that DCs secrete different cytokines throughout the immune response, changing the conditions under which T cell activation occurs (52). The early immune response is characterised by “active” DCs which secrete IL-12, while “exhausted” DCs secrete IL-4 and are characteristic of the late immune response (52). Furthermore, duration of DC-T cell interaction has been implicated in Th1/Th2 polarisation (33). *In vivo* imaging of mouse lymph nodes by two-photon microscopy has demonstrated that Th1 responses arise upon long and sustained interactions between DCs and $CD4^+$ T cells. Conversely, in Th2 responses T cells display multiple brief interactions with DCs (33). A similar study confirmed that sustained interactions cause secretion of IFN-γ by T cells (53). Together these studies suggest that T cell polarisation is guided by DCs in the lymph nodes and changes throughout the immune response.

Cytokine induced polarisation is known to modify the migratory capacity of T cells by inducing expression of specific homing receptors (54, 55). T cells can then migrate to inflamed tissues where they are exposed to different stimuli and acquire new functions. For example, a mouse model of infection showed that Th17 differentiation can be locally induced in the gut by changes in the microbiota (56). Other stimuli different from cytokines are also involved in this process. For instance, it was found that DCs in the Peyer’s patch can induce expression of the gut homing receptor CCR9 by mouse T cells (57). This phenotype was not induced by DCs from other locations. This tropism is mediated by retinoic acid produced *in situ* (58). The same is observed in the skin, where DCs process vitamin D3 into its active form $1,25(OH)_2D_3$, inducing the expression of CCR10 by T cells which can then migrate to the skin (59). This process is restricted to the skin, with $1,25(OH)_2D_3$ inhibiting T cell homing to the gut (59). Consequently, it is increasingly appreciated that upon polarisation $CD4^+$ T cells home to inflamed tissue, where differentiation is completed.

### 1.1.4 T cell polarisation states retain functional plasticity

T cell polarisation states are mutually exclusive. Th2 differentiation, for example, is inhibited by IFN-γ (60, 61). Moreover, Th17 differentiation requires blockade of both IFN-γ and IL-4 (25). This suggests that throughout the immune response one lineage might dominate over others. This is enhanced by the autocrine action of endogenous cytokines, which promote

self-sustained T cell polarisation via a positive feedback loop. Th1 cells, for example, secrete IFN-γ, which itself induces the expression of T-bet (62). Furthermore, IL-12 also induces the expression of its own receptor (63). Similarly, Th2 cells secrete IL-4, which enhances the expression of GATA-3 (36). Consequently, it is thought that mutually exclusive T cell phenotypes arise upon responses to different stimuli and cytokine milieus, and that each lineage is expanded by a positive feedback loop.

Despite this mutual exclusivity, T cell polarisation states are also highly plastic (3) and under certain conditions cells can acquire a new phenotype upon re-stimulation with different cytokines. For instance, GATA-3$^+$ cells committed to the Th2 lineage can still secrete IFN-γ if transferred to a mouse infected with lymphocytic choriomeningitis virus (LCMV), known to promote Th1 responses (64). This study reported stable co-expression of GATA-3 and T-bet (64). Furthermore, iTreg and Th17 cells are able to interconvert, despite their opposing functional roles (65, 66). This plasticity is likely mediated by epigenetic mechanisms (67). It has been demonstrated that CD4$^+$ T cells from one lineage suppress the secretion of cytokines from other lineages by temporarily silencing those genomic regions, as suggested by global mapping of histone marks in Th1, Th2, and Th17 mouse cells (68). However, the promoter region of master regulator TFs such as T-bet shows both accessible and repressive chromatin marks which coexist, suggesting complex regulatory mechanisms (68). In conclusion, CD4$^+$ T cell polarisation generally results in mutually exclusive lineages, but the resulting cells also retain functional plasticity and can adapt in response to their environment.

## 1.2 Cytokine induced polarisation of macrophages

### 1.2.1 Macrophages are key players of the innate immune response

The phagocyte mononuclear system is composed of monocytes and tissue macrophages, in charge of clearing infecting pathogens through phagocytosis, as well as maintaining tissue homeostasis (69). Following maturation, monocytes egress to the periphery, where they express the surface marker CD14 (70), a co-receptor for bacterial LPS (71). Monocytes have been classified into two groups: “classical” monocytes (CD14$^+$CD16$^-$), and “alternative” monocytes (CD14$^+$CD16$^+$) (72, 73). Upon tissue damage, classical monocytes are recruited to the affected area via the chemokine CCL2, where they preferentially differentiate into monocyte derived macrophages. This differentiation is mostly triggered by macrophage

colony stimulating factor (M-CSF) (72). Conversely, $CD14^+CD16^+$ monocytes seem to migrate into the tissues under healthy conditions via chemokines as $CX_3CL1$, and differentiate mostly into dendritic cells (DCs) (74, 75). This differentiation process is triggered by granulocyte/monocyte-colony stimulating factor (GM-CSF) and IL-4 (72).

Macrophages show phenotypic diversity across different tissues: Langerhans cells in the skin, alveolar macrophages in the lungs, microglia in the brain, and osteoclasts in the bones, among other examples (76-79). However, they share common functions. Firstly, they are professional phagocytes which participate in cellular immunity by engulfing pathogenic particles and targeting them to the phagolysosome, where they are degraded by proteolytic enzymes and reactive oxygen/nitrogen species (ROS/NOS) (80). Secondly, macrophages also mediate homeostasis by clearing apoptotic cells and debris via phagocytosis, and repairing tissue (81, 82).

In order to carry out their functions, macrophages must be activated. Activation is triggered by binding of an alarm signal such as LPS to pattern recognition receptors (PRRs), for example Toll-like receptors (TLRs) (80, 83, 84). The molecules that bind PRRs commonly belong to one of two families: pathogen associated molecular patterns (PAMPs), and damage associated molecular patterns (DAMPs) (85), with this last group consisting of intracellular antigens such as dsDNA which are released to the microenvironment upon tissue destruction. Macrophages also produce pro-inflammatory cytokines such as IL-1β and tumour necrosis factor (TNF) (86). Furthermore, their activation can be modified or fully triggered by the cytokine milieu (83, 87). This process is referred to as cytokine induced macrophage polarisation.

### 1.2.2 Th1/Th2 cytokines polarise macrophages to an M1/M2 phenotype

Cytokine induced macrophage polarisation was first described by Mills et al., who proposed the existence of two functional classes of macrophages: M1 and M2 (88). M1 macrophages arise upon stimulation with IFN-γ in the presence or absence of LPS, and have enhanced inflammatory and phagocytic capacity (11, 83). On the other hand, polarisation with IL-4, IL-10 or IL-13 generates M2 macrophages (83, 89), which are central to the immune response against parasites (90). M2 macrophages also mediate tumour immune evasion (91). The M1/M2 nomenclature comes from the fact that, as described before, IFN-γ is produced by Th1 cells while IL-4, IL-10 and IL-13 are signature Th2 cytokines. Thus, a functional equivalence between $CD4^+$ T cell and macrophage subsets was proposed (88).

Subsequently, the response of macrophages to IFN-γ and IL-4 has been characterised in more depth. For instance, it is now known that M1 polarisation is mostly mediated by STAT1, while STAT6 coordinates M2 polarisation (87, 92). Furthermore, the mammalian target of rapamycin complex 1 (mTORC1) is also involved in macrophage activation, with constitutive induction of mTORC1 preventing development of the M2 phenotype (93). Transcriptional profiling of M1/M2 macrophages has also been performed using microarrays, which revealed crucial differences between both phenotypes such as the expression levels of mannose receptors and cyclooxygenases (94). Efforts to identify M1 and M2 specific surface markers have suggested M2 macrophages express the mannose receptor Mrc2, as well as Ym1, FIZZ1, and Arginase 1 (Arg1) (94-96). On the other hand, the inducible nitric oxide synthase (iNOS) is the gold standard for M1 identification (83). However, Arg1 is also expressed in other subsets, such as tissue resident macrophages and in other cells involved in the responses to intracellular pathogens (97), questioning the validity of single surface markers. Thus, an in-depth description of the full transcriptome upon M1/M2 polarisation is still necessary.

### 1.2.3 Macrophage polarisation beyond the M1/M2 paradigm

Despite the widely accepted classification, it is now known that M1 and M2 are not the only macrophage subtypes (98). For example, polarisation of mouse bone marrow macrophages with LPS and ovalbumin immune complexes (IgG-OVA) generated a third type of macrophage population capable of secreting IL-10 but not IL-12 (99). This suggested that IgG-OVA polarised macrophages have a regulatory function. Based on this observation, it is hypothesized that at least three groups of macrophages exist: proinflammatory (M1), tissue-remodelling (M2), and immunoregulatory (99, 100). These last had been formerly included in the M2 category. Furthermore, polarisation with several other stimuli such as IL-10 and TGF-β followed by transcriptional profiling revealed even more subgroups (101). Thus, M1 and M2 are currently regarded as extremes of a broader functional continuum that spans various proinflammatory and tissue remodelling functions (100). As such, a more consistent macrophage nomenclature and a set of experimental guidelines were proposed in 2013 (102). This nomenclature expands the M1/M2 paradigm to include the outcome of a variety of cytokine induced polarisations.

Macrophage as opposed to T cell polarisation causes phenotypic changes as early as six hours after stimulation, which disappear at later time points (103). Furthermore, macrophage subsets are also highly plastic and their biology is heavily influenced by the tissue in which

they reside (86). Research on macrophage plasticity points to epigenetic mechanisms (104). For example, marks of active chromatin such as H3K4me3 selectively appear at the promoters of M2 genes shortly after stimulation with IL-4 or IL-13 (103). These are replaced by the repressive mark H3K27me3 once the stimulus disappears (103). These chromatin modifications are mediated by histone methylases like Jmjd3, whose expression is induced by IL-4 (103, 105). This suggests a functional explanation for macrophage plasticity, since the induction of different chromatin modifying enzymes by environmental cues could allow rapid shifts in macrophage function.

## 1.3 Cytokine induced polarisation mediates pathologic inflammation in autoimmunity

In addition to its fundamental role in the immune response against pathogens, cytokine induced cell polarisation is also involved in driving chronic inflammation (2). Evidence for the role of cytokines in autoimmune and autoinflammatory disease comes from different sources. For example, studies of experimental autoimmune encephalomyelitis (EAE), the animal model of multiple sclerosis (MS), have identified increased levels of IL-1β in cerebrospinal fluid of animals with active disease (106-108). This observation has also been recapitulated in cerebrospinal fluid of MS patients (108, 109). During the course of disease, IL-1β is produced by macrophages via the inflammasome pathway, among other myeloid cells (110, 111), and it has been suggested that it acts by polarising $CD4^+$ T cells to the Th17 phenotype (112). IL-1β also induces secretion of GM-CSF by Th17 cells (113, 114).

Moreover, targeting cytokines and their receptors with monoclonal antibodies is an efficient therapy for several diseases such as rheumatoid arthritis (RA) and psoriasis (2, 115). For example, blockade of IL-17 and IL-23 signalling is effective for treating psoriasis, which suggests the involvement of Th17 responses (116). Similarly, it has been demonstrated that patients with RA respond well to IL-6 blockade, which is also a cytokine involved in Th17 differentiation (117). More recently, subcutaneous administration of anti-IL17A monoclonal antibodies was proven efficient in the treatment of ankylosing spondylitis in a randomised trial with placebo controls (118).

Importantly, some cytokines associated to autoimmunity go beyond the classical definition of T cell and macrophage polarisation described above. For example, TNF blockade is to different extents a successful therapy for RA, giant-cell arteritis (GCA), Crohn's disease

(CD), ulcerative colitis (UC), psoriasis and ankylosing spondylitis (2, 119, 120). TNF is a cytokine of the innate immune response which induces secretion of inflammatory cytokines, apoptosis and necroptosis (119, 121, 122). Interestingly, TNF blockade in MS exacerbates disease (123). This is likely due to the regulatory functions of TNF in cells of the central nervous system (CNS) (124), although further research is necessary to investigate the role of TNF in MS. IL-21, IL-27, and type I IFN are also involved in RA, where they are thought to modify the function of $CD4^+$ T cells, especially follicular helper T (Tfh) cells (115, 125). In addition, it has been proposed that IL-23 might mediate autoimmune inflammation of the brain via its action in macrophages (126).

Despite the success of IL-6 and TNF blockade in RA, not all cytokines and receptors investigated have been efficient drug targets. For example, administration of subcutaneous IFN-β to patients with RA caused no changes in their radiological scores when compared to individuals treated with a placebo in a randomised, double blind trial (127). This suggests that IFN-β might not be crucial for RA pathology. Surprisingly, a randomised phase II study of intravenous and subcutaneous anti-IL17A antibody found no significant differences in ACR scores between patients with active RA who received the treatment and those who did not (128). This despite the same antibody being effective for treating ankylosing spondylitis (118). However, the treatment did achieve mild reduction of disease activity, C-reactive protein levels and self-reported pain (128), suggesting that IL-17 is involved in RA pathology but its blockade is not enough for treating the disease. Taken together, this evidence suggests that even though cytokine induced polarisation is central to autoimmunity, research is needed to design more precise and efficient therapeutic strategies. To achieve this, a deeper characterisation of the effect of cytokines across different cell types is necessary.

## 1.4 Project description

### 1.4.1 Project aims

It has become increasingly evident that a deeper cellular characterisation is necessary to explain how cytokines contribute to autoimmunity. This thesis describes a study that aimed to generate gene expression data of cytokine induced cell states in $CD4^+$ T cells and macrophages using RNA-sequencing (RNA-seq). Even though several studies have addressed this question before, they have either focused on mouse lymphocytes (129), assessed the cell states of interest without studying the process that generates them (130), been limited to very few states (131), or sampled subsets of the transcriptome (94). We

believe that this study contributes to fill this gap by asking fundamental questions of cytokine biology not previously answered for human immune cells. Specifically, we asked if previously described subsets of cells such as Th1, Th2, Th17 or M1 and M2 macrophages showed a stable or a transitional transcriptome, and how their gene expression changed throughout time. We wanted to determine if any evident gene expression program existed and at which time point it was triggered. We also aimed to characterise the key aspects of these cell states, extending the definition of cell subsets, currently relying almost solely on cytokine secretion profiles. Furthermore, we wanted to determine which cell type was affected by cytokines associated with autoimmunity, as well as which genes or pathways were activated by these cytokines. This has, to our best knowledge, not been assessed in these cell types before. By doing this, we wanted to determine if any of these cytokines could be a suitable drug target for the autoimmune diseases under consideration.

### 1.4.2 Experimental design

In order to achieve our aims, we devised an experimental design based on low coverage RNA-seq. Briefly, we stimulated and polarised naive $CD4^+$ T cells and monocyte derived macrophages from two healthy individuals using cytokines associated to autoimmunity. Details of the stimulatory conditions are presented in the methodology section. Macrophages were analysed after six hours, while T cells were assessed 16 hours and five days after stimulation. Next, we isolated RNA and performed low coverage RNA-seq, and used these data to carry out a differential gene expression analysis between cells stimulated in the presence and in the absence of cytokines. Finally, we identified pathways, TFs, and gene co-expression modules relevant to these cell states (**Figure 1.1**).

It has been shown that the statistical power of RNA-seq studies increases in proportion to gene coverage and sample size (132-134), being this last factor the most important determinant of sensitivity (133). In order to account for the caveats in our experimental design, which has both low sample size and low coverage, we used the statistical method for differential expression analysis “DESeq2”, specifically designed for low sample size (135) and which has been shown to achieve good power under similar circumstances (132). A thorough analysis of the statistical power of this study was also carried out and is presented in the results section.

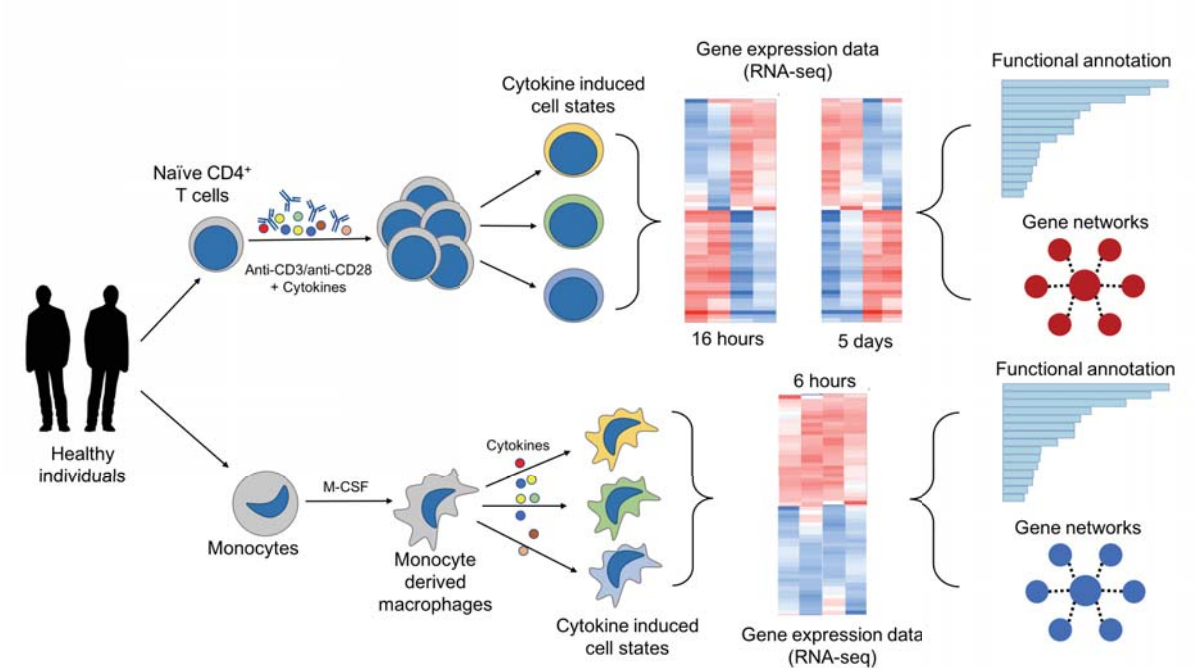


**Figure 1.1 Overview of the experimental design** In this study, two cell types were isolated from two healthy blood donors. Cytokine induced polarisation followed by RNA sequencing was performed on these cells. The resulting data was used to perform differential expression analysis, pathway enrichment analysis, and gene co-expression network analysis.

## 1.5 Thesis outline

In chapter 2, I present an in-depth description of the experimental methodology and data analysis techniques. Chapter 3 contains the results from optimisation experiments used to determine the optimal conditions for isolation, cell culture, and stimulation of human immune cells. Subsequently, chapter 4 describes the results from RNA-seq data analysis, including statistical power estimations, differential gene expression analysis and identification of relevant pathways and TFs. Finally, chapter 5 summarises the conclusions of the study and presents a brief discussion on future perspectives.

# 2. Methods

## 2.1 Cytokine induced polarisation of human immune cells

### 2.1.1 Isolation of human $CD4^+$ T cells and monocytes from peripheral blood

Blood from healthy donors was obtained as leukocyte reduction cones from the NHS Blood and Transplant, Cambridge, UK. Upon collection, 10 ml of blood was diluted in 50 ml of RPMI-1640 culture medium supplemented with 10% foetal calf serum (FCS, Sigma Aldrich) and 1 mM EDTA (Sigma Aldrich) to avoid clotting. Each 25 ml of blood in RPMI was layered on top of 17 ml of Ficoll-Paque (GE Life Sciences) and gradient centrifugation was performed at 830 g for 20 minutes without break. Peripheral blood mononuclear cells (PBMCs) were recovered from the middle layer using a pasteur pipette and washed twice in 50 ml FACS buffer (Dulbecco's Phosphate Buffer Saline (PBS, Sigma), supplemented with 1mM EDTA and 2% FCS). The cells were then resuspended at 50 x $10^6$ cells/ml.

Approximately 100 x $10^6$ PBMCs were transferred to a 15 ml tube (Thermo Scientific) for monocyte isolation. This procedure was carried out via positive magnetic beads cell selection using the Human $CD14^+$ Positive Selection Kit (EasySep™, STEMCELL Technologies) following the manufacturer's instructions. The remaining PBMCs were used for $CD4^+$ T cell enrichment, which was carried out via negative magnetic beads cell selection using the Human $CD4^+$ T Cell Enrichment Kit (EasySep™, STEMCELL Technologies). Samples enriched in $CD4^+$ cells were resuspended at 100 x $10^6$ cells/ml and incubated for 30 minutes with FACS antibodies against the following surface markers: CD4, CD25, CD127, and CD45RA (**Table 2.1**). Finally, cells were washed in 2 ml FACS buffer. For each fluorophore, single stain compensation controls were prepared using 1x$10^6$ cells from the same sample for each individual stain. Shortly before sorting, cells were incubated with a 1:3000 dilution of the nucleic acid stain 4',6-diamidino-2-phenylindole (DAPI) (Sigma Aldrich) for 5 minutes in order to label dead cells.

**Table 2.1**. Product description of the FACS antibodies used throughout this thesis

| Antibody | Fluorophore | Manufacturer | Clone | Volume per 100 µl sample |
|---|---|---|---|---|
| Anti-human CD4 | APC | BioLegend | OKT4 | 3 µl |
| Anti-human CD25 | PE | BioLegend | M-A251 | 8 µl |
| Anti-human CD127 | FITC | eBioscience, Thermo Scientific | RDR5 | 3 µl |
| Anti-human CD45RA | BV785 | BioLegend | HI100 | 6 µl |
| Anti-human CD69 | PE-Cyanine7 | eBioscience, Thermo Scientific | FN50 | 4 µl |
| Anti-T-bet MAb | PE-Cyanine7 | eBioscience, Thermo Scientific | 4B10 | 5 µl |
| Anti-Gata-3 MAb | PE-Cyanine7 | eBioscience, Thermo Scientific | TWAJ | 5 µl |
| Anti-FoxP3 MAb | BV421 | BioLegend | 206D | 5 µl |
| Anti-human CD14 | Alexa Fluor 647 | BD Pharmigen | MphilP9 | 2 µl |
| Anti-human CD68 | PE-Cyanine7 | BioLegend | Y1/82A | 2 µl |
| Anti- human MerTK | BV421 | BioLegend | 590H11G1E3 | 5 µl |
| Anti-human HLA-DR | PE | BioLegend | L243 | 5 µl |

Fluorescence-activated cell sorting (FACS) was performed on the samples in a MoFlo XDP sorter (Beckman Coulter). Naïve T cells, defined as $DAPI^{-}$ $CD4^{+}$ $CD25^{low}$ $CD127^{high}$ $CD45RA^{+}$, were recovered. Cell sorting was performed by the Cytometry Facility of the Wellcome Trust Sanger Institute. Following sorting, naïve T cells were washed in 50 ml FACS buffer and resuspended at $2x10^{6}$ cells/ml in RPMI-1640 medium supplemented with 10% FCS, 2 mM L-glutamine (Sigma-Aldrich), and 1X Penicillin-Streptomycin (Gibco™, Thermo Scientific) (further referred to as complete RPMI).

### 2.1.2 Activation and cytokine polarisation of $CD4^+$ naïve T cells

Human T-activator CD3/CD28 dynabeads (Gibco™, Thermo Scientific) were washed and diluted in complete RPMI medium. Naïve T cells were plated in a 24-well plate (Corning) at $1x10^6$ cells per well in 2 ml volume, and supplemented with dynabead solution when appropriate. Unless otherwise stated, the ratio of cells to dynabeads was kept at 2:1. The control samples were supplemented with complete RPMI medium. Where required, polarising cytokines were added in combinations and concentrations shown in **Table 2.2**. All cytokines used in this study were purchased from PeproTech, while all antibodies used for polarisations were obtained from R&D. Cells were incubated at 37˚C for 16 hours or 5 days, respectively.

Activation beads were removed after either 16 hours or five days of stimulation. In order to do so, the cell suspension for each condition was transferred into a 1.5 ml Eppendorf tube. Tubes were then incubated for five minutes in a DynaMag™ magnet (Thermo Scientific) for 1.5 ml tubes, after which the media containing cells was carefully transferred to new Eppendorf tubes without touching the wall closest to the magnet in order not to transfer beads.

After beads removal, 20 µl of cells were mixed with 20 µl of Cellometer ViaStain™ AOPI (Nexcelom Bioscience) solution to assess their viability and counted in an automated cell counter (Cellometer Auto 2000™ Cell Viability Counter). Additionally, for a selection of samples, cells were also counted in a flow cytometer using AccuCheck™ counting beads.

### 2.1.4 Differentiation and stimulation of monocyte derived macrophages

Isolated $CD14^+$ cells were seeded into 6-well culture plates (Corning), $2.5 \times 10^5$ cells in 2 ml complete RPMI per well. For macrophage differentiation, the media was supplemented with 50 ng/ml M-CSF (PeproTech). Cultures were incubated for 7 days at 37 ˚C.

Following 7 days of culture, the media was supplemented with cytokine (PeproTech) polarisation cocktails (**Table 2.3)**. After 6 hours, the supernatant containing the cytokines was removed and cells were washed twice with PBS.

**Table 2.2** Composition of $CD4^+$ naïve T cells cytokine-polarisation cocktails

| POLARISING CONDITION | ACTIVATION BEADS RATIO | CYTOKINE COMBINATION | CYTOKINE CONCENTRATIONS |
|---|---|---|---|
| Unstimulated | -- | No cytokines | --- |
| Th0 | 1:2 | No cytokines | -- |
| Th1 | 1:2 | IL-12 | 50 ng/ml |
| | | Anti-human IL-4 antibody | 1 ng/ml |
| Th2 | 1:2 | IL-4 | 10 ng/ml |
| | | Anti-human IFN-γ antibody | 1 ng/ml |
| Th17 | 1:2 | IL-6 | 50 ng/ml |
| | | IL-23 | 20 ng/ml |
| | | IL-1β | 10 ng/ml |
| | | TGF-β1 | 5 ng/ml |
| | | Anti-human IL-4 antibody | 1 ng/ml |
| | | Anti-human IFN-γ antibody | 1 ng/ml |
| iTreg | 1:2 | TGF-β1 | 5 ng/ml |
| TNF-α | 1:2 | TNF-α | 20 ng/ml |
| IL-10 | 1:2 | IL-10 | 50 ng/ml |
| IL-21 | 1:2 | IL-21 | 50 ng/ml |
| IFN-β | 1:2 | IFN-β | 10 ng/ml |
| IL-21 | 1:2 | IL-21 | 20 ng/ml |

**Table 2.3**. Composition of macrophage cytokine-polarisation cocktails

| POLARISING CONDITION | CYTOKINE COCKTAIL | CONCENTRATION |
|---|---|---|
| Unstimulated (M0) | No cytokines | --- |
| M1 | IFN-γ | 50 ng/ml |
| M2 | IL-4 | 50 ng/ml |
| TNF-α | TNF-α | 50 ng/ml |
| IL-23 | IL-23 | 20 ng/ml |
| IL-26 | IL-26 | 20 ng/ml |

## 2.1.5 Flow cytometry

All the samples described below were analysed with a LSR Fortessa (BD) FACS analysers.

### 2.1.5.1 Assessing T cell activation

Following 16 hours and five days of T cell stimulation, cells were transferred into a 96-well plate (Corning), washed once with 200 µl FACS buffer, and incubated with FACS antibodies against CD69 and CD25 for 20 minutes. Cells were then incubated with 1:3000 DAPI solution for 5 minutes and washed twice with FACS buffer to remove unbound antibody and DAPI. Compensation controls for each fluorophore were prepared by incubating UltraComp eBeads™ compensation beads (Thermo Scientific) with 1 µl of the respective antibody.

### 2.1.5.2 Immunophenotyping of monocyte derived macrophages

Following seven days of differentiation, monocyte derived macrophages were detached from the plate by incubating them with 1X Non-enzymatic Cell Dissociation Solution (Sigma Aldrich). Cells were resuspended in 1 X Fix/Perm Buffer (BioLegend) containing Human TruStain FcX (BioLegend) Fc receptor blocking solution for 10 minutes. After FcR blocking, the cells were incubated for 30 minutes at room temperature with antibodies against CD14, CD68, MerTK and HLA-DR. (**Table 2.1**). Cells were then washed in 1 ml 1 X Fix/Perm Buffer and resuspended in 200 µl FACS buffer.

#### 2.1.5.3 Immunophenotyping of polarised $CD4^+$ T cells

After five days of cytokine polarising stimulation, T cells from the Th1, Th2, Th17 and iTreg conditions were phenotyped for expression of relevant transcription factors. Cells were fixed and permeabilized using the FOXP3 Fix/Perm Buffer Set (BioLegend), according to the manufacturer's instructions. Permeabilized cells were incubated for 30 minutes with FACS antibodies against the transcription factors T-bet, GATA3, and FoxP3. Each of these stainings was performed separately and independently across all conditions.

#### 2.1.5.4 Data analysis

All data obtained by flow cytometry was analysed with FlowJo™ version 10 (TreeStar). FlowJo was used to quantify the relative percentages and median fluorescence intensities (MFI) of cell populations. The results from this analysis were then imported into the R programming environment (version 3.1.1), where they were visualized as scatter plots and boxplots using ggplot2 library.

## 2.2 Analysis of gene expression in cytokine polarised cells

### 2.2.1 Isolation of RNA from T cells and monocyte derived macrophages

Following polarisation of monocyte derived macrophages and naive $CD4^+$ T cells, total RNA was isolated from all conditions by resuspending 3 x $10^5$ cells in 500 µl of TRIzol™ (Invitrogen, Thermo Scientific). Samples were stored at -80˚C until RNA extraction was performed. Thawed cell suspension was transferred to a 1.5 ml MaXtract High Density tube (Qiagen), and 100 µl of chloroform (Sigma Aldrich) was added to each sample. The tubes were vigorously mixed for 15 seconds and incubated at room temperature for 10 minutes. Following incubation, samples were centrifuged at 21,000 g for 5 minutes at 4˚C. The 300 µl of aqueous phase from each sample was used for RNA isolation with the RNeasy™ MinElute Cleanup Kit (Qiagen) as instructed in the manufacturer's handbook.

### 2.2.2 Library preparation and RNA-sequencing

The quality of total RNA was assessed using RNA 6000 Nano Chip (Agilent Technologies) on a 2100 Bioanalyzer Instrument (Agilent Technologies) according to the manufacturer's instructions. Only samples with an RNA integrity number (RIN) higher than eight were processed for library preparation, which was performed by the Sequencing Pipelines Facility at The Sanger Institute, following the TruSeq mRNA Sample Preparation Guide by Illumina

(136). Briefly, 1 µg total RNA was used for mRNA purification using poly-T oligo attached magnetic beads in two rounds of washing and elution. The resulting mRNA was transferred to a PCR tube and fragmented under high temperature. The fragmented mRNA was resuspended in RNAse free water, and the first cDNA strand was synthesised using random primers and reverse transcriptase. The second cDNA strand was then synthesised using RNAse to remove the RNA template. The overhangs were converted into blunt ends using and “End Repair Mix” and the blunt ends were adenylated using the Klenow fragment and dATP in an A-tailing buffer. Following A-tailing, index adapters were ligated to the ends of the DNA, and the cDNA was amplified by PCR, generating a library suitable for sequencing. The adapters used contained barcode sequences which allowed multiplexing of the 56 samples in the same flow cell. The libraries were finally spread across two lanes of an Illumina HiSeq 2500 for clustering and sequencing.

### 2.2.3 RNA-seq data analysis

#### Read mapping

Sequencing data was aligned, demultiplexed and quality assessed by the Sequencing Facility at The Sanger Institute. It was released in CRAM format. Once receiving the data, the CRAM files were converted to FASTQ using BioBamBam release 2.0.8 (137). Next, FASTQ files with the same barcodes were merged. Reads were mapped to the hg38 release of the Human Reference Genome using the Spliced-Transcripts Alignment to a Reference (STAR) software version 2.5.3 (138) with the default parameters. The output of STAR mapping, obtained in a Binary Alignment Map (BAM) format, was filtered for high-quality reads using SAMtools version 1.3.1 (139). Only reads with a minimum mapping quality (MAPQ) of 20 were kept for further analysis. Gene expression quantification was estimated using featureCounts version 1.22.2 (140).

#### Quality control and exploratory data analysis

To reduce sources of variability unrelated to the study, counts from non protein-coding genes, the HLA region on chromosome 6 (chr6:25,000,000-47,825,000), and the Y chromosome were removed. Next, genes showing low expression levels, defined as a sum of counts lower than 20 (considering all samples), were also removed from the analysis. A table with sample information was built, which included: cell type, polarising condition assayed, time point, and batch number. Principal component analysis (PCA) (141, 142) was performed using DESeq2 (135). To stabilize the variance of lowly expressed genes, the count data was transformed using the regularized logarithmic transformation before

performing PCA (135). Throughout this thesis, DESeq2 version 1.16.1 (Bioconductor release 3.5) was used.

Finally, the Euclidean distance between samples was calculated and used to perform hierarchical clustering and build heatmaps using “pheatmap” R package (143). Batch correction was performed using a linear model with the batch correction function included in the “limma” R package (144). R version 3.1.1 is used throughout this study.

### Statistical power estimation

In order to estimate the statistical power of the study across several comparisons, we divided the data into three smaller data sets: macrophages (12 samples), CD4+ T cells 16 hours (22 samples) and CD4+ T cells 5 days (22 samples). These same data sets were later use for analysing differential gene expression. DESeq2 was used to estimate the coefficient of variation (CV) of each gene in the three data sets. To do so, the CV of each gene was defined as approximately equal to the squared root of its dispersion, as suggested by the package developers (135). Next, the global CV of each group was estimated as the median CV of all genes.

Following CV estimation, we modelled the statistical power as a function of gene coverage. Coverage was defined as the number of raw counts detected for each gene (134). For this calculation, we used the R package “RNASeqPower”, which estimates power using a generalised linear model (GLM) based on the Negative Binomial (NB) distribution (134). Throughout these estimations, we considered a sample size of 2 and assumed an average effect size (fold change) of 2, and an FDR of 0.05.

Finally, we used “RNASeqPower” (134) to estimate the global power of the study. We did this separately for each of the three sample groups. First, we obtained the median gene coverage using the counts() function of DESeq2 (135) and used this median value to calculate the power of detecting genes with a fold change of 2 at an FDR of 0.05, given the CV and sample size of the study.

## Differential expression analysis

The RNA counts table was used to assess differential gene expression in R. Separate analyses were performed for T cells and macrophages across different time points. To analyse transcriptional changes due to cytokine polarisation of monocyte derived macrophages, RNA counts were compared against unstimulated cells. Conversely, to analyse transcriptional changes upon cytokine polarisation in $CD4^+$ T cells, Th0 cells were used as a baseline for the comparison in order to identify only differences explained by cytokine polarisation as opposed to T cell activation. For this, P values were computed using Wald's Test and the negative binomial (NB) distribution in DESeq2, with gene size and sequencing depth correction (135, 145). The Benjamini-Hochberg (BH) method was applied for multiple testing correction (146). All genes with a BH-adjusted P value ≤ 0.05 and an absolute log2 fold change ≥ 1 were classified as differentially expressed. When loading the data into DESeq2, the following linear models were used to represent the null and alternative hypotheses:

$$H_0: \quad \mathbf{Y} = \mathbf{B_0} + \mathbf{B_1 D} + \boldsymbol{\varepsilon}$$

$$H_A: \quad \mathbf{Y} = \mathbf{B_0} + \mathbf{B_1 D} + \mathbf{B_2 C} + \boldsymbol{\varepsilon}$$

Where **Y** is a vector containing the observed RNA counts, $\mathbf{B_0}$ an intercept term (mean of counts), $\mathbf{B_1}$ and $\mathbf{B_2}$ the linear model coefficients, **D** the categorical variable batch number, **C** the cytokine-polarising condition (treatment), and **ε** a random error term.

## Functional annotation of differentially expressed genes and overrepresentation analysis (OA)

Up and down regulated genes were functionally annotated using gene ontology (GO) (147, 148). Upregulation was defined as a log2 fold change ≥ 1, and downregulation as a log2 fold change ≤ -1. The R package gProfileR (149) was used to annotate each gene to its respective cellular component (CC), molecular function (MF), and biological process (BP) GO terms. Next, an overrepresentation analysis of GO terms was performed using gProfileR. The observed proportion of genes assigned to each term was compared to the expected proportion, assuming a hypergeometric distribution (149). The complete list of genes used for differential expression analysis (14,399 protein-coding genes) was used as a background, and the hypergeometric P values were corrected for multiple testing using Benjamini-Hochberg's FDR method (146).

## Gene co-expression network analysis

To analyse shared gene regulation in response to cytokine stimulation, correlation networks were inferred. To do this, a variation from the standard workflow for weighted gene co-expression network analysis (150) was implemented. The Pearson correlation coefficient of each pair of genes across all samples was selected as a measure of similarity between genes and calculated as specified below. Firstly, a correlation matrix was built using gene expression data from all the samples of interest. The correlation matrix was defined as follows:

$$\mathbf{X} = \begin{pmatrix} \mathrm{X}_1 \\ \mathrm{X}_2 \\ \vdots \\ \mathrm{X}_n \end{pmatrix} = \begin{pmatrix} & \text{Samples} & & & \\ \text{Genes} & x_{1\,1} & x_{1\,2} & \cdots & x_{1\,m} \\ & x_{2\,1} & x_{2\,2} & \cdots & x_{2\,m} \\ & \vdots & \vdots & \ddots & \vdots \\ & x_{n\,1} & x_{n\,2} & \cdots & x_{n\,m} \end{pmatrix}$$

$$\boldsymbol{\rho} = \begin{pmatrix} & \text{Genes} & & & \\ \text{Genes} & 1 & \rho_{1\,2} & \cdots & \rho_{1\,n} \\ & \rho_{2\,1} & 1 & \cdots & \rho_{2\,n} \\ & \vdots & \vdots & \ddots & \vdots \\ & \rho_{n\,1} & \rho_{n\,2} & \cdots & 1 \end{pmatrix} = \begin{pmatrix} \frac{cov(\mathrm{X}_1, \mathrm{X}_1)}{\sigma_{\mathrm{X}_1} * \sigma_{\mathrm{X}_1}} & \frac{cov(\mathrm{X}_1, \mathrm{X}_2)}{\sigma_{\mathrm{X}_1} * \sigma_{\mathrm{X}_2}} & \cdots & \frac{cov(\mathrm{X}_1, \mathrm{X}_n)}{\sigma_{\mathrm{X}_1} * \sigma_{\mathrm{X}_n}} \\ \frac{cov(\mathrm{X}_2, \mathrm{X}_1)}{\sigma_{\mathrm{X}_2} * \sigma_{\mathrm{X}_1}} & \frac{cov(\mathrm{X}_2, \mathrm{X}_2)}{\sigma_{\mathrm{X}_2} * \sigma_{\mathrm{X}_2}} & \cdots & \frac{cov(\mathrm{X}_2, \mathrm{X}_n)}{\sigma_{\mathrm{X}_2} * \sigma_{\mathrm{X}_n}} \\ \vdots & \vdots & & \vdots \\ \frac{cov(\mathrm{X}_n, \mathrm{X}_1)}{\sigma_{\mathrm{X}_n} * \sigma_{\mathrm{X}_1}} & \frac{cov(\mathrm{X}_n, \mathrm{X}_2)}{\sigma_{\mathrm{X}_n} * \sigma_{\mathrm{X}_2}} & \ddots & \frac{cov(\mathrm{X}_n, \mathrm{X}_n)}{\sigma_{\mathrm{X}_n} * \sigma_{\mathrm{X}_n}} \\ & & \cdots & \end{pmatrix}$$

With **X** being the expression matrix containing regularized log-transformed counts of the 14,399 protein-coding genes across all samples, and **ρ** a matrix containing the Pearson correlation coefficients of gene pairs. We then proceeded to find the main co-expression partners of the genes of interest. To define the co-expression network, the gene of interest was set to be the central node and a signum adjacency function with threshold  (150, 151) was used to determine its interactors. This adjacency function was defined as follows:

$$\boldsymbol{a}_{i,j}(\boldsymbol{\rho}_{i,j}) = \begin{cases} 1 & if\ \rho_{i,j} \geq \tau \\ 0 & if\ \rho_{i,j} < \tau \end{cases}$$

With $\mathbf{a_{ij}}$ equaling 1 when the two genes **i** and **j** belong to the same co-expression network, and 0 when the two genes do not show a sufficiently strong co-expression pattern. For consistency of the network topology, the network size rather than value of **τ** was kept constant, as suggested in the literature (150, 151). To achieve this, the correlation coefficients of the gene of interest with all the remaining genes were extracted from the correlation matrix and approximated by a normal distribution. The threshold  was defined as the correlation coefficient equivalent to the 99th percentile of this distribution. In sum, genes with the 1% highest correlation coefficients with the gene of interest were defined as its interactors.

Genes within each co-expression network of interest were then tested for common transcriptional regulation. To do this, TRANSFAC (149, 152) was used to perform an overrepresentation analysis for transcription factor binding sites (TFBS) with the same statistical models and corrections described above. Shared TFBS were ranked by FDR-adjusted P value.

## 2.3 Protein expression analysis of activated T cells

### 2.3.1 Isolation and quantification of protein from T cells

For proteome quantification, unstimulated T cells, Th0 and Th1 cells were used in two technical replicates. Only three cell states were selected in order to test the technique's reproducibility and optimise the experimental protocols, with the plan on profiling all studied conditions in the future.

Pellets from $3x10^6$ cells were washed twice with PBS, the supernatant removed, and dried cell pellets were stored at -20˚C until protein isolation was performed. For protein quantification, the cell pellets were thawed and resuspended in 150 µl 0.1 M triethylammonium bicarbonate (TEAB) buffer (Sigma Aldrich) supplemented with 0.1% SDS. Pulse probe sonication was performed with 40% power (EpiShear™) on ice for 20 seconds, after which the samples were boiled for 10 minutes at 96˚C in a heat block. This procedure was performed twice. Lysed cells were then centrifuged at 12,000 rpm for 10 minutes in order to remove cellular debris, and protein quantification was performed using the Quick Start Bradford Protein Assay (Bio-Rad) as specified by the manufacturer's instructions. Protein samples were then divided into 100 µg aliquots.

### 2.3.2 Protein digestion, TMT labeling, and HPLC

Protein digestion, TMT labelling, and HPLC analysis were performed by Marta Baldrighi in collaboration with Theodoros Roumeliotis and the proteomics facility at The Sanger Institute, as specified in the initial collaboration note to this dissertation. Briefly, protein aliquots were resuspended in a 5 mM solution of tris-2-carboxymethyl phosphine (TCEP) buffer (Sigma Aldrich) and incubated for 1 hour at 60˚C in order to reduce the disulfide bonds. Iodoacetamide (IAA) was added to the sample and adjusted to a final concentration of 10 mM, in which the sample was incubated for 30 minutes at room temperature, in the dark. MS grade Pierce Trypsin (Thermo Scientific) was added at a mass ratio of 1:30, and the samples were incubated overnight for peptide digestion.

The digested protein samples were diluted to a total volume of 100 µl in 0.1 M TEAB buffer. A volume of 41 µl anhydrous acetonitrile was added to each vial of TMT reagents (Thermo Scientific) and vortexed. The content of each TMT vial was then transferred to the corresponding protein sample. After 1 hour, the reaction was quenched by adding 8 µl of 5% hydroxylamine. All the protein samples were combined into a single tube and dried using a speedvac concentrator. Samples were stored at -20˚C until fractionation could be performed.

High pH Reverse Phase (RP) peptide fractionation was performed with the Waters XBridge C18 column (2.1 x 150 mm, 3.5 µm, 120 Ä) on a Dionex™ UltiMate 3000 HPLC system (Thermo Scientific). A 0.1% solution of ammonium hydroxide was used as mobile phase A, while mobile phase B was composed of 99.9% acetonitrile with 0.1% ammonium hydroxide. The TMT-labelled samples were reconstituted in 100 µl mobile phase A, centrifuged and injected into the column, which operated at 0.2 ml/min. The fractions collected from the column were dried with the SpeedVac concentrator and stored at -20˚C until MS could be performed.

### 2.3.3 LC-MS/MS

Liquid Chromatography-Mass Spectrometry (LC-MS) was performed using a Dionex™ UltiMate 3000 HPLC system (Thermo Scientific) coupled with the Orbitrap Fusion Tribrid Mass Spectrometer (Thermo Scientific). This was performed by the Proteomics Facility at The Sanger Institute.

Dried samples were reconstituted in 40 µl 0.1% formic acid, of which 7 µl were loaded to the Acclaim PepMap 100 trapping column (100 µm x 2 cm, C18, 5 µl, 100 Ä) at a flow rate of 10 µl/min. Then, multi-step gradient elution was performed at 45˚C using the Dionex™ Acclaim PepMap RSLC capillary column (75 µm x 50 cm, 2 µm, 100 Ä). A 0.1% solution of formic acid was used as mobile phase A, and a 80% acetonitrile, 0.1% formic acid solution as mobile phase B. Precursors with mass resolution of 120k, AGC 3 x 105 and IT 100 ms were isolated for CID fragmentation with quadrupole isolation width of 1.2 Th. Collision energy was set at 35%. Furthermore, MS3 quantification spectra were acquired via further fragmentation for the top 10 most abundant CID fragments.

### 2.3.4 Proteomics data analysis

#### Protein identification and quantification

Protein discovery analysis was performed by Theodoros Roumeliotis and the proteomics facility at The Sanger Institute. Briefly, the obtained mass spectra were submitted to Sequest HT search in Proteome Discoverer™ 2.1 (Thermo Scientific). Spectra were searched for tryptic peptides with maximum 2 miscleavage events and a minimum length of 6 amino acids. The TMT 6-plex at N-terminus were defined as static modifications. Peptide confidence was estimated with the Percolator node, and the FDR was set at 0.01 and validation was based on q-values. Spectra were then searched against 20,165 reviewed human entries of UniProt. TMT quantification was performed with the Reporter Ion Quantifier node, and a window tolerance of 15 ppm. Only peptides belonging to protein groups were used for quantification.

#### Quality control

Raw protein counts were normalised to the sample median. Next, the data was imported to the R programing environment and a $\log_2$ transformation was applied to improve data visualization. PCA was performed on the transformed protein counts using the “prcomp” package of base R.

#### RNA-protein correlation analysis

Raw RNA counts and median normalised protein counts were imported to R, and a $\log_2$ transformation was applied to both data sets. Next, the RNA-seq biological replicates and MS technical replicates were averaged, and the Pearson correlation between both molecular traits was calculated. Finally, the $\log_2$ fold change between unstimulated T cells and each polarising condition (Th0 and Th1) were calculated for both data sets, and a Pearson correlation coefficient was computed.

# 3. Optimisation of methods for cytokine induced polarisation of primary human immune cells

## 3.1 Overview

Throughout this study, we aimed to characterise the response to cytokine induced polarisation in immune cells by analysing specific cell states generated *in vitro*. In this chapter, I describe the optimisation of our experimental setup for isolation, stimulation and polarisation of human naive $CD4^+$ T cells and monocyte derived macrophages. Finally, I summarise the results of a phenotypic characterisation of the cytokine polarisation cell states generated.

## 3.2 Differentiation and phenotyping of monocyte derived macrophages

To promote monocyte to macrophage differentiation, we cultured $CD14^+$ monocytes with M-CSF for 7 days and evaluated the efficiency of the differentiation compared with untreated monocytes. We observed that the expression of CD14, CD68, MerTK, and HLA-DR increased after seven days of differentiation (**Figure 3.1**), indicating that our cell culture conditions successfully induced monocyte to macrophage differentiation (153).

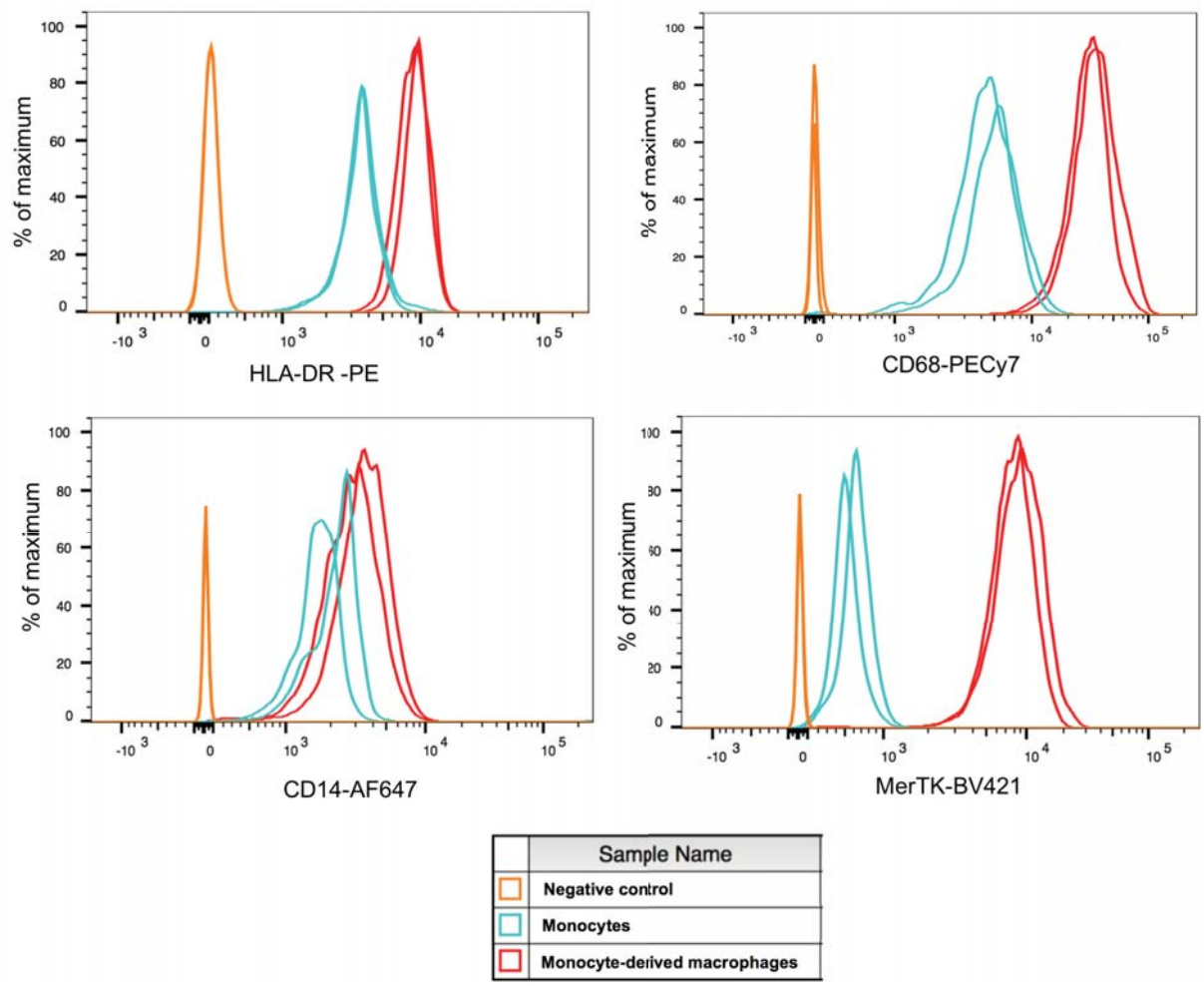


**Figure 3.1 M-CSF promotes monocyte to macrophage differentiation.** Following seven days of treatment with M-CSF, macrophages were stained for HLA-DR, CD68, CD14 and MErTK, and analysed via flow cytometry. Monocytes kept in culture without M-CSF for seven days as well as unstained cells were used as negative controls. Results are shown as percentage of maximum (normalised to mode measurements), with each color representing a different culture condition.

## 3.3 Isolation and stimulation of naïve CD4$^+$ T cells

Naive CD4$^+$ T cells were isolated from peripheral blood using magnetic selection followed by FACS. Isolated cells were of high purity, positive for CD45RA, and expressed low levels of CD25 and CD127 (**Figure 3.2**). Thus, we concluded that the population obtained was mostly composed of naive CD4$^+$ T cells and proceeded to use this method throughout our study.

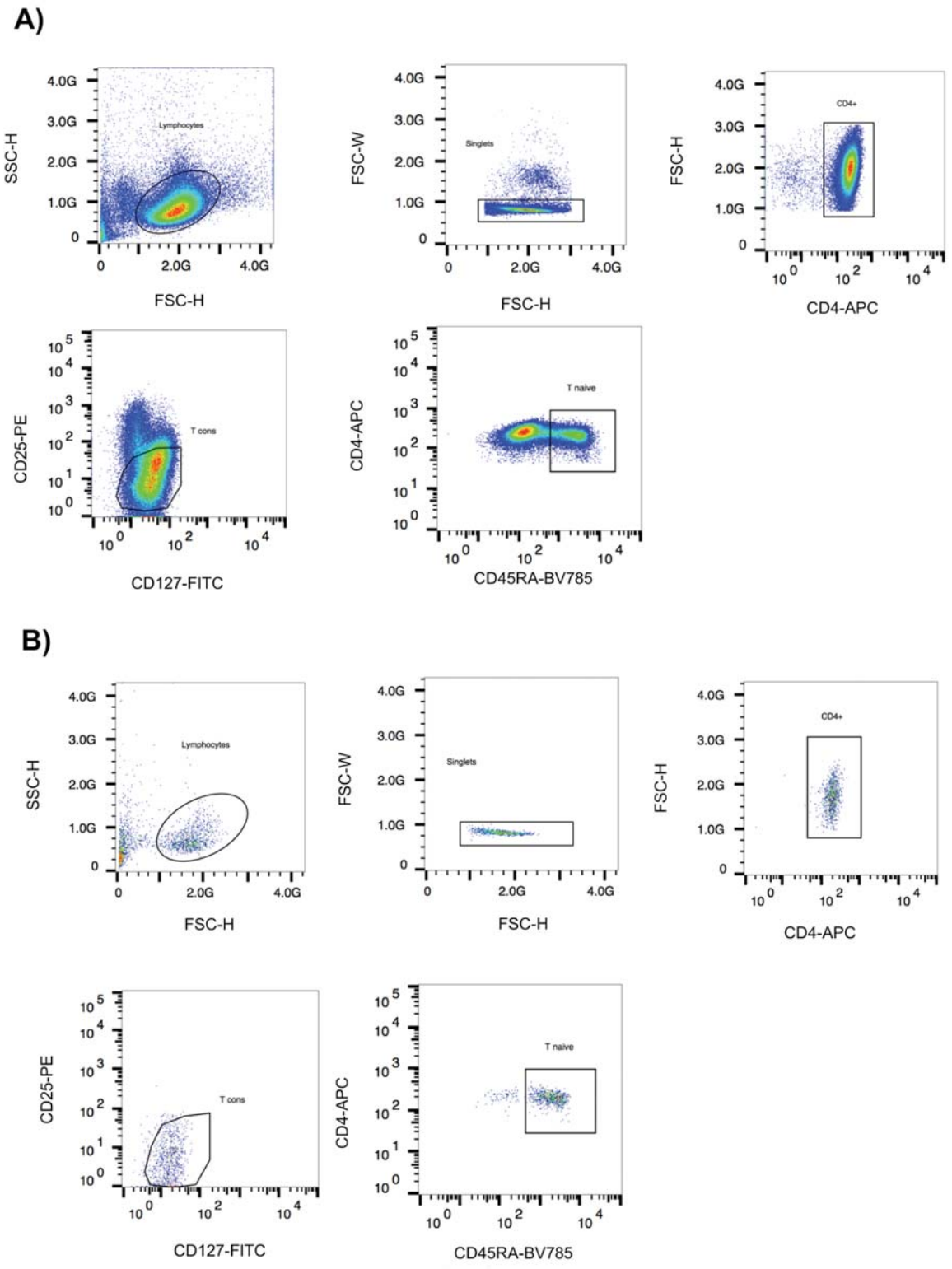


**Figure 3.2 Naïve CD4$^+$ T cells are isolated using fluorescence activated cell sorting.** **A)** CD4$^+$ cells were enriched from PBMCs, stained and separated via flow cytometry using the gating scheme in this figure. "Conventional T cells" ($T_{cons}$) were identified as CD25$^{low}$ and naïve T cells as CD4$^+$ CD127$^{high}$ CD25$^{low}$ CD45RA$^+$. Example performed on PBMCs from one individual. **B)** After CD4$^+$ T cell isolation, purity was assessed by flow cytometry. On average, 90% of cells were CD4$^+$CD25$^{low}$CD127$^{low}$CD45RA$^+$. This is an example of such purity analysis performed on cells from one individual.

To assess the efficiency of T cell activation, following stimulation with anti-CD3/anti-CD28 antibodies we stained cells for the expression of the activation markers CD25 and CD69 (154). We observed that on average 85% of cells expressed CD69, and 80% increased CD25 expression after 16 hours of activation. A large $CD25^{+}CD69^{+}$ population emerged which was not present in the unstimulated samples (**Figure 3.3**). We thus concluded that stimulation was effective.

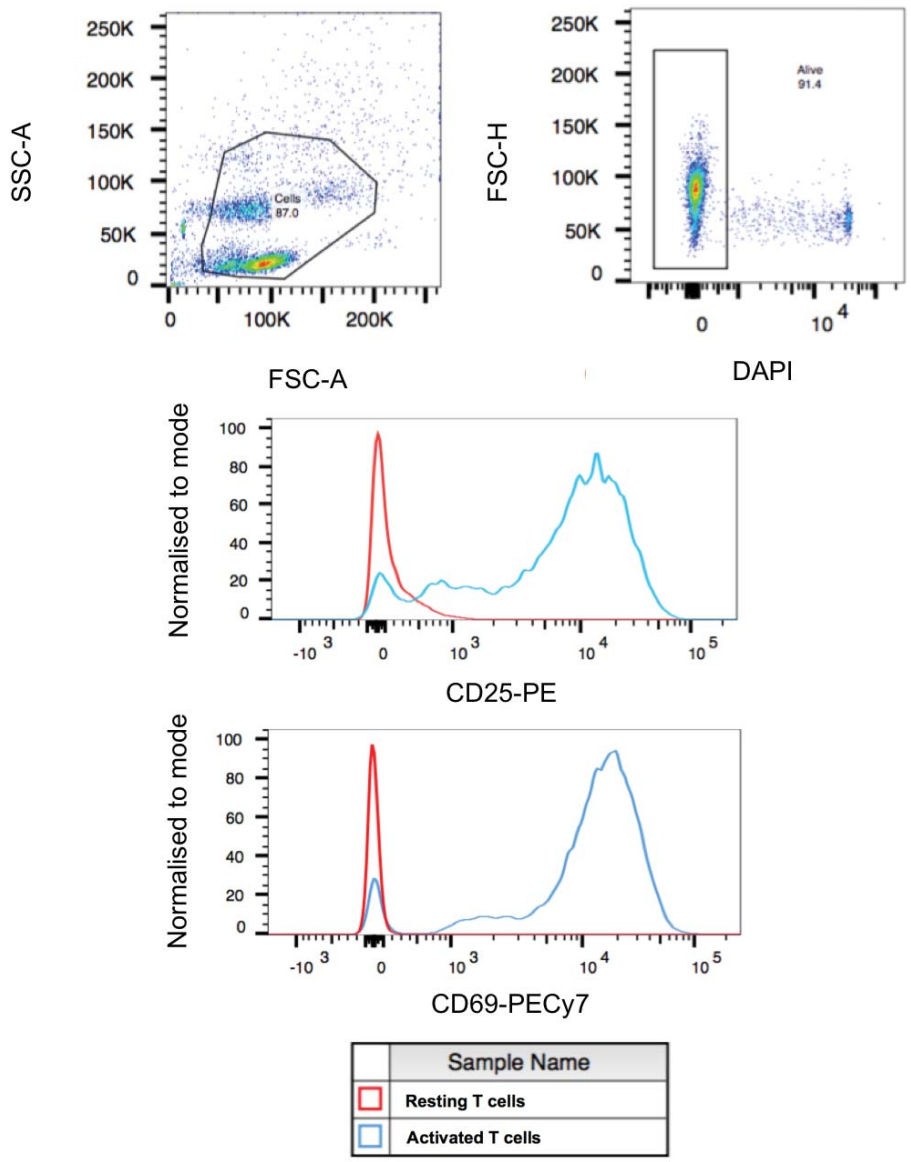


**Figure 3.3 T cells express CD25 and CD69 following activation.** After 16 hours of activation, the viability and surface marker expression of $CD4^{+}$ T cells were analysed by flow cytometry. Only $DAPI^{-}$ cells were used to determine the percentage of CD69 and CD25 expressing cells.

## 3.4 Determination of optimal T cell activation conditions

Given that activation beads tightly interact with T cells, their mechanical removal inherently results in cell loss. Thus, we proceeded to estimate the ratio of beads to cells that achieved the maximum efficiency of activation with the minimal cell loss upon beads removal. To do this, we stimulated naïve $CD4^+$ T cells with a decreasing beads-to-cells ratio and assessed the activation efficiency through the expression of CD69 at 16 hours. The data from these experiments was used to build a titration curve (**Figure 3.4A**). We found that both a 1:1 and a 1:2 beads to cells ratio achieved on average over 90% CD69 expressing cells (**Figure 3.4A**). Since the difference in activation was minimal, we decided to measure the cell loss observed with a 1:2 beads to cells ratio. To estimate the percentage of cells lost due to beads removal, we stimulated naive $CD4^+$ T cells and magnetically removed the beads after 16 hours of culture. The cells were then counted via flow cytometry using counting beads. The total counts were compared with a sample from the same individual in which no removal of beads was performed. On average, magnetic removal of activation beads at the beads-to-cells ratio of 1:2 caused 30% cell loss (**Figure 3.4**). We considered this number acceptable to use throughout the rest of the study.

We wanted to ensure that the presence of cytokines would not affect the efficiency of T cell activation. To assess this, we stimulated naïve $CD4^+$ T cells for 16 hours as previously described in the presence or absence of polarising cytokines. Following cell culture, the expression of CD69 and CD25 was measured by flow cytometry and compared to unstimulated $CD4^+$ T cells cultured for 16 hours. We observed a clear upregulation of both CD69 and CD25 in $CD4^+$ T cells upon activation which was independent from the polarising condition (**Figure 3.5**). More than 90% cells expressed CD69 regardless of the cytokines they were polarised with, and on average 75% expressed CD25. Therefore, these results implicated that cytokines did not affect the percentages of activated T cells.

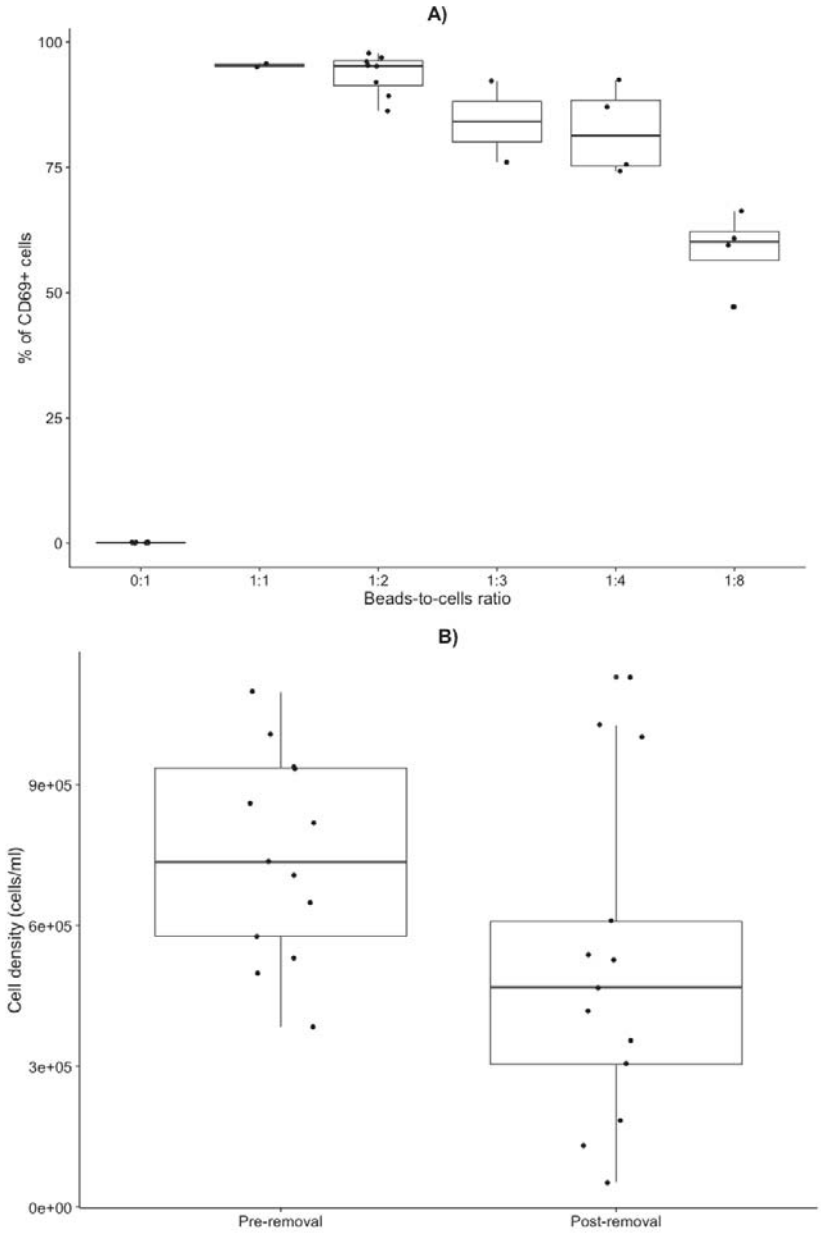


**Figure 3.4 Determination of the optimal ratio of T cells to activation beads.** Naive $CD4^+$ T cells were incubated for 16 hours with activation beads. Next, beads were removed and cells counted using flow cytometry. Boxplots represent data from nine independent experiments. **A)** Titration curve showing the percentage of CD69 expressing cells at different cells-to-beads ratios. **B)** Number of cells per millilitre before and after magnetic removal of activation beads at a 1:2 ratio. A 30% cell loss was observed.

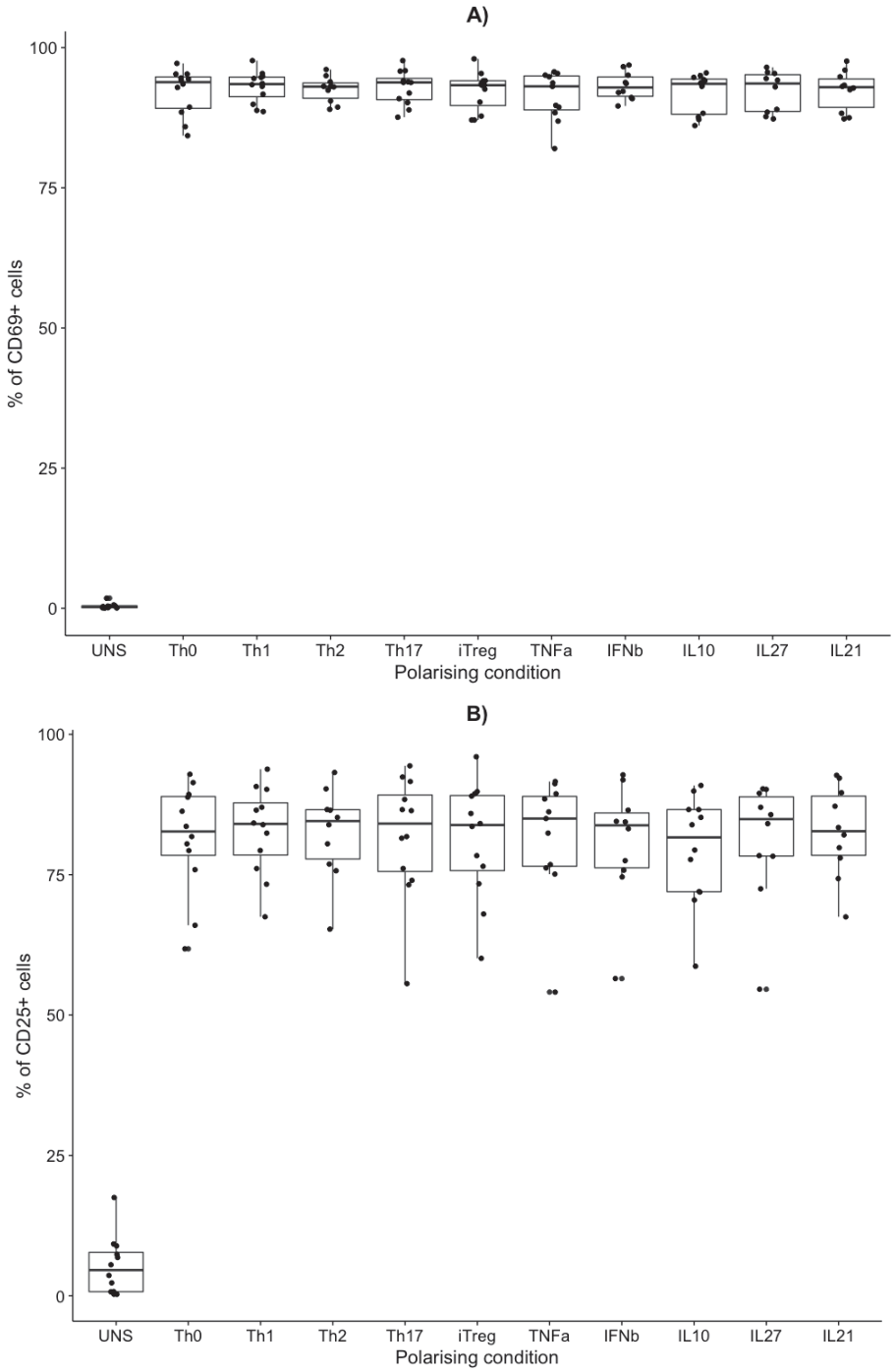


**Figure 3.5 Cytokine polarising conditions do not modify activation efficiency.** Naive $CD4^+$ T cells were incubated with polarising cytokine cocktails and activation beads. Percentage of live cells expressing **A)** CD69 and **B)** CD25 expression was assessed by flow cytometry after 16 hours. Box plots represent 12 independent biological replicates.

## 3.5 Cytokine polarisation of naive CD4$^+$ T cells

Next, we sought to investigate whether cytokines polarised CD4$^+$ T cells to known cell states. In order to assess the expression of Tbet, Gata3, and FoxP3, we stimulated and polarised naïve CD4$^+$ T cells to Th1, Th2, Th17 and iTreg lineages for 5 days. Cells were then fixed, permeabilised, and stained with antibodies against these proteins. The percentage of TF-expressing cells was estimated by flow cytometry. We observed increased expression of GATA-3 and FoxP3 in Th2 and iTreg lineages, respectively. Approximately 75% of cells stimulated with IL-4 expressed GATA-3, and on average 65% of TGF-β stimulated cells were FoxP3$^+$ (**Figure 3.6**). Therefore, we concluded that our Th2- and iTreg-polarising cocktails efficiently triggered the respective differentiation programs. These results also confirmed that the concentration of cytokines used was appropriate. Since Th17 and iTreg polarisation both need TGF-β, and yet Th17 cells did not express FoxP3 (**Figure 3.6A**), these results indirectly suggested a good efficiency of Th17-polarisation.

Since T-bet was expressed at variable levels across all lineages, reporting percentages of Tbet-expressing cells was not as informative as for the other TFs. However, we observed that the expression level of T-bet, measured as MFI, was higher in Th1 cells as compared to other polarised cell fates (**Figure 3.6C**). Therefore, we concluded that our cocktail successfully polarised CD4$^+$ T cells to the Th1 phenotype.

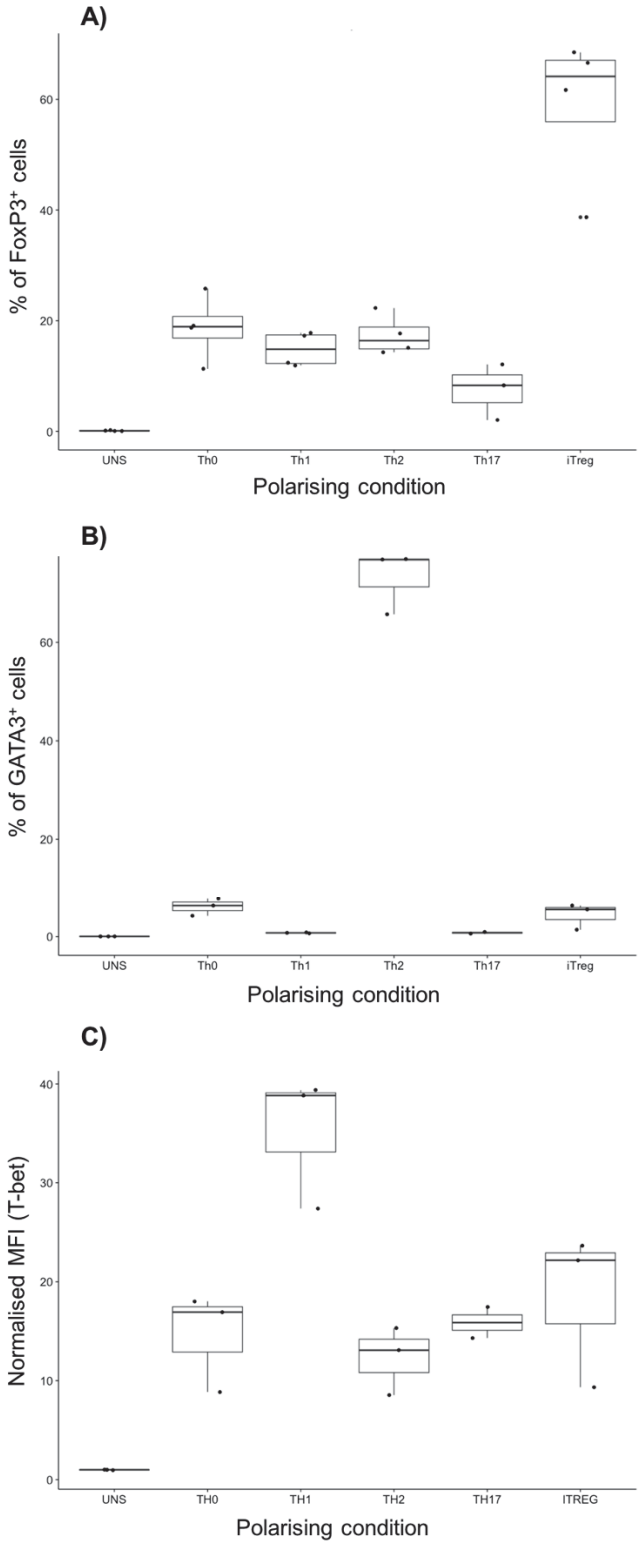


**Figure 3.6 Cytokines polarise CD4$^+$ T cells towards Th2 and iTreg lineages.** Polarisation of CD4$^+$ T cells to Th1, Th2 and iTreg was assessed by flow cytometry after five days. **A)** Percentages of cells expressing Gata3 and **B)** FoxP3 were calculated. **C)** T-bet expression was represented as MFIs normalised to the negative control. Box plots correspond to observations from three independent biological replicates.

## 3.6 Discussion

In this study we optimised a system for assessing cytokine polarisation of human immune cells *in vitro*. We demonstrated that in our experimental set up human monocytes expressed high levels of CD14, a well known marker of the monocyte/macrophage lineage (72), as well as medium levels of HLA-DR, CD68 and MerTK. *In viv*o, human monocytes differentiate into DCs or macrophages upon migration to the tissues (73-75). Each of these differentiation programs is triggered by the presence of specific stimuli. Whereas GM-CSF with IL-4 induces differentiation into DCs, M-CSF induces differentiation into macrophages (155). We used M-CSF to induce the monocyte to macrophage differentiation program (94). When comparing the phenotype of monocyte derived macrophages with monocytes, we saw a sharp upregulation of CD68, MerTK and HLA-DR. MHC-II molecules, including HLA-DR, are known to be upregulated in both DCs and macrophages as compared to monocytes, and are thus a general marker of differentiation (153). On the other hand, MerTK is a known marker of mature tissue macrophages not expressed by DCs (153), informing on the type of differentiation. Thus, this indicated that our protocols for $CD14^+$ cell isolation followed by M-CSF treatment yielded high purity monocyte derived macrophages.

Naïve $CD4^+$ T cells can be identified based on the expression of the splice variant of the CD45 molecule ($CD45RA^+$ cells) as opposed to the effector and memory cells that express the CD45RO isoform (156). In our study, cells were selected based on low expression of CD25, and high CD127 and CD45RA expression. Flow cytometry analysis consistently showed high purity of this population. *In viv*o, naïve $CD4^+$ T cells egress from the thymus and circulate through peripheral blood before homing to secondary lymphoid organs such as lymph nodes in response to a chemokine gradient (157). In the lymph nodes, naive $CD4^+$ T cells are stimulated by DCs, who provide two signals necessary to successfully drive activation (48-53). In order to mimic this process *in vitro,* we stimulated T cells with beads coated with anti-CD3 and anti-CD28 antibodies. This stimulation induced an increase in CD25 and CD69 expression. This is expected, as CD25 allows the cell to respond to IL-2, a cytokine essential for T cell proliferation in response to activation signals (158). This upregulation was observed even at 16 hours, generally thought of as an early time point. Furthermore, expression of CD69, a transmembrane lectin protein upregulated shortly after T cell activation (154, 158), was also seen at 16 hours and further confirmed that cells responded to activation. These results suggested that our T cell activation method was efficient. Furthermore, they also validated the choice of 16 hours as a relevant time point for transcriptional analysis. This time point was chosen so as to characterise the transcriptome

before the activation of cell cycle genes. At five days, on the other hand, we expect to find more defined lineage specific signatures.

Magnetic removal of activation beads is an important cause of cell loss. For this reason, we decided to reduce by half the number of activation beads in the cell culture. Our results showed almost no difference in activation efficiency between the two bead ratios. Thus, this reduction maintained the efficiency of activation in our cell population, while cell loss was reduced to approximately 30%.

Next, we proved experimentally that cytokine stimuli did not affect the percentage of stimulated cells, even when regulatory (anti-inflammatory) cytokines such as IL-10 were used. Then, we verified that each T cell subset expressed its master regulatory TF (35, 36, 159, 160). We also found that T cell polarisation to Th1, Th2, Th17 and iTreg occurred at a later time point of T cell activation, since lineage specifying TFs were not expressed at 16 hours but rather appeared at high levels after five days. We observed that cytokines seemed to act in addition to T cell activation, triggering further specialisation. These results are in agreement with the two-step model of T cell polarisation proposed in the literature (161-163).

Our results suggest that T cell activation itself is enough to induce expression of T-bet regardless of cytokines in the microenvironment. The addition of IL-12, however, caused significant upregulation of this TF. These results reflect the fact that T cell lineages sometimes share the expression of master regulators, and are not clearly defined cell types, but rather functional states with remarkable plasticity (29, 43, 64, 67, 164-166). This is in agreement with previous observations of interconversion between T cell polarisation states upon stimulation with cytokines (65). However, the effect of autocrine cytokines cannot be ruled out and might explain the induction of T-bet even in Th0 cells. To test this, we would need to perform a new experiment, adding anti-IFNg antibody to the culture media. Furthermore, strong TCR stimulation can also induce Th1 polarisation (33).

In summary, we have optimised a methodology for studying cytokine induced polarisation of human primary immune cells *in vitro*. The populations of human monocytes and naïve $CD4^+$ T cells obtained with this methodology appeared to be highly pure and could respond efficiently to monocyte to macrophage differentiation and T cell activation. Polarised cells expressed phenotypes previously described in the literature, implicating that our experimental setup provides a valid model for studying human cytokine biology *in vitro*.

# 4. Analysis of gene expression in cytokine polarised cell states

## 4.1 Overview

Throughout this study we sought to delineate the differences between cytokine induced cell states by studying their gene expression. In this chapter, I describe the results of a low coverage RNA-seq study of $CD4^+$ T cells polarised to four known lineages (Th1, Th2, Th17 and iTreg) and the additional five conditions treated with different cytokines linked to autoimmunity (IL-10, IL-21, IL-27, IFN-β, and TNF-α). These cells were assessed after 16 hours and 5 days of stimulation. Additionally, I describe the results from RNA-seq performed on macrophages polarised for six hours towards the classical M1 and M2 phenotypes, as well as with the additional conditions with three different cytokines linked to autoimmunity (IL-23, IL-26, and TNFα). Finally, I describe the results of differential gene expression analysis followed by pathway enrichment and gene co-expression network analysis.

## 4. 2 Quality control of sequencing data

Quality assessment was performed by the Sequencing Facility at The Sanger Institute (**Table 4.1** and **4.2**). We observed a median fragment size of 177 bp. Approximately 91% fragments matched with the human genome. The GC fraction was close to the expected value. Furthermore, we observed that multiplexing barcodes were efficiently decoded, with an average 98% perfect matches, and only 0.83% sequences with no match. We also observed high accuracy throughout the sequencing run, as determined by quality scores throughout cycles (**Figure 4.1**). We concluded that sequencing had been performed appropriately, generating high quality data.

**Table 4.1** Global quality metrics of two lanes sequenced run in an Illumina HiSeq 2500

| Lane Number | Number of Cycles | Tag Decode Rate (%) | Tag Decode CV | Median Insert Size | Top Reference Matches (%) |
|---|---|---|---|---|---|
| 1 | 158 | 99.17 | 7.06 | 177 | *Homo sapiens* 91.6<br>*Pan troglodytes* 84.6 |
| 2 | 158 | 99.16 | 7.10 | 177 | *Homo sapiens* 91.9<br>*Pan troglodytes* 84.6 |

**Table 4.2** Read specific quality metrics of two lanes sequenced in an Illumina HiSeq 2500

| Lane Number | Read | Adapters (%) | GC Fraction (%) | Yield (kb above Q20) | Average mismatch (%) |
|---|---|---|---|---|---|
| 1 | Forward | 0.06 | 48.0 | 11,123,259 | 2.56 |
| | Reverse | 0.03 | 49.1 | 10,965,772 | 2.52 |
| 2 | Forward | 0.06 | 48.0 | 11,160,621 | 2.52 |
| | Reverse | 0.03 | 49.1 | 11,013,167 | 2.46 |

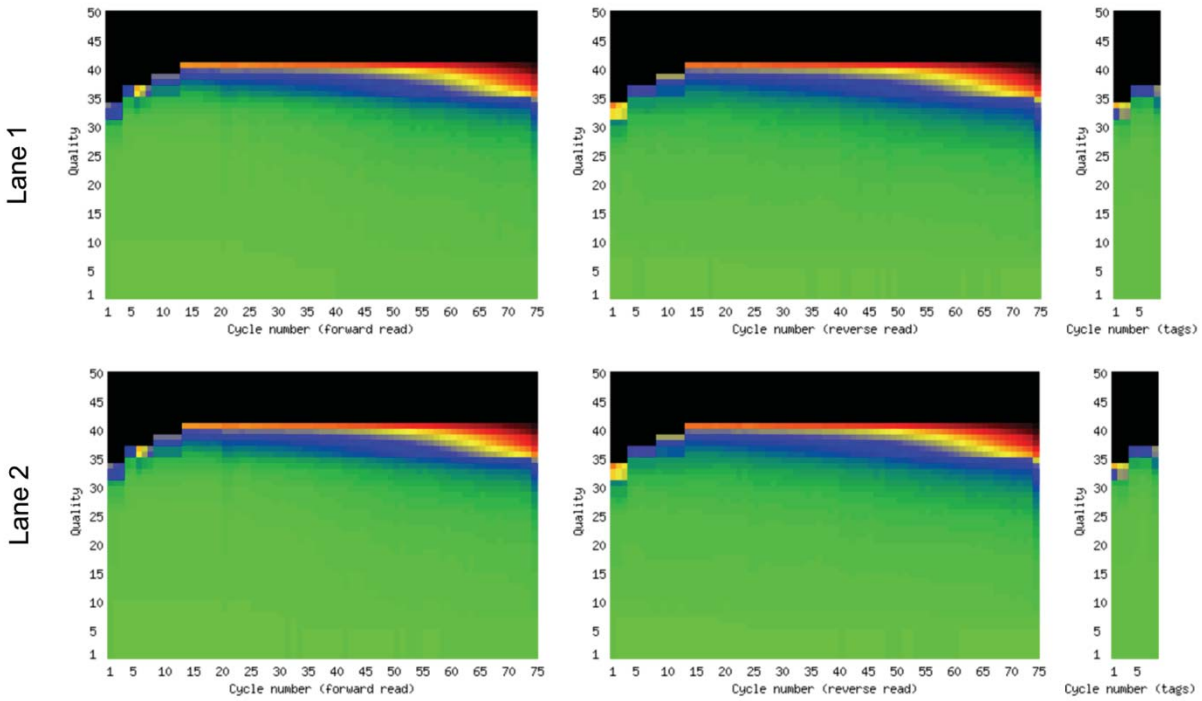


**Figure 4.1 Sequencing quality is high throughout the run** Following library preparation, the mRNA library was spread across two lanes of an Illumina HiSeq 2500 for clustering and sequencing. The average quality score at each cycle was plotted for the forward and reverse reads, as well as the tags. Each sequencing lane was analysed separately.

Following quality control, we re-mapped the 5.25 x $10^6$ paired-end reads per sample using STAR (138). Approximately 89.5% of reads were uniquely mapped. Next, we used featureCounts (140) and obtained 83% of reads assigned to features. We concluded that mapping efficiency was high.

To estimate the reproducibility, we compared the expression values of two replicates of the same condition. This analysis was done using biological replicates, since the study included no technical replicates. We transformed the data using the log2 function. We observed that for three selected conditions the log2 counts were highly correlated upon visual inspection (**Figure 4.2**). Hence, we calculated the Pearson correlation for all pairs of replicates and observed an average correlation coefficient higher than 0.96 (**Table 4.3**). We concluded that the RNA-seq results were reproducible.

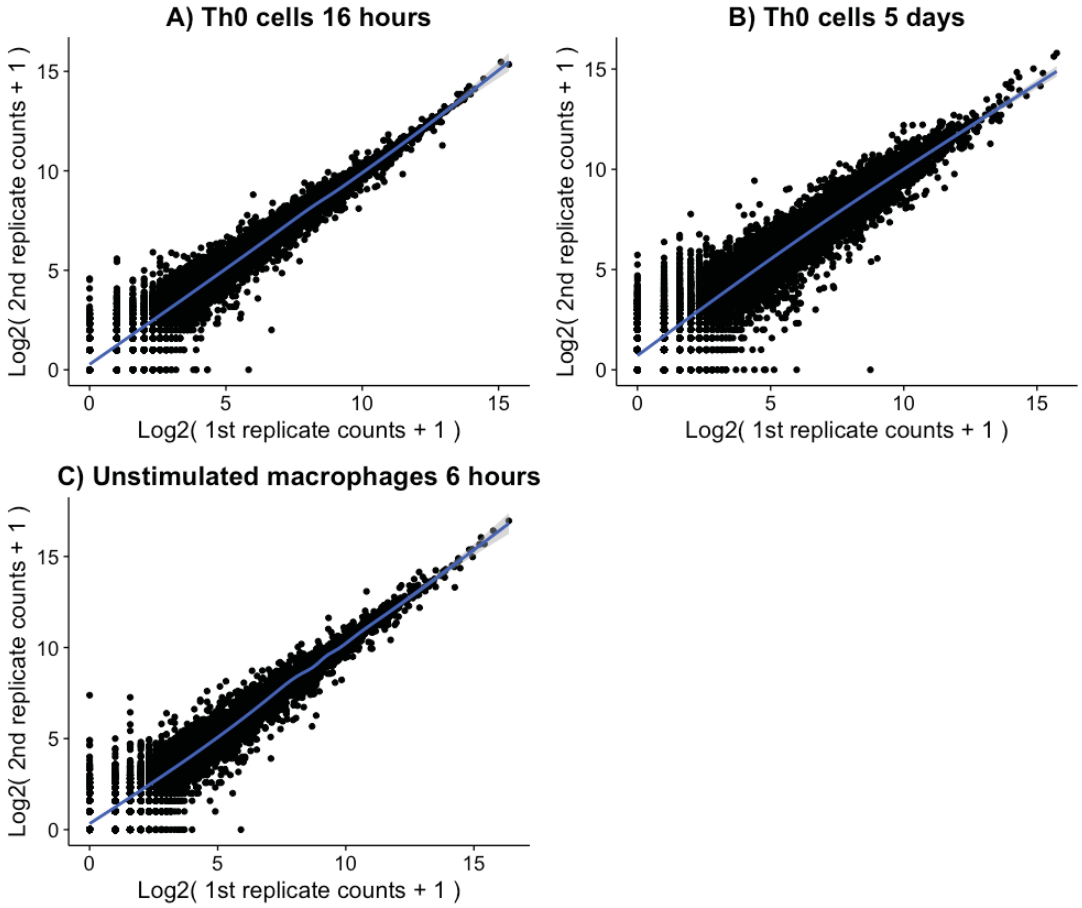


**Figure 4.2 RNA-seq results are reproducible** Following mapping and summarisation, the RNA counts of two biological replicates of three representative were plotted against each other. The samples were selected so as to include all cell types and time points and log2 transformed counts were used.

**Table 4.3** Correlation coefficient of log transformed RNA counts for the two biological replicates of each condition.

| Cell Type | Time Point | Condition | Pearson Correlation |
|---|---|---|---|
| T cell | 16 hours | Unstimulated | 0.977 |
| | | Th0 | 0.981 |
| | | Th1 | 0.981 |
| | | Th2 | 0.981 |
| | | Th17 | 0.981 |
| | | iTreg | 0.981 |
| | | IL-10 | 0.981 |
| | | IL-21 | 0.981 |
| | | IL-27 | 0.981 |
| | | IFN-β | 0.982 |
| | | TNF-α | 0.981 |
| | 5 days | Unstimulated | 0.963 |
| | | Th0 | 0.958 |
| | | Th1 | 0.963 |
| | | Th2 | 0.966 |
| | | Th17 | 0.961 |
| | | iTreg | 0.966 |
| | | IL-10 | 0.967 |
| | | IL-21 | 0.962 |
| | | IL-27 | 0.965 |
| | | IFN- β | 0.971 |
| | | TNF-α | 0.965 |
| Macrophage | 6 hours | Unstimulated | 0.978 |
| | | M1 | 0.98 |
| | | M2 | 0.979 |
| | | IL-23 | 0.971 |
| | | IL-26 | 0.977 |
| | | TNF-α | 0.977 |

## 4. 3 Estimation of statistical power

To determine how powered the study was, we estimated the statistical power to detect genes with 2-fold change differential expression at an FDR of 0.05. We divided the samples in three groups according to cell type and time point and used DESeq2 and “RNASeqPower” (134) to model power as a function of the expression level. We observed that power increased for genes with higher counts (**Figure 4.3**) to a similar extent in all groups. On average, power was larger than 0.6 for genes with raw counts larger than 20, and above 0.8 for genes with raw counts higher than 50. We concluded that the study might be powered for detecting differences in genes with expression levels of 50 counts or more.

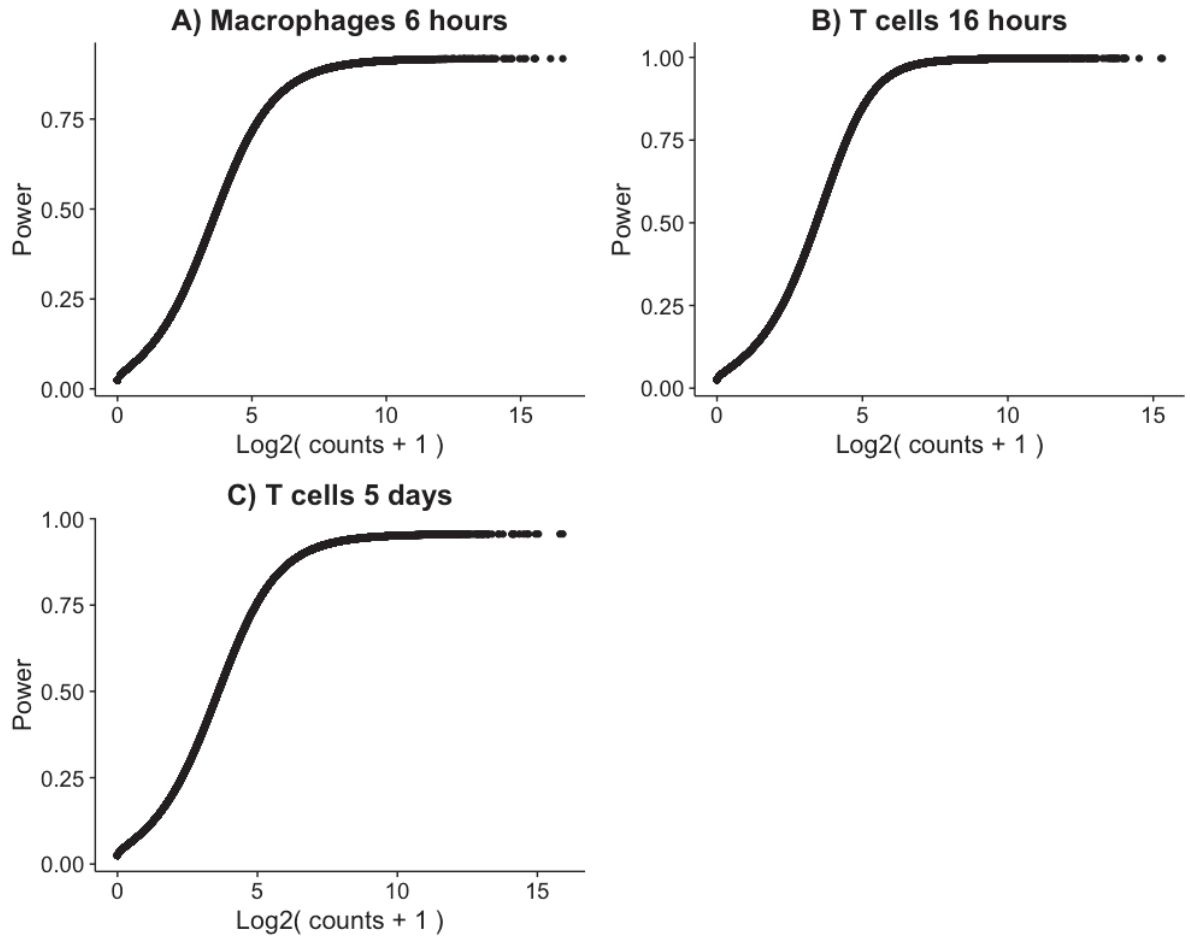


**Figure 4.3 Statistical power increases for highly expressed genes** Gene expression data was divided in three groups, and DESeq2 was used to estimate their coefficient of variation. This coefficient was used to model the statistical power for detecting a gene as a function of its coverage (RNA count) using “RNASeqPower”. For this calculation, we specified an FDR of 0.05, a sample size of 2, and a fold change (effect size) of 2. The power to detect each gene was plotted against its log2-transformed counts.

New we estimated the average statistical power per group. We used DESeq2 to compute the overall median of RNA counts for each group and concluded that, on average, the study had 0.8 power to detect genes with a fold change of 2 at 0.05 FDR (**Table 4.4**).

**Table 4.3** Average power for detecting genes with a fold change of 2 in each group of samples.

| Cell type | Time point | Median of Counts | Median CV | Fold Change | Average Power |
|---|---|---|---|---|---|
| T cell | 16 hours | 53 | 0.147 | 2 | 0.93 |
| | 5 days | 73 | 0.189 | 2 | 0.88 |
| Macrophage | 6 hours | 59 | 0.207 | 2 | 0.81 |

## 4.4 Exploratory data analysis

To explore the data in more detail, we used DESeq2 (135) to perform data transformation and PCA in all samples of the data set. We observed a clear clustering by cell type, with PC1 separating monocytes from T cells (**Figure 4.4A**). This separation accounted for 83% of the variance. On the other hand, PC2 explained 12% of the variance and separated the two different time points within the $CD4^+$ T cell samples. We recapitulated these results by performing PCA on T cell samples only (**Figure 4.4C**). Here, PC1 accounted for 75% of the variance and separated cells stimulated for 16 hours from cells stimulated for five days. We also observed a separate cluster containing four samples, these conditions corresponded to unstimulated cells at both time points. Therefore, PC2 might separate resting cells from the remaining conditions.

To obtain more detailed insights into the data, we repeated the PCA separately for each cell type. We observed that PC1 separated M1 macrophages from the rest of the samples (**Figure 4.4B**) and explained more than 50% of the variance. This analysis also showed separation of the unstimulated, M2, TNF and IL26 macrophage conditions, with both biological replicates clustering tightly together. However, macrophage samples stimulated with IL-23 did not cluster together in the PCA plot.

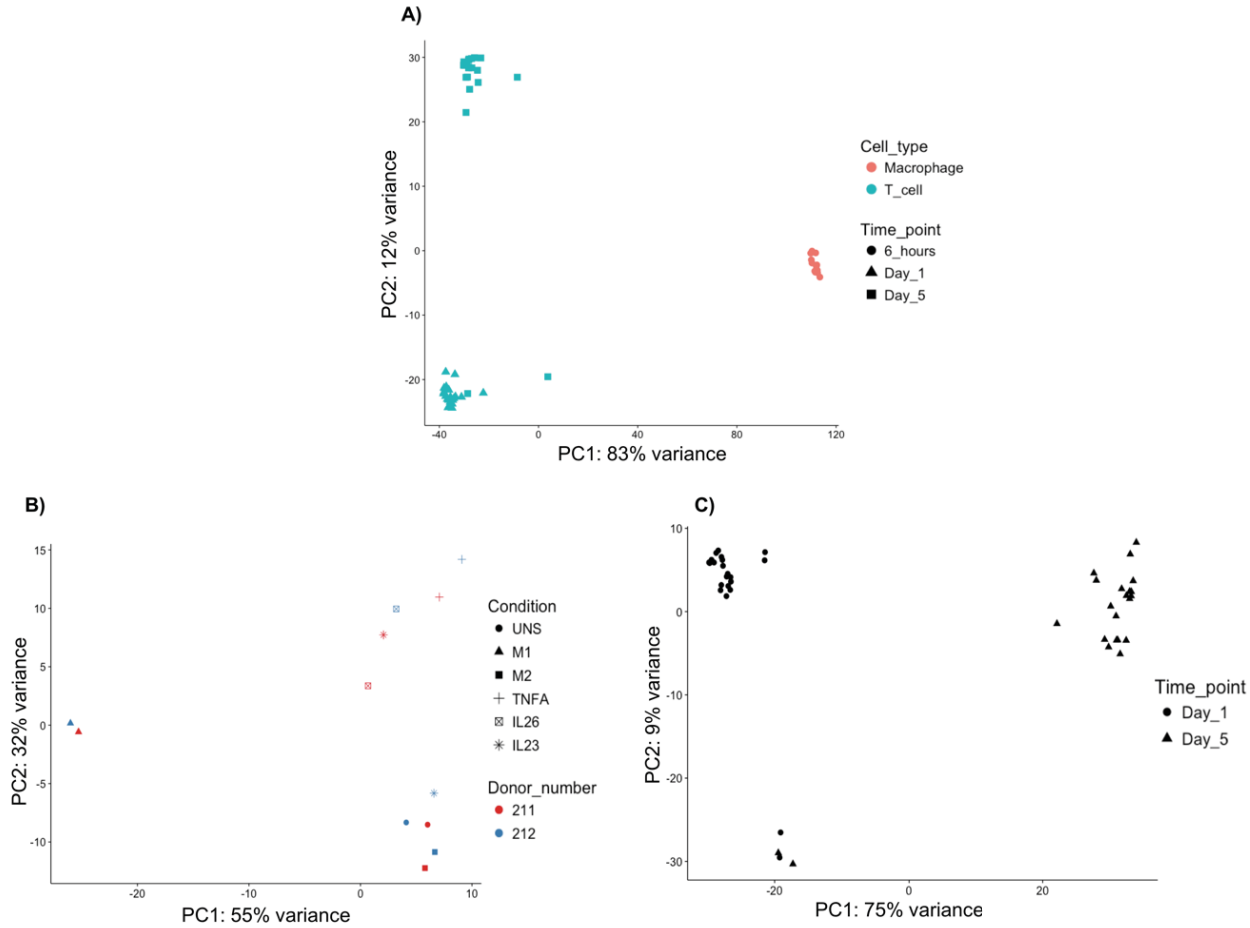


**Figure 4.4 PCA separates different cell types, stimulation time points and conditions.** PCA was performed on RNA counts from: **A)** All samples in the study, with colours represent different cell types and shapes different stimulation times. **B)** Monocyte derived macrophages from two independent biological replicates, with different shapes represent cytokine polarising conditions and colours biological replicates. **C)** $CD4^+$ T cells from two independent biological replicates, with shapes representing stimulation times. Here, the four unstimulated T cell samples clustered separately to the rest of the conditions near the bottom of the plot.

Next, we assessed the differences between polarisations in $CD4^+$ T cells. We removed the unstimulated samples from the analysis and asked whether samples separated by condition. Using transformed RNA counts, we calculated the distance between samples and performed hierarchical clustering using DESeq2. We observed a batch effect between the two individuals, which were also processed on different days (**Figure 4.5A**). Thus, we removed the batch effect using limma (144) and repeated the distance calculation and hierarchical clustering. We observed clustering of biological replicates in the dendrogram at both time points (**Figure 4.5B**). This suggested the presence of different transcriptional responses to different cytokine polarisations. However, we found that several conditions clustered with the control samples. Specifically, iTreg, TNFα, IL-10 and IL-23 were close to the Th0 control at

16 hours. The same was true for IL-10, TNF-α, IL-27 and IL-21 at five days. On the other hand, IFN-β, Th2, and IL-27, clustered separately to the rest of the samples at 16 hours. This was also true for Th1, Th2, Th17 and iTreg cells at five days.

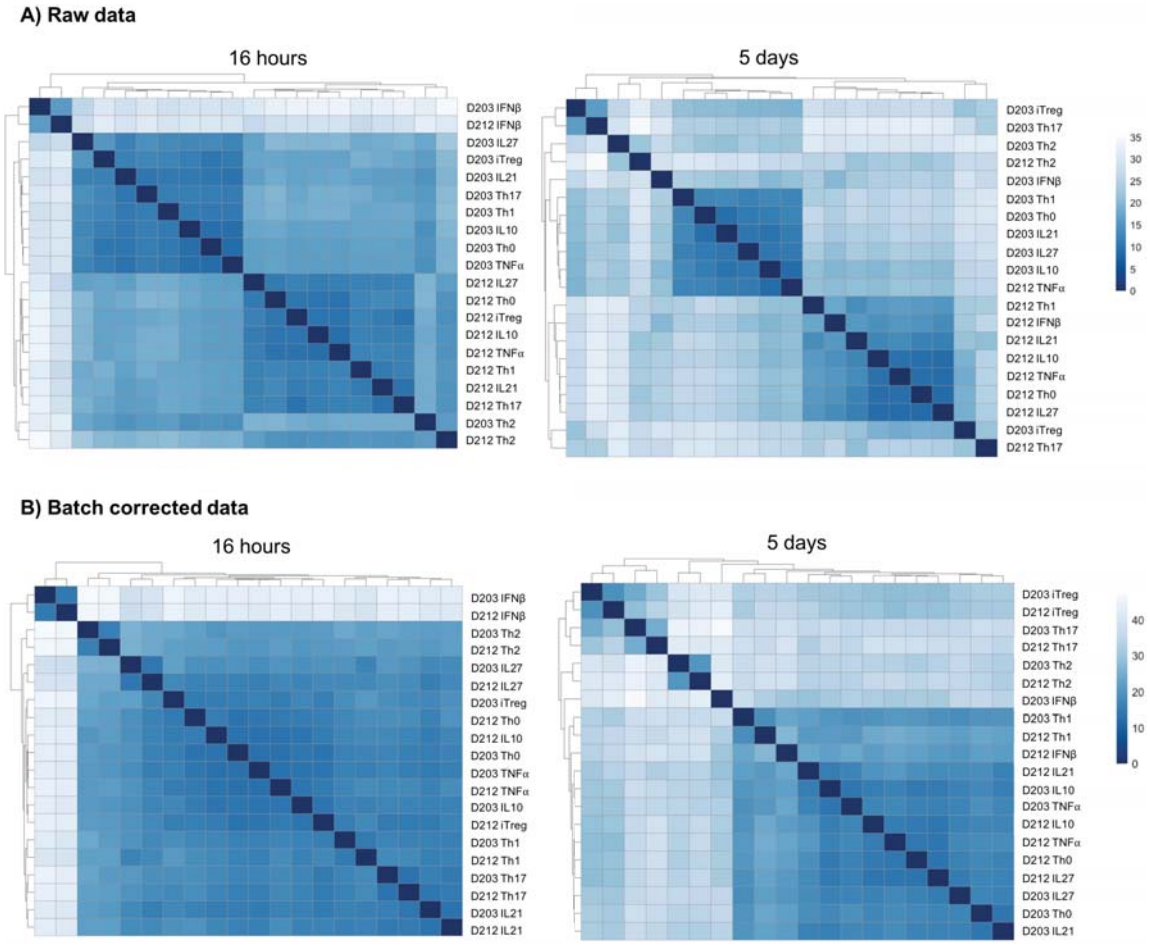


**Figure 4.5 Batch correction improves the separation of polarising conditions in CD4$^+$ T cells** Calculation of Euclidean distance between samples followed by hierarchical clustering was performed. Results are displayed as a heat map, with a colour gradient proportional to the distance between two samples. **A)** Samples from two different batches are shown. **B)** The same samples are shown after implementation of the batch correction. The labels indicate the batch number and the polarising condition of each sample.

We then asked whether transcriptional profiles agreed with descriptions of macrophage and T cell lineages in the literature. We analysed the RNA counts of the M1 macrophage markers IL-12, CXCL11, and COX-2 (94) and observed upregulation in the M1 samples as compared with M2 macrophages (**Figure 4.6A**). CXCL11 expression increased 7-fold in M1 macrophages. We repeated this analysis for the M2 markers COX-1 and MRC1 (94) and confirmed that their expression seemed higher in M2 than in M1 (**Figure 4.6B**). Notably, COX-1 and COX-2 seemed to have opposite expression patterns at the RNA level. Consequently, we concluded that polarisation with IFN-γ and IL4, respectively, induced the M1 and M2 polarisation in macrophages.

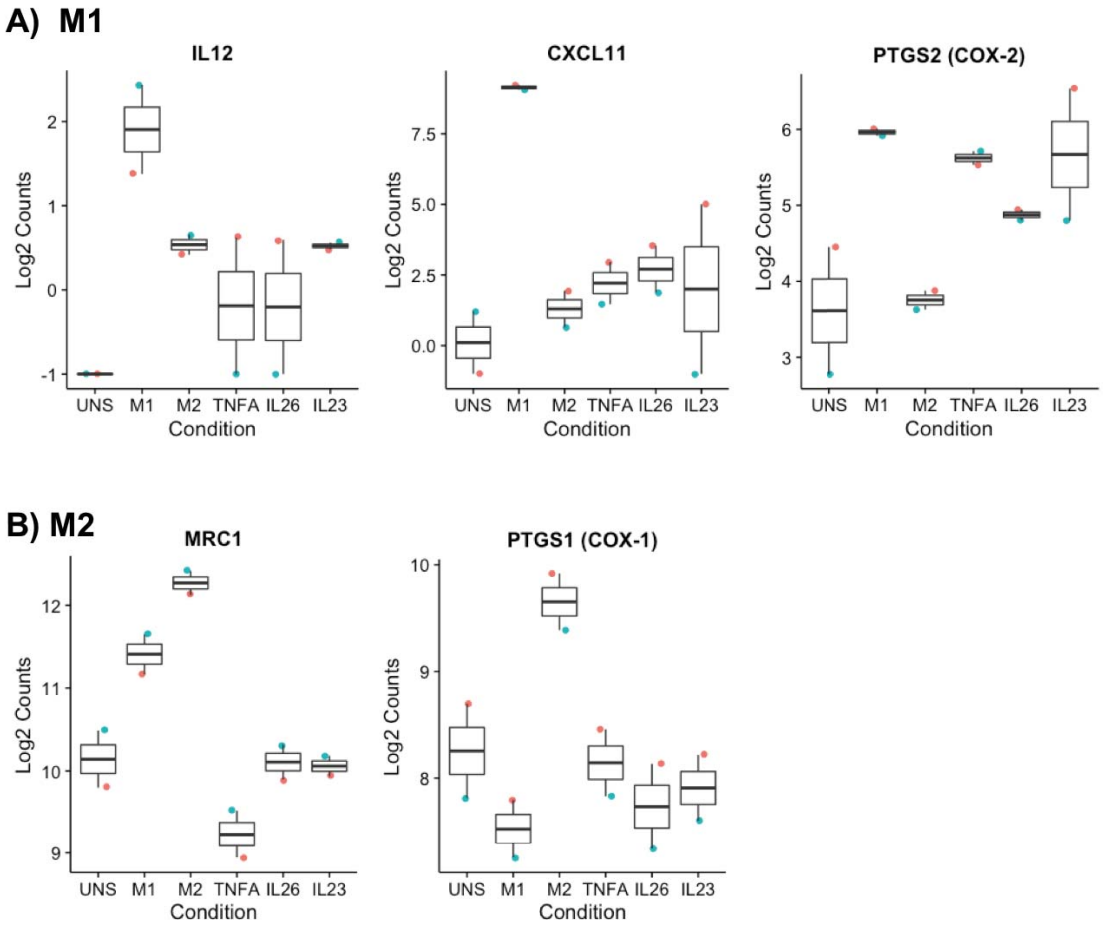


**Figure 4.6 Lineage specific genes are expressed in M1 and M2 macrophages** Bar plots of regularised log2 (rlog) values of RNA counts of macrophage specific. Different colours indicate two independent biological replicates. **A)** M1 macrophages were inspected for expression of IL12, CXCL11 and COX2. **B)** M2 macrophages were inspected for expression of MRC1 and COX1.

Next, we analysed the expression of lineage markers in $CD4^+$ T cells at five days. Th1 cells upregulated T-bet and IFN-γ relative to all other conditions (**Figure 4.7.1A**). In addition, we confirmed that Th2 cells (**Figure 4.7.1B**) expressed three fold more GATA-3 than other activated cells. We also observed expression of IL-4 and IL-13. Conversely, Th17 cells significantly downregulated GATA-3 but showed higher expression of RORC, IL17F, and CCR6 (**Figure 4.7.2C**). CCR6 was also upregulated by iTreg cells, which expressed two fold more FoxP3 than other lineages (**Figure 4.7.2D**). Moreover, we found upregulation of CTLA-4 in iTreg cells. The expression of the regulatory cytokine IL-10 did not change upon iTreg polarisation. We concluded that stimulation with cytokines for the Th1 (IL-12), Th2 (IL-4), Th17 (IL-23, TGF-β, IL-6), and iTreg (TGF-β) lineages effectively induced polarisation in $CD4^+$ cells.

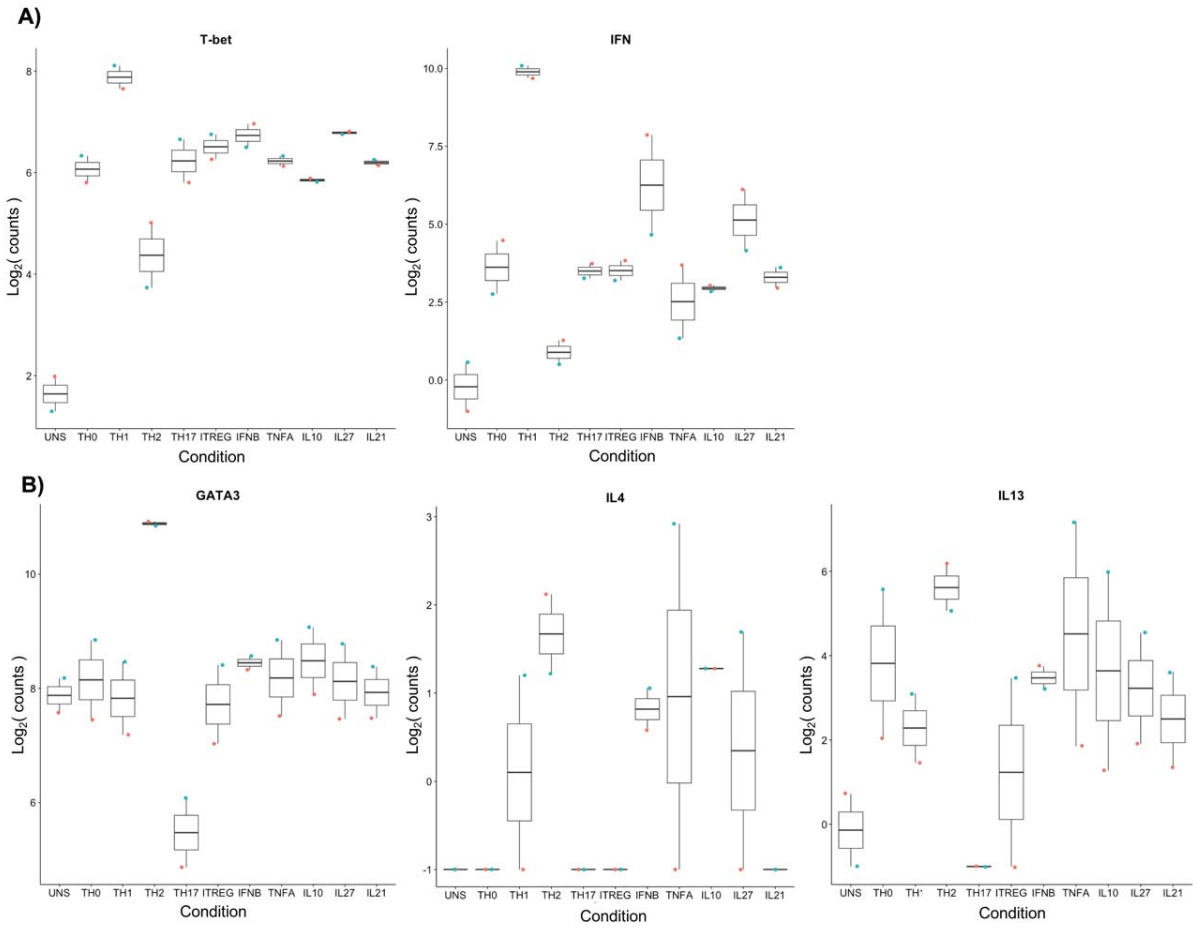


**Figure 4.7.1 Hallmark genes are upregulated after T cell polarisation** Bar plots of logarithmic values of RNA counts of T cell lineage specific genes. Different colours correspond to two independent biological replicates. Expression of **A)** T-bet and IFN-γ in Th1 and **B)** GATA3 and IL-4 in Th2.

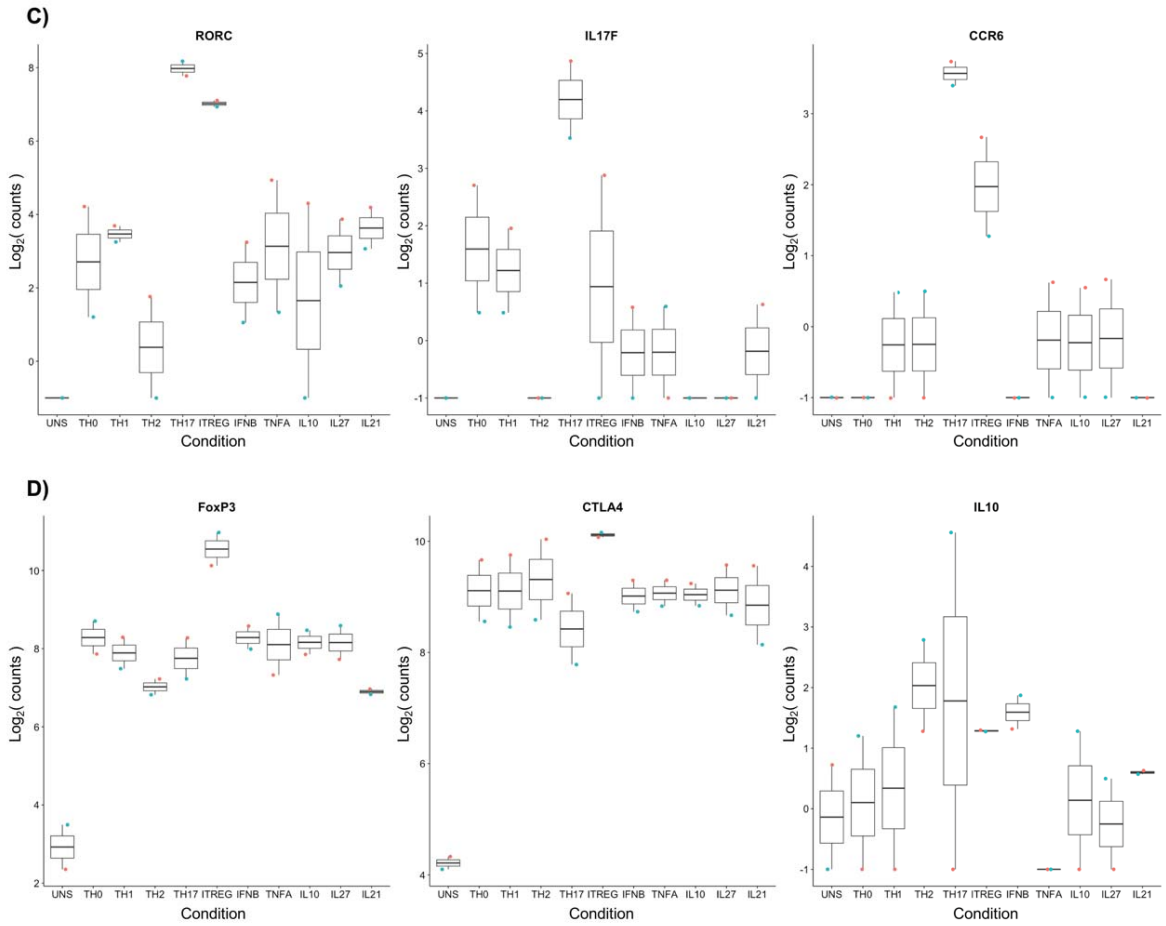


**Figure 4.7.2 Hallmark genes are upregulated after T cell polarisation** Bar plots of regularised log2 (rlog) values of RNA counts of T cell lineage specific genes. Different colours correspond to two independent biological replicates. Expression of **C)** IL-17F, RORC and CCR6 in Th17, and **D)** FoxP3 and CTLA-4 in iTreg cells.

## 4.5 Differential gene expression in polarised CD4$^+$ T cells

To identify genes specifically expressed in different CD4$^+$ T cell polarisation states we performed differential expression analysis. We did pairwise comparisons of RNA counts between each condition and non-polarised Th0 cells, which were used as negative control. Genes with an absolute $\log_2$ fold change larger than 1 and an adjusted P-value lower than 0.05 were considered significantly differentially expressed. At the 16-hour time point, we identified 140 and 29 differentially expressed genes in IFN-β and Th2 conditions, respectively. However, in the remaining conditions practically no genes reached statistical significance at this time point (**Figure 4.8A**). In contrast, after five days of polarisation we identified differential gene expression for all the lineages: 45 genes were differentially expressed in Th1, 361 in Th2, 489 in Th17, and 260 in iTreg cells (**Figure 4.8A**). However, we only found 63 differentially expressed genes upon IFN-β polarisation for five days.

Detailed information concerning differential expression analysis of these conditions, such as fold changes, P-values and mean gene counts, is presented at the end of this thesis (**Appendix**).

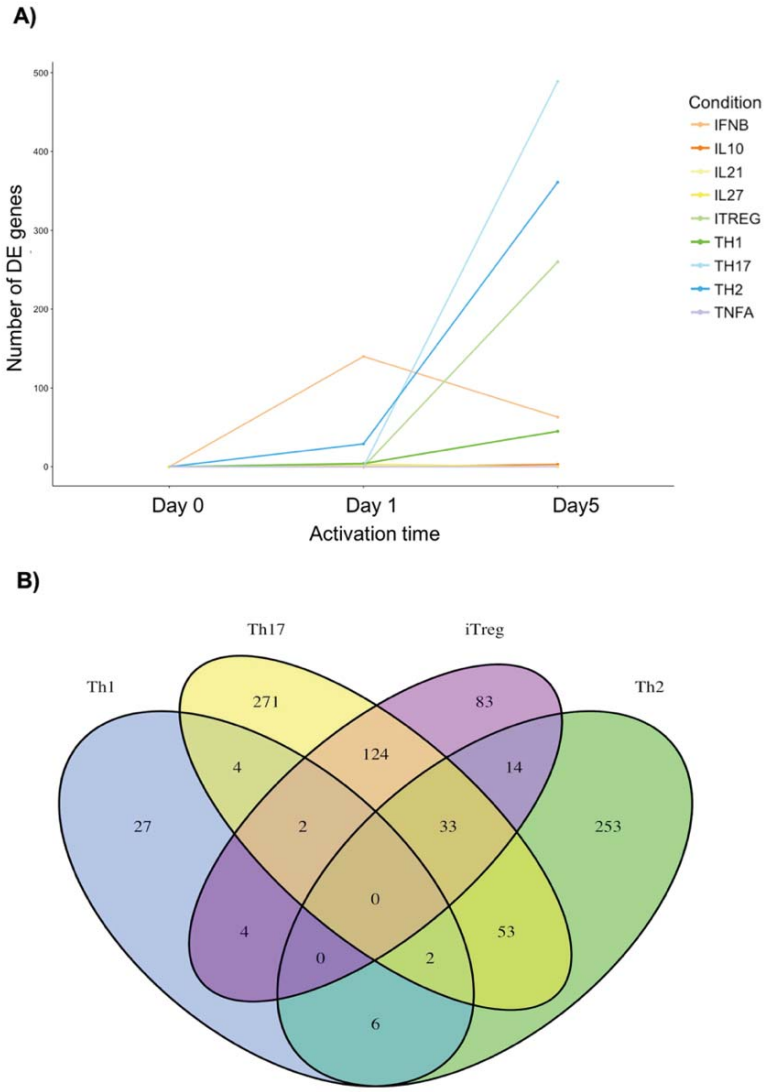


**Figure 4.8 Transcriptional responses to cytokine induced polarisation are condition specific** Differentially expressed genes were defined by comparing CD4+ T cells polarised with cytokines to unpolarised Th0 cells. Genes with an adjusted P-value ≤ 0.05 and an absolute $\log_2$ fold change ≥ 1 were considered differentially expressed. **A)** The numbers of differentially expressed genes per condition were plotted with respect to polarisation time, with each colour representing a condition. **B)** Overlap of differentially expressed genes across Th1, Th2, Th17 and iTreg cells at five days.

Next, we looked for shared differential gene expression across conditions. We overlapped the lists of differentially expressed genes obtained for all T cell conditions at day five and quantified the overlap. IFN-β stimulation was not included in this analysis since most changes appeared at a different time point and displayed entirely different transcriptional dynamics. No genes seemed to be shared between the conditions (**Figure 4.8B**). Th2 and Th17 appeared to have the most different transcriptional profiles, with 253 genes only present in Th2 and 271 only in Th17. On the contrary, iTreg shared approximately 60% of its transcriptional profile with Th17 cells, with only 83 apparently unshared genes. Furthermore, there were 27 genes with differential expression only detected in Th1 cells.

We hypothesised that responses to different cytokines have different transcriptional dynamics. To test this, we analysed the time trajectory of each differentially expressed gene in IFN-β and Th2 polarisation, the condition with the most differentially expressed genes (**Figure 4.9**). We observed substantial, stable expression changes between the first and fifth day in Th2 polarisation, with two large blocks of genes showing up and downregulation, respectively. On the contrary, most genes of the IFN-β response seemed to increase at 16 hours but to decrease at five days. To test for pathway enrichment, we analysed differential expression in Th1, Th2, Th17 and iTreg polarisations at the 5-day time point, while using the 16-hour time point for IFN-β stimulation.

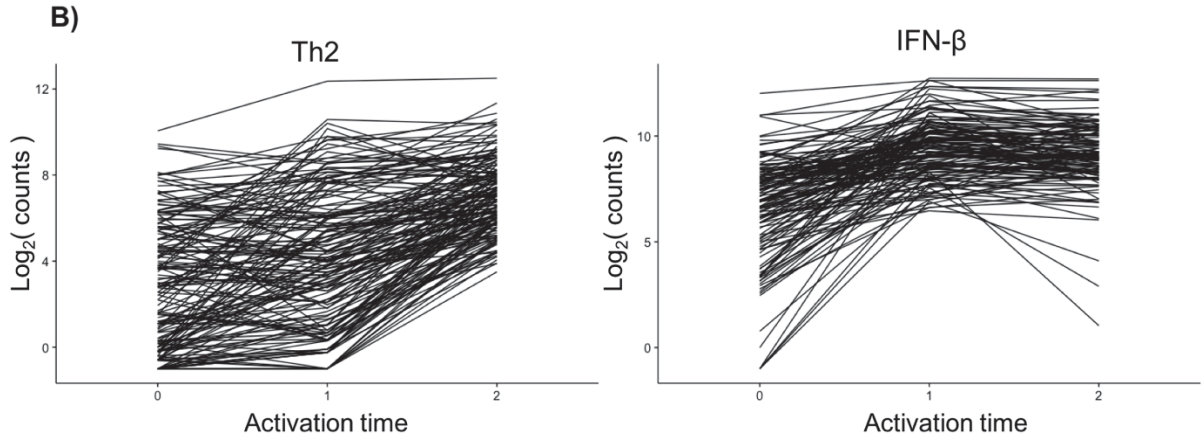


**Figure 4.9 Different transcriptional dynamics between different induced T cell statesB)** The time trajectory of each differentially expressed gene was plotted for Th2 cells and IFNβ stimulated cells. Regularised log2 (rlog) transformation was used.

Next, we functionally annotated the differentially expressed genes in each condition. First, we classified genes as upregulated or downregulated based on their $\log_2$ fold change. Using gProfileR (149), we annotated the genes in each group with GO terms for the cellular component (CC), molecular function (MF), and biological process (BP) categories (147). Next, we analysed which GO terms were overrepresented. We confirmed that the genes upregulated after 16 hours of IFN-β stimulation were enriched in interferon signalling pathways (**Figure 4.10**). Furthermore, their molecular function was mostly related to RNA binding. The genes driving this enrichment included interferon induced protein kinases and helicases, and 2'-5'-oligoadenylate synthetases (OAS). All of these terms characterise processes involved in the antiviral response (167, 168).

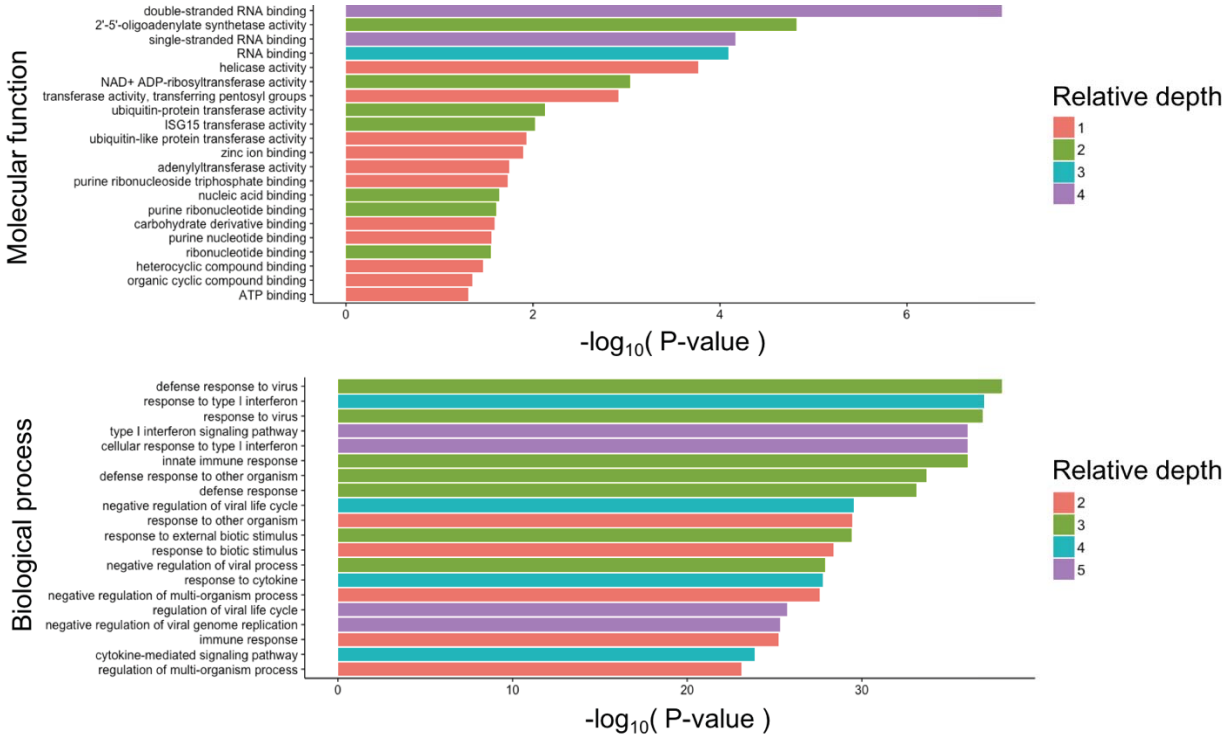


**Figure 4.10 Polarisation of CD4$^+$ T cells with IFNβ activates the antiviral response** The differentially upregulated genes upon polarisation with IFN-β were used to perform a GO term overrepresentation analysis using gProfileR. Results were ordered by adjusted P-value, with different colours representing relative depths within the ontology.

To determine whether the genes which contributed to the enrichment corresponded to functional blocks at the protein level, we built a protein interaction network using 133 upregulated genes as an input for STRING (169). Only interactions from experimental, co-expression and neighbourhood data were kept in the network. We observed a block of tightly interconnected proteins composed of genes from the OAS, and MX families (**Figure 4.11**).

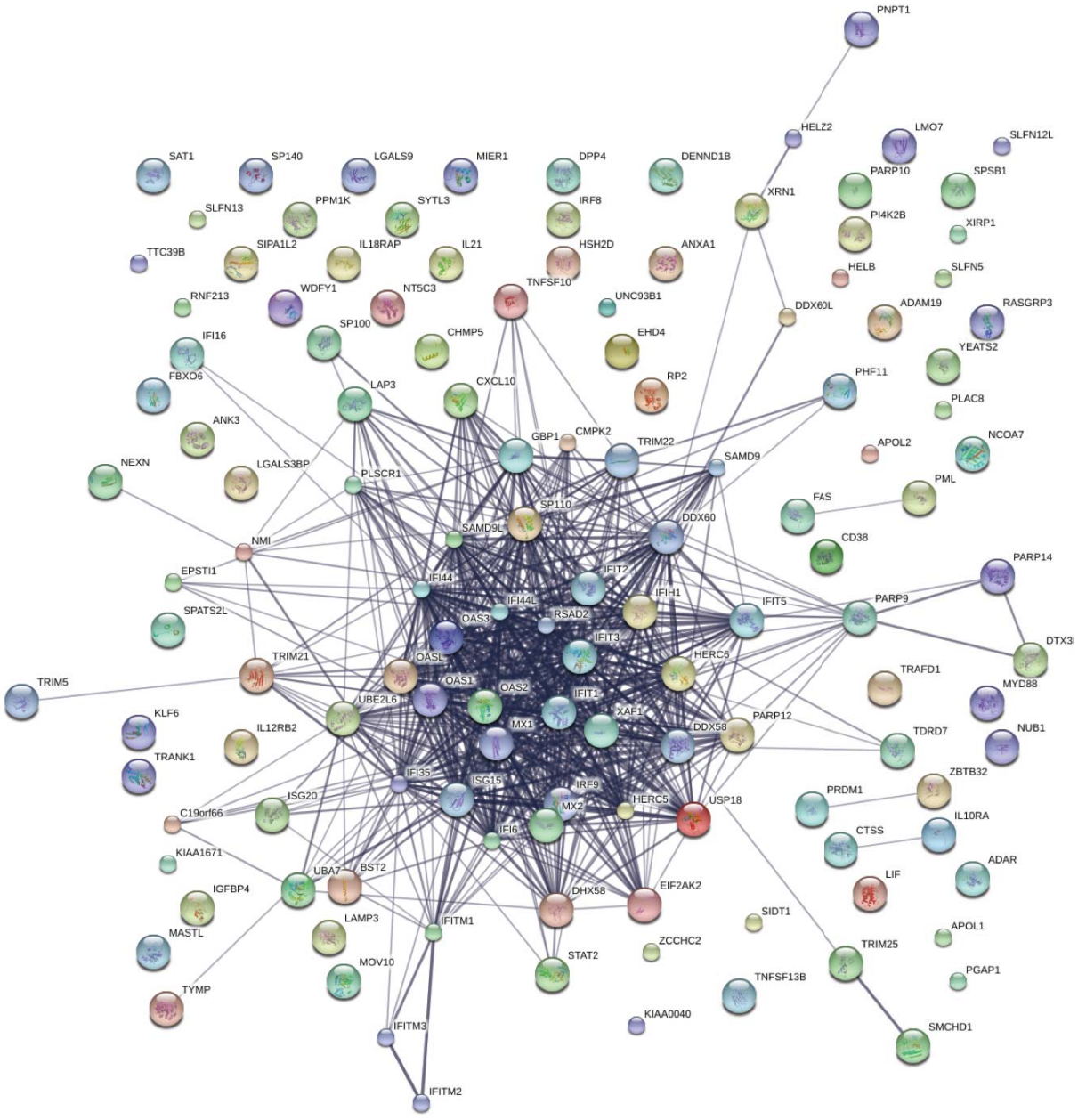


**Figure 4.11 Protein network in CD4$^+$ T cells polarised with IFNβ** Genes driving the enrichment in GO terms for antiviral response upon IFNβ stimulation were used to build STRING network. Connections represent protein interactions and co-expression expression. The width of each line is proportional to the strength of evidence for the interaction.

Then, we performed the same analysis for genes differentially upregulated in $CD4^+$ T cells. We used the results from T cell polarisation states at five days and observed that the genes upregulated in Th1 cells were enriched in signalling and response to cytokines (**Figure 4.12**). Specifically, Th1 cells upregulated the receptors for IFN-γ, IL-1, IL-18, and IL-33, as well as integrins and laminins. When analysing the 192 differentially upregulated genes in iTreg cells, we also observed enrichment in signalling and cell communication pathways (**Figure 4.13**). Here, the most represented molecular functions were chemokine receptors (CCRs), cytokine receptors and ion channels. Furthermore, we found that the genes upregulated in Th17 cells localised to integrin complexes and had membrane receptor or signal transducer activity. However, the upregulation of genes in Th2 cells seemed to be unspecific, with few GO terms showing only nominally significant P-values.

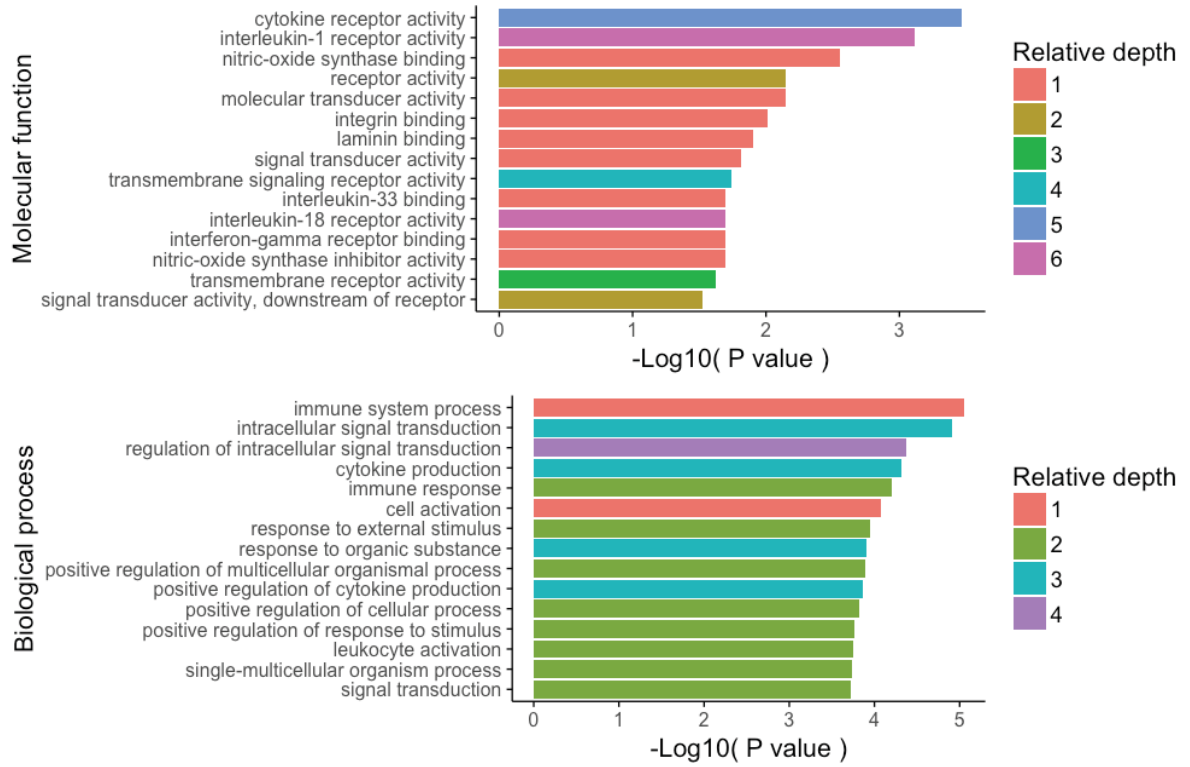


**Figure 4.12 Genes involved in IFN and IL1 signalling are upregulated in Th1 cells** Genes differentially upregulated upon polarisation to the Th1 lineage were used to perform a GO term overrepresentation analysis in gProfileR. The results were ordered by their adjusted P value, with different colours representing relative depths within the ontology. X axis represents the significance of the enrichment of molecular function and biological processes terms.

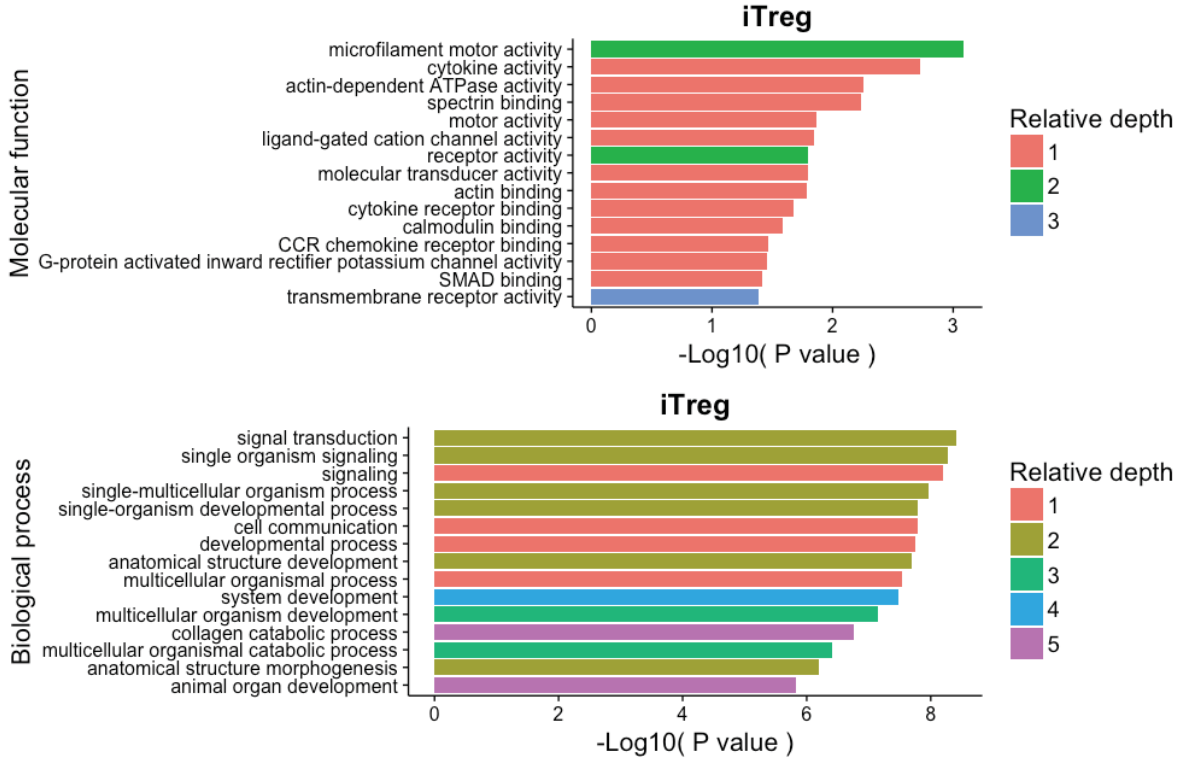


**Figure 4.13 Genes upregulated by iTreg cells are enriched in chemokine and cytokine receptors** Genes differentially upregulated upon polarisation to the iTreg lineage were used to perform a GO term overrepresentation analysis in gProfileR. The results were ordered by their adjusted P-values, with different colors representing relative depths within the ontology. Enrichment in molecular function and biological process terms in shown.

Next, we repeated the previous analysis for genes downregulated in $CD4^+$ T cells at five days. In Th1 cells we detected only 10 downregulated genes, therefore, we excluded this condition from the analysis. We observed that the 199 genes downregulated in Th2 cells were highly enriched in response to viruses, type I interferons (enrichment in the IFN response reactome pathway was also significant), and cytokines, with adjusted P values smaller than $1 \times 10^{-20}$ (**Figure 4.14**). We also observed significant enrichment of IL-1 production pathways. The molecular function of these genes was annotated to families such as OAS, RNA-binding proteins and signal transducer terms.

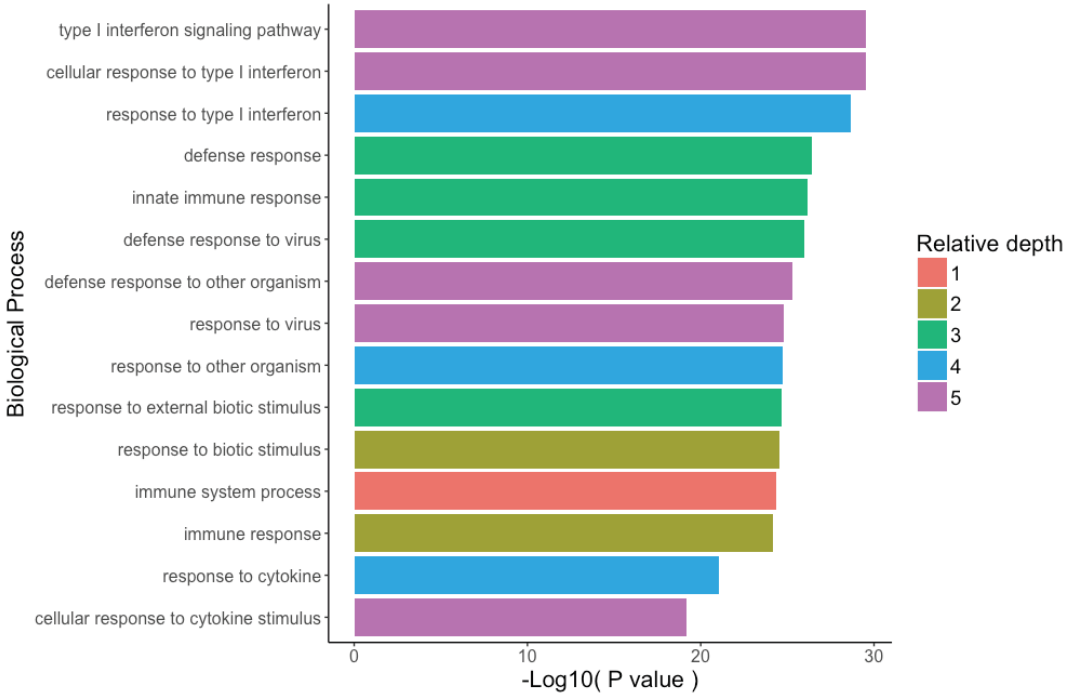


**Figure 4.14 Genes involved in IFN signalling are downregulated in Th2 cells** Genes differentially downregulated upon polarisation to the Th2 lineage were used to perform a GO term overrepresentation analysis in gProfileR. Results were ordered by their adjusted P-values, with different colours representing relative depths within the ontology.

Lastly, we analysed the downregulated genes in Th17 and iTreg cells. Th17 cells seemed to downregulate cell surface components such as integral membrane proteins. Interestingly, some of these genes localised specifically to phosphatidylinositol-3-kinase (PI3K) complexes. Furthermore, we also observed an enrichment in tyrosine kinase and PI3K activity (**Figure 4.15A**) and obtained similar results in iTreg cells (**4.15B**). Consequently, it is possible that downregulation of the PI3K pathway plays a role in Th17 and iTreg differentiation.

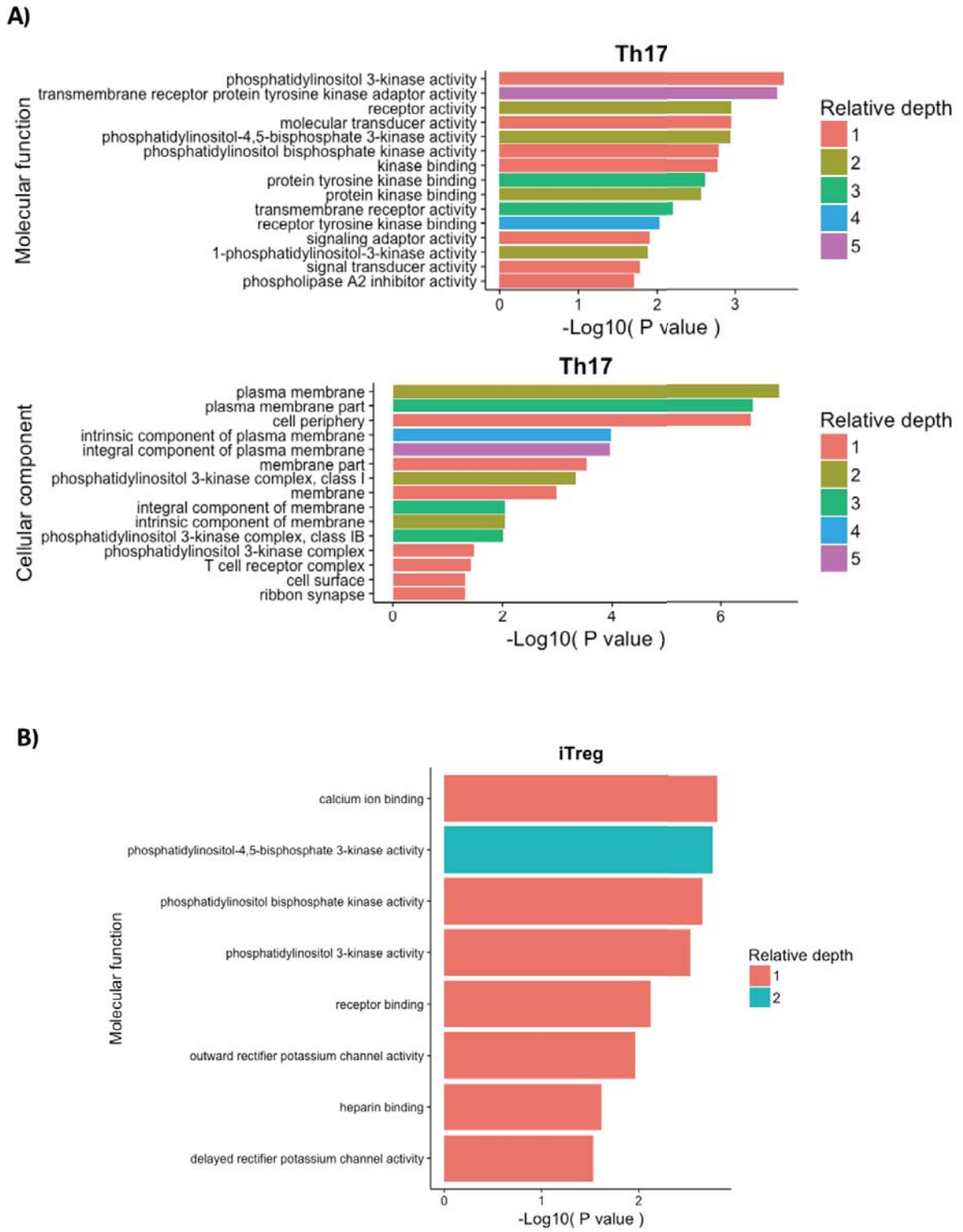


**Figure 4.15 Genes of the PI3K pathway are downregulated in Th17 and iTreg cells** Genes differentially upregulated upon polarisation to the Th17 and iTreg lineages were used to perform a GO term overrepresentation analysis in gProfileR. The results are ordered by adjusted P-values, with different colours representing relative depths within the ontology. **A)** Cellular component and molecular function term enrichment in Th17 cells. **B)** Molecular function term enrichment in iTreg cells.

## 4.6 Identification of potential lineage specific surface markers

Specific surface markers are necessary to study the role of cytokine induced polarisation *in vivo*. To address this issue, we tried to identify potential markers to isolate $CD4^+$ T cell subsets from the blood. We performed GO term overrepresentation analysis on the differentially upregulated genes which appeared only in one T cell state, but not in the others. Next, we examined the expression levels of the genes enriched in cell membrane categories. We identified five membrane receptors upregulated in Th2 cells: CD86, FZD3, ADGRA3, and the receptors for TGFβ and IL17 (TGFBR3 and L17RB) (**Figure 4.16**). We also observed TLR1 was differentially upregulated by Th1 cells (**Figure 4.17A**). Furthermore, four membrane receptors were upregulated only by Th17 cells: Lyn, TLR2, IL13RA, and integrin-β4 (IGB4) (**Figure 4.17B**). Finally, we identified three surface genes only present in iTregs: CD82, CD83, and CD101 (**Figure 4.17C**).

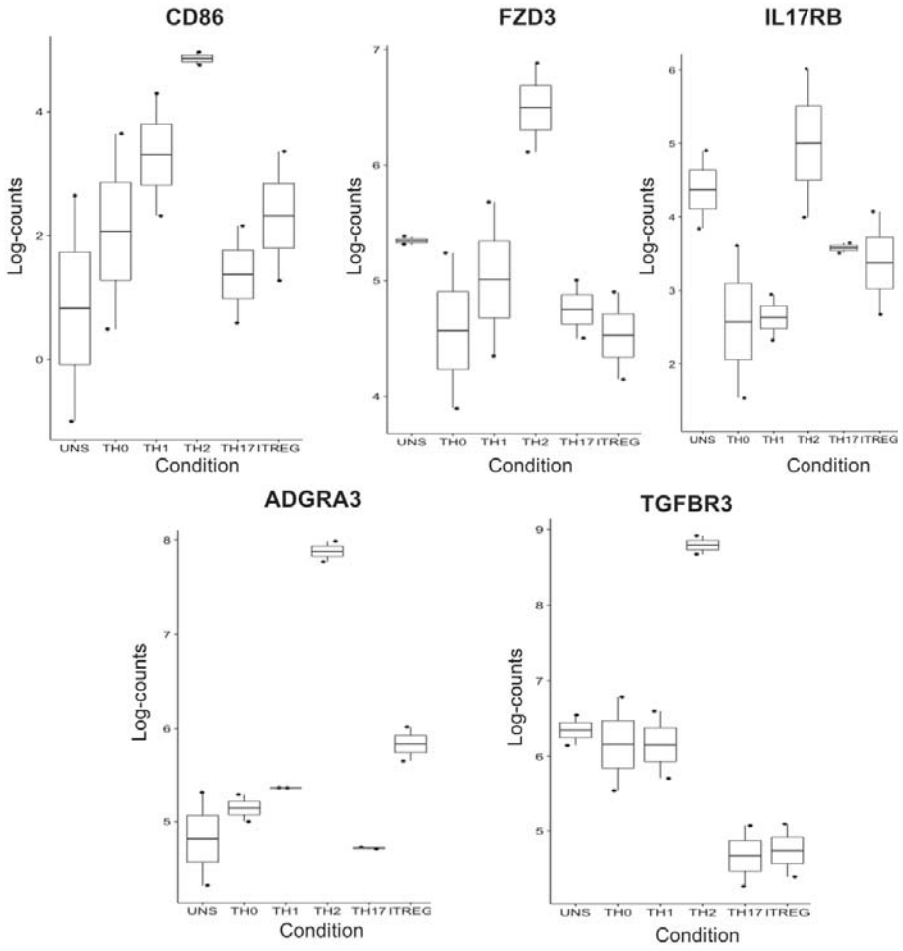


**Figure 4.16 Differential expression analysis identifies potential surface markers for Th2 cells** Upregulated gene specific to Th2 cells were used to perform a GO term overrepresentation analysis in gProfileR. The regularised log2 (rlog) counts for genes in cellular component category “membrane receptors” were inspected using bar plots.

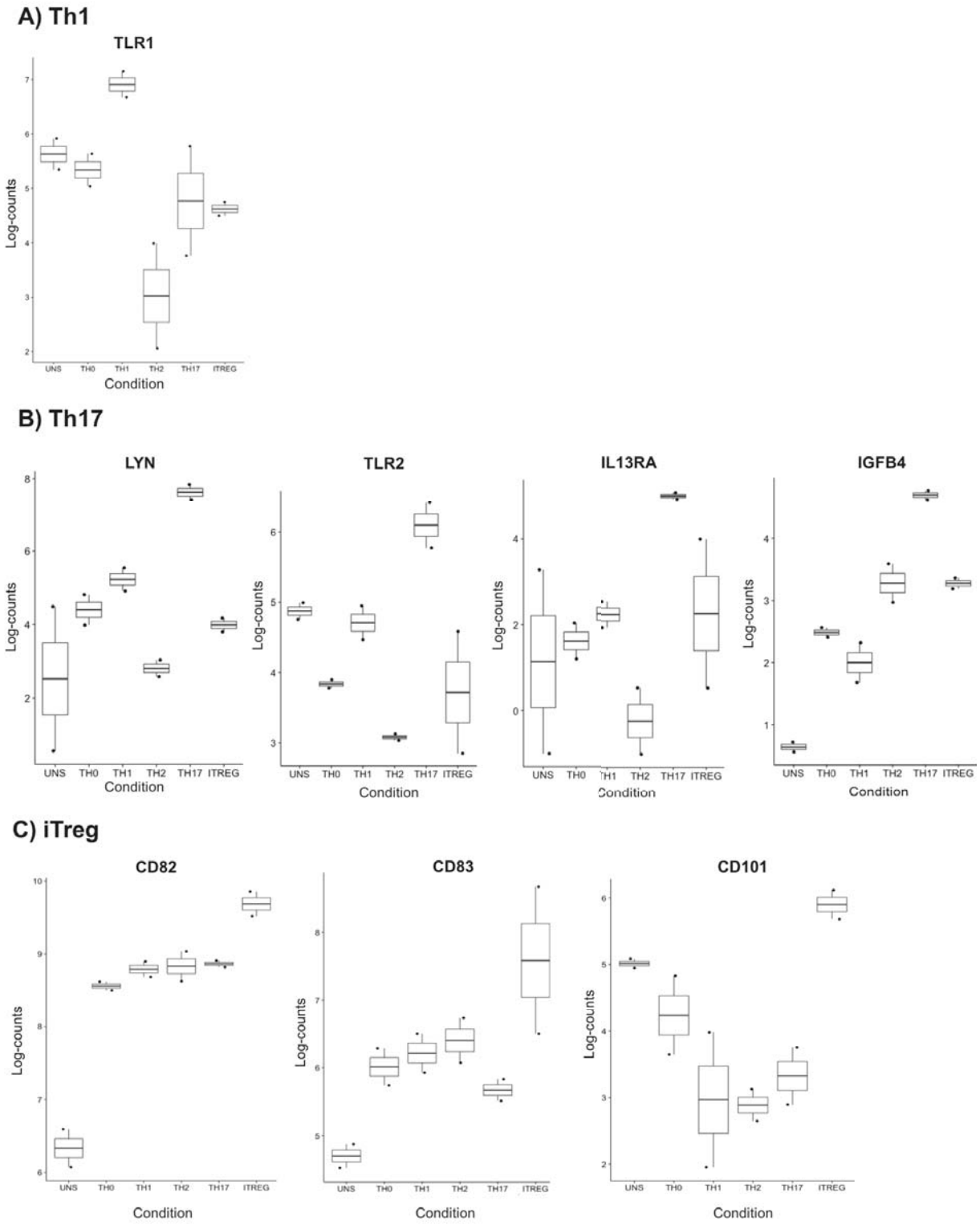


**Figure 4.17 Differential expression analysis identifies potential surface markers for Th1, Th17 and iTreg cells** Upregulated genes specific to each T cell subset were used to perform a GO term overrepresentation analysis in gProfileR. The regularised log2 (rlog) counts of genes in the cellular component category “membrane receptors” were inspected using bar plots. **A)** Th1, **B)** Th17, and **C)** iTreg cells.

## 4.7 Gene co-expression network analysis

We asked whether functional gene blocks were associated to specific transcriptional regulation mechanisms. For this, we performed a co-expression network analysis using the RNA counts from $CD4^+$ T cells stimulated for five days. At first, we focused on the type I interferon signalling pathway, which was downregulated in Th2 differentiation. We selected the interferon induced protein 35 (IFI35) gene, since it was present repeatedly in all the enriched GO terms related to IFN signalling. We calculated IFI35's co-expression network and annotated the genes in the network using the TRANSFAC tool for TF binding prediction (149, 170) Finally, we performed an overrepresentation analysis for TFBSs. We observed a significant enrichment in binding sites for the interferon response factors IRF9 (ISGF3), IRF8 (ICSBP), IRF1 and IRF7 (**Figure 4.18A**). This suggested that IRFs could be downregulated in Th2 cells, subsequently not binding to its targets and suppressing the IFN response. We confirmed that IRF8 and IRF9 expression was lower in Th2 cells than in other conditions (**Figure 4.18B**).

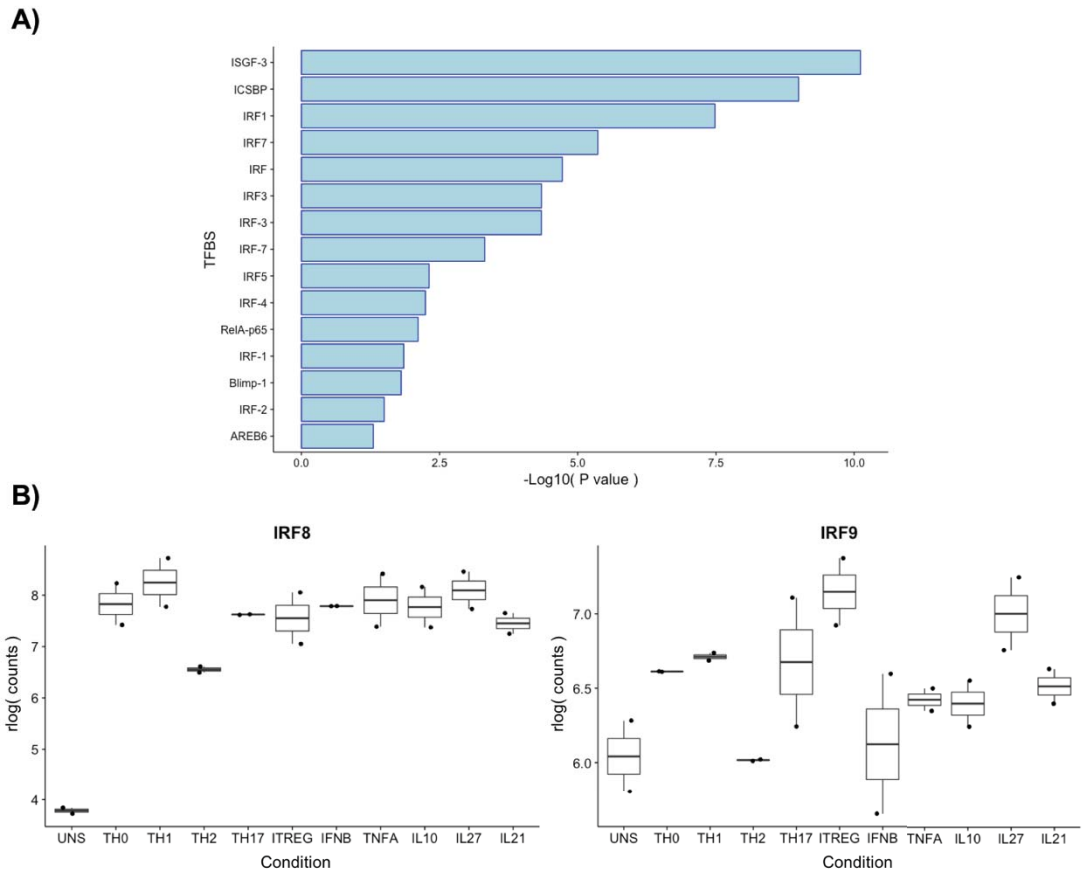


**Figure 4.18 Downregulation of IRFs may suppress type I interferon responses in Th2 cells** The gene IFI35 was used to build a co-expression network based on gene wise Pearson correlations. The members of this network were later used in a TFBS overrepresentation analysis with TRANSFAC in gProfileR. **A)** Enriched TFBS ordered by the adjusted P-values. **B)** Regularised log2 (rlog) RNA counts for IRF8 and IRF9.

Next, we applied the same approach to study the PI3K pathway, downregulated in Th17 and iTreg cells. To do so, PI3KR1 was used to build a co-expression network, since it was present in all the enriched terms related to PI3K activity. We evaluated the genes in this network using TRANSFAC and found a significant enrichment in TFBS for Sox4 and Msx2 (**Figure 4.19**).

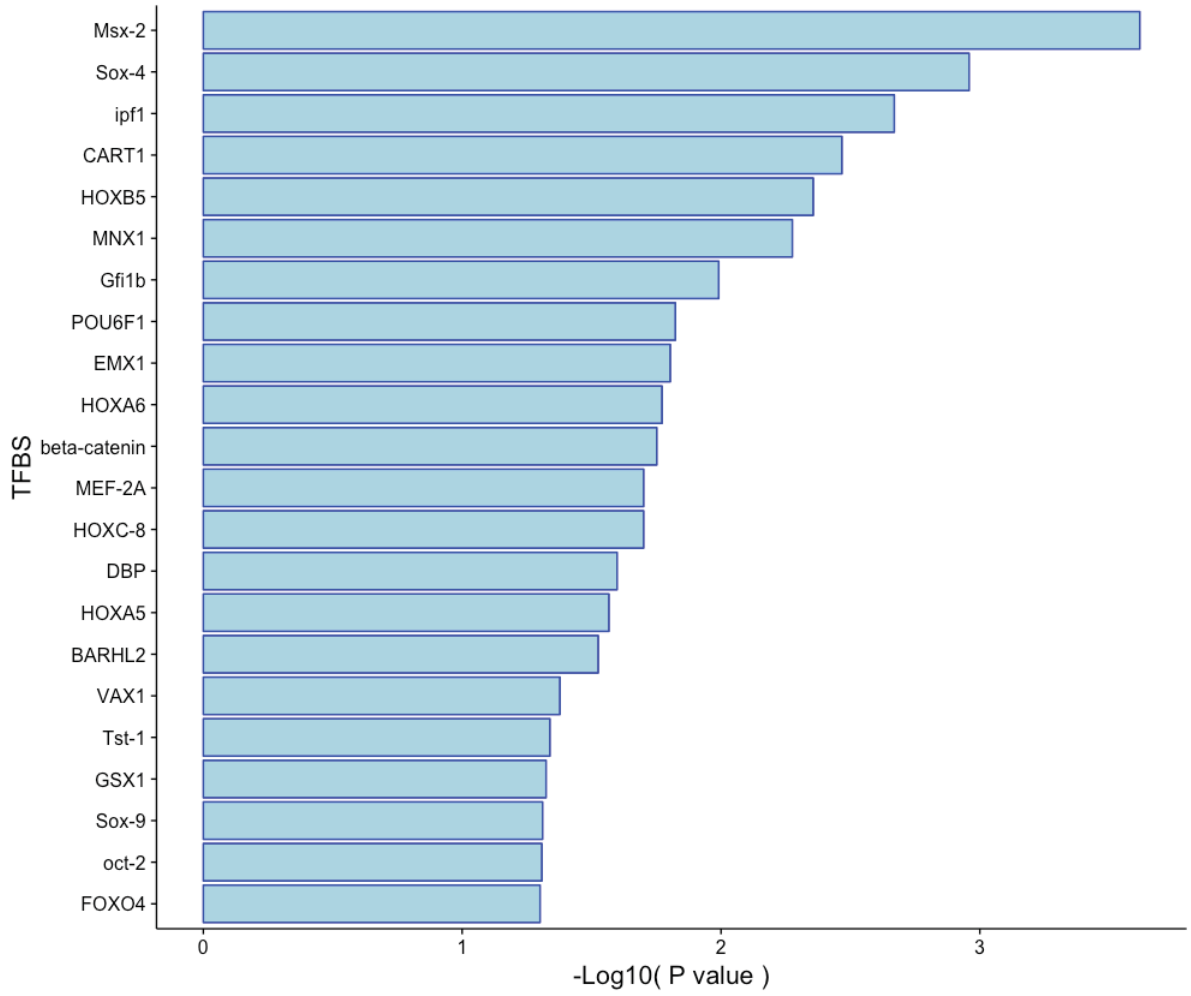


**Figure 4.19 Downregulated genes in Th17 and iTreg cells are enriched in binding sites for Msx-2 and Sox-4** The gene PI3KR1 was used to build a co-expression network based on gene-wise Pearson correlations. The members of this network were later used to perform a TFBS overrepresentation analysis with TRANSFAC in gProfileR. The genes were ordered by the adjusted P-values.

## 4.8 Differential gene expression analysis in polarised macrophages

We were interested in functionally characterising the response of macrophages to cytokines. Consequently, we performed differential expression analysis to compare the different conditions with unstimulated macrophages. Approximately 690 genes were differentially expressed in M1 macrophages, and 500 in macrophages polarised with TNF-α. Moreover, we observed more than 200 differentially expressed genes in both M2 and IL-26 polarisation. On the contrary, stimulation with IL-23 caused no observable changes (**Figure 4.20A**). Detailed information concerning differential expression analysis of these conditions, such as fold changes, P-values and mean gene counts, is presented in the end of this thesis (**Appendix**).

Next, we asked whether transcriptional responses to cytokines were condition specific. We intersected the lists of differentially expressed genes of each condition and observed genes which seemed to only be present upon M1, M2, and TNF-α induced polarisation (**Figure 4.20B**). On the contrary, more than 50% of the genes upregulated in the IL-26 condition were shared with TNF-α (**Figure 4.20B**). We concluded that macrophages acquired different functions in response to different cytokines, and hypothesised that IL-26 activated similar pathways than TNF-α.

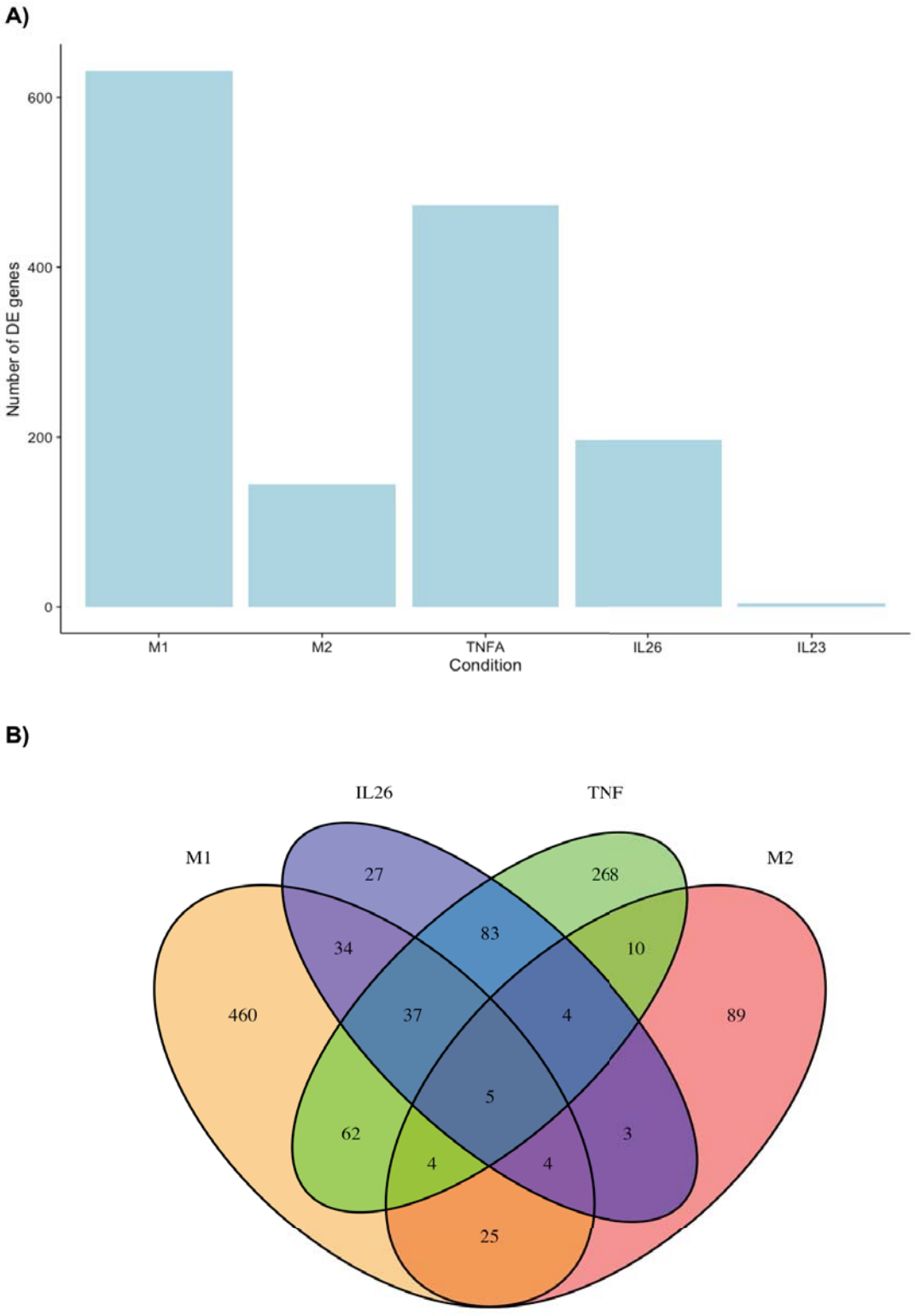


**Figure 4.20** Number of differentially expressed genes upon cytokine induced macrophage polarisation Differentially expressed genes were defined by comparing macrophages polarised with cytokines to unstimulated macrophages. Genes with an adjusted P value ≤ 0.05 and an absolute $\log_2$ fold change ≥ 1 were considered differentially expressed. **A)** The numbers of differentially expressed genes after six hours were plotted. **B)** Overlap of differentially expressed genes across macrophage polarisation states at six hours.

To verify this, we performed GO term annotation followed by overrepresentation analysis in TNF-α and IL-26 stimulated macrophages. Both conditions were enriched in binding sites for NFκB (**Figure 4.21**). However, some of the molecular functions enriched in TNF-α were not present in IL-26 polarisation. For example, activation of the death domain and the PI3K pathway (**Figure 4.22**). We concluded that macrophage responses to TNF and IL-26 share a common regulation involving NFκB, but that TNF generated a broader response.

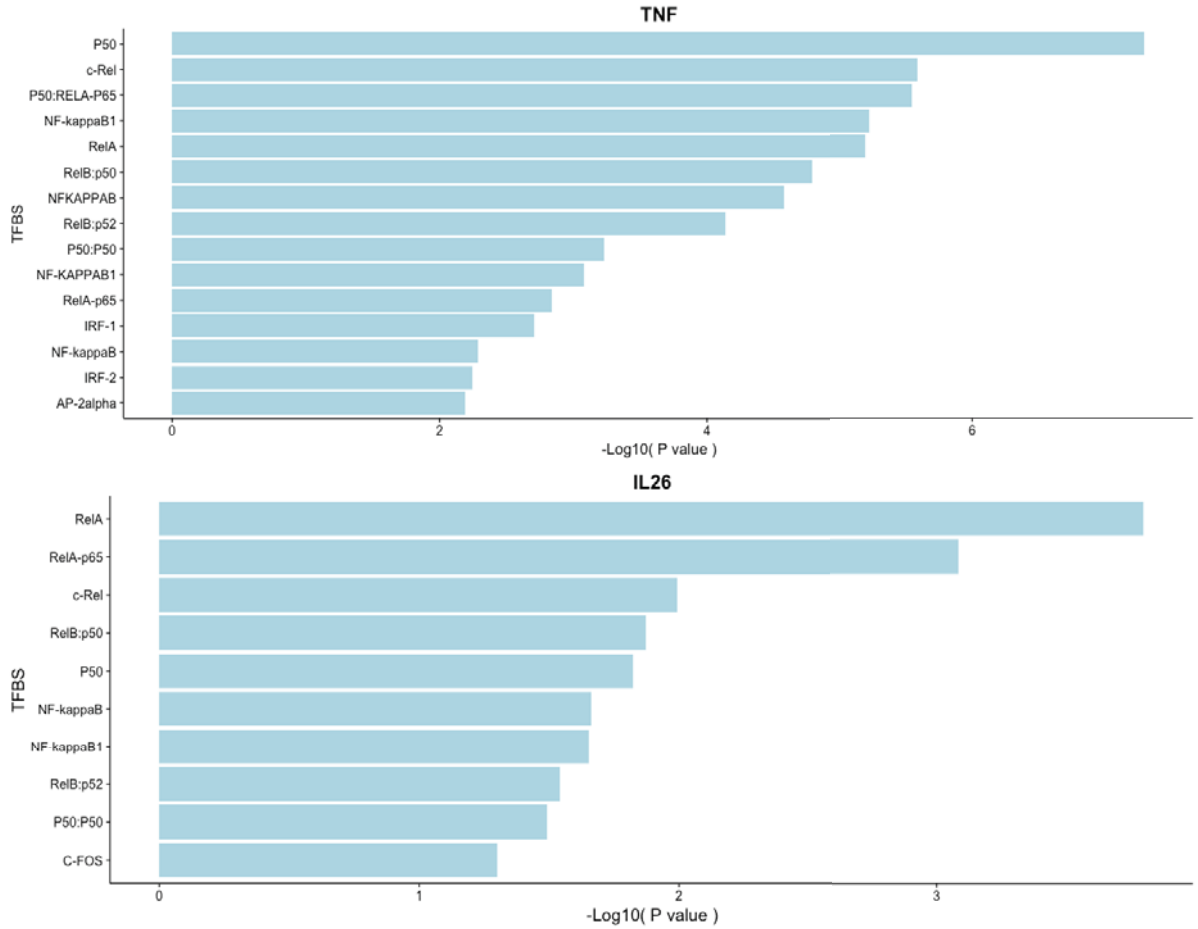


**Figure 4.21 The responses to TNF and IL26 in macrophages are regulated by NFκB** Genes differentially upon macrophage polarisation with TNF-α and IL26 were used to perform a TFBS overrepresentation analysis in gProfileR and TRANSFAC. Results were ordered by adjusted P-values.

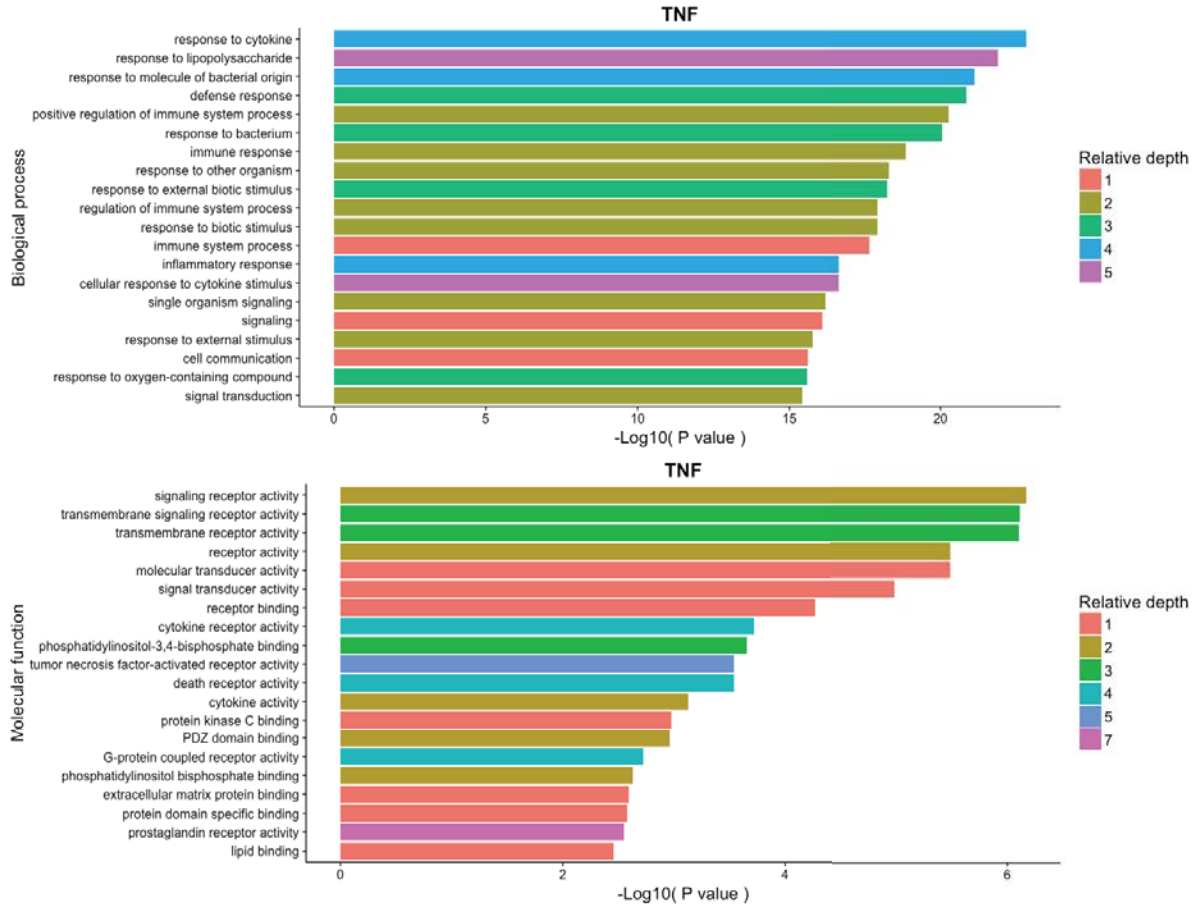


**Figure 4.22 Macrophages upregulate proinflammatory in response to TNF-α** Genes differentially upregulated upon macrophage polarisation with TNF-α were used to perform a GO term overrepresentation analysis in gProfileR. The results were ordered by adjusted P-values, with colours representing different depths within the ontology.

Finally, we characterised the effects of IFN-γ (M1) and IL-4 (M2) on the transcriptome of macrophages using GO term overrepresentation analysis. We found that genes upregulated in M1 macrophages were enriched in functions such as synthesis of OAS, ribonucleotide binding, cysteine peptidases, and other antiviral response pathways. (**Figure 4.23**). Consequently, we confirmed that macrophage polarisation with IFN-γ generated a proinflammatory phenotype tailored to respond against viral infections. On the other hand, half of the genes differentially expressed in M2 macrophages were downregulated. These genes were enriched in cytokine production pathways (**Figure 4.24**). Specifically, we found significant downregulation of IL-6 and IL-1β synthesis. Furthermore, we observed that genes upregulated in M1 macrophages are enriched in TFBS for STAT1, while those upregulated in M2 macrophages are enriched in TFBS for STAT6 (**Figure 4.25**). We concluded that M2 macrophages do not display an inflammatory phenotype, in contrast to their M1 counterpart, and that each polarisation acts via a different STAT.

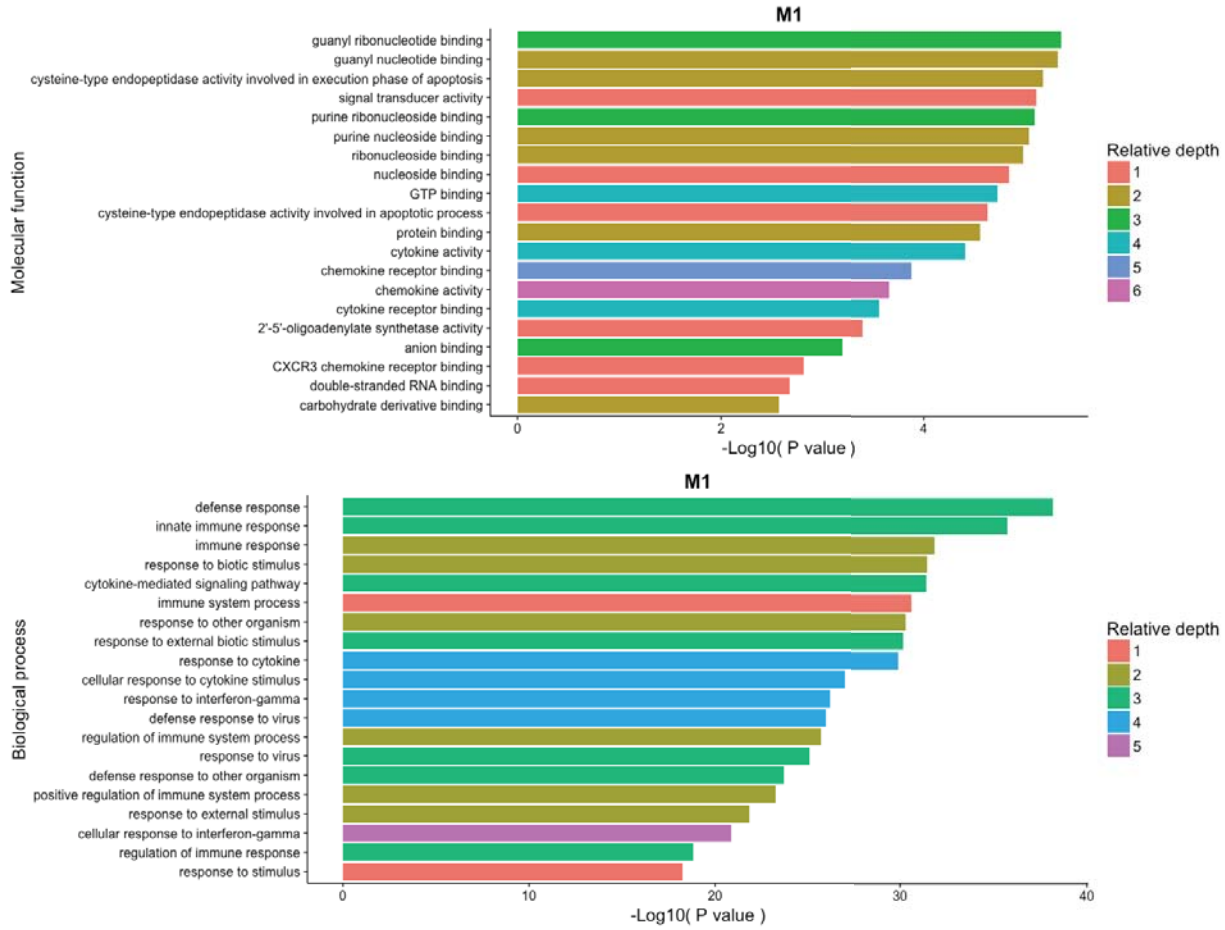


**Figure 4.23 Macrophages activate the antiviral response upon M1 differentiation** Genes differentially upregulated upon macrophage polarisation with IFN-γ were used to perform a GO term overrepresentation analysis in gProfileR. Results were ordered by adjusted P-values, with colours representing different depths within the ontology.

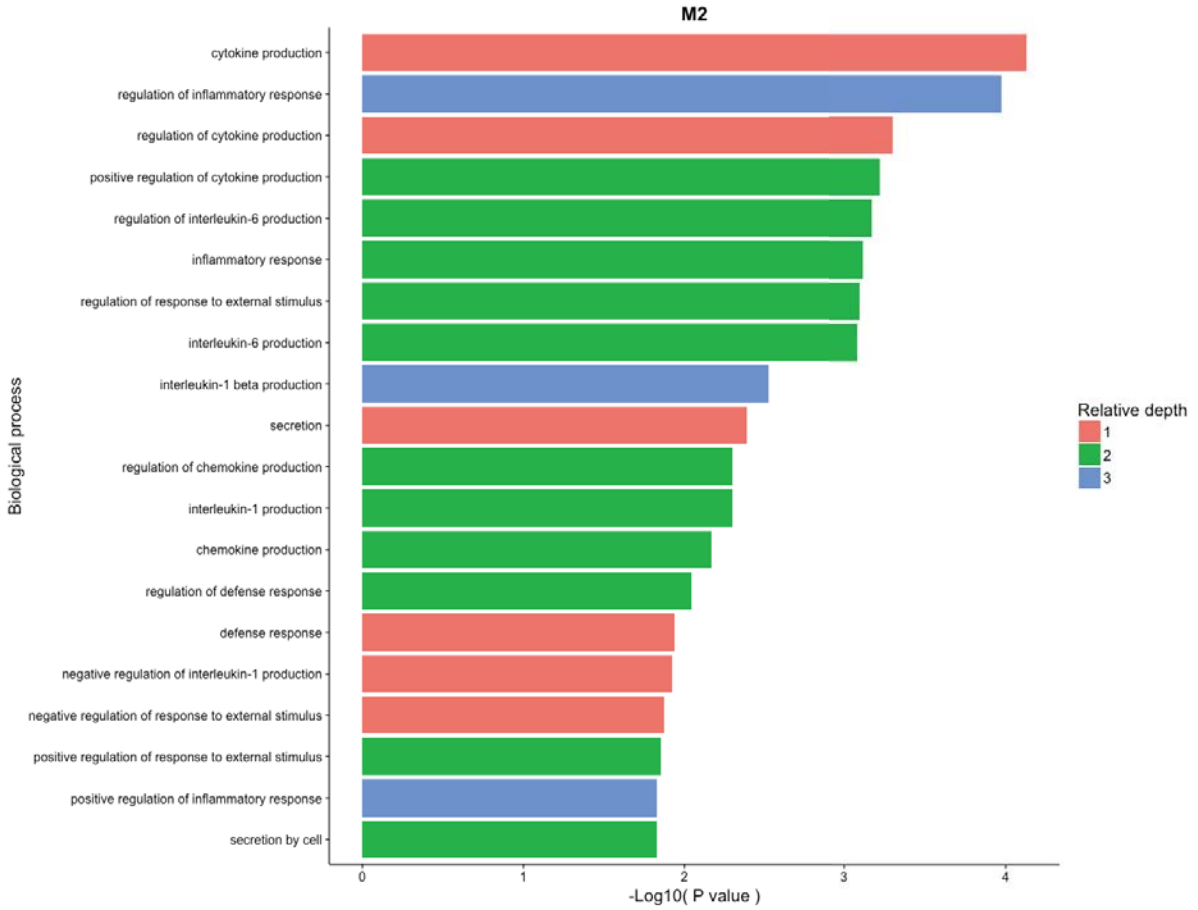


**Figure 4.24 Macrophages downregulate the production of IL6 and IL1β upon M2 differentiation** Genes differentially downregulated upon macrophage polarisation with IL-4 were used to perform a GO term overrepresentation analysis in gProfileR. Results were ordered by adjusted P value, with colours representing different depths within the ontology.

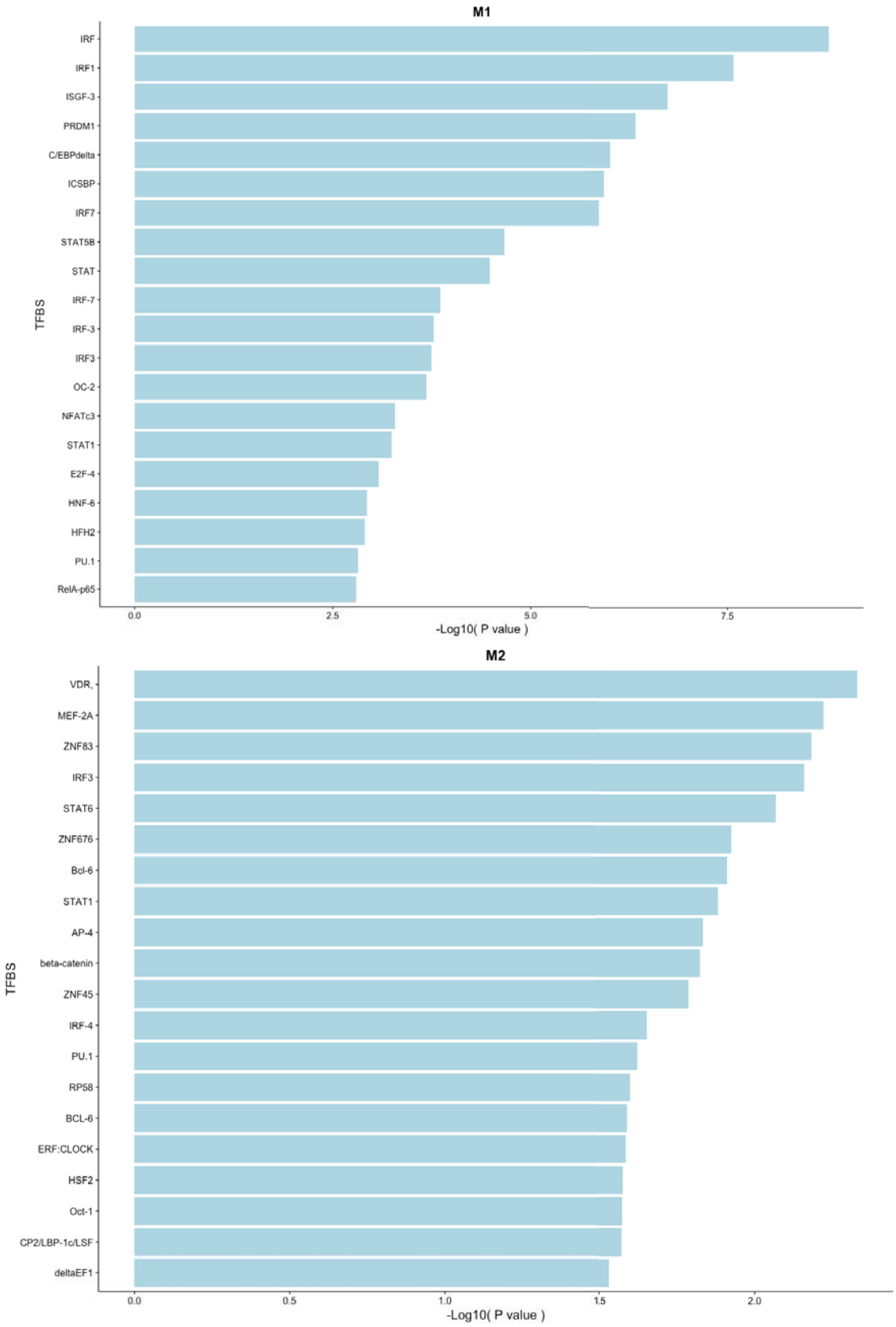


**Figure 4.25 M1 and M2 macrophages activate signalling via STAT1 and STAT6** Genes differentially upregulated in M1 and M2 macrophages were used to perform a TFBS overrepresentation in TRANSFAC. Results were ordered by P-values.

## 4.9 Analysis of protein expression in stimulated CD4$^+$ T cells

Next, we asked if the results from RNA-seq of CD4$^+$ T cells could be reproduced at the protein level. We isolated the whole proteome of unstimulated CD4$^+$ T cells, Th0 cells and Th1 cells, and performed LC-MS/MS for protein identification and quantification. In order to assess the reproducibility of the technique, we conducted the experiment using two technical replicates of each condition. When comparing the raw counts from both technical replicates, we obtained a correlation coefficient of 0.99 across all conditions (**Figure 4.26**). Thus, we concluded that LC-MS/MS with isobaric tagging is a highly reproducible technique for protein quantification. Next, we performed data normalisation and PCA. We saw a clear separation by polarising condition, with the technical replicates clustering tightly together (**Figure 4.26**). PC1 separated the unstimulated samples from the remaining conditions and accounted for 71% of the observed variance. Conversely, PC2 explained separated Th0 and Th1 cells and explained 15% of the variance. We concluded that the technique was suitable for evaluating protein expression in CD4$^+$ T cells.

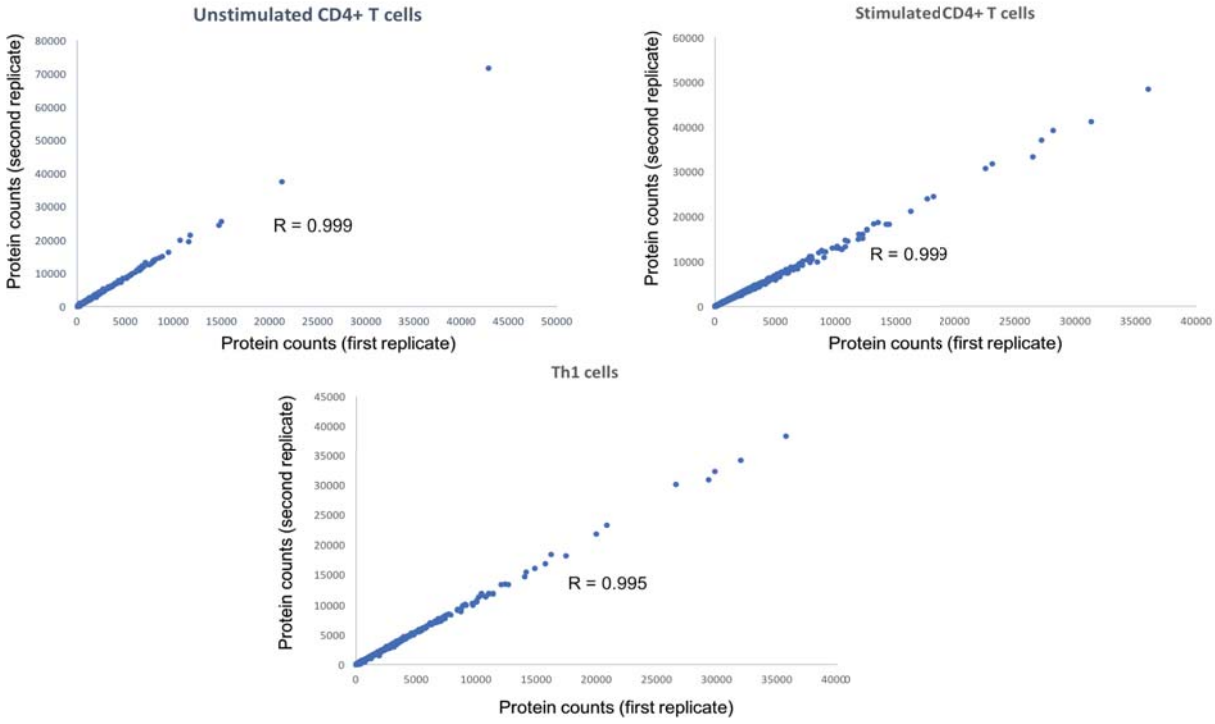


**Figure 4.26 LC-MS/MS reproducibly quantifies protein expression in CD4$^+$ T cells** Proteins from unstimulated CD4$^+$ T cells, stimulated CD4$^+$ T cells and Th1 cells were quantified with TMT-labelling and LC-MS/MS. The results from two technical replicates were compared using scatter plots. The Pearson correlation coefficient of both replicates is shown in each plot.

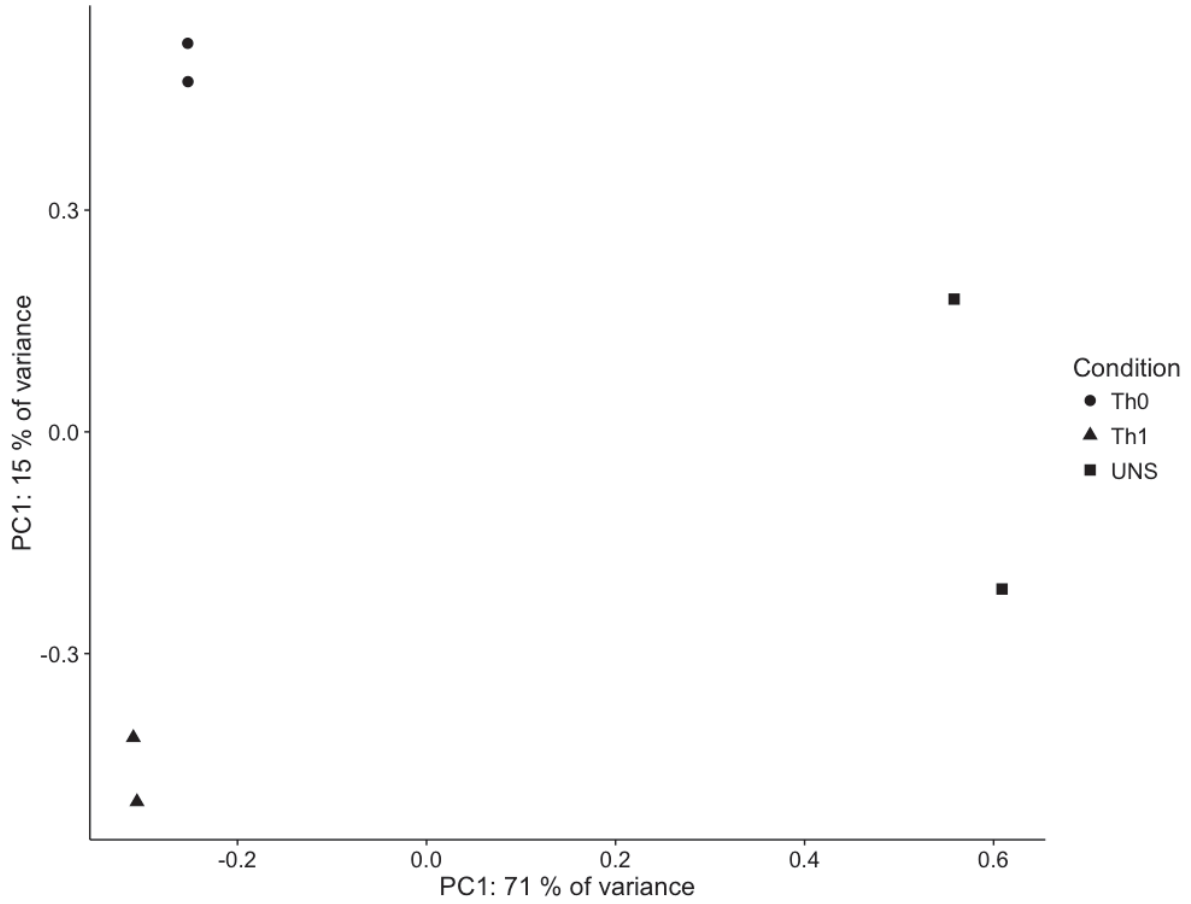


**Figure 4.27 PCA separates stimulatory conditions in LC-MS/MS data** Protein counts were normalized to the sample median and used to perform PCA. Different shapes represent different polarising conditions.

To quantify the similarity between RNA-seq and LC-MS/MS results, we computed the correlation of both data sets. To do this, we calculated the $\log_2$ fold changes between unstimulated cells and Th0 or Th1 cells at both the protein and RNA level. Next, we computed the sample wise Pearson correlation between both methods. We concluded that the changes in mRNA and protein levels were correlated (**Figure 4.27**), with Pearson coefficients close to 0.5. Through visual inspection, we identified genes with particularly high correlations between RNA-seq and LC-MS/MS (**Figure 4.27**). These genes were enriched in cell cycle functions. Based on these results, we concluded that RNA and protein changes in $CD4^+$ T cells were correlated and reproducible, and that both techniques could be used to study cytokine induced cell polarisation.

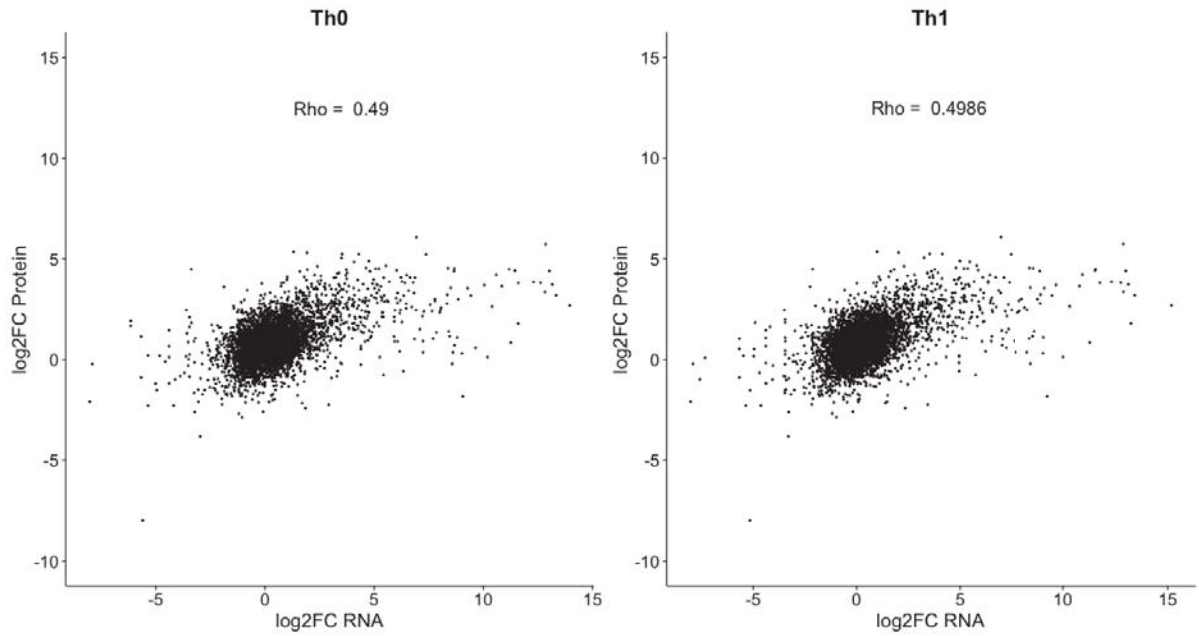


**Figure 4.28 RNA-seq and LC-MS/MS data are highly correlated** Log2 fold changes between Th0/Th1 and unstimulated $CD4^+$ T cells were calculated using LC-MS/MS and RNA-seq data. Next, a scatter plot of both data sets was built. The Pearson correlation coefficient between both methods is shown in each plot.

## 4.10 Discussion

In this chapter, I showed a characterisation of the transcriptional response to cytokines in human macrophages and T cells. This characterisation was performed using low coverage RNA-seq, an affordable approach to examine a large number of conditions (171). At first, I summarised the most important sequencing quality metrics. These results suggested that the RNA-seq run was not only performed adequately, but also generated reproducible data.

We acknowledged that a variety of power limitations might be present in this study. This is due to the fact that, to evaluate a large number of conditions with a limited budget, sequencing depth was kept at $5x10^6$ PE reads and the sample size was only two replicates. Since it is known that statistical power depends on the effect size, coverage and sample size (132-134), this raises potential issues. Hence, we modelled the power of the study to detect differences in genes with varying expression levels. We concluded that, if an average fold change of two is assumed, we might be powered to confidently detect differential expression in genes with raw counts higher than 50. Since the average count of genes in this study is 52, we concluded that our power is close to 0.8. Despite the small sample size, we achieve a relatively high power. This might be explained by the statistical model implemented in

DESeq2, specifically tailored for low sample size (135) and shown to achieve the highest power under these circumstances (132). Since our starting material are cells belonging to the same cell type and kept in cell culture, a tightly controlled environment, the coefficient of variation is also relatively low, which might contribute to the relatively high sensitivity (132). Nonetheless, there exist power limitations, particularly for lowly expressed genes. These should be acknowledged when evaluating aspects as condition specific gene expression or conditions with no observable differences. Each conclusion will be dependent on the mean expression level of the genes in question, which can be accessed via the Appendix to this thesis.

Having investigated our power limitations, we analysed differential gene expression. Initial inspection of the data revealed several combinations of cytokines and time points which seemed to show no effect. For example, we observed no differential gene expression after 16 hours of $CD4^+$ T cell polarisation to Th1, Th17 and iTreg. However, we did find large differences compared to Th0 after five days of stimulation. This suggests that Th1 and Th17 differentiation occurs in the later stages of the immune response. However, since some of the effect sizes observed at these early time points might be relatively small, this must be verified in a more powered study, with more biological replicates and a larger sequencing depth. On the other hand, we observed Th2 differentiation in early stages of activation, and it persisted during the course of five days. The opposite is true for IFN-β, which induced major effects in T cells at 16 hours but almost no effect after five days. Macrophages also showed prominent transcriptional responses to IFN-γ, IL-4, TNF-α, and IL-26 after six hours. On the other hand, polarisation of $CD4^+$ T cells with TNF-α, IL-10, IL-21 and IL-27, and polarisation of macrophages with IL-23 revealed no changes at any time point, but it remains unclear whether this is biologically true or a consequence of the low power of this study: we cannot completely rule out an effect of these cytokines given the small sample size and low coverage. For the purpose of the following discussions I only consider conditions which showed differential gene expression.

The response of $CD4^+$ T cells to IFN-β was strikingly different to that to other cytokines. Consequently, we hypothesised that transcriptional changes upon IFN-β stimulation were transitional, while polarisation to other cell subsets was stable. However, this observation should be confirmed by examining more time points following T cell activation. An analysis of genes upregulated upon stimulation with IFN-β revealed that most of these genes act at an early time point. This is expected, as type I interferons are involved in the cellular response to viruses (172), which must be triggered immediately upon infection in order to prevent exponential reproduction of the pathogen. Our functional enrichment analysis also supported

this explanation. It revealed a network of tightly connected genes composed of oligoadenylate synthetases (OAS), involved in the activation of RNAse L, and IRFs (167, 173). The difference between transcriptional dynamics in Th2 (the Th subset with the largest number of differentially expressed genes) and IFN-β could be explained by the differentiation model to lineages proposed in the literature in which initial activation of a master regulator TF induces expression of signature cytokines. These cytokines then induce the expression of the regulator TF in a self-sustaining positive feedback loop (25, 62, 174-176).

When analysing known T cell polarisation states, we observed that the cells obtained agreed with their descriptions in the literature. For example, Th1 and Th2 cells were originally described as $CD4^+$ T cells with distinct, mutually exclusive cytokine secretion profiles (14, 177). These observations have been extensively reproduced, with Th1 cells secreting IL-12 and IFN-γ, and Th2 cells producing IL-4, IL-10 and IL-13. These phenotypes are induced by the activation of the TFs T-bet and GATA-3, respectively (35, 36). All of these observations are reproduced in our data set. We observe a higher level of IFN-γ and T-bet mRNA in Th1 cells, and higher IL-4 and GATA3 transcription in Th2. The same is true for Th17 cells, which in our study express higher levels of IL17F and RORC at the mRNA level, as has been described elsewhere (25, 27, 37, 178). Furthermore, Treg cells are known to express the master regulator TF FoxP3 (179), which was also observed in our RNA-seq study of iTreg differentiation. It is worth noting that, in contrast to the common conception derived from mouse models that $CD4^+$ regulatory T cell function is dependent on IL10 and TGF-β (180-182), we only found slight upregulation of the IL-10 and unaltered expression of TGF-β. This, however, cannot be ruled out given our sample size and has to be verified in a study with larger power. Conversely, we saw upregulation of CTLA-4, which has been proposed as a key mechanism of Treg mediated immune regulation (182-185).

Macrophages polarised to the M1 phenotype are known to upregulate IL-12 and COX-1, while M2 macrophages express mannose receptors and COX-2 (83, 94, 95). We also recapitulated these findings. Taken together, our observations suggest that cytokine polarisation with this experimental approach is effective for both $CD4^+$ T cells and macrophages.

Next, we compared polarised $CD4^+$ T cells upon five days of stimulation against Th0 cells. We found only 45 differentially expressed genes between Th1 and Th0 cells, compared to over 250 in all other comparisons, which suggested that Th0 cells might polarise to a default functional state similar to Th1. This might be explained by the autocrine action of cytokines, since our cytometry data proved that TCR stimulation alone upregulates T-bet, which can

induce IFN-γ (35) and trigger a positive feedback loop (62). Furthermore, strong TCR stimulation could also explain this observation, since it is known that the strength and duration of TCR signalling can influence cell fate (33, 52, 186), with strong and prolonged TCR signalling generating Th1 cells (31). To disentangle the causes of this observation, we would need to perform another experiment using anti-IFN-γ antibodies to block the effects of autocrine cytokines.

When comparing the remaining lineages with Th0, we observed a combination of gene expression changes which appeared to be unique and non-overlapping for each condition. Given that the average power of our study is close to 80%, it is not possible to definitely state that these changes are condition specific. There is a possibility that these genes were indeed differentially expressed in other conditions to a smaller extent, and thus not identified by our statistical analysis. However, since the cytokine secretion profiles of Th1, Th2 and Th17 cells are known to be mutually exclusive (14, 16, 25, 187), we think that these observations might suggest the existence of transcriptional profiles specific to each condition. Next, we used the lists of differentially expressed genes only observed in each lineage and used them for surface marker discovery. This was motivated by the lack of markers for the isolation of specific $CD4^+$ T cell subsets *in vivo*, given that most of the surface receptors proposed in the literature have either not been sufficiently specific (54, 188), or been dependent on particular pathogenic stimuli (189). We identified a variety of potential markers, including TLR1 upregulated in Th1 cells, and TLR2 upregulated in Th17 cells. A comparatively large set of potential markers was obtained for Th2 cells, which included ADGRA3 and TGFBR3. Because marker discovery was solely based on RNA level and the study is not fully powered, further validation is needed. Our confidence on the specificity of each of these markers increases with their expression level, since we determined that the study is more powered to detect differential expression in highly expressed genes. In order to validate these markers, we would need to perform further experiments, using antibodies to stain the markers of interest and to purify populations enriched in them. Next, the cytokine secretion patterns of these populations would need to be characterised using Luminex or enzyme-linked immunosorbent assay (ELISA). We would expect, for example, cells enriched in markers identified here as Th2 specific to secrete IL-4, IL-10 and IL-13.

We also asked whether LC-MS/MS coupled with quantification by isobaric labelling is a reproducible technique for analysing protein expression in $CD4^+$ T cells. Our results indicated that this technique was not only highly reproducible, but also correlated well with the observations from RNA-seq in sample wise comparisons. These results suggested that

LC-MS/MS might be a powerful platform for surface marker discovery in $CD4^+$ T cells too, because it would allow unbiased screening of the cell's proteome. However, we would need to evaluate the efficiency of this technique for identifying membrane bound proteins.

Next, we focused on determining the functional context of differential gene upregulation and downregulation in each condition. We did this by gene ontology annotation followed by overrepresentation analysis of the GO terms. Some of the genes downregulated in Th2 cells were involved in the response to IFN-γ, the hallmark Th1 cytokine. Furthermore, the response to type I interferons was downregulated to an even larger extent. It is known that Th2 and Th17 differentiation are inhibited by both IFN-γ and IFN-α (25, 190). However, once differentiation has occurred Th17 cells are able to retain their phenotype even in the presence of IFN-α (25), while the Th2 phenotype can be reversed (190). Thus, these results point to the activity of IFNα/β signalling being a crucial, tightly regulated determinant of Th1/Th2 responses. When using co-expression network analysis to study the type I IFN enriched pathways, it became clear that most of the genes have binding sites for IRFs, specially IRF9 and IRF8. IRF9 is necessary for the response to IFN-α, IFN-β, and also IFN-γ (173, 191). On the other hand, IRF8 is specifically induced by IFN-γ, but not by type I interferons, and it interacts with PU.1 to drive T cell differentiation (173). This suggests that the response to IFN-γ is downregulated in Th2 cells, which might be seen as a suppression of the Th1 differentiation program. These observations seem to support the mutual exclusivity model of Th1/Th2/Th17 differentiation discussed above.

By performing a gene co-expression analysis of downregulated genes, we observed enrichment in binding sites for Sox4 in iTreg and Th17 cells. A Sox4 *knock in* study in $CD4^+$ T cells showed that this TF is directly induced by TGF-β and is involved in suppression of Th2 differentiation (192). As a part of that study, ChIP-seq for Sox4 in $CD4^+$ T cells was performed, and it was concluded that Sox4 suppresses Th2 differentiation by directly inhibiting GATA-3 binding (192). Furthermore, Sox4 also modifies the chromatin landscape by regulating the expression of histone deacetylases in T cells (193). This evidence suggests multiple functional roles for this protein. Results from our RNA-seq analysis contribute to this discussion by suggesting a potentially new functional mechanism: direct downregulation of Th2 related genes by Sox4. However, this hypothesis must be validated by functional studies capable of revealing TFBS occupancy in Sox4 targets upon cytokine induced polarisation and no definitive conclusions can be reached so far.

When analysing gene expression in iTreg cells, we found that iTregs share a large proportion of their transcriptional program with Th17 cells. This is expected, as both cell

types have been previously associated in the literature. For example, iTreg cells can convert to Th17 cells in response to pathogenic signals (65, 178). We also identified several overlapping functions between these lineages. For example, downregulated genes are enriched in the PI3K pathway in both cell types. This pathway is involved in T cell polarisation (194), where PI3Ks phosphorylate $PIP_2$ and generate $PIP_3$, which in turn causes the activation of Akt, a central component of the mTORC pathway (195). Since Akt inhibits the function of FoxO1 and FoxO3a (195), regulators of FoxP3 (196), inhibiting the PI3K pathway is necessary for Treg differentiation (197). This agrees with our observations. However, downregulation of PI3Ks in Th17 cells is puzzling, since the PI3K-Akt-mTORC1 axis is thought to promote Th17 differentiation through translocation of RORγ to the nucleus (195, 198, 199). Given the fact that PI3K downregulation is highly enriched in Th17 cells in our data set, our observations seem to contradict this model. Functional validation of these observations is needed to clarify whether up or downregulation of this pathway is necessary for Th17 differentiation. The observations described above highlight crucial aspects of Th17 biology. They are of particular importance in the study of MS, which is largely driven by Th17 responses (108, 200, 201). Disentangling the contributions of these factors in $CD4^+$ T cell fate decision towards the Th17 lineage, and specially in the balance between Th17 and Treg cells, could aid in proposing new drug targets for MS treatment, which is unresponsive to widely used autoimmunity therapies such as TNF blockade (123).

Unlike MS, RA is usually responsive to TNF-α and IL-6 blockade (2, 115, 119). As a matter of fact, TNF-α is involved in multiple autoimmune diseases (119). This encouraged us to characterise the effects of TNF-α in different cell subsets. TNF-α is usually regarded as a cytokine of the innate immunity (2) which acts on macrophages and mononuclear phagocytes (119). Our results suggest that, indeed, stimulated $CD4^+$ T cells might not respond to TNF-α treatment. However, the power limitations of our study make it difficult to draw any definitive conclusions. Conversely, macrophages upregulated more than 400 genes in response to TNF-α. The response of macrophages to TNF-α was apparent at six hours, and a more detailed analysis revealed that upregulated genes were enriched in TFBS for NFκB and IRFs. These same genes were also enriched in death domain activity and receptors for cytokines and prostaglandins. The fact that both the death domain and NFκB are enriched suggests that macrophages might be responding by activating more than one of these pathways.

Furthermore, IL-26 has also been associated to autoimmunity (202). Interestingly, macrophages responded to IL-26 in a similar way as to TNF-α, with 83 out of 200 differentially expressed genes being shared between both conditions. The IL-26 response

was also enriched in genes controlled by NFκB, but the results from pathway enrichment analysis suggested a slightly different profile, which did not include activation of the death domain. This suggests that the overlap between the response to IL-26 and TNF-α might be due to the shared elements in their signalling cascade and not to TNF-α autocrine secretion in response to IL-26. However, to completely rule out the role of autocrine cytokines we would have to conduct an experiment in which macrophages were stimulated with IL-26 while supplementing the culture with antibodies against TNF-α. It is important to determine the source of this shared signalling in light of the currently existing TNF-blockade therapeutics. Given that anti-TNF therapy is not effective in a subset of patients, and having shown that TNF-α generates prominent effects in macrophages, it would be interesting to determine whether the patients who do not respond to therapy show any additional IL-26 signalling. If this is proven true, therapies focused on IL-26 blockade could be investigated.

IL-23 has also been linked with autoimmune reactions involving macrophages, particularly in the context of MS and inflammation of the central nervous system (126). However, our study was unable to identify any transcriptional response to IL-23. This might be explained by power limitations, especially given our small sample size and the fact that the biological replicates of IL-23 stimulation appear quite separate from each other in the PCA plot. However, it is also possible that this cytokine might act in a different cell type, for example in the polarisation of Th17 cells (25, 203).

Even though macrophages are not considered drivers of autoimmunity, their role in several immune diseases is well established (4, 87, 204). As a result, we analysed the gene expression profile of macrophages polarised to M1 and M2 phenotypes. We observed transcriptional responses with 460 differentially expressed genes only observed in M1, 89 only in M2, and 25 genes shared. A comparison of their enrichments in GO terms revealed that the M1 response might be coordinated by STAT1 and IRFs. On the other hand, STAT6 could be coordinating the M2 response, which agrees with the literature (87, 92). This duality of transcriptional regulation is mirrored at the functional level, with M1 macrophages showing upregulation of chemokine receptors and genes necessary for the antiviral response (RNAses and OAS), and M2 macrophages downregulating genes in the IL-1 and IL-6 synthesis and signalling pathways. These observations agree with the generally accepted idea of M2 macrophages being involved in tissue repair and wound healing (83, 87).

In summary, there appear to be two patterns of transcriptional dynamics upon cytokine induced polarisation of $CD4^+$ T cells: steadily increasing changes in gene expression (known lineages) and transitional changes, (IFN-β). We identified pathways which are relevant for

the function of each of these cell states using pathway enrichment analysis followed by overrepresentation analysis. For instance, we observed that downregulation of the PI3K pathway might be involved in Th17 and iTreg differentiation and that IFN-β might induce components of the antiviral response, among other examples. Furthermore, we hypothesised possible mechanisms of gene regulation using gene co-expression network analysis such as downregulation of IRFs in Th2 cells and Sox4 in Th17 cells. Last, we also characterised the transcriptome of known macrophage polarisation states and proposed that the effect of IL-26 could act via the TF NFκB, sharing some aspects with TNF-α polarisation.

# 5. Conclusions and future perspectives

## 5.1 Conclusions

Throughout this thesis I presented the results of a transcriptional characterisation of cytokine induced cell states. For this study, we focused on human $CD4^+$ T cells and macrophages, assessing their response to cytokines associated to autoimmunity. At first, we optimised experimental protocols to isolate, stimulate and polarise naive $CD4^+$ T cells and monocyte derived macrophages, ensuring that the phenotypes obtained agreed with their description in the literature. These findings were confirmed by low coverage RNA-seq, where we identified expression of known markers such as T-bet and IL-12 in Th1 cells, GATA3 and IL-4 in Th2 cells, IL-17F and RORC in Th17 cells, FoxP3 and CTLA-4 in iTregs, COX-1 in M1 macrophages and COX-2 in M2 macrophages. Furthermore, we also proposed possible surface markers for $CD4^+$ T cell subsets using an unbiased approach that combines gene ontology annotation, GO term overrepresentation analysis and differential gene expression.

We performed differential expression analysis and identified combinations of cytokines and time points which might cause transcriptional changes in each cell type. Based on this analysis, we hypothesise that polarisation of $CD4^+$ T cells to known lineages is long lasting, with steadily increasing changes only slightly apparent at 16 hours. On the other hand, polarisation with IFN-β seemed to cause more immediate and transitory changes.

We proposed functional implications of transcriptional changes. For example, we observed similarity between the Th0 and Th1 transcriptomes, which suggested that $CD4^+$ T cells stimulated with our method might acquire a state similar to Th1. We also hypothesise that Th2 cells downregulate the type I IFN signalling pathway, and proposed that this downregulation could be mediated by IRFs. Moreover, we observed that downregulation of the PI3K pathway might be involved in differentiation of iTreg and Th17 cells. Using gene co-expression network analysis, we hypothesised that this might involve suppression of the Th2 differentiation program by the TF Sox4.

We also seemed to confirm the proinflammatory phenotype of M1 and the anti-inflammatory phenotype of M2 macrophages. Furthermore, we observed that M1 differentiation might be mediated by STAT1, and M2 differentiation by STAT6. When studying the effect of cytokines associated to autoimmunity, we observed that TNF-α seems to have no effect on $CD4^+$ T cells but significant effects on macrophages, where it promotes secretion of proinflammatory

cytokines, apoptosis and necroptosis. Polarisation of macrophages with IL-26 shared some of these features, possibly regulated by NFκB. Conversely, there seems to be no effect in macrophages stimulated with IL-23 or in T cells stimulated with IL-21, IL-27, and IL-10.

Finally, we assessed the reproducibility of LC-MS/MS coupled to TMT-labelling for quantitative proteomic analysis in $CD4^+$ T cells. The results of this methodology appear to be reproducible and correlate well with observations at the RNA level.

## 5.2 Future perspectives

### 5.2.1 Characterisation of heterogeneity and plasticity in cytokine induced cell polarisation

Despite our success in identifying pathways and possibly involved in cytokine induced cell polarisation, the results from this study suggest that cells in culture respond differently to the same cytokine stimulus. For example, we observed that TGF-β only induces FoxP3 expression in 65% of cells, and the same is true for other conditions and TFs. Thus, it is unclear if the remaining cells do not respond to the stimulus, or if several types of response coexist, generating a heterogeneous population. Furthermore, polarised cells are plastic and can interconvert from one phenotype to another (3, 65). Single-cell RNA-sequencing (scRNA-seq) is a high-resolution technique which can successfully identify subsets of cells that display characteristic gene expression profiles within a population (205, 206). Thus, performing a similar study using scRNA-seq instead of bulk RNA-seq would inform on the existence of subpopulations of cells upon cytokine induced polarisation. According to our results, this would be particularly useful for studying Th2, Th17 and iTreg cells stimulated for five days. Furthermore, scRNA-seq can also characterise changes in gene expression throughout time with higher resolution, accounting for differences in response time between individual cells (207).

### 5.2.2 Identification of novel drug targets

Some of the results of this study are particularly relevant for drug development. For example, TNF-α blockade is a major therapeutic strategy for treating conditions such as RA (2, 119), however the role of TNF-α in disease is still unclear and some patients are unresponsive to treatment. Here we found that the effects of this cytokine on macrophages are very similar to those of IL-26. An immediate question is if the combination of IL-26 and TNF-α blockade

would improve the current treatment. To evaluate this, we would need to recapitulate the results in a more powered study and to characterise the mechanism behind this observation. For example, the effect of autocrine TNF-α secretion would need to be discarded. Furthermore, characterising the response to cytokines like IL-1β, IL-23, and IL-27 on different cell types might help identifying more specific strategies for cytokine blockade which could be used as therapies.

### 5.2.3 Surface marker validation and characterisation of cytokine induced cell states *in vivo*

In this study, we identified potential novel markers to isolate $CD4^+$ T cell subset directly from blood. However, these markers were only based on mRNA levels and need further validation, specially given our power limitations. In the short term these markers should be used for staining cells with antibodies specific for them, and further isolating cell subsets enriched in the expression of these markers from peripheral blood using flow cytometry. The cytokine secretion pattern of these cells could then be characterised using flow cytometry, Luminex and ELISA. Direct isolation of cytokine induced cell states from peripheral blood would significantly improve our understanding of cell subsets in the human immune system, reducing the need of *in vitro* models.

In the long term, developing a proteomics based approach to identify surface markers would be useful. Based on the high correlation of our LC-MS/MS and RNA-seq data, we hypothesise that LC-MS/MS would be an appropriate methodology. To achieve this, the next step would be to quantify the full proteome of specific cell types using TMT LC-MS/MS. This study has already been started in our group for the cell states here described.

### 5.2.4 Intersection with GWAS variants and prioritisation of cell states relevant to autoimmunity

Improving our understanding of diseases like MS, RA and IBD is a major motivation for genetic studies. Genome wide association studies (GWAS) have identified hundreds of variants linked to autoimmunity (208-210). Most of these localise to non-coding regions (211) and are difficult to interpret. The study of their contribution to disease is complicated by the multiplicity of cell types and cell states in the immune system (44) and it remains unclear in which cell states these variants have a functional implication.

To assess the implication of risk variants in each cell state, gene expression data from this study could be intersected with catalogues of GWAS SNPs linked to immune disease (212). If variants are highly enriched within genes differentially expressed in a particular cell state, this cell might be prioritised for the studied disease (212). In the short term, this is attainable with our. Moreover, a similar study with larger sample size and sequencing depth is already being carried out by our research group.

However, most risk variants are non-coding and will not be unequivocally assigned to a target gene based solely on genomic proximity. Hence, in the longer term a characterisation of the epigenetic context and chromatin landscape upon cytokine induced polarisation is needed. To this end, ChIP-seq (213, 214) can be performed on the cytokine induced cell states described here. Next, specific chromatin modifications which mark active enhancers, active promoters or inactive chromatin (213) can be identified. These annotations can then be used to prioritise relevant cell states by intersecting the chromatin marks with GWAS SNPs (215). This approach is expected to achieve a better resolution than enrichment analyses which use only RNA-seq data. ChIP-seq is already being performed in our research group for the cell states here described.

### 5.2.5 Epigenetic characterisation of cytokine induced cell states

Throughout this study we failed to identify substantial differences in gene expression after 16 hours of cytokine polarisation in $CD4^+$ T cells. The next step would be to repeat the analysis for selected conditions using a more powered design. However, it is also possible that only epigenetic changes are apparent at this time point. To assess this, we would need to characterise the chromatin landscape, as well as the activity of specific TFs in these cell states. This could be done using the assay of transposase accessible chromatin followed by sequencing (ATAC-seq) (216), which has been successful in mapping chromatin accessibility and TFBS occupancy (217). This approach would help us assess hypotheses generated by our results, for example whether Sox4 and Msx2 really coordinate part of the Th17 and iTreg differentiation programs.

# 6. References


1. O'Shea JJ. Helper T-cell differentiation and plasticity. In: Paul WE, editor. *Fundamental Immunology*. 7th ed. Philadelphia, USA: Lippincott Williams & Wilkins; 2013. p. 1824-52.
2. Schett G, Elewaut D, McInnes IB, Dayer JM, Neurath MF. How cytokine networks fuel inflammation: Toward a cytokine-based disease taxonomy. *Nat Med*. 2013;19(7):822-4.
3. Hirahara K, Poholek A, Vahedi G, Laurence A, Kanno Y, Milner JD, et al. Mechanisms underlying helper T-cell plasticity: implications for immune-mediated disease. *J Allergy Clin Immunol*. 2013;131(5):1276-87.
4. Haringman JJ, Gerlag DM, Zwinderman AH, Smeets TJ, Kraan MC, Baeten D, et al. Synovial tissue macrophages: a sensitive biomarker for response to treatment in patients with rheumatoid arthritis. *Ann Rheum Dis*. 2005;64(6):834-8.
5. Guermonprez P, Valladeau J, Zitvogel L, Théry C, Amigorena S. Antigen presentation and T cell stimulation by dendritic cells. *Annu Rev Immunol*. 2002;20:621-67.
6. Smith-Garvin JE, Koretzky GA, Jordan MS. T cell activation. *Annu Rev Immunol*. 2009;27:591-619.
7. Rudolph MG, Stanfield RL, Wilson IA. How TCRs bind MHCs, peptides, and coreceptors. *Annu Rev Immunol*. 2006;24:419-66.
8. Acuto O, Michel F. CD28-mediated co-stimulation: a quantitative support for TCR signalling. *Nat Rev Immunol*. 2003;3(12):939-51.
9. Annunziato F, Romagnani S. Heterogeneity of human effector CD4+ T cells. *Arthritis Res Ther*. 2009;11(6):257.
10. Reinhardt RL, Liang HE, Locksley RM. Cytokine-secreting follicular T cells shape the antibody repertoire. *Nat Immunol*. 2009;10(4):385-93.
11. Dalton DK, Pitts-Meek S, Keshav S, Figari IS, Bradley A, Stewart TA. Multiple defects of immune cell function in mice with disrupted interferon-gamma genes. *Science*. 1993;259(5102):1739-42.
12. Leonard WJ. Type I cytokines and interferons, and their receptors. In: Paul WE, editor. *Fundamental Immunology*. 7th ed. Philadelphia, USA: Lippincott Williams & Wilkins; 2013. p. 1542-666.
13. Zhu J, Yamane H, Paul WE. Differentiation of effector CD4 T cell populations. *Annu Rev Immunol*. 2010;28:445-89.
14. Mosmann TR, Cherwinski H, Bond MW, Giedlin MA, Coffman RL. Two types of murine helper T cell clone. I. Definition according to profiles of lymphokine activities and secreted proteins. *J Immunol*. 1986;136(7):2348-57.

15. Bottomly K. A functional dichotomy in CD4+ T lymphocytes. *Immunol Today*. 1988;9(9):268-74.

16. Gor DO, Rose NR, Greenspan NS. TH1-TH2: a procrustean paradigm. *Nat Immunol*. 2003;4(6):503-5.

17. Romagnani S. Lymphokine production by human T cells in disease states. *Annu Rev Immunol.* 1994;12:227-57.

18. Heinzel FP, Sadick MD, Holaday BJ, Coffman RL, Locksley RM. Reciprocal expression of interferon gamma or interleukin 4 during the resolution or progression of murine leishmaniasis. Evidence for expansion of distinct helper T cell subsets. *J Exp Med*. 1989;169(1):59-72.

19. Scott P, Natovitz P, Coffman RL, Pearce E, Sher A. Immunoregulation of cutaneous leishmaniasis. T cell lines that transfer protective immunity or exacerbation belong to different T helper subsets and respond to distinct parasite antigens. *J Exp Med*. 1988;168(5):1675-84.

20. Pirmez C, Yamamura M, Uyemura K, Paes-Oliveira M, Conceição-Silva F, Modlin RL. Cytokine patterns in the pathogenesis of human leishmaniasis. *J Clin Invest*. 1993;91(4):1390-5.

21. Nagata K, Tanaka K, Ogawa K, Kemmotsu K, Imai T, Yoshie O, et al. Selective expression of a novel surface molecule by human Th2 cells in vivo. *J Immunol*. 1999;162(3):1278-86.

22. Chan SH, Perussia B, Gupta JW, Kobayashi M, Pospísil M, Young HA, et al. Induction of interferon gamma production by natural killer cell stimulatory factor: characterization of the responder cells and synergy with other inducers. *J Exp Med*. 1991;173(4):869-79.

23. Le Gros G, Ben-Sasson SZ, Seder R, Finkelman FD, Paul WE. Generation of interleukin 4 (IL-4)-producing cells in vivo and in vitro: IL-2 and IL-4 are required for in vitro generation of IL-4-producing cells. *J Immunol*. 2008;181(5):2943-51.

24. Kaplan MH, Schindler U, Smiley ST, Grusby MJ. Stat6 is required for mediating responses to IL-4 and for development of Th2 cells. *Immunity*. 1996;4(3):313-9.

25. Harrington LE, Hatton RD, Mangan PR, Turner H, Murphy TL, Murphy KM, et al. Interleukin 17-producing CD4+ effector T cells develop via a lineage distinct from the T helper type 1 and 2 lineages. *Nat Immunol*. 2005;6(11):1123-32.

26. Langrish CL, Chen Y, Blumenschein WM, Mattson J, Basham B, Sedgwick JD, et al. IL-23 drives a pathogenic T cell population that induces autoimmune inflammation. *J Exp Med*. 2005;201(2):233-40.

27. Park H, Li Z, Yang XO, Chang SH, Nurieva R, Wang YH, et al. A distinct lineage of CD4 T cells regulates tissue inflammation by producing interleukin 17. *Nat Immunol*. 2005;6(11):1133-41.

28. Chen W, Jin W, Hardegen N, Lei KJ, Li L, Marinos N, et al. Conversion of peripheral CD4+CD25- naive T cells to CD4+CD25+ regulatory T cells by TGF-beta induction of transcription factor Foxp3. *J Exp Med*. 2003;198(12):1875-86.

29. Veldhoen M, Uyttenhove C, van Snick J, Helmby H, Westendorf A, Buer J, et al. Transforming growth factor-beta 'reprograms' the differentiation of T helper 2 cells and promotes an interleukin 9-producing subset. *Nat Immunol*. 2008;9(12):1341-6.

30. Trifari S, Kaplan CD, Tran EH, Crellin NK, Spits H. Identification of a human helper T cell population that has abundant production of interleukin 22 and is distinct from T(H)-17, T(H)1 and T(H)2 cells. *Nat Immunol*. 2009;10(8):864-71.

31. Lanzavecchia A, Sallusto F. Progressive differentiation and selection of the fittest in the immune response. *Nat Rev Immunol*. 2002;2(12):982-7.

32. Iezzi G, Scotet E, Scheidegger D, Lanzavecchia A. The interplay between the duration of TCR and cytokine signaling determines T cell polarization. *Eur J Immunol*. 1999;29(12):4092-101.

33. van Panhuys N, Klauschen F, Germain RN. T-cell-receptor-dependent signal intensity dominantly controls CD4(+) T cell polarization In Vivo. *Immunity*. 2014;41(1):63-74.

34. Purvis HA, Stoop JN, Mann J, Woods S, Kozijn AE, Hambleton S, et al. Low-strength T-cell activation promotes Th17 responses. *Blood*. 2010;116(23):4829-37.

35. Szabo SJ, Kim ST, Costa GL, Zhang X, Fathman CG, Glimcher LH. A novel transcription factor, T-bet, directs Th1 lineage commitment. *Cell*. 2000;100(6):655-69.

36. Zheng W, Flavell RA. The transcription factor GATA-3 is necessary and sufficient for Th2 cytokine gene expression in CD4 T cells. *Cell*. 1997;89(4):587-96.

37. Yang XO, Pappu BP, Nurieva R, Akimzhanov A, Kang HS, Chung Y, et al. T helper 17 lineage differentiation is programmed by orphan nuclear receptors ROR alpha and ROR gamma. *Immunity*. 2008;28(1):29-39.

38. Chang HC, Sehra S, Goswami R, Yao W, Yu Q, Stritesky GL, et al. The transcription factor PU.1 is required for the development of IL-9-producing T cells and allergic inflammation. *Nat Immunol*. 2010;11(6):527-34.

39. Fantini MC, Becker C, Monteleone G, Pallone F, Galle PR, Neurath MF. Cutting edge: TGF-beta induces a regulatory phenotype in CD4+CD25- T cells through Foxp3 induction and down-regulation of Smad7. *J Immunol*. 2004;172(9):5149-53.

40. Fu S, Zhang N, Yopp AC, Chen D, Mao M, Zhang H, et al. TGF-beta induces Foxp3 + T-regulatory cells from CD4 + CD25 - precursors. *Am J Transplant*. 2004;4(10):1614-27.

41. Vahedi G, Takahashi H, Nakayamada S, Sun HW, Sartorelli V, Kanno Y, et al. STATs shape the active enhancer landscape of T cell populations. *Cell*. 2012;151(5):981-93.
42. Samstein RM, Arvey A, Josefowicz SZ, Peng X, Reynolds A, Sandstrom R, et al. Foxp3 exploits a pre-existent enhancer landscape for regulatory T cell lineage specification. *Cell*. 2012;151(1):153-66.
43. Kanhere A, Hertweck A, Bhatia U, Gökmen MR, Perucha E, Jackson I, et al. T-bet and GATA3 orchestrate Th1 and Th2 differentiation through lineage-specific targeting of distal regulatory elements. *Nat Commun*. 2012;3:1268.
44. Sallusto F. Heterogeneity of Human CD4(+) T Cells Against Microbes. *Annu Rev Immunol*. 2016;34:317-34.
45. Noël W, Raes G, Hassanzadeh Ghassabeh G, De Baetselier P, Beschin A. Alternatively activated macrophages during parasite infections. *Trends Parasitol*. 2004;20(3):126-33.
46. Hurst SD, Muchamuel T, Gorman DM, Gilbert JM, Clifford T, Kwan S, et al. New IL-17 family members promote Th1 or Th2 responses in the lung: in vivo function of the novel cytokine IL-25. *J Immunol*. 2002;169(1):443-53.
47. Ouyang W, Kolls JK, Zheng Y. The biological functions of T helper 17 cell effector cytokines in inflammation. *Immunity*. 2008;28(4):454-67.
48. Rissoan MC, Soumelis V, Kadowaki N, Grouard G, Briere F, de Waal Malefyt R, et al. Reciprocal control of T helper cell and dendritic cell differentiation. *Science*. 1999;283(5405):1183-6.
49. Maldonado-López R, De Smedt T, Michel P, Godfroid J, Pajak B, Heirman C, et al. CD8alpha+ and CD8alpha- subclasses of dendritic cells direct the development of distinct T helper cells in vivo. *J Exp Med*. 1999;189(3):587-92.
50. Macatonia SE, Hosken NA, Litton M, Vieira P, Hsieh CS, Culpepper JA, et al. Dendritic cells produce IL-12 and direct the development of Th1 cells from naive CD4+ T cells. *J Immunol*. 1995;154(10):5071-9.
51. Whelan M, Harnett MM, Houston KM, Patel V, Harnett W, Rigley KP. A filarial nematode-secreted product signals dendritic cells to acquire a phenotype that drives development of Th2 cells. *J Immunol*. 2000;164(12):6453-60.
52. Langenkamp A, Messi M, Lanzavecchia A, Sallusto F. Kinetics of dendritic cell activation: impact on priming of TH1, TH2 and nonpolarized T cells. *Nat Immunol*. 2000;1(4):311-6.
53. Celli S, Garcia Z, Bousso P. CD4 T cells integrate signals delivered during successive DC encounters in vivo. *J Exp Med*. 2005;202(9):1271-8.

54. Bonecchi R, Bianchi G, Bordignon PP, D'Ambrosio D, Lang R, Borsatti A, et al. Differential expression of chemokine receptors and chemotactic responsiveness of type 1 T helper cells (Th1s) and Th2s. *J Exp Med*. 1998;187(1):129-34.

55. Annunziato F, Cosmi L, Santarlasci V, Maggi L, Liotta F, Mazzinghi B, et al. Phenotypic and functional features of human Th17 cells. *J Exp Med*. 2007;204(8):1849-61.

56. Wang J, Li F, Wei H, Lian ZX, Sun R, Tian Z. Respiratory influenza virus infection induces intestinal immune injury via microbiota-mediated Th17 cell-dependent inflammation. *J Exp Med*. 2014;211(12):2397-410.

57. Mora JR, Bono MR, Manjunath N, Weninger W, Cavanagh LL, Rosemblatt M, et al. Selective imprinting of gut-homing T cells by Peyer's patch dendritic cells. *Nature*. 2003;424(6944):88-93.

58. Iwata M, Hirakiyama A, Eshima Y, Kagechika H, Kato C, Song SY. Retinoic acid imprints gut-homing specificity on T cells. *Immunity*. 2004;21(4):527-38.

59. Sigmundsdottir H, Pan J, Debes GF, Alt C, Habtezion A, Soler D, et al. DCs metabolize sunlight-induced vitamin D3 to 'program' T cell attraction to the epidermal chemokine CCL27. *Nat Immunol*. 2007;8(3):285-93.

60. Gajewski TF, Fitch FW. Anti-proliferative effect of IFN-gamma in immune regulation. I. IFN-gamma inhibits the proliferation of Th2 but not Th1 murine helper T lymphocyte clones. *J Immunol*. 1988;140(12):4245-52.

61. Seder RA, Paul WE, Davis MM, Fazekas de St Groth B. The presence of interleukin 4 during in vitro priming determines the lymphokine-producing potential of CD4+ T cells from T cell receptor transgenic mice. *J Exp Med*. 1992;176(4):1091-8.

62. Lighvani AA, Frucht DM, Jankovic D, Yamane H, Aliberti J, Hissong BD, et al. T-bet is rapidly induced by interferon-gamma in lymphoid and myeloid cells. *Proc Natl Acad Sci USA*. 2001;98(26):15137-42.

63. Becskei A, Grusby MJ. Contribution of IL-12R mediated feedback loop to Th1 cell differentiation. *FEBS Lett*. 2007;581(27):5199-206.

64. Hegazy AN, Peine M, Helmstetter C, Panse I, Fröhlich A, Bergthaler A, et al. Interferons direct Th2 cell reprogramming to generate a stable GATA-3(+)T-bet(+) cell subset with combined Th2 and Th1 cell functions. *Immunity*. 2010;32(1):116-28.

65. Komatsu N, Okamoto K, Sawa S, Nakashima T, Oh-hora M, Kodama T, et al. Pathogenic conversion of Foxp3+ T cells into TH17 cells in autoimmune arthritis. *Nat Med*. 2014;20(1):62-8.

66. Gagliani N, Amezcua Vesely MC, Iseppon A, Brockmann L, Xu H, Palm NW, et al. Th17 cells transdifferentiate into regulatory T cells during resolution of inflammation. *Nature*. 2015;523(7559):221-5.

67. Kanno Y, Vahedi G, Hirahara K, Singleton K, O'Shea JJ. Transcriptional and epigenetic control of T helper cell specification: molecular mechanisms underlying commitment and plasticity. *Annu Rev Immunol*. 2012;30:707-31.

68. Wei G, Wei L, Zhu J, Zang C, Hu-Li J, Yao Z, et al. Global mapping of H3K4me3 and H3K27me3 reveals specificity and plasticity in lineage fate determination of differentiating CD4+ T cells. *Immunity*. 2009;30(1):155-67.

69. Varol C, Mildner A, Jung S. Macrophages: development and tissue specialization. *Annu Rev Immunol*. 2015;33:643-75.

70. Passlick B, Flieger D, Ziegler-Heitbrock HW. Identification and characterization of a novel monocyte subpopulation in human peripheral blood. *Blood*. 1989;74(7):2527-34.

71. Ziegler-Heitbrock HW, Ulevitch RJ. CD14: cell surface receptor and differentiation marker. *Immunol Today*. 1993;14(3):121-5.

72. Gordon S, Taylor PR. Monocyte and macrophage heterogeneity. *Nat Rev Immunol*. 2005;5(12):953-64.

73. Ziegler-Heitbrock HW, Fingerle G, Ströbel M, Schraut W, Stelter F, Schütt C, et al. The novel subset of CD14+/CD16+ blood monocytes exhibits features of tissue macrophages. *Eur J Immunol*. 1993;23(9):2053-8.

74. Randolph GJ, Sanchez-Schmitz G, Liebman RM, Schäkel K. The CD16(+) (FcgammaRIII(+)) subset of human monocytes preferentially becomes migratory dendritic cells in a model tissue setting. *J Exp Med*. 2002;196(4):517-27.

75. Sánchez-Torres C, García-Romo GS, Cornejo-Cortés MA, Rivas-Carvalho A, Sánchez-Schmitz G. CD16+ and CD16- human blood monocyte subsets differentiate in vitro to dendritic cells with different abilities to stimulate CD4+ T cells. *Int Immunol*. 2001;13(12):1571-81.

76. Teitelbaum SL, Ross FP. Genetic regulation of osteoclast development and function. *Nat Rev Genet*. 2003;4(8):638-49.

77. Mildner A, Schmidt H, Nitsche M, Merkler D, Hanisch UK, Mack M, et al. Microglia in the adult brain arise from Ly-6ChiCCR2+ monocytes only under defined host conditions. *Nat Neurosci*. 2007;10(12):1544-53.

78. Merad M, Manz MG, Karsunky H, Wagers A, Peters W, Charo I, et al. Langerhans cells renew in the skin throughout life under steady-state conditions. *Nat Immunol*. 2002;3(12):1135-41.

79. Hussell T, Bell TJ. Alveolar macrophages: plasticity in a tissue-specific context. *Nat Rev Immunol*. 2014;14(2):81-93.

80. Gordon S. Macrophages and phagocytosis. In: Paul WE, editor. *Fundamental Immunology*. 7th ed. Philadelphia, USA: Lippincott Williams & Wilkins; 2013. p. 1178-213.

81. Yamasaki R, Lu H, Butovsky O, Ohno N, Rietsch AM, Cialic R, et al. Differential roles of microglia and monocytes in the inflamed central nervous system. *J Exp Med*. 2014;211(8):1533-49.
82. Chazaud B. Macrophages: supportive cells for tissue repair and regeneration. *Immunobiology*. 2014;219(3):172-8.
83. Gordon S. Alternative activation of macrophages. *Nat Rev Immunol.* 2003;3(1):23-35.
84. Nau GJ, Richmond JF, Schlesinger A, Jennings EG, Lander ES, Young RA. Human macrophage activation programs induced by bacterial pathogens. *Proc Natl Acad Sci USA*. 2002;99(3):1503-8.
85. O'Neill LAJ. The innate immune system. In: Paul WE, editor. *Fundamental Immunology*. 7th ed. Philadelphia, USA: Lippincott Williams & Wilkins; 2013. p. 897-935.
86. Martinez FO, Sica A, Mantovani A, Locati M. Macrophage activation and polarization. *Front Biosci*. 2008;13:453-61.
87. Sica A, Mantovani A. Macrophage plasticity and polarization: in vivo veritas. *J Clin Invest*. 2012;122(3):787-95.
88. Mills CD, Kincaid K, Alt JM, Heilman MJ, Hill AM. M-1/M-2 macrophages and the Th1/Th2 paradigm. *J Immunol*. 2000;164(12):6166-73.
89. Stein M, Keshav S, Harris N, Gordon S. Interleukin 4 potently enhances murine macrophage mannose receptor activity: a marker of alternative immunologic macrophage activation. *J Exp Med*. 1992;176(1):287-92.
90. Herbert DR, Hölscher C, Mohrs M, Arendse B, Schwegmann A, Radwanska M, et al. Alternative macrophage activation is essential for survival during schistosomiasis and downmodulates T helper 1 responses and immunopathology. *Immunity*. 2004;20(5):623-35.
91. Mantovani A, Sozzani S, Locati M, Allavena P, Sica A. Macrophage polarization: tumor-associated macrophages as a paradigm for polarized M2 mononuclear phagocytes. *Trends Immunol*. 2002;23(11):549-55.
92. Sica A, Bronte V. Altered macrophage differentiation and immune dysfunction in tumor development. *J Clin Invest*. 2007;117(5):1155-66.
93. Byles V, Covarrubias AJ, Ben-Sahra I, Lamming DW, Sabatini DM, Manning BD, et al. The TSC-mTOR pathway regulates macrophage polarization. *Nat Commun*. 2013;4:2834.
94. Martinez FO, Gordon S, Locati M, Mantovani A. Transcriptional profiling of the human monocyte-to-macrophage differentiation and polarization: new molecules and patterns of gene expression. *J Immunol*. 2006;177(10):7303-11.
95. Raes G, De Baetselier P, Noël W, Beschin A, Brombacher F, Hassanzadeh Gh G. Differential expression of FIZZ1 and Ym1 in alternatively versus classically activated macrophages. *J Leukoc Biol*. 2002;71(4):597-602.

96. Welch JS, Escoubet-Lozach L, Sykes DB, Liddiard K, Greaves DR, Glass CK. TH2 cytokines and allergic challenge induce Ym1 expression in macrophages by a STAT6-dependent mechanism. *J Biol Chem*. 2002;277(45):42821-9.

97. El Kasmi KC, Qualls JE, Pesce JT, Smith AM, Thompson RW, Henao-Tamayo M, et al. Toll-like receptor-induced arginase 1 in macrophages thwarts effective immunity against intracellular pathogens. *Nat Immunol*. 2008;9(12):1399-406.

98. Martinez FO, Gordon S. The M1 and M2 paradigm of macrophage activation: time for reassessment. *F1000Prime Rep*. 2014;6:13.

99. Edwards JP, Zhang X, Frauwirth KA, Mosser DM. Biochemical and functional characterization of three activated macrophage populations. *J Leukoc Biol*. 2006;80(6):1298-307.

100. Mosser DM, Edwards JP. Exploring the full spectrum of macrophage activation. *Nat Rev Immunol*. 2008;8(12):958-69.

101. Xue J, Schmidt SV, Sander J, Draffehn A, Krebs W, Quester I, et al. Transcriptome-based network analysis reveals a spectrum model of human macrophage activation. *Immunity*. 2014;40(2):274-88.

102. Murray PJ, Allen JE, Biswas SK, Fisher EA, Gilroy DW, Goerdt S, et al. Macrophage activation and polarization: nomenclature and experimental guidelines. *Immunity*. 2014;41(1):14-20.

103. Ishii M, Wen H, Corsa CA, Liu T, Coelho AL, Allen RM, et al. Epigenetic regulation of the alternatively activated macrophage phenotype. *Blood*. 2009;114(15):3244-54.

104. Ivashkiv LB. Epigenetic regulation of macrophage polarization and function. *Trends Immunol.* 2013;34(5):216-23.

105. De Santa F, Totaro MG, Prosperini E, Notarbartolo S, Testa G, Natoli G. The histone H3 lysine-27 demethylase Jmjd3 links inflammation to inhibition of polycomb-mediated gene silencing. *Cell*. 2007;130(6):1083-94.

106. Bauer J, Berkenbosch F, Van Dam AM, Dijkstra CD. Demonstration of interleukin-1 beta in Lewis rat brain during experimental allergic encephalomyelitis by immunocytochemistry at the light and ultrastructural level. *J Neuroimmunol*. 1993;48(1):13-21.

107. Baker D, O'Neill JK, Turk JL. Cytokines in the central nervous system of mice during chronic relapsing experimental allergic encephalomyelitis. *Cell Immunol*. 1991;134(2):505-10.

108. Lin CC, Edelson BT. New Insights into the Role of IL-1β in Experimental Autoimmune Encephalomyelitis and Multiple Sclerosis. *J Immunol*. 2017;198(12):4553-60.

109. Woodroofe MN, Cuzner ML. Cytokine mRNA expression in inflammatory multiple sclerosis lesions: detection by non-radioactive in situ hybridization. *Cytokine*. 1993;5(6):583-8.

110. Ronchi F, Basso C, Preite S, Reboldi A, Baumjohann D, Perlini L, et al. Experimental priming of encephalitogenic Th1/Th17 cells requires pertussis toxin-driven IL-1β production by myeloid cells. *Nat Commun*. 2016;7:11541.

111. Jha S, Srivastava SY, Brickey WJ, Iocca H, Toews A, Morrison JP, et al. The inflammasome sensor, NLRP3, regulates CNS inflammation and demyelination via caspase-1 and interleukin-18. *J Neurosci*. 2010;30(47):15811-20.

112. Sutton C, Brereton C, Keogh B, Mills KH, Lavelle EC. A crucial role for interleukin (IL)-1 in the induction of IL-17-producing T cells that mediate autoimmune encephalomyelitis. *J Exp Med*. 2006;203(7):1685-91.

113. Codarri L, Gyülvészi G, Tosevski V, Hesske L, Fontana A, Magnenat L, et al. RORγt drives production of the cytokine GM-CSF in helper T cells, which is essential for the effector phase of autoimmune neuroinflammation. *Nat Immunol*. 2011;12(6):560-7.

114. El-Behi M, Ciric B, Dai H, Yan Y, Cullimore M, Safavi F, et al. The encephalitogenicity of T(H)17 cells is dependent on IL-1- and IL-23-induced production of the cytokine GM-CSF. *Nat Immunol*. 2011;12(6):568-75.

115. McInnes IB, Buckley CD, Isaacs JD. Cytokines in rheumatoid arthritis - shaping the immunological landscape. *Nat Rev Rheumatol*. 2016;12(1):63-8.

116. Nickoloff BJ. Cracking the cytokine code in psoriasis. *Nat Med*. 2007;13(3):242-4.

117. Kume K, Amano K, Yamada S, Hatta K, Ohta H, Kuwaba N. Tocilizumab monotherapy reduces arterial stiffness as effectively as etanercept or adalimumab monotherapy in rheumatoid arthritis: an open-label randomized controlled trial. *J Rheumatol*. 2011;38(10):2169-71.

118. Baeten D, Sieper J, Braun J, Baraliakos X, Dougados M, Emery P, et al. Secukinumab, an Interleukin-17A Inhibitor, in Ankylosing Spondylitis. *N Engl J Med*. 2015;373(26):2534-48.

119. Kalliolias GD, Ivashkiv LB. TNF biology, pathogenic mechanisms and emerging therapeutic strategies. *Nat Rev Rheumatol*. 2016;12(1):49-62.

120. Monaco C, Nanchahal J, Taylor P, Feldmann M. Anti-TNF therapy: past, present and future. *Int Immunol*. 2015;27(1):55-62.

121. Brenner D, Blaser H, Mak TW. Regulation of tumour necrosis factor signalling: live or let die. *Nat Rev Immunol*. 2015;15(6):362-74.

122. Micheau O, Tschopp J. Induction of TNF receptor I-mediated apoptosis via two sequential signaling complexes. *Cell*. 2003;114(2):181-90.

123. TNF neutralization in MS: results of a randomized, placebo-controlled multicenter study. The Lenercept Multiple Sclerosis Study Group and The University of British Columbia MS/MRI Analysis Group. *Neurology*. 1999;53(3):457-65.

124. Probert L. TNF and its receptors in the CNS: The essential, the desirable and the deleterious effects. *Neuroscience*. 2015;302:2-22.

125. Di Fusco D, Izzo R, Figliuzzi MM, Pallone F, Monteleone G. IL-21 as a therapeutic target in inflammatory disorders. *Expert Opin Ther Targets*. 2014;18(11):1329-38.

126. Cua DJ, Sherlock J, Chen Y, Murphy CA, Joyce B, Seymour B, et al. Interleukin-23 rather than interleukin-12 is the critical cytokine for autoimmune inflammation of the brain. *Nature*. 2003;421(6924):744-8.

127. van Holten J, Pavelka K, Vencovsky J, Stahl H, Rozman B, Genovese M, et al. A multicentre, randomised, double blind, placebo controlled phase II study of subcutaneous interferon beta-1a in the treatment of patients with active rheumatoid arthritis. *Ann Rheum Dis*. 2005;64(1):64-9.

128. Tlustochowicz W, Rahman P, Seriolo B, Krammer G, Porter B, Widmer A, et al. Efficacy and Safety of Subcutaneous and Intravenous Loading Dose Regimens of Secukinumab in Patients with Active Rheumatoid Arthritis: Results from a Randomized Phase II Study. *J Rheumatol*. 2016;43(3):495-503.

129. Stubbington MJ, Mahata B, Svensson V, Deonarine A, Nissen JK, Betz AG, et al. An atlas of mouse CD4(+) T cell transcriptomes. *Biol Direct*. 2015;10:14.

130. Bonnal RJ, Ranzani V, Arrigoni A, Curti S, Panzeri I, Gruarin P, et al. De novo transcriptome profiling of highly purified human lymphocytes primary cells. *Sci Data*. 2015;2:150051.

131. Kanduri K, Tripathi S, Larjo A, Mannerström H, Ullah U, Lund R, et al. Identification of global regulators of T-helper cell lineage specification. *Genome Med*. 2015;7:122.

132. Ching T, Huang S, Garmire LX. Power analysis and sample size estimation for RNA-Seq differential expression. *RNA*. 2014;20(11):1684-96.

133. Liu Y, Zhou J, White KP. RNA-seq differential expression studies: more sequence or more replication? *Bioinformatics*. 2014;30(3):301-4.

134. Hart SN, Therneau TM, Zhang Y, Poland GA, Kocher JP. Calculating sample size estimates for RNA sequencing data. *J Comput Biol*. 2013;20(12):970-8.

135. Love MI, Huber W, Anders S. Moderated estimation of fold change and dispersion for RNA-seq data with DESeq2. *Genome Biol*. 2014;15(12):550.

136. Illumina. *TruSeq RNA sample preparation guide*. 2009.

137. Tischler G, Leonard S. biobambam: tools for read pair collation based algorithms on BAM files. *Source code for biology and medicine*. 2014;9(13).

138. Dobin A, Davis CA, Schlesinger F, Drenkow J, Zaleski C, Jha S, et al. STAR: ultrafast universal RNA-seq aligner. *Bioinformatics*. 2013;29(1):15-21.

139. Li H, Handsaker B, Wysoker A, Fennell T, Ruan J, Homer N, et al. The Sequence Alignment/Map format and SAMtools. *Bioinformatics*. 2009;25(16):2078-9.

140. Liao Y, Smyth GK, Shi W. featureCounts: an efficient general purpose program for assigning sequence reads to genomic features. *Bioinformatics*. 2014;30(7):923-30.

141. Ringnér M. What is principal component analysis? *Nat Biotechnol*. 2008;26(3):303-4.

142. Abdi H, Williams LJ. Principal component analysis. *WIREs Comp Stat*. 2010;2:433-59.

143. Kolde R. Pretty heat maps (pheatmaps). 1.0.8 ed: *CRAN*; 2015.

144. Ritchie ME, Phipson B, Wu D, Hu Y, Law CW, Shi W, et al. limma powers differential expression analyses for RNA-sequencing and microarray studies. *Nucleic Acids Res*. 2015;43(7):e47.

145. Anders S, Huber W. Differential expression analysis for sequence count data. *Genome Biol*. 2010;11(10):R106.

146. Benjamini Y, Hochberg Y. Controlling the false discovery rate: a practical and powerful approach to multiple testing. *Journal of the Royal Statistical Society Series B (Methodological)*. 1995;57(1):289-300.

147. Consortium GO. Gene Ontology Consortium: going forward. *Nucleic Acids Res*. 2015;43(Database issue):D1049-56.

148. Ashburner M, Ball CA, Blake JA, Botstein D, Butler H, Cherry JM, et al. Gene ontology: tool for the unification of biology. The Gene Ontology Consortium. *Nat Genet*. 2000;25(1):25-9.

149. Reimand J, Arak T, Adler P, Kolberg L, Reisberg S, Peterson H, et al. g:Profiler-a web server for functional interpretation of gene lists (2016 update). *Nucleic Acids Res*. 2016;44(W1):W83-9.

150. Zhang B, Horvath S. A general framework for weighted gene co-expression network analysis. *Stat Appl Genet Mol Biol*. 2005;4:Article17.

151. Bergmann S, Ihmels J, Barkai N. Similarities and differences in genome-wide expression data of six organisms. *PLoS Biol*. 2004;2(1):E9.

152. Wingender E. The TRANSFAC project as an example of framework technology that supports the analysis of genomic regulation. *Brief Bioinform*. 2008;9(4):326-32.

153. Gautier EL, Shay T, Miller J, Greter M, Jakubzick C, Ivanov S, et al. Gene-expression profiles and transcriptional regulatory pathways that underlie the identity and diversity of mouse tissue macrophages. *Nat Immunol*. 2012;13(11):1118-28.

154. Shipkova M, Wieland E. Surface markers of lymphocyte activation and markers of cell proliferation. *Clin Chim Acta*. 2012;413(17-18):1338-49.

155. Geissmann F, Manz MG, Jung S, Sieweke MH, Merad M, Ley K. Development of monocytes, macrophages, and dendritic cells. *Science*. 2010;327(5966):656-61.

156. Rosenblum MD, Way SS, Abbas AK. Regulatory T cell memory. *Nat Rev Immunol*. 2016;16(2):90-101.

157. von Andrian UH, Mempel TR. Homing and cellular traffic in lymph nodes. *Nat Rev Immunol*. 2003;3(11):867-78.

158. Fazekas de St Groth B, Smith AL, Higgins CA. T cell activation: in vivo veritas. I*mmunol Cell Biol*. 2004;82(3):260-8.

159. Hori S, Nomura T, Sakaguchi S. Control of regulatory T cell development by the transcription factor Foxp3. *Science*. 2003;299(5609):1057-61.

160. Wang C, Collins M, Kuchroo VK. Effector T cell differentiation: are master regulators of effector T cells still the masters? *Curr Opin Immunol*. 2015;37:6-10.

161. Yamane H, Zhu J, Paul WE. Independent roles for IL-2 and GATA-3 in stimulating naive CD4+ T cells to generate a Th2-inducing cytokine environment. *J Exp Med*. 2005;202(6):793-804.

162. Wang X, Mosmann T. In vivo priming of CD4 T cells that produce interleukin (IL)-2 but not IL-4 or interferon (IFN)-gamma, and can subsequently differentiate into IL-4- or IFN-gamma-secreting cells. *J Exp Med*. 2001;194(8):1069-80.

163. Yamane H, Paul WE. Early signaling events that underlie fate decisions of naive CD4(+) T cells toward distinct T-helper cell subsets. *Immunol Rev*. 2013;252(1):12-23.

164. Oestreich KJ, Huang AC, Weinmann AS. The lineage-defining factors T-bet and Bcl-6 collaborate to regulate Th1 gene expression patterns. *J Exp Med*. 2011;208(5):1001-13.

165. Wohlfert EA, Grainger JR, Bouladoux N, Konkel JE, Oldenhove G, Ribeiro CH, et al. GATA3 controls Foxp3$^+$ regulatory T cell fate during inflammation in mice. *J Clin Invest*. 2011;121(11):4503-15.

166. Feng T, Cao AT, Weaver CT, Elson CO, Cong Y. Interleukin-12 converts Foxp3+ regulatory T cells to interferon-γ-producing Foxp3+ T cells that inhibit colitis. *Gastroenterology*. 2011;140(7):2031-43.

167. Drappier M, Michiels T. Inhibition of the OAS/RNase L pathway by viruses. *Curr Opin Virol*. 2015;15:19-26.

168. Justesen J, Hartmann R, Kjeldgaard NO. Gene structure and function of the 2'-5'-oligoadenylate synthetase family. *Cell Mol Life Sci*. 2000;57(11):1593-612.

169. Szklarczyk D, Franceschini A, Wyder S, Forslund K, Heller D, Huerta-Cepas J, et al. STRING v10: protein-protein interaction networks, integrated over the tree of life. *Nucleic Acids Res*. 2015;43(Database issue):D447-52.

170. Matys V, Kel-Margoulis OV, Fricke E, Liebich I, Land S, Barre-Dirrie A, et al. TRANSFAC and its module TRANSCompel: transcriptional gene regulation in eukaryotes. *Nucleic Acids Res*. 2006;34(Database issue):D108-10.

171. Moyerbrailean GA, Davis GO, Harvey CT, Watza D, Wen X, Pique-Regi R, et al. A high-throughput RNA-seq approach to profile transcriptional responses. *Sci Rep*. 2015;5:14976.

172. Katze MG, He Y, Gale M. Viruses and interferon: a fight for supremacy. *Nat Rev Immunol*. 2002;2(9):675-87.

173. Taniguchi T, Ogasawara K, Takaoka A, Tanaka N. IRF family of transcription factors as regulators of host defense. *Annu Rev Immunol*. 2001;19:623-55.

174. Ouyang W, Löhning M, Gao Z, Assenmacher M, Ranganath S, Radbruch A, et al. Stat6-independent GATA-3 autoactivation directs IL-4-independent Th2 development and commitment. *Immunity*. 2000;12(1):27-37.

175. Liu Z, Liu Q, Hamed H, Anthony RM, Foster A, Finkelman FD, et al. IL-2 and autocrine IL-4 drive the in vivo development of antigen-specific Th2 T cells elicited by nematode parasites. *J Immunol*. 2005;174(4):2242-9.

176. Gutcher I, Donkor MK, Ma Q, Rudensky AY, Flavell RA, Li MO. Autocrine transforming growth factor-β1 promotes in vivo Th17 cell differentiation. *Immunity*. 2011;34(3):396-408.

177. Mosmann TR, Coffman RL. TH1 and TH2 cells: different patterns of lymphokine secretion lead to different functional properties. *Annu Rev Immunol*. 1989;7:145-73.

178. Bettelli E, Carrier Y, Gao W, Korn T, Strom TB, Oukka M, et al. Reciprocal developmental pathways for the generation of pathogenic effector TH17 and regulatory T cells. *Nature*. 2006;441(7090):235-8.

179. Hori S, Nomura T, Sakaguchi S. Pillars Article: Control of Regulatory T Cell Development by the Transcription Factor Foxp3. Science 2003. 299: 1057-1061. *J Immunol*. 2017;198(3):981-5.

180. Nakamura K, Kitani A, Strober W. Cell contact-dependent immunosuppression by CD4(+)CD25(+) regulatory T cells is mediated by cell surface-bound transforming growth factor beta. *J Exp Med*. 2001;194(5):629-44.

181. Burkhart C, Liu GY, Anderton SM, Metzler B, Wraith DC. Peptide-induced T cell regulation of experimental autoimmune encephalomyelitis: a role for IL-10. *Int Immunol*. 1999;11(10):1625-34.

182. Rubtsov YP, Rasmussen JP, Chi EY, Fontenot J, Castelli L, Ye X, et al. Regulatory T cell-derived interleukin-10 limits inflammation at environmental interfaces. *Immunity*. 2008;28(4):546-58.

183. Sansom DM, Walker LS. The role of CD28 and cytotoxic T-lymphocyte antigen-4 (CTLA-4) in regulatory T-cell biology. *Immunol Rev*. 2006;212:131-48.

184. Wing K, Onishi Y, Prieto-Martin P, Yamaguchi T, Miyara M, Fehervari Z, et al. CTLA-4 control over Foxp3+ regulatory T cell function. *Science*. 2008;322(5899):271-5.

185. Ueda H, Howson JM, Esposito L, Heward J, Snook H, Chamberlain G, et al. Association of the T-cell regulatory gene CTLA4 with susceptibility to autoimmune disease. *Nature*. 2003;423(6939):506-11.

186. Iezzi G, Karjalainen K, Lanzavecchia A. The duration of antigenic stimulation determines the fate of naive and effector T cells. *Immunity*. 1998;8(1):89-95.

187. Karulin AY, Hesse MD, Tary-Lehmann M, Lehmann PV. Single-cytokine-producing CD4 memory cells predominate in type 1 and type 2 immunity. *J Immunol*. 2000;164(4):1862-72.

188. Sallusto F, Mackay CR, Lanzavecchia A. Selective expression of the eotaxin receptor CCR3 by human T helper 2 cells. *Science*. 1997;277(5334):2005-7.

189. Acosta-Rodriguez EV, Rivino L, Geginat J, Jarrossay D, Gattorno M, Lanzavecchia A, et al. Surface phenotype and antigenic specificity of human interleukin 17-producing T helper memory cells. *Nat Immunol*. 2007;8(6):639-46.

190. Huber JP, Ramos HJ, Gill MA, Farrar JD. Cutting edge: Type I IFN reverses human Th2 commitment and stability by suppressing GATA3. *J Immunol*. 2010;185(2):813-7.

191. Bluyssen AR, Durbin JE, Levy DE. ISGF3 gamma p48, a specificity switch for interferon activated transcription factors. *Cytokine Growth Factor Rev*. 1996;7(1):11-7.

192. Kuwahara M, Yamashita M, Shinoda K, Tofukuji S, Onodera A, Shinnakasu R, et al. The transcription factor Sox4 is a downstream target of signaling by the cytokine TGF-β and suppresses T(H)2 differentiation. *Nat Immunol*. 2012;13(8):778-86.

193. Higuchi T, Nakayama T, Arao T, Nishio K, Yoshie O. SOX4 is a direct target gene of FRA-2 and induces expression of HDAC8 in adult T-cell leukemia/lymphoma. *Blood*. 2013;121(18):3640-9.

194. Okkenhaug K, Patton DT, Bilancio A, Garçon F, Rowan WC, Vanhaesebroeck B. The p110delta isoform of phosphoinositide 3-kinase controls clonal expansion and differentiation of Th cells. *J Immunol*. 2006;177(8):5122-8.

195. Nagai S, Kurebayashi Y, Koyasu S. Role of PI3K/Akt and mTOR complexes in Th17 cell differentiation. *Ann N Y Acad Sci*. 2013;1280:30-4.

196. Harada Y, Elly C, Ying G, Paik JH, DePinho RA, Liu YC. Transcription factors Foxo3a and Foxo1 couple the E3 ligase Cbl-b to the induction of Foxp3 expression in induced regulatory T cells. *J Exp Med*. 2010;207(7):1381-91.

197. Sauer S, Bruno L, Hertweck A, Finlay D, Leleu M, Spivakov M, et al. T cell receptor signaling controls Foxp3 expression via PI3K, Akt, and mTOR. *Proc Natl Acad Sci USA*. 2008;105(22):7797-802.

198. Kurebayashi Y, Nagai S, Ikejiri A, Ohtani M, Ichiyama K, Baba Y, et al. PI3K-Akt-mTORC1-S6K1/2 axis controls Th17 differentiation by regulating Gfi1 expression and nuclear translocation of RORγ. *Cell Rep*. 2012;1(4):360-73.

199. Lainé A, Martin B, Luka M, Mir L, Auffray C, Lucas B, et al. Foxo1 Is a T Cell-Intrinsic Inhibitor of the RORγt-Th17 Program. *J Immunol*. 2015;195(4):1791-803.

200. Tzartos JS, Friese MA, Craner MJ, Palace J, Newcombe J, Esiri MM, et al. Interleukin-17 production in central nervous system-infiltrating T cells and glial cells is associated with active disease in multiple sclerosis. *Am J Pathol*. 2008;172(1):146-55.

201. Fletcher JM, Lalor SJ, Sweeney CM, Tubridy N, Mills KH. T cells in multiple sclerosis and experimental autoimmune encephalomyelitis. *Clin Exp Immunol*. 2010;162(1):1-11.

202. Stephen-Victor E, Fickenscher H, Bayry J. IL-26: An Emerging Proinflammatory Member of the IL-10 Cytokine Family with Multifaceted Actions in Antiviral, Antimicrobial, and Autoimmune Responses. *PLoS Pathog*. 2016;12(6):e1005624.

203. Schmitt N, Ueno H. Regulation of human helper T cell subset differentiation by cytokines. *Curr Opin Immunol*. 2015;34:130-6.

204. Paulson JC. Innate immune response triggers lupus-like autoimmune disease. *Cell*. 2007;130(4):589-91.

205. Vieira Braga FA, Teichmann SA, Chen X. Genetics and immunity in the era of single-cell genomics. *Hum Mol Genet*. 2016;25(R2):R141-R8.

206. Mahata B, Zhang X, Kolodziejczyk AA, Proserpio V, Haim-Vilmovsky L, Taylor AE, et al. Single-cell RNA sequencing reveals T helper cells synthesizing steroids de novo to contribute to immune homeostasis. *Cell Rep*. 2014;7(4):1130-42.

207. Trapnell C, Cacchiarelli D, Grimsby J, Pokharel P, Li S, Morse M, et al. The dynamics and regulators of cell fate decisions are revealed by pseudotemporal ordering of single cells. *Nat Biotechnol*. 2014;32(4):381-6.

208. Okada Y, Wu D, Trynka G, Raj T, Terao C, Ikari K, et al. Genetics of rheumatoid arthritis contributes to biology and drug discovery. *Nature*. 2014;506(7488):376-81.

209. Beecham AH, Patsopoulos NA, Xifara DK, Davis MF, Kemppinen A, Cotsapas C, et al. Analysis of immune-related loci identifies 48 new susceptibility variants for multiple sclerosis. *Nat Genet*. 2013;45(11):1353-60.

210. Liu JZ, van Sommeren S, Huang H, Ng SC, Alberts R, Takahashi A, et al. Association analyses identify 38 susceptibility loci for inflammatory bowel disease and highlight shared genetic risk across populations. *Nat Genet*. 2015;47(9):979-86.

211. Farh KK, Marson A, Zhu J, Kleinewietfeld M, Housley WJ, Beik S, et al. Genetic and epigenetic fine mapping of causal autoimmune disease variants. *Nature*. 2015;518(7539):337-43.

212. Hu X, Kim H, Stahl E, Plenge R, Daly M, Raychaudhuri S. Integrating autoimmune risk loci with gene-expression data identifies specific pathogenic immune cell subsets. *Am J Hum Genet*. 2011;89(4):496-506.

213. Barski A, Cuddapah S, Cui K, Roh TY, Schones DE, Wang Z, et al. High-resolution profiling of histone methylations in the human genome. *Cell*. 2007;129(4):823-37.

214. Johnson DS, Mortazavi A, Myers RM, Wold B. Genome-wide mapping of in vivo protein-DNA interactions. *Science*. 2007;316(5830):1497-502.

215. Trynka G, Sandor C, Han B, Xu H, Stranger BE, Liu XS, et al. Chromatin marks identify critical cell types for fine mapping complex trait variants. *Nat Genet*. 2013;45(2):124-30.

216. Buenrostro JD, Giresi PG, Zaba LC, Chang HY, Greenleaf WJ. Transposition of native chromatin for fast and sensitive epigenomic profiling of open chromatin, DNA-binding proteins and nucleosome position. *Nat Methods*. 2013;10(12):1213-8.

217. Raj A, Shim H, Gilad Y, Pritchard JK, Stephens M. msCentipede: Modeling Heterogeneity across Genomic Sites and Replicates Improves Accuracy in the Inference of Transcription Factor Binding. *PLoS One*. 2015;10(9):e0138030.

# 7. Appendix

In this appendix I present the complete data from the differential gene expression analysis for conditions discussed throughout this thesis. These analyses were performed using the Wald's Test implemented in DESeq2 version 1.16.1 with thresholds of BH-adjusted P value < 0.05 and log-fold changes > 1. The conditions for which almost no differential expression is observed, as well as the genes for which no annotated protein was found, have been omitted from this appendix.

**Supplementary table 1** Genes differentially expressed in $CD4^+$ T cells 16 hours of polarisation with IFN-ß. Gene expression was compared to stimulated, unpolarised (Th0) cells used as control. Genes are ordered by Log2-fold change.

| Gene Name | Log2(Base Mean Count) | Log2FC | P adjusted |
|---|---|---|---|
| MX1 | 9.48 | 5.31 | 6.18E-236 |
| IFI6 | 7.02 | 5.15 | 4.19E-235 |
| OAS1 | 6.63 | 4.93 | 4.25E-214 |
| IFIT2 / ISG54 | 7.53 | 4.68 | 1.34E-201 |
| HERC6 | 7.24 | 4.65 | 5.79E-202 |
| IFI44L | 8.99 | 4.49 | 2.87E-163 |
| MX2 | 8.19 | 4.37 | 3.98E-155 |
| USP18 / ISG43 | 5.99 | 4.36 | 2.72E-165 |
| IFI44 | 7.31 | 4.23 | 5.81E-164 |
| IFIT3 / ISG60 | 9.47 | 4.21 | 2.03E-143 |
| OAS2 | 9.45 | 4.14 | 0.00E+00 |
| CXCL10 | 7.92 | 3.91 | 4.14E-132 |
| ISG20 | 7.19 | 3.90 | 2.28E-144 |
| HERC5 / CEBP1 | 6.06 | 3.72 | 7.86E-117 |
| TNFSF10 / APO2L | 7.91 | 3.60 | 9.06E-159 |
| PLSCR1 | 6.95 | 3.52 | 4.06E-108 |
| DDX60 | 7.23 | 3.49 | 9.63E-115 |
| IFIT1 / ISG56 | 7.15 | 3.48 | 3.38E-132 |
| CMPK2 | 6.99 | 3.47 | 3.40E-100 |
| SAMD9L | 8.38 | 3.46 | 2.79E-105 |
| OAS3 | 8.36 | 3.44 | 1.38E-95 |
| ISG15 | 6.09 | 3.39 | 8.11E-97 |
| EIF2AK2 | 8.61 | 3.36 | 1.66E-185 |
| SPATS2L | 5.56 | 3.19 | 2.58E-85 |
| HSH2D | 6.29 | 3.12 | 3.57E-83 |
| DDX60L | 6.98 | 3.08 | 1.36E-94 |
| OASL | 5.39 | 2.99 | 9.29E-79 |
| TRIM22 | 9.51 | 2.93 | 2.50E-146 |
| CD38 | 8.40 | 2.92 | 3.91E-100 |
| RSAD2 | 7.62 | 2.91 | 1.68E-73 |
| LAMP3 | 8.21 | 2.85 | 1.01E-108 |
| CD225 / IFI7 | 7.65 | 2.79 | 1.40E-100 |
| DDX58 | 6.46 | 2.73 | 4.91E-65 |
| TRANK1 | 7.10 | 2.69 | 2.98E-64 |

| | | | |
|---|---|---|---|
| SAMD9 | 6.86 | 2.67 | 1.25E-63 |
| ZBTB32 | 6.10 | 2.65 | 6.40E-59 |
| IFI35 | 6.94 | 2.65 | 1.22E-67 |
| DHX58 | 5.91 | 2.63 | 1.84E-57 |
| HELZ2 | 6.94 | 2.61 | 5.18E-62 |
| IFIH1 | 7.52 | 2.60 | 5.23E-81 |
| NT5C3A | 8.37 | 2.60 | 9.91E-120 |
| XAF1 | 6.59 | 2.50 | 1.11E-57 |
| SAT1 | 7.59 | 2.42 | 2.24E-73 |
| NEXN | 5.45 | 2.22 | 5.71E-40 |
| EPSTI1 | 7.49 | 2.19 | 8.83E-39 |
| IFIT5 / ISG58 | 7.61 | 2.09 | 3.69E-55 |
| SSTR3 | 4.90 | 2.08 | 5.84E-39 |
| TYMP / ECGF1 | 6.46 | 2.07 | 6.44E-38 |
| PARP10 | 6.79 | 2.06 | 1.73E-37 |
| STAT2 | 8.23 | 2.05 | 1.51E-62 |
| TRIM25 / ZNF147 | 9.21 | 2.03 | 1.20E-83 |
| PARP9 | 8.37 | 1.99 | 4.32E-62 |
| LGALS9 | 6.33 | 1.94 | 3.81E-32 |
| SP100 | 9.08 | 1.93 | 3.52E-71 |
| KIAA1671 | 6.54 | 1.89 | 1.11E-34 |
| DTX3L | 8.55 | 1.84 | 6.21E-50 |
| SLFN12L | 6.77 | 1.83 | 3.82E-33 |
| SP110 | 6.58 | 1.83 | 5.78E-33 |
| PARP12 | 7.04 | 1.80 | 2.52E-30 |
| BST2 | 7.11 | 1.79 | 1.13E-35 |
| TNFSF13B / BAFF | 4.77 | 1.79 | 1.46E-27 |
| NMI | 7.57 | 1.78 | 4.22E-41 |
| RYDEN | 6.50 | 1.76 | 1.07E-29 |
| PPM1K | 8.10 | 1.75 | 1.33E-45 |
| TDRD7 | 5.01 | 1.69 | 1.99E-23 |
| XIRP1 | 6.91 | 1.66 | 2.90E-26 |
| LMO7 / FBX20 | 7.16 | 1.66 | 8.04E-26 |
| IGFBP4 | 6.20 | 1.66 | 5.59E-24 |
| PHF11 | 7.95 | 1.64 | 2.35E-34 |
| PARP14 / BAL2 | 10.00 | 1.63 | 3.79E-30 |
| WDFY1 | 8.33 | 1.61 | 3.05E-34 |
| SP140 | 7.11 | 1.55 | 1.77E-27 |
| LGALS3BP | 6.88 | 1.54 | 9.54E-25 |
| DPP4 / CD26 | 7.24 | 1.54 | 8.19E-22 |
| NUB1 | 7.99 | 1.53 | 1.01E-38 |
| ADAM19 | 7.19 | 1.50 | 3.97E-22 |
| EHD4 | 8.64 | 1.49 | 9.90E-49 |
| PI4K2B | 6.83 | 1.45 | 7.72E-18 |
| GBP1 | 9.85 | 1.44 | 3.23E-39 |
| IFI16 | 10.45 | 1.40 | 1.93E-64 |
| CHMP5 | 7.51 | 1.38 | 1.19E-20 |
| IL18RAP / IL1R7 | 6.30 | 1.38 | 4.11E-17 |
| IRF8 | 10.78 | 1.37 | 8.27E-53 |
| APOL1 | 8.47 | 1.37 | 8.93E-23 |
| MOV10 | 6.31 | 1.36 | 1.59E-16 |
| LIF | 9.90 | 1.36 | 2.29E-15 |

| | | | |
|---|---|---|---|
| FBXO6 | 5.96 | 1.36 | 2.92E-15 |
| PGAP1 | 7.98 | 1.35 | 1.21E-14 |
| ZCCHC2 | 8.23 | 1.33 | 4.65E-31 |
| TRAFD1 | 8.55 | 1.33 | 2.06E-34 |
| SLFN13 | 5.06 | 1.32 | 3.71E-14 |
| HELB | 7.93 | 1.31 | 2.13E-25 |
| TRIM5 | 6.52 | 1.31 | 7.50E-16 |
| PML | 7.52 | 1.29 | 5.43E-21 |
| SIDT1 | 6.45 | 1.28 | 3.73E-15 |
| TRIM21 | 7.33 | 1.27 | 1.70E-20 |
| IL12RB2 | 9.49 | 1.26 | 9.13E-14 |
| RASGRP3 | 4.50 | 1.25 | 3.69E-14 |
| IFITM3 | 4.80 | 1.25 | 2.62E-13 |
| LAP3 | 8.66 | 1.24 | 1.60E-32 |
| DENND1B | 6.36 | 1.22 | 7.20E-14 |
| RP2 | 5.90 | 1.22 | 2.09E-12 |
| XRN1 | 9.57 | 1.20 | 3.55E-22 |
| PRDM1 | 5.69 | 1.19 | 1.07E-11 |
| IL21 | 5.66 | 1.19 | 1.93E-11 |
| PLAC8 | 5.67 | 1.18 | 2.49E-11 |
| MYD88 | 7.93 | 1.18 | 1.40E-21 |
| RNF213 | 11.46 | 1.17 | 7.92E-13 |
| SPSB1 | 4.59 | 1.17 | 3.27E-12 |
| UBE2L6 | 9.00 | 1.17 | 8.84E-28 |
| SLFN5 | 7.46 | 1.17 | 4.87E-11 |
| MIER1 | 9.40 | 1.14 | 1.20E-23 |
| NCOA7 | 9.13 | 1.14 | 5.11E-30 |
| MASTL | 6.28 | 1.12 | 5.38E-11 |
| KIAA0040 | 7.03 | 1.11 | 1.28E-12 |
| IL10RA | 6.40 | 1.10 | 6.63E-10 |
| CTSS | 7.93 | 1.09 | 1.02E-18 |
| KLF6 | 10.02 | 1.08 | 5.91E-30 |
| IFITM2 | 6.70 | 1.07 | 1.31E-11 |
| ANXA1 | 7.03 | 1.07 | 5.91E-12 |
| PNPT1 | 9.80 | 1.06 | 2.28E-32 |
| YEATS2 | 8.13 | 1.05 | 8.15E-16 |
| ANK3 | 8.49 | 1.04 | 2.61E-17 |
| UBA7 | 6.54 | 1.04 | 1.17E-09 |
| ADAR | 11.41 | 1.04 | 4.63E-43 |
| APOL2 | 8.97 | 1.04 | 7.98E-19 |
| SYTL3 | 6.52 | 1.04 | 2.20E-09 |
| UNC93B1 | 5.08 | 1.03 | 1.12E-08 |
| SIPA1L2 | 6.61 | 1.02 | 7.12E-09 |
| SMCHD1 | 10.36 | 1.01 | 6.04E-33 |
| FAS | 7.68 | 1.01 | 2.35E-12 |
| IRF9 / ISGF3G | 6.53 | 1.00 | 1.94E-08 |
| TTC39B | 6.86 | 1.00 | 7.82E-10 |

**Supplementary table 2** Genes differentially expressed in Th1 cells after five days of polarisation. Gene expression was compared to stimulated, unpolarised (Th0) cells used as control. Genes are ordered by Log2-fold change, and up and downregulation are separated within the table.

| Gene Name | Log2( Base Mean Count) | Log2FC | P adjusted |
|---|---|---|---|
| IFNG | 6.91 | 3.19 | 1.07E-20 |
| IL12RB | 5.36 | 1.66 | 1.46E-04 |
| IL1RL1 | 3.59 | 1.65 | 1.80E-04 |
| MYO1B | 2.35 | 1.59 | 2.52E-06 |
| AT2B4 | 4.69 | 1.58 | 1.80E-04 |
| IL18RAP | 6.99 | 1.54 | 2.21E-05 |
| GTPB8 | 4.45 | 1.52 | 1.12E-03 |
| ANXA3 | 4.76 | 1.47 | 1.16E-03 |
| TBX21 / TBET | 6.54 | 1.46 | 3.47E-05 |
| AT8B4 | 2.68 | 1.39 | 3.27E-04 |
| BBS12 | 4.72 | 1.39 | 2.00E-03 |
| STEA1 | 9.74 | 1.39 | 1.67E-06 |
| IL31R | 4.81 | 1.37 | 2.43E-03 |
| TIAM2 | 5.13 | 1.35 | 4.18E-03 |
| COE4 | 7.31 | 1.33 | 3.47E-05 |
| GRAH | 5.16 | 1.29 | 1.05E-02 |
| IL18R | 4.82 | 1.26 | 1.97E-02 |
| SKT | 2.04 | 1.26 | 2.88E-03 |
| IRAK3 | 6.62 | 1.24 | 3.47E-05 |
| BCAP | 6.99 | 1.21 | 2.73E-03 |
| CBPM | 6.66 | 1.20 | 9.44E-03 |
| MCTP2 | 7.03 | 1.20 | 2.73E-03 |
| WNT11 | 7.03 | 1.20 | 5.02E-03 |
| EPS8 | 5.76 | 1.19 | 1.86E-02 |
| ITA3 | 6.50 | 1.16 | 1.12E-03 |
| ITAX | 5.51 | 1.15 | 3.45E-02 |
| P2RX5 | 7.42 | 1.15 | 4.61E-03 |
| M3K8 | 7.13 | 1.14 | 4.43E-03 |
| LAS2 | 8.71 | 1.11 | 1.57E-03 |
| ITA6 | 6.30 | 1.10 | 8.90E-03 |
| DMD | 8.46 | 1.08 | 9.91E-06 |
| TLR1 | 5.63 | 1.08 | 2.66E-02 |
| DGKI | 7.12 | 1.07 | 4.61E-03 |
| CLMN | 10.25 | 1.03 | 1.46E-05 |
| TIFA | 6.89 | 1.02 | 2.50E-03 |
| IL21 | 8.31 | 1.00 | 2.82E-02 |
| S100A4 | 9.06 | -1.00 | 7.07E-06 |
| C1orf162 | 6.23 | -1.02 | 1.51E-02 |
| STMN3 | 5.70 | -1.04 | 2.06E-02 |
| VIM | 11.64 | -1.07 | 1.65E-05 |
| SESN3 | 10.13 | -1.17 | 1.86E-02 |
| ITM2C | 7.42 | -1.18 | 8.16E-03 |
| LY9 | 6.96 | -1.20 | 1.31E-02 |
| NEK6 | 6.27 | -1.30 | 6.99E-03 |
| MAN1C1 | 7.64 | -1.40 | 2.74E-04 |

**Supplementary table 3** Genes differentially expressed in Th2 after five days of polarisation. Gene expression was compared to stimulated, unpolarised (Th0) cells used as control. Genes are ordered by Log2-fold change, and up and downregulation are separated within the table.

| Gene Name | Log2( Base Mean ) | Log2FC | P adjusted |
|---|---|---|---|
| ENPP1 | 4.57 | 4.66 | 3.02E-47 |
| MYO3B | 4.22 | 4.43 | 1.57E-43 |
| PTGIS | 4.91 | 4.36 | 3.89E-40 |
| AKAP12 | 6.52 | 4.16 | 4.94E-43 |
| TPRG1 | 6.00 | 3.49 | 5.27E-41 |
| DYNC2LI1 | 6.27 | 3.05 | 2.26E-24 |
| IL1RA | 6.28 | 2.88 | 3.04E-18 |
| ANK1 | 5.21 | 2.87 | 4.71E-18 |
| CALD1 | 5.14 | 2.72 | 8.56E-15 |
| BATF3 | 6.95 | 2.61 | 2.72E-17 |
| ABHD6 | 5.06 | 2.60 | 1.03E-16 |
| AGAP9 | 4.80 | 2.59 | 4.20E-15 |
| TNFSF11 | 3.50 | 2.58 | 6.44E-14 |
| PLEKHH2 | 4.24 | 2.51 | 9.60E-13 |
| MRPS26 | 7.40 | 2.50 | 5.70E-26 |
| DAPK1 | 3.95 | 2.44 | 6.01E-12 |
| HOMER2 | 5.08 | 2.42 | 1.60E-12 |
| SLC39A14 | 8.14 | 2.38 | 3.11E-18 |
| NCS1 | 5.99 | 2.38 | 6.44E-14 |
| CLDN1 | 5.29 | 2.37 | 1.95E-11 |
| PPP1R14A | 2.55 | 2.36 | 1.68E-18 |
| GATA3 | 8.79 | 2.35 | 3.04E-18 |
| ADGRA3 | 5.88 | 2.33 | 1.58E-17 |
| LIMA1 | 9.28 | 2.27 | 1.49E-18 |
| HIP1 | 5.49 | 2.26 | 6.44E-14 |
| TGFBR3 | 6.73 | 2.18 | 1.79E-14 |
| RRS1 | 6.64 | 2.17 | 5.07E-11 |
| RNF125 | 8.37 | 2.14 | 1.53E-18 |
| MRC2 | 5.54 | 2.09 | 1.92E-10 |
| BCAR3 | 4.89 | 2.09 | 8.35E-09 |
| MYL9 | 3.16 | 2.05 | 3.66E-09 |
| PIP5K1B | 4.03 | 2.01 | 3.51E-08 |
| SLIT3 | 3.48 | 1.99 | 2.33E-08 |
| IGF2BP3 | 3.44 | 1.98 | 2.92E-08 |
| C10orf128 | 4.76 | 1.92 | 1.54E-07 |
| GAD1 | 4.17 | 1.86 | 6.31E-07 |
| RNF43 | 4.44 | 1.82 | 3.29E-07 |
| PLA2G4A | 2.67 | 1.80 | 5.85E-08 |
| SPINT2 | 7.47 | 1.79 | 1.05E-11 |
| HRH1 | 2.47 | 1.78 | 4.28E-08 |
| RBM47 | 5.52 | 1.77 | 6.41E-07 |
| GPC1 | 4.28 | 1.76 | 1.83E-06 |
| RXRA | 5.63 | 1.75 | 7.07E-07 |
| DUSP6 | 7.86 | 1.75 | 1.22E-08 |
| ATP6V0A2 | 8.14 | 1.71 | 2.73E-09 |

| | | | |
|---|---|---|---|
| IGSF3 | 4.20 | 1.69 | 9.77E-06 |
| GNRH2 | 2.11 | 1.68 | 8.35E-09 |
| PDE7B | 4.66 | 1.68 | 7.00E-06 |
| PPCDC | 5.31 | 1.66 | 2.44E-07 |
| FBLN5 | 5.58 | 1.65 | 5.44E-06 |
| RAB6B | 3.75 | 1.63 | 2.16E-05 |
| AOAH | 6.12 | 1.62 | 3.16E-07 |
| NRP1 | 2.76 | 1.59 | 2.53E-06 |
| ITPRIPL2 | 4.84 | 1.54 | 7.07E-05 |
| GAB2 | 7.71 | 1.54 | 4.33E-06 |
| ALDH2 | 3.53 | 1.51 | 0.000125207 |
| ENPP3 | 3.85 | 1.51 | 9.07E-05 |
| CDC42BPA | 6.11 | 1.50 | 3.05E-06 |
| NDFIP2 | 9.12 | 1.49 | 1.82E-22 |
| EGR1 | 7.89 | 1.48 | 1.95E-07 |
| KIAA1462 | 3.26 | 1.48 | 0.000142763 |
| FZD3 | 5.12 | 1.45 | 3.11E-05 |
| MGST3 | 6.89 | 1.43 | 5.14E-09 |
| CSF1 | 7.80 | 1.43 | 6.10E-07 |
| PTGS2 / COX2 | 3.59 | 1.41 | 0.000181351 |
| SEMA4A | 6.45 | 1.41 | 0.000315121 |
| SLC7A8 | 5.12 | 1.40 | 0.000506262 |
| KLF7 | 8.34 | 1.39 | 8.31E-08 |
| ASIC1 / BNAC2 | 5.22 | 1.39 | 5.27E-05 |
| NFIL3 / L3BP1 | 8.95 | 1.39 | 6.01E-12 |
| LRRC32 | 3.82 | 1.38 | 0.00054911 |
| NEK6 | 6.27 | 1.38 | 0.000180809 |
| UBP41 | 2.63 | 1.37 | 0.000311074 |
| LMNA | 7.97 | 1.37 | 1.65E-06 |
| CDC45 | 7.99 | 1.37 | 6.75E-11 |
| S1PR3 | 2.45 | 1.34 | 0.000131901 |
| RGS9 | 4.50 | 1.34 | 0.000566806 |
| CMSS1 | 6.96 | 1.34 | 7.75E-06 |
| PLAU | 3.29 | 1.32 | 0.000878379 |
| PTPN14 | 6.78 | 1.32 | 0.00142904 |
| RAI14 | 3.30 | 1.32 | 0.001088782 |
| TBC1D4 | 8.57 | 1.31 | 1.06E-12 |
| FOXB1 | 4.39 | 1.31 | 0.001563392 |
| IL17RB | 3.57 | 1.31 | 0.001481053 |
| CTH | 5.78 | 1.31 | 0.000377895 |
| EGR3 | 7.30 | 1.31 | 7.46E-06 |
| EML5 | 5.01 | 1.29 | 0.00130589 |
| EGR2 | 7.01 | 1.28 | 3.53E-05 |
| DFNA5 | 6.38 | 1.28 | 0.000109718 |
| GJB6 | 3.83 | 1.27 | 0.002359302 |
| S100P | 1.94 | 1.27 | 0.000180611 |
| CTNNBIP1 | 5.94 | 1.26 | 0.000210807 |
| CEP55 | 9.03 | 1.25 | 2.15E-09 |
| EVI5 | 7.29 | 1.24 | 1.09E-06 |
| ENTPD1 | 5.06 | 1.24 | 0.002939732 |
| CHDH | 2.44 | 1.24 | 0.000445207 |
| SLC37A3 | 8.05 | 1.23 | 1.68E-09 |

| | | | |
|---|---|---|---|
| ETFB | 7.08 | 1.23 | 3.34E-06 |
| ZBED3 | 5.11 | 1.23 | 0.001914833 |
| MAOA | 6.41 | 1.22 | 5.81E-10 |
| SH3RF2 | 2.18 | 1.22 | 0.000733861 |
| ATF5 | 6.50 | 1.22 | 0.000153517 |
| TP63 | 2.12 | 1.22 | 0.000629179 |
| SCPEP1 | 6.24 | 1.21 | 0.000129851 |
| KCNC4 | 7.18 | 1.21 | 6.23E-05 |
| CALCB | 4.07 | 1.21 | 0.004258309 |
| ABCC4 | 6.05 | 1.21 | 0.00030792 |
| ITGA11 | 3.94 | 1.21 | 0.003963703 |
| NTRK1 | 5.64 | 1.20 | 0.003082133 |
| PHEX | 4.88 | 1.20 | 0.001686029 |
| SIGLEC10 | 3.05 | 1.19 | 0.004302236 |
| TNFSF14 | 7.19 | 1.19 | 1.83E-05 |
| CD86 / CD28L2 | 3.26 | 1.19 | 0.003882017 |
| FAM110B | 2.83 | 1.17 | 0.002292625 |
| NKG7 | 5.95 | 1.16 | 0.003521039 |
| OPLAH | 4.81 | 1.15 | 0.004632217 |
| IL10RA | 8.70 | 1.14 | 6.10E-07 |
| TUBB4A | 3.89 | 1.14 | 0.008398702 |
| IFFO2 | 7.81 | 1.13 | 7.93E-07 |
| B3GNT5 | 5.63 | 1.13 | 0.001587811 |
| CAPSL | 2.67 | 1.13 | 0.006101939 |
| THBS4 | 3.53 | 1.13 | 0.009928716 |
| CTNS | 6.84 | 1.12 | 6.23E-05 |
| SLC26A6 | 7.04 | 1.12 | 0.000131856 |
| PSTPIP2 | 6.73 | 1.12 | 2.16E-05 |
| OCC1 | 8.13 | 1.12 | 2.53E-07 |
| GPR35 | 4.93 | 1.11 | 0.006914292 |
| VSIG10L | 4.92 | 1.11 | 0.01026285 |
| IKZF2 / HELIOS | 4.30 | 1.11 | 0.0116774 |
| ZNF697 | 3.09 | 1.11 | 0.010084007 |
| PLCL1 | 5.42 | 1.11 | 0.007666693 |
| KIF1A | 6.45 | 1.11 | 0.003738018 |
| PIGM | 6.17 | 1.10 | 0.00039659 |
| RNF11 | 7.50 | 1.09 | 3.05E-06 |
| MAP1B | 4.86 | 1.09 | 0.014619415 |
| ZNF282 | 8.18 | 1.09 | 9.38E-06 |
| CTNNAL1 | 7.60 | 1.08 | 0.000109718 |
| ABCD3 | 7.05 | 1.08 | 1.35E-05 |
| MICAL2 | 9.76 | 1.08 | 3.13E-07 |
| PHLDA1 | 7.08 | 1.08 | 0.002787641 |
| EPHB1 | 1.50 | 1.07 | 0.000293062 |
| SLC26A4 | 4.14 | 1.07 | 0.014588392 |
| SLC26A11 | 5.12 | 1.06 | 0.007443992 |
| TNFRSF9 / CD137 | 6.61 | 1.06 | 0.008492994 |
| HSPA5 / GRP78 | 11.65 | 1.06 | 9.78E-07 |
| RASGRP4 | 7.08 | 1.06 | 0.00319166 |
| ZFYVE28 | 5.50 | 1.06 | 0.002981664 |
| REEP2 | 4.30 | 1.06 | 0.014344994 |
| CTTN | 6.51 | 1.05 | 0.003769034 |

| | | | |
|---|---|---|---|
| SIGLEC12 | 2.25 | 1.05 | 0.00268142 |
| CAMK1 | 5.69 | 1.04 | 0.004505279 |
| CA2 | 5.20 | 1.04 | 0.012921107 |
| TRAM2 | 6.43 | 1.03 | 0.001934363 |
| ARG2 | 5.55 | 1.03 | 0.010299273 |
| RABL2A | 4.75 | 1.03 | 0.010479042 |
| NME4 | 6.10 | 1.02 | 0.003660987 |
| ADGRD1 | 1.23 | 1.02 | 0.000513897 |
| HECW2 | 4.67 | 1.02 | 0.028010754 |
| HLF | 5.34 | 1.02 | 0.022677431 |
| COL6A3 | 8.35 | 1.02 | 0.020384731 |
| ID2 | 9.05 | 1.01 | 0.022803706 |
| PALD1 | 3.87 | 1.01 | 0.030286777 |
| MX1 | 12.15 | -2.48 | 1.78E-21 |
| XAF1 | 8.53 | -2.44 | 3.51E-19 |
| MX2 | 9.91 | -2.39 | 4.22E-17 |
| EPSTI1 | 9.65 | -2.33 | 1.33E-26 |
| KLF2 | 6.39 | -2.27 | 8.26E-12 |
| GBP5 | 11.05 | -2.20 | 1.65E-32 |
| GIMAP7 | 8.80 | -2.15 | 2.33E-21 |
| TRANK1 | 9.66 | -2.09 | 8.22E-16 |
| GIMAP4 | 10.49 | -2.06 | 2.14E-18 |
| TXK | 7.65 | -2.03 | 3.11E-18 |
| LGALS9 | 9.25 | -1.98 | 2.06E-13 |
| PPFIBP1 | 8.85 | -1.98 | 6.73E-11 |
| IFIT1 / ISG56 | 9.15 | -1.96 | 1.41E-08 |
| GBP4 | 9.38 | -1.96 | 1.30E-12 |
| OAS1 | 10.01 | -1.96 | 2.81E-12 |
| ANXA3 | 7.31 | -1.94 | 9.56E-12 |
| STAT1 | 13.24 | -1.94 | 8.85E-63 |
| GIMAP8 | 7.39 | -1.90 | 6.68E-13 |
| SAMD9L | 10.91 | -1.90 | 9.97E-14 |
| DPP4 / CD26 | 10.12 | -1.83 | 9.34E-14 |
| TCF7 | 10.20 | -1.78 | 3.51E-14 |
| ENPP2 | 6.89 | -1.74 | 3.37E-09 |
| DDX60 | 10.17 | -1.73 | 3.15E-09 |
| TRAT1 | 8.71 | -1.73 | 4.98E-14 |
| TNFSF10 / APO2L | 10.11 | -1.73 | 4.57E-07 |
| IFIH1 | 9.67 | -1.69 | 8.69E-12 |
| ALPK1 | 8.36 | -1.68 | 1.21E-08 |
| BHLHE40 | 11.84 | -1.67 | 1.35E-10 |
| OAS2 | 11.99 | -1.66 | 6.23E-16 |
| EIF2AK2 | 10.84 | -1.66 | 9.95E-12 |
| TYMP | 8.56 | -1.66 | 1.80E-07 |
| IFIT5 / ISG58 | 8.05 | -1.66 | 2.98E-10 |
| OASL | 9.18 | -1.65 | 2.17E-10 |
| OAS3 | 11.65 | -1.63 | 8.61E-06 |
| G0S2 | 6.03 | -1.63 | 1.45E-05 |
| IFI44L | 11.31 | -1.62 | 5.46E-06 |
| LGALS3BP | 9.87 | -1.61 | 3.26E-09 |
| DDX60L | 8.92 | -1.60 | 2.24E-05 |
| CEACAM1 | 7.41 | -1.60 | 5.14E-06 |

| | | | |
|---|---|---|---|
| SAMD9 | 10.08 | -1.60 | 4.33E-12 |
| RGS1 | 7.56 | -1.59 | 3.26E-06 |
| PARP9 | 9.91 | -1.56 | 2.39E-08 |
| SDK2 | 6.26 | -1.56 | 2.95E-05 |
| SMAD3 | 9.08 | -1.55 | 8.35E-09 |
| TNFSF13B / BAFF | 6.63 | -1.55 | 7.58E-06 |
| FXYD7 | 4.30 | -1.54 | 8.81E-05 |
| WIPF1 | 11.31 | -1.54 | 6.70E-24 |
| GBP1 | 9.71 | -1.52 | 4.88E-09 |
| KAT2B | 8.28 | -1.52 | 2.17E-12 |
| DTX3L | 9.90 | -1.52 | 1.63E-07 |
| RHOU | 7.05 | -1.51 | 1.64E-08 |
| IFI6 | 10.23 | -1.51 | 8.26E-05 |
| MAP3K8 | 7.03 | -1.50 | 1.10E-05 |
| SESN3 | 10.13 | -1.50 | 2.23E-05 |
| GPRIN3 | 9.72 | -1.50 | 2.33E-08 |
| CMPK2 | 8.91 | -1.50 | 9.29E-05 |
| RORA / NR1F1 | 9.11 | -1.50 | 2.81E-06 |
| PARP12 | 8.77 | -1.49 | 3.12E-07 |
| SEPT11 | 6.84 | -1.48 | 4.05E-05 |
| PITPNC1 | 8.69 | -1.47 | 7.93E-07 |
| IFI44 | 9.93 | -1.47 | 7.18E-07 |
| ADAM19 | 10.76 | -1.46 | 1.18E-09 |
| HERC5 / CEBP1 | 9.77 | -1.46 | 2.86E-08 |
| LSR | 6.86 | -1.44 | 7.65E-07 |
| NETO2 | 4.96 | -1.43 | 0.000220469 |
| ISG15 | 10.32 | -1.43 | 0.000163479 |
| NEXN | 6.55 | -1.43 | 1.70E-06 |
| PARP14 | 10.73 | -1.40 | 2.15E-09 |
| TRIM22 | 10.45 | -1.40 | 4.83E-08 |
| UNC93B1 | 7.73 | -1.38 | 6.27E-07 |
| PDE4B | 9.18 | -1.38 | 0.000479977 |
| GCSAM | 7.07 | -1.38 | 3.94E-06 |
| IGFBP4 | 8.75 | -1.38 | 9.33E-08 |
| SAT1 | 10.36 | -1.37 | 9.34E-10 |
| MAP3K5 | 7.03 | -1.37 | 2.15E-07 |
| STAT2 | 10.12 | -1.36 | 9.70E-09 |
| NUAK2 | 5.52 | -1.35 | 0.000216192 |
| SSTR3 | 7.77 | -1.33 | 1.14E-05 |
| GIMAP6 | 8.98 | -1.33 | 1.59E-12 |
| HERC6 | 8.41 | -1.33 | 6.08E-05 |
| TTC39C | 7.92 | -1.32 | 1.35E-08 |
| GRAMD1B | 8.08 | -1.32 | 2.11E-07 |
| IFI16 | 11.63 | -1.31 | 6.81E-19 |
| TRPS1 | 6.63 | -1.31 | 0.000130175 |
| LAMP3 | 8.94 | -1.30 | 0.000709311 |
| ENC1 | 4.43 | -1.30 | 0.001372873 |
| TSHZ2 | 8.54 | -1.28 | 1.69E-06 |
| GPR155 | 8.01 | -1.28 | 0.000269855 |
| CLEC2B | 9.07 | -1.28 | 0.002262302 |
| IL18RAP / IL1R7 | 6.99 | -1.28 | 0.000260671 |
| SSBP3 | 9.18 | -1.27 | 8.52E-10 |

| | | | |
|---|---|---|---|
| IFITM3 | 8.08 | -1.26 | 0.000143286 |
| IFIT2 / ISG54 | 9.79 | -1.25 | 6.53E-07 |
| SPATS2L | 8.65 | -1.25 | 3.51E-08 |
| MTSS1 | 6.93 | -1.24 | 9.42E-05 |
| ISG20 | 9.07 | -1.24 | 0.000169076 |
| HPGD | 4.11 | -1.23 | 0.003521039 |
| CHI3L2 | 7.41 | -1.23 | 7.71E-05 |
| MYO1E | 7.45 | -1.22 | 0.000647572 |
| IFIT3 / ISG60 | 10.16 | -1.22 | 0.002787641 |
| SLFN5 | 10.37 | -1.21 | 4.51E-05 |
| ISG43 | 8.61 | -1.21 | 0.003147667 |
| CXCR3 | 6.33 | -1.21 | 0.001967548 |
| HIC1 | 7.08 | -1.21 | 0.000787761 |
| PTPRO | 5.44 | -1.21 | 0.004162812 |
| IPCEF1 | 6.13 | -1.20 | 0.000124007 |
| ITGA2 / CD49B | 6.00 | -1.20 | 0.0009622 |
| GIMAP1 IMAP1 | 7.41 | -1.20 | 0.00014703 |
| DDX58 | 8.77 | -1.19 | 0.003222583 |
| DNAJC12 | 7.38 | -1.18 | 0.00014703 |
| PGAP1 | 9.06 | -1.18 | 1.14E-05 |
| TDRD7 | 7.86 | -1.18 | 0.000598729 |
| ADGRG1 | 6.88 | -1.18 | 0.003598197 |
| PLSCR1 | 9.00 | -1.18 | 0.002914871 |
| BST2 | 8.80 | -1.18 | 0.000172717 |
| IRF7 | 5.54 | -1.18 | 0.0026115 |
| SYNE2 | 10.08 | -1.17 | 3.37E-06 |
| ITM2B | 9.00 | -1.17 | 2.17E-09 |
| MAST4 | 8.81 | -1.17 | 9.85E-07 |
| FAM110A | 7.68 | -1.17 | 0.00022615 |
| MALT1 | 10.11 | -1.17 | 1.09E-05 |
| RIPK2 | 4.66 | -1.16 | 0.003738018 |
| NT5C3A | 9.39 | -1.15 | 0.003653008 |
| RAB11FIP5 | 7.71 | -1.15 | 0.000188105 |
| MLLT3 AF9 YEATS3 | 9.40 | -1.15 | 3.04E-05 |
| ODF3B | 6.41 | -1.15 | 0.001063876 |
| JAZF1 | 5.48 | -1.14 | 0.002022688 |
| GNPDA1 | 9.11 | -1.14 | 2.74E-05 |
| HHLA2 | 6.38 | -1.14 | 0.000575643 |
| KSR1 | 9.17 | -1.14 | 3.79E-10 |
| NPTX1 | 8.20 | -1.14 | 7.87E-05 |
| LGMN | 4.47 | -1.13 | 0.008349345 |
| SLC44A1 / CD92 | 7.57 | -1.13 | 3.20E-06 |
| PRR5L | 5.61 | -1.12 | 0.007134049 |
| TRPM2 | 5.88 | -1.12 | 0.001950818 |
| ENOX1 | 4.88 | -1.12 | 0.010479042 |
| ETV6 | 9.01 | -1.12 | 1.32E-05 |
| IFITM2 | 10.44 | -1.11 | 4.70E-07 |
| TLR1 | 5.76 | -1.11 | 0.007666693 |
| TRIM14 | 9.48 | -1.11 | 4.55E-09 |
| GADD45B | 7.22 | -1.11 | 0.000824057 |
| PLAC8 | 8.84 | -1.11 | 0.008349345 |
| KCNA2 | 4.89 | -1.11 | 0.010084007 |

| | | | |
|---|---|---|---|
| IL12RB2 | 9.74 | -1.10 | 4.51E-05 |
| PLEKHO1 | 7.52 | -1.10 | 9.68E-05 |
| UBE2L6 | 9.95 | -1.10 | 9.65E-07 |
| SLC35F3 | 7.44 | -1.09 | 0.000787761 |
| LPAR3 | 4.23 | -1.09 | 0.01401738 |
| TBX21 / TBET | 6.54 | -1.09 | 0.002676763 |
| ATM | 9.69 | -1.09 | 8.72E-07 |
| DLG4 | 6.63 | -1.09 | 0.000773677 |
| CASP7 | 6.44 | -1.08 | 0.001774372 |
| SLAMF7 | 7.91 | -1.08 | 0.003198506 |
| C5orf56 | 6.69 | -1.08 | 0.005155167 |
| SCML4 | 6.66 | -1.08 | 0.000711083 |
| CD96 | 10.12 | -1.08 | 1.75E-09 |
| RAPGEF2 | 7.79 | -1.07 | 0.000113105 |
| TNFRSF1B / TNFR2 | 9.86 | -1.07 | 8.09E-05 |
| ZC3H4 | 9.63 | -1.07 | 9.15E-09 |
| IFITM1 / CD225 | 11.00 | -1.07 | 1.97E-08 |
| RARRES3 | 6.53 | -1.07 | 0.003071558 |
| B3GALNT1 | 5.03 | -1.07 | 0.01425511 |
| HAVCR2 | 8.81 | -1.07 | 0.001654113 |
| OTUD1 | 7.46 | -1.07 | 0.00059722 |
| DGKA | 10.45 | -1.07 | 3.05E-08 |
| HBEGF | 7.58 | -1.06 | 0.002332997 |
| MEOX1 | 6.08 | -1.06 | 0.00551506 |
| AFDN | 7.94 | -1.06 | 0.002401693 |
| ZCCHC2 | 8.93 | -1.05 | 4.09E-10 |
| ARAP2 | 8.61 | -1.05 | 0.000406173 |
| CD38 | 9.83 | -1.05 | 1.92E-05 |
| KCNA3 | 7.97 | -1.05 | 0.000299251 |
| TRIM21 | 8.45 | -1.05 | 7.03E-05 |
| GBP2 | 11.09 | -1.05 | 9.35E-08 |
| RUFY4 | 5.02 | -1.04 | 0.022618538 |
| NOG | 4.32 | -1.04 | 0.022983569 |
| BSPRY | 7.36 | -1.04 | 0.000289666 |
| GPR174 / GPCR17 | 6.61 | -1.04 | 0.000641376 |
| GBP3 | 6.25 | -1.04 | 0.002118448 |
| TC2N | 4.52 | -1.04 | 0.018640979 |
| CXorf21 | 5.91 | -1.04 | 0.00551506 |
| IRF8 | 7.80 | -1.04 | 0.000684965 |
| SP110 | 7.85 | -1.03 | 0.000494367 |
| HELZ2 | 9.64 | -1.03 | 0.025236013 |
| CYSLTR1 | 7.48 | -1.03 | 0.000526103 |
| TP53INP1 | 8.31 | -1.02 | 0.025366567 |
| SELL | 11.67 | -1.02 | 4.54E-09 |
| IFI35 | 8.47 | -1.01 | 0.003762157 |
| SOCS2 / STATI2 | 8.46 | -1.01 | 0.025890024 |
| SP100 | 10.86 | -1.01 | 3.38E-09 |
| LIF | 11.31 | -1.01 | 0.000886745 |
| EURL | 7.28 | -1.01 | 0.000352608 |
| PYHIN1 | 6.60 | -1.01 | 0.001676872 |
| CHST2 | 7.46 | -1.01 | 0.006626567 |
| UBA7 | 9.34 | -1.00 | 2.16E-05 |

| | | | |
|---|---|---|---|
| PML | 9.59 | -1.00 | 4.57E-07 |
| CTSH | 6.81 | -1.00 | 0.007443992 |
| SAMHD1 | 9.40 | -1.00 | 0.000153221 |
| PYCARD | 5.86 | -1.00 | 0.003166189 |

**Supplementary table 4** Genes differentially expressed in Th17 cells after five days of polarisation. Gene expression was compared to stimulated, unpolarised (Th0) cells used as control. Genes are ordered by Log2-fold change, and up and downregulation are separated within the table.

| Gene Name | Log2( Base Mean Count ) | Log2FC | P adjusted |
|---|---|---|---|
| CXCL13 | 5.15 | 3.97 | 8.24E-32 |
| CTSL | 7.01 | 3.41 | 3.86E-23 |
| FNBP1L | 6.08 | 3.32 | 7.04E-24 |
| NCS1 | 5.99 | 3.31 | 1.90E-27 |
| EFR3B | 3.96 | 3.25 | 7.82E-22 |
| ALPK2 | 3.99 | 3.09 | 1.31E-19 |
| BCAR3 | 4.89 | 3.06 | 5.39E-19 |
| DSE | 4.76 | 2.97 | 3.62E-18 |
| COL15A1 | 4.39 | 2.93 | 1.44E-17 |
| NIPAL4 | 4.96 | 2.92 | 2.86E-17 |
| CLEC17A | 3.58 | 2.82 | 3.67E-17 |
| SEMA7A | 7.83 | 2.81 | 4.11E-32 |
| COL6A3 | 8.35 | 2.81 | 4.61E-17 |
| BASP1 | 4.64 | 2.80 | 8.19E-16 |
| KIF5A | 6.05 | 2.75 | 2.14E-23 |
| CSF1R | 3.94 | 2.71 | 2.43E-15 |
| SERPINA1 | 3.62 | 2.60 | 1.16E-14 |
| AHCYL2 | 9.21 | 2.59 | 1.18E-30 |
| PMEPA1 | 5.41 | 2.55 | 1.34E-15 |
| DHRS9 | 4.85 | 2.50 | 1.19E-12 |
| S100A2 | 3.28 | 2.46 | 1.97E-13 |
| LYN | 5.51 | 2.45 | 2.79E-14 |
| IL1R2 | 5.90 | 2.40 | 1.32E-11 |
| BARX2 | 5.25 | 2.40 | 1.33E-11 |
| IL1R1 | 6.61 | 2.37 | 3.61E-14 |
| GRHL3 | 2.66 | 2.35 | 3.08E-15 |
| PSD3 | 5.46 | 2.31 | 1.47E-12 |
| LPL | 4.73 | 2.30 | 6.39E-11 |
| GPR161 | 4.28 | 2.28 | 1.55E-10 |
| RYR1 | 6.71 | 2.26 | 3.67E-17 |
| MRC2 | 5.54 | 2.25 | 2.66E-12 |
| MMP2 | 3.85 | 2.24 | 7.37E-11 |
| TMPRSS6 | 6.82 | 2.24 | 6.37E-13 |
| LMNA | 7.97 | 2.21 | 4.68E-17 |
| BATF3 | 6.95 | 2.19 | 3.64E-12 |
| CCNA1 | 4.30 | 2.18 | 9.23E-10 |
| CDH1 | 6.65 | 2.14 | 1.36E-10 |
| GPR157 | 6.73 | 2.13 | 1.21E-10 |
| MYO5B | 5.64 | 2.09 | 7.23E-09 |
| NTRK3 | 3.58 | 2.02 | 4.92E-09 |
| HGNC:18790 | 4.03 | 2.00 | 3.75E-08 |
| LAMB3 | 6.16 | 1.99 | 3.54E-09 |
| IGFBP6 | 3.77 | 1.98 | 4.74E-08 |
| TIAM2 | 6.50 | 1.97 | 4.90E-14 |
| RASGRP4 | 7.08 | 1.96 | 8.78E-11 |

| | | | |
|---|---|---|---|
| C1QL1 | 2.64 | 1.96 | 9.96E-10 |
| CHST3 | 4.06 | 1.96 | 6.19E-08 |
| AQP3 | 8.20 | 1.95 | 6.63E-18 |
| TUFT1 | 5.33 | 1.95 | 3.71E-09 |
| PERP | 7.21 | 1.95 | 1.26E-10 |
| IKZF3 | 9.26 | 1.95 | 1.63E-13 |
| THBS1 | 5.54 | 1.95 | 9.56E-08 |
| ELOVL7 | 4.71 | 1.91 | 1.62E-07 |
| KCNJ10 | 2.72 | 1.91 | 1.02E-08 |
| CAMSAP2 | 5.68 | 1.90 | 6.71E-10 |
| KLF7 | 8.34 | 1.89 | 1.16E-14 |
| NCEH1 | 6.13 | 1.87 | 7.16E-12 |
| CCL22 | 3.86 | 1.87 | 5.39E-08 |
| USP43 | 2.68 | 1.86 | 4.42E-08 |
| FNDC9 | 3.54 | 1.86 | 6.19E-09 |
| RUBCNL | 5.32 | 1.85 | 1.13E-08 |
| CDC42BPB | 4.57 | 1.85 | 9.84E-08 |
| ITGAX | 7.42 | 1.84 | 2.94E-10 |
| DHRS2 | 4.05 | 1.83 | 1.39E-07 |
| CTNND1 | 6.72 | 1.81 | 1.23E-09 |
| F5 | 9.37 | 1.81 | 9.43E-23 |
| NAPSA | 6.95 | 1.81 | 1.03E-08 |
| EPHA4 | 4.60 | 1.80 | 1.10E-06 |
| ASCL1 | 3.39 | 1.80 | 3.42E-07 |
| CCL20 | 3.15 | 1.80 | 2.15E-08 |
| KCNJ9 | 2.59 | 1.79 | 1.81E-08 |
| APLP1 | 4.19 | 1.78 | 8.11E-07 |
| PTK2 | 6.48 | 1.78 | 8.08E-10 |
| ITGA3 | 7.13 | 1.75 | 1.83E-09 |
| PRG4 | 9.49 | 1.74 | 7.30E-07 |
| RAI14 | 3.30 | 1.72 | 2.73E-06 |
| LGALS3 | 6.70 | 1.71 | 2.67E-08 |
| VASH1 | 5.80 | 1.70 | 3.18E-07 |
| CIITA | 6.83 | 1.70 | 6.00E-07 |
| RORC | 5.53 | 1.70 | 1.13E-07 |
| FUT7 | 4.80 | 1.70 | 4.14E-06 |
| ATP6V0A4 | 3.39 | 1.70 | 2.92E-07 |
| LPCAT2 | 4.75 | 1.70 | 2.96E-06 |
| ABCG2 | 4.00 | 1.70 | 3.94E-06 |
| MCAM | 5.74 | 1.69 | 1.89E-07 |
| SYN1 | 3.27 | 1.68 | 2.23E-06 |
| FGD6 | 3.52 | 1.68 | 7.41E-06 |
| RUNX1 | 8.65 | 1.67 | 1.90E-11 |
| NRIP3 | 5.34 | 1.67 | 9.60E-07 |
| AKAP12 | 6.52 | 1.66 | 1.23E-06 |
| EBI3 | 5.59 | 1.65 | 2.97E-06 |
| TNFRSF8 | 7.39 | 1.64 | 4.12E-06 |
| CA12 | 5.06 | 1.64 | 1.38E-05 |
| SKIL | 7.23 | 1.63 | 2.54E-11 |
| KIF1A | 6.45 | 1.63 | 1.05E-06 |
| MYO10 | 2.59 | 1.62 | 3.13E-07 |
| DUSP6 | 7.86 | 1.62 | 1.46E-07 |

| | | | |
|---|---|---|---|
| GALNT10 | 8.81 | 1.61 | 6.78E-09 |
| DFNA5 | 6.38 | 1.61 | 1.52E-07 |
| CCDC3 | 2.19 | 1.60 | 2.12E-07 |
| FURIN | 12.03 | 1.60 | 6.77E-17 |
| ATP1B1 | 6.04 | 1.60 | 5.07E-06 |
| HMCN1 | 2.10 | 1.59 | 1.13E-07 |
| SELENON | 7.91 | 1.59 | 3.68E-13 |
| DGKG | 3.87 | 1.58 | 2.61E-06 |
| ARHGAP31 | 6.28 | 1.58 | 2.33E-08 |
| IL2 | 7.36 | 1.58 | 3.13E-05 |
| EHD2 | 3.67 | 1.58 | 2.89E-05 |
| ZFYVE28 | 5.50 | 1.58 | 3.13E-07 |
| FAM110B | 2.83 | 1.58 | 4.98E-06 |
| IVNS1ABP | 10.54 | 1.56 | 2.17E-15 |
| PFKFB3 | 10.40 | 1.56 | 4.62E-08 |
| EML5 | 5.01 | 1.56 | 2.29E-05 |
| TLR2 | 4.50 | 1.56 | 1.96E-05 |
| HLX | 3.06 | 1.56 | 1.84E-06 |
| NRSN2 | 5.10 | 1.56 | 3.22E-06 |
| TNFRSF12A | 3.92 | 1.55 | 5.07E-05 |
| SLC16A2 | 2.44 | 1.55 | 2.94E-06 |
| RBPJ | 10.56 | 1.55 | 6.24E-09 |
| ZNF282 | 8.18 | 1.53 | 1.52E-11 |
| QSOX1 | 7.75 | 1.53 | 2.00E-08 |
| PTPN14 | 6.78 | 1.51 | 8.93E-05 |
| SLC39A14 | 8.14 | 1.51 | 2.09E-07 |
| GPR132 | 7.38 | 1.51 | 1.17E-10 |
| ADAM19 | 10.76 | 1.50 | 1.17E-10 |
| SYNGR3 | 5.85 | 1.50 | 1.01E-06 |
| EPAS1 | 8.39 | 1.50 | 7.33E-05 |
| ALDH7A1 | 4.26 | 1.49 | 7.45E-05 |
| DIXDC1 | 8.17 | 1.48 | 0.000127563 |
| ABCC4 | 6.05 | 1.48 | 1.88E-06 |
| CXCL12 | 1.75 | 1.48 | 2.21E-09 |
| CEP112 | 3.39 | 1.47 | 0.000125299 |
| MAPK12 | 4.61 | 1.47 | 0.00010145 |
| SMYD3 | 6.66 | 1.47 | 1.86E-09 |
| DAPK2 | 2.94 | 1.47 | 5.38E-05 |
| ATP6V0A2 | 8.14 | 1.46 | 5.51E-07 |
| FLVCR2 | 4.36 | 1.46 | 9.22E-05 |
| C15orf48 | 5.43 | 1.46 | 0.000171434 |
| ADPRH | 5.48 | 1.44 | 4.70E-05 |
| SH3RF1 | 2.99 | 1.44 | 0.000155183 |
| STRIP2 | 9.86 | 1.43 | 9.96E-10 |
| TBC1D16 | 5.06 | 1.43 | 5.30E-05 |
| CHRNA6 | 6.38 | 1.42 | 3.55E-05 |
| S100A6 | 9.70 | 1.42 | 1.77E-13 |
| RIMS3 | 6.93 | 1.42 | 3.08E-06 |
| SIPA1L2 | 4.39 | 1.42 | 0.000198035 |
| JAKMIP1 | 6.15 | 1.42 | 0.000118632 |
| KIFC3 | 2.24 | 1.42 | 2.02E-05 |
| CDC42BPA | 6.11 | 1.41 | 1.23E-05 |

| | | | |
|---|---|---|---|
| FEZ1 | 2.89 | 1.40 | 0.000131128 |
| RGCC | 8.68 | 1.40 | 3.97E-06 |
| MAST4 | 8.81 | 1.39 | 1.79E-10 |
| CGN | 3.35 | 1.39 | 0.00028541 |
| CACHD1 | 3.89 | 1.38 | 0.000430885 |
| PNOC | 2.23 | 1.38 | 2.70E-06 |
| HECTD2 | 4.70 | 1.38 | 0.000239176 |
| MAF | 9.00 | 1.37 | 9.20E-06 |
| GJC1 | 3.16 | 1.37 | 0.000388286 |
| TIMP1 | 7.04 | 1.36 | 0.000554147 |
| REEP2 | 4.30 | 1.36 | 0.00034879 |
| CTTN | 6.51 | 1.36 | 3.26E-05 |
| THEM5 | 5.38 | 1.36 | 0.000271647 |
| MAP1A | 5.28 | 1.35 | 5.97E-05 |
| DIS3L2 | 6.68 | 1.35 | 1.46E-07 |
| SPEF2 | 6.80 | 1.35 | 3.40E-07 |
| AHR | 9.76 | 1.35 | 2.75E-10 |
| FNIP2 | 8.10 | 1.35 | 3.04E-08 |
| ITGA2 | 6.00 | 1.34 | 2.04E-05 |
| SPSB1 | 6.89 | 1.34 | 0.000125299 |
| CD22 | 6.65 | 1.33 | 6.72E-05 |
| KCNC4 | 7.18 | 1.33 | 4.10E-06 |
| SPOCD1 | 2.04 | 1.33 | 7.94E-06 |
| SYP | 5.44 | 1.32 | 0.000319847 |
| RASGRP3 | 7.08 | 1.32 | 3.56E-05 |
| PALLD | 8.45 | 1.32 | 0.000924877 |
| DOCK4 | 2.17 | 1.32 | 2.85E-05 |
| GSN | 5.21 | 1.32 | 0.000473016 |
| PLEC | 10.97 | 1.31 | 1.15E-11 |
| TYRO3 | 2.33 | 1.31 | 0.000231642 |
| EPHA10 | 3.31 | 1.30 | 0.000770088 |
| GCNT4 | 4.70 | 1.30 | 0.000885331 |
| CCR4 | 10.17 | 1.30 | 6.46E-06 |
| MED12L | 3.95 | 1.29 | 0.001365322 |
| IL13RA1 | 2.80 | 1.29 | 0.000208751 |
| ITPKC | 6.15 | 1.29 | 3.56E-05 |
| LOXL3 | 3.55 | 1.28 | 0.001472173 |
| TSHZ3 | 3.49 | 1.28 | 0.001414569 |
| SLC4A7 | 7.39 | 1.27 | 3.84E-05 |
| SUSD6 | 9.64 | 1.26 | 1.46E-13 |
| GDPD5 | 6.17 | 1.25 | 0.000285195 |
| NLGN2 | 6.58 | 1.25 | 1.96E-05 |
| AREG | 3.36 | 1.25 | 0.002179566 |
| PLS3 | 3.99 | 1.25 | 0.002035959 |
| IFNL1 | 3.81 | 1.24 | 0.001729888 |
| CAMSAP1 | 8.86 | 1.24 | 2.22E-07 |
| KLF4 | 4.36 | 1.24 | 0.001466572 |
| NOTCH1 | 9.24 | 1.24 | 1.75E-07 |
| HAGHL | 4.60 | 1.24 | 0.002363963 |
| EVA1C | 5.15 | 1.23 | 0.000687379 |
| APOD | 6.39 | 1.23 | 0.000609655 |
| ETS2 | 8.79 | 1.23 | 8.74E-05 |

| | | | |
|---|---|---|---|
| KCNN4 | 7.73 | 1.22 | 3.77E-09 |
| SLC22A17 | 5.63 | 1.22 | 0.000198498 |
| SHC2 | 1.54 | 1.22 | 9.53E-06 |
| CYTH3 | 4.53 | 1.22 | 0.001856577 |
| CARMIL3 | 3.63 | 1.22 | 0.002883579 |
| POMT2 | 4.76 | 1.22 | 0.001358548 |
| MYOF | 7.71 | 1.22 | 1.58E-05 |
| ATP9A | 4.29 | 1.21 | 0.002268242 |
| NCKAP1 | 5.32 | 1.21 | 0.000269549 |
| SPHK1 | 3.94 | 1.21 | 0.003545994 |
| CAVIN3 | 5.19 | 1.20 | 0.00221296 |
| PCNX1 | 9.47 | 1.19 | 2.07E-09 |
| TNFRSF25 | 7.91 | 1.19 | 2.04E-09 |
| FOSL2 | 9.20 | 1.19 | 3.54E-09 |
| PPARG | 4.60 | 1.18 | 0.000425662 |
| ITGB4 | 3.02 | 1.18 | 0.004280956 |
| IGSF3 | 4.20 | 1.18 | 0.004807287 |
| KIF5C | 5.98 | 1.17 | 0.000264272 |
| CALCB | 4.07 | 1.17 | 0.005027574 |
| GALNT2 | 8.73 | 1.16 | 2.09E-07 |
| DLGAP4 | 7.69 | 1.16 | 6.20E-05 |
| RORA | 9.11 | 1.16 | 0.000440511 |
| ZBED2 | 11.20 | 1.15 | 0.00202837 |
| RPP30 | 7.83 | 1.15 | 1.76E-08 |
| SLAMF1 | 8.72 | 1.14 | 3.66E-05 |
| SH2D2A | 9.25 | 1.14 | 2.16E-07 |
| ZFP92 | 4.43 | 1.14 | 0.004878454 |
| PNMA2 | 6.18 | 1.14 | 0.002583344 |
| TNFSF14 | 7.19 | 1.14 | 3.78E-05 |
| RYR2 | 1.60 | 1.14 | 6.98E-05 |
| SMIM3 | 6.79 | 1.13 | 2.29E-05 |
| HOXB9 | 2.38 | 1.13 | 0.001883563 |
| TSHZ2 | 8.54 | 1.13 | 1.68E-05 |
| LMCD1 | 4.84 | 1.12 | 0.007403074 |
| CASKIN2 | 3.06 | 1.12 | 0.00527785 |
| NFATC4 | 2.83 | 1.12 | 0.002551464 |
| RNF217 | 4.11 | 1.12 | 0.00863 |
| MAPK11 | 6.60 | 1.12 | 0.0002557 |
| SPINT1 | 5.78 | 1.11 | 0.006334168 |
| ITPR2 | 8.95 | 1.11 | 4.98E-08 |
| F2RL1 | 3.68 | 1.11 | 0.009104566 |
| DNMBP | 5.09 | 1.10 | 0.002016945 |
| CD226 | 9.29 | 1.10 | 2.10E-06 |
| PDLIM7 | 6.79 | 1.10 | 0.000378639 |
| MAML2 | 8.41 | 1.10 | 3.32E-07 |
| C2CD4D | 4.28 | 1.09 | 0.009708077 |
| TMOD1 | 4.14 | 1.09 | 0.011151813 |
| IL4I1 | 5.84 | 1.09 | 0.006749981 |
| ATF3 | 8.00 | 1.09 | 3.21E-09 |
| WDFY3 | 2.83 | 1.08 | 0.001942707 |
| NACAD | 2.83 | 1.08 | 0.006180211 |
| B4GALT5 | 7.90 | 1.08 | 2.92E-06 |

| | | | |
|---|---|---|---|
| AHRR | 8.23 | 1.07 | 1.97E-07 |
| KCTD15 | 4.03 | 1.07 | 0.012905985 |
| SPARC | 1.93 | 1.07 | 0.000278643 |
| ACSL4 | 9.23 | 1.07 | 1.06E-05 |
| GRB7 | 3.69 | 1.07 | 0.013483144 |
| MCF2L2 | 4.78 | 1.07 | 0.007833559 |
| SLC35E4 | 5.51 | 1.06 | 0.007051111 |
| ITGA1 | 4.55 | 1.06 | 0.010304079 |
| MYO7A | 1.96 | 1.06 | 0.000913109 |
| RAB13 | 6.41 | 1.06 | 0.001820666 |
| RNF213 | 12.54 | 1.06 | 3.13E-07 |
| SLC25A4 | 4.96 | 1.06 | 0.011708599 |
| FAM83G | 6.92 | 1.06 | 0.000202177 |
| TRO | 4.73 | 1.06 | 0.011126061 |
| CKAP4 | 6.44 | 1.05 | 3.49E-05 |
| BRSK1 | 5.06 | 1.05 | 0.006324732 |
| BCL6 | 9.10 | 1.05 | 0.012275978 |
| DYNC2H1 | 4.13 | 1.05 | 0.016607512 |
| IRS2 | 6.66 | 1.04 | 0.000177225 |
| ARHGEF5 | 5.13 | 1.04 | 0.005526584 |
| EGR2 | 7.01 | 1.04 | 0.001359256 |
| HMSD | 5.30 | 1.04 | 0.011338871 |
| ATP2B4 | 10.25 | 1.03 | 3.42E-07 |
| RAVER2 | 4.28 | 1.03 | 0.015081849 |
| HOPX | 5.89 | 1.03 | 0.014802712 |
| HERC6 | 8.41 | 1.03 | 0.002602044 |
| PRDX1 | 9.05 | 1.02 | 2.47E-05 |
| CCDC88A | 6.65 | 1.02 | 0.000125299 |
| OCIAD2 | 7.65 | 1.02 | 5.99E-07 |
| CH25H | 2.00 | 1.02 | 0.002929208 |
| TNFRSF9 | 6.61 | 1.02 | 0.010668163 |
| CPXM1 | 3.15 | 1.02 | 0.018564588 |
| PKN3 | 5.73 | 1.02 | 0.00202837 |
| DOCK6 | 4.84 | 1.01 | 0.016451629 |
| USP45 | 5.88 | 1.01 | 0.00272293 |
| NLRP3 | 3.67 | 1.01 | 0.016237165 |
| SLC7A5 | 11.07 | 1.01 | 2.22E-05 |
| C3orf67 | 4.24 | 1.01 | 0.019546819 |
| NCBP3 | 8.38 | 1.01 | 1.61E-09 |
| ITGAV | 6.36 | 1.00 | 0.000430704 |
| CYP1B1 | 7.15 | 1.00 | 0.001158647 |
| INTS7 | 7.89 | 1.00 | 7.17E-05 |
| SLC35F3 | 7.44 | -2.96 | 4.79E-24 |
| KLF2 | 6.39 | -2.85 | 4.23E-18 |
| HHLA2 | 6.38 | -2.68 | 1.21E-18 |
| SESN3 | 10.13 | -2.45 | 2.94E-14 |
| BTBD11 | 7.85 | -2.44 | 1.26E-20 |
| HS3ST3B1 | 6.26 | -2.33 | 6.79E-13 |
| HIC1 | 7.08 | -2.26 | 1.64E-12 |
| TRIB2 | 6.75 | -2.25 | 1.81E-12 |
| ANXA1 | 8.76 | -2.19 | 2.43E-16 |
| MAL | 8.90 | -2.17 | 4.46E-25 |

| | | | |
|---|---|---|---|
| FGFR1 | 8.22 | -2.16 | 1.76E-13 |
| EGFL6 | 6.34 | -2.16 | 2.27E-11 |
| TRAT1 | 8.71 | -2.14 | 7.30E-21 |
| PIK3CG | 8.31 | -2.12 | 4.49E-17 |
| NCALD | 5.35 | -2.10 | 2.45E-10 |
| GATA3 | 8.79 | -1.99 | 3.96E-12 |
| RDH10 | 7.67 | -1.97 | 6.48E-10 |
| PDE3B | 9.83 | -1.95 | 3.50E-20 |
| PLXNC1 | 8.04 | -1.94 | 2.85E-17 |
| CST7 | 8.00 | -1.92 | 6.71E-15 |
| KLF3 | 6.53 | -1.92 | 2.48E-10 |
| CYSLTR1 | 7.48 | -1.92 | 8.83E-13 |
| ST3GAL1 | 9.16 | -1.90 | 2.65E-11 |
| TC2N | 4.52 | -1.88 | 2.08E-07 |
| MEOX1 | 6.08 | -1.84 | 2.65E-08 |
| RNF157 | 8.56 | -1.83 | 2.56E-11 |
| SDK2 | 6.26 | -1.82 | 3.13E-07 |
| PRDM1 | 7.65 | -1.81 | 4.58E-09 |
| FADS2 | 9.21 | -1.81 | 1.92E-19 |
| ADA2 | 6.59 | -1.80 | 2.05E-07 |
| MYO1F | 7.53 | -1.79 | 3.93E-10 |
| PLEKHA7 | 6.67 | -1.77 | 1.82E-07 |
| SEPT11 | 6.84 | -1.76 | 2.69E-07 |
| NOD2 | 5.70 | -1.76 | 2.09E-07 |
| LRRN3 | 7.99 | -1.74 | 8.78E-08 |
| POU2AF1 | 5.89 | -1.73 | 1.12E-07 |
| AOAH | 6.12 | -1.73 | 3.01E-07 |
| CD38 | 9.83 | -1.72 | 3.94E-14 |
| WIPF1 | 11.31 | -1.69 | 1.66E-28 |
| ST3GAL5 | 6.55 | -1.68 | 3.10E-07 |
| TRPM2 | 5.88 | -1.68 | 3.10E-07 |
| GBP3 | 6.25 | -1.64 | 8.78E-08 |
| DPP4 | 10.12 | -1.64 | 3.42E-11 |
| GBP5 | 11.05 | -1.64 | 7.29E-18 |
| PSTPIP2 | 6.73 | -1.63 | 5.25E-09 |
| DHRS3 | 8.77 | -1.61 | 1.02E-05 |
| SYTL2 | 7.15 | -1.60 | 6.34E-10 |
| HRH2 | 6.67 | -1.60 | 1.28E-06 |
| ANKRD55 | 5.73 | -1.55 | 1.23E-05 |
| B3GALNT1 | 5.03 | -1.53 | 5.13E-05 |
| ANXA3 | 7.31 | -1.52 | 1.39E-07 |
| CHI3L2 | 7.41 | -1.52 | 2.37E-07 |
| GSAP | 4.87 | -1.52 | 5.30E-05 |
| PPFIBP1 | 8.85 | -1.51 | 1.55E-06 |
| CD200R1 | 4.97 | -1.50 | 5.33E-05 |
| PLAC8 | 8.84 | -1.49 | 5.92E-05 |
| NFIL3 | 8.95 | -1.49 | 1.93E-12 |
| ATP12A | 4.62 | -1.48 | 0.000105937 |
| STX3 | 7.43 | -1.47 | 7.49E-06 |
| PTPRO | 5.44 | -1.45 | 0.000171434 |
| ATM | 9.69 | -1.45 | 6.86E-12 |
| CABLES1 | 6.43 | -1.45 | 0.000119994 |

| | | | |
|---|---|---|---|
| MYBL1 | 6.27 | -1.44 | 1.89E-05 |
| CD48 | 9.78 | -1.44 | 3.68E-12 |
| EGLN3 | 5.72 | -1.43 | 0.000209007 |
| WWC3 | 7.40 | -1.43 | 8.22E-09 |
| STAT4 | 9.59 | -1.42 | 8.41E-08 |
| CD59 | 6.99 | -1.41 | 7.95E-06 |
| ENPP2 | 6.89 | -1.41 | 2.15E-06 |
| SLC39A8 | 9.31 | -1.40 | 1.80E-16 |
| IL18R1 | 8.71 | -1.40 | 5.17E-07 |
| SELPLG | 9.65 | -1.39 | 1.65E-13 |
| SNX18 | 6.98 | -1.39 | 4.32E-06 |
| KIF3A | 7.90 | -1.39 | 2.41E-05 |
| PAG1 | 8.90 | -1.37 | 3.97E-14 |
| GPRIN3 | 9.72 | -1.37 | 3.67E-07 |
| PRF1 | 7.27 | -1.36 | 0.000105784 |
| GBP4 | 9.38 | -1.36 | 2.31E-06 |
| UBASH3A | 8.27 | -1.36 | 4.88E-08 |
| SMAD3 | 9.08 | -1.36 | 5.42E-07 |
| AUH | 7.36 | -1.36 | 1.55E-06 |
| HBEGF | 7.58 | -1.35 | 2.32E-05 |
| VPS37B | 6.47 | -1.35 | 9.86E-06 |
| ABCD2 | 7.48 | -1.35 | 3.24E-08 |
| JAZF1 | 5.48 | -1.35 | 0.00010914 |
| SOCS2 | 8.46 | -1.35 | 0.000572 |
| GPR18 | 6.25 | -1.34 | 2.48E-05 |
| GPR15 | 4.97 | -1.32 | 0.000603734 |
| GCSAM | 7.07 | -1.32 | 8.18E-06 |
| RBM47 | 5.52 | -1.32 | 0.000770088 |
| AFF3 | 4.62 | -1.31 | 0.001071251 |
| CLMN | 5.63 | -1.30 | 0.000335903 |
| KAT2B | 8.28 | -1.30 | 2.80E-09 |
| OSTM1 | 6.36 | -1.29 | 1.28E-05 |
| NLRP6 | 4.46 | -1.29 | 0.001211763 |
| FHIT | 7.43 | -1.29 | 2.10E-06 |
| PDE7B | 4.66 | -1.28 | 0.001466572 |
| PRKX | 9.29 | -1.28 | 3.08E-15 |
| C16orf54 | 7.48 | -1.28 | 6.89E-05 |
| KIF2A | 10.61 | -1.27 | 3.23E-10 |
| CYLD | 10.70 | -1.26 | 2.79E-14 |
| ADORA2B | 5.09 | -1.24 | 0.0008259 |
| LAYN | 6.82 | -1.24 | 0.002035959 |
| OXNAD1 | 8.49 | -1.24 | 4.54E-09 |
| PHEX | 4.88 | -1.24 | 0.001575376 |
| CD52 | 8.92 | -1.24 | 1.27E-05 |
| GFI1 | 8.67 | -1.23 | 3.74E-07 |
| ARL4C | 10.91 | -1.22 | 2.79E-14 |
| IL32 | 10.98 | -1.21 | 1.93E-15 |
| APOBR | 6.27 | -1.21 | 0.000913109 |
| RASGRP2 | 6.85 | -1.20 | 3.18E-05 |
| PECAM1 | 6.60 | -1.20 | 0.000320403 |
| STRADB | 7.68 | -1.19 | 4.24E-07 |
| HSF4 | 7.14 | -1.19 | 0.000356084 |

| | | | |
|---|---|---|---|
| HDGFL3 | 7.70 | -1.18 | 0.000267137 |
| PRKACB | 8.22 | -1.18 | 4.61E-06 |
| STAP1 | 7.08 | -1.18 | 0.000473794 |
| FAM105A | 6.93 | -1.17 | 0.000652322 |
| XBP1 | 10.10 | -1.16 | 1.85E-11 |
| DUSP10 | 7.43 | -1.15 | 2.48E-05 |
| TOX | 4.73 | -1.15 | 0.006156694 |
| CPOX | 8.03 | -1.15 | 2.18E-08 |
| HCAR1 | 4.28 | -1.14 | 0.006596471 |
| TRIB1 | 7.90 | -1.14 | 0.000725556 |
| SERTAD2 | 8.51 | -1.14 | 5.19E-05 |
| NEDD9 | 7.79 | -1.13 | 1.53E-07 |
| AXIN2 | 5.34 | -1.13 | 0.004702477 |
| SFMBT2 | 8.36 | -1.13 | 8.83E-09 |
| ACSS1 | 7.17 | -1.13 | 2.41E-05 |
| RPS6KA5 | 7.15 | -1.13 | 2.25E-05 |
| TLE4 | 6.85 | -1.12 | 8.29E-05 |
| CLEC2B | 9.07 | -1.12 | 0.008271526 |
| L3MBTL3 | 6.09 | -1.12 | 0.000549718 |
| RAB37 | 6.12 | -1.12 | 0.001627163 |
| TMSB10 | 13.26 | -1.12 | 1.09E-07 |
| SKAP1 | 8.67 | -1.12 | 4.42E-08 |
| LPAR6 | 6.78 | -1.12 | 4.44E-05 |
| SETBP1 | 5.27 | -1.12 | 0.005308143 |
| IFT57 | 6.82 | -1.11 | 7.97E-05 |
| HAVCR2 | 8.81 | -1.11 | 0.000633765 |
| HPGD | 4.11 | -1.11 | 0.00893099 |
| C10orf128 | 4.76 | -1.11 | 0.00899212 |
| SREBF1 | 9.30 | -1.11 | 8.38E-14 |
| TGFBR3 | 6.73 | -1.11 | 0.001395947 |
| DLG3 | 7.42 | -1.11 | 0.000266579 |
| CACNA1I | 5.13 | -1.10 | 0.008828196 |
| MGAT5 | 7.53 | -1.10 | 0.000675767 |
| ACSBG1 | 3.78 | -1.10 | 0.008210485 |
| TRABD2A | 8.42 | -1.10 | 9.61E-09 |
| NUCB2 | 8.65 | -1.10 | 0.000103798 |
| TMEM71 | 8.42 | -1.10 | 9.07E-05 |
| KLHL29 | 5.79 | -1.10 | 0.005861522 |
| PPP3CA | 6.24 | -1.10 | 0.000431373 |
| TNFSF8 | 8.06 | -1.09 | 3.68E-05 |
| LRRC8C | 9.36 | -1.09 | 1.07E-07 |
| SNRK | 8.03 | -1.09 | 2.81E-06 |
| LPAR3 | 4.23 | -1.09 | 0.011295859 |
| CLECL1 | 4.09 | -1.09 | 0.011009633 |
| MCOLN3 | 3.71 | -1.09 | 0.011344991 |
| RFLNB | 9.27 | -1.08 | 4.52E-06 |
| SP4 | 7.38 | -1.08 | 0.00010352 |
| RCSD1 | 9.72 | -1.08 | 7.66E-09 |
| STC1 | 4.75 | -1.07 | 0.013004904 |
| SOS1 | 9.43 | -1.07 | 1.14E-05 |
| HPSE | 7.40 | -1.07 | 5.94E-06 |
| CASP9 | 6.74 | -1.07 | 0.001190971 |

| | | | |
|---|---|---|---|
| LYST | 9.07 | -1.07 | 0.011474345 |
| CCNI2 | 4.45 | -1.05 | 0.01243014 |
| MLLT3 | 9.40 | -1.05 | 0.00013046 |
| RIN3 | 7.86 | -1.05 | 0.002838482 |
| HSBP1L1 | 5.90 | -1.05 | 0.006334168 |
| XYLT1 | 7.74 | -1.05 | 2.33E-05 |
| ZDHHC14 | 5.44 | -1.05 | 0.006302555 |
| CEACAM1 | 7.41 | -1.04 | 0.007033897 |
| PHTF2 | 8.07 | -1.04 | 8.30E-05 |
| PCSK6 | 3.37 | -1.04 | 0.015705555 |
| INPP4A | 8.64 | -1.04 | 3.18E-08 |
| TMC8 | 9.69 | -1.04 | 1.12E-08 |
| PPP2R2B | 3.48 | -1.03 | 0.016212957 |
| FCMR | 6.92 | -1.03 | 0.001137424 |
| FXYD7 | 4.30 | -1.03 | 0.019998034 |
| PIK3R1 | 9.50 | -1.03 | 9.44E-08 |
| GBP2 | 11.09 | -1.02 | 1.39E-07 |
| SPIN1 | 8.30 | -1.02 | 7.39E-07 |
| RASGRF2 | 6.31 | -1.02 | 0.004866051 |
| CDHR1 | 5.05 | -1.02 | 0.019863418 |
| KCNQ5 | 5.86 | -1.02 | 0.004255084 |
| ANTXR2 | 6.72 | -1.01 | 0.008890539 |
| PIK3R5 | 8.22 | -1.01 | 0.000185235 |
| MAP3K5 | 7.03 | -1.01 | 0.000208763 |
| CASP3 | 9.21 | -1.01 | 3.20E-07 |
| TIAM1 | 8.77 | -1.01 | 0.000243103 |
| ACTN1 | 9.55 | -1.00 | 1.80E-05 |
| GIMAP6 | 8.98 | -1.00 | 2.37E-07 |

**Supplementary table 5** Genes differentially expressed in iTreg after five days of polarisation. Gene expression was compared to stimulated, unpolarised (Th0) cells used as control. Genes are ordered by Log2-fold change, and up and downregulation are separated within the table.

| Gene Name | Log2( Base Mean Count ) | Log2FC | P adjusted |
|---|---|---|---|
| FNBP1L | 6.08 | 3.59 | 2.32E-27 |
| CTSL | 7.01 | 3.28 | 3.52E-21 |
| PMEPA1 | 5.41 | 3.25 | 4.15E-25 |
| MMP2 | 3.85 | 3.12 | 1.55E-20 |
| MRC2 | 5.54 | 2.76 | 2.26E-18 |
| CHST3 | 4.06 | 2.59 | 2.18E-13 |
| COL15A1 | 4.39 | 2.57 | 3.50E-13 |
| MYO5B | 5.64 | 2.53 | 1.55E-12 |
| KIF5A | 6.05 | 2.52 | 2.48E-19 |
| LPL | 4.73 | 2.50 | 1.75E-12 |
| SEMA7A | 7.83 | 2.48 | 8.52E-25 |
| ANK1 | 5.21 | 2.39 | 4.78E-12 |
| VASH1 | 5.80 | 2.36 | 2.18E-13 |
| HGNC:18790 | 4.03 | 2.32 | 1.26E-10 |
| RYR1 | 6.71 | 2.31 | 9.71E-18 |
| CAMSAP2 | 5.68 | 2.23 | 2.04E-13 |
| LMNA | 7.97 | 2.22 | 6.59E-17 |
| NCS1 | 5.99 | 2.20 | 1.36E-11 |
| ATP1B1 | 6.04 | 2.19 | 1.09E-10 |
| TMPRSS6 | 6.82 | 2.17 | 1.02E-11 |
| LPCAT2 | 4.75 | 2.15 | 1.33E-09 |
| RASGRP4 | 7.08 | 2.12 | 2.60E-12 |
| AHCYL2 | 9.21 | 2.10 | 7.82E-20 |
| IL1A | 3.53 | 2.05 | 1.32E-08 |
| CLEC17A | 3.58 | 2.04 | 9.70E-09 |
| NR4A3 | 7.00 | 2.01 | 1.48E-09 |
| BASP1 | 4.64 | 1.99 | 1.08E-07 |
| SKIL | 7.23 | 1.98 | 1.92E-16 |
| RGS16 | 8.02 | 1.97 | 1.06E-07 |
| CCL22 | 3.86 | 1.94 | 3.17E-08 |
| NFATC4 | 2.83 | 1.88 | 3.85E-08 |
| SLC14A1 | 4.44 | 1.86 | 8.11E-07 |
| CAVIN3 | 5.19 | 1.85 | 2.56E-07 |
| BCAR3 | 4.89 | 1.84 | 1.23E-06 |
| ALPK2 | 3.99 | 1.84 | 1.07E-06 |
| LMCD1 | 4.84 | 1.82 | 1.63E-06 |
| PTK2 | 6.48 | 1.81 | 7.43E-10 |
| COL6A1 | 3.96 | 1.81 | 1.46E-06 |
| COL6A3 | 8.35 | 1.81 | 8.73E-07 |
| APOD | 6.39 | 1.79 | 1.31E-07 |
| EGR2 | 7.01 | 1.79 | 7.47E-10 |
| EFR3B | 3.96 | 1.79 | 2.42E-06 |
| TIAM2 | 6.50 | 1.78 | 4.59E-11 |
| TNFRSF9 | 6.61 | 1.78 | 3.87E-07 |
| SPTBN5 | 4.25 | 1.77 | 2.85E-06 |

| | | | |
|---|---|---|---|
| SARDH | 4.72 | 1.76 | 2.61E-06 |
| F5 | 9.37 | 1.76 | 3.35E-21 |
| CYTH3 | 4.53 | 1.74 | 1.98E-06 |
| CCR4 | 10.17 | 1.73 | 6.10E-10 |
| NIPAL4 | 4.96 | 1.71 | 1.12E-05 |
| IGSF3 | 4.20 | 1.69 | 1.45E-05 |
| KCNJ9 | 2.59 | 1.69 | 3.03E-07 |
| KLF7 | 8.34 | 1.67 | 4.81E-11 |
| IKZF4 | 8.02 | 1.67 | 3.70E-10 |
| ARHGAP31 | 6.28 | 1.64 | 1.32E-08 |
| EGR1 | 7.89 | 1.63 | 9.41E-09 |
| ITPRIPL2 | 4.84 | 1.61 | 3.85E-05 |
| CSGALNACT1 | 5.58 | 1.60 | 7.34E-06 |
| SPON1 | 4.92 | 1.60 | 5.56E-05 |
| IVNS1ABP | 10.54 | 1.59 | 9.14E-16 |
| LGALS3 | 6.70 | 1.58 | 1.05E-06 |
| EBI3 | 5.59 | 1.57 | 2.44E-05 |
| GPR157 | 6.73 | 1.57 | 1.58E-05 |
| SLC39A14 | 8.14 | 1.56 | 1.50E-07 |
| CCL20 | 3.15 | 1.56 | 4.21E-06 |
| GCNT1 | 6.32 | 1.55 | 0.000114233 |
| COL5A2 | 5.36 | 1.52 | 4.59E-05 |
| PLAGL1 | 6.74 | 1.51 | 1.62E-06 |
| GLT1D1 | 4.69 | 1.50 | 0.000156807 |
| CA12 | 5.06 | 1.49 | 0.000252775 |
| CXCL13 | 5.15 | 1.47 | 0.000272749 |
| IL4I1 | 5.84 | 1.46 | 0.000122079 |
| HECTD2 | 4.70 | 1.45 | 0.000160317 |
| GPR161 | 4.28 | 1.45 | 0.00039296 |
| MYH6 | 3.98 | 1.44 | 0.000170672 |
| EVA1C | 5.15 | 1.44 | 6.57E-05 |
| DNAJC12 | 7.38 | 1.44 | 5.65E-07 |
| CDK14 | 3.48 | 1.43 | 0.000483014 |
| TUFT1 | 5.33 | 1.43 | 0.000110627 |
| IL2 | 7.36 | 1.42 | 0.000557068 |
| PGM2L1 | 7.90 | 1.42 | 3.93E-08 |
| KIAA1522 | 3.86 | 1.41 | 0.000587426 |
| FOXP3 | 8.60 | 1.40 | 0.000725121 |
| IL1RN | 6.28 | 1.40 | 0.000358955 |
| RTKN | 4.09 | 1.39 | 0.00085465 |
| GPR132 | 7.38 | 1.39 | 1.13E-08 |
| DFNA5 | 6.38 | 1.38 | 3.00E-05 |
| CD200 | 7.61 | 1.38 | 3.56E-07 |
| DSE | 4.76 | 1.37 | 0.000916956 |
| CTTN | 6.51 | 1.37 | 5.88E-05 |
| TNFRSF12A | 3.92 | 1.36 | 0.001155274 |
| DHRS2 | 4.05 | 1.35 | 0.00060561 |
| CDC42BPB | 4.57 | 1.34 | 0.000711746 |
| ALDH7A1 | 4.26 | 1.34 | 0.001054666 |
| NYNRIN | 2.25 | 1.34 | 0.000114488 |
| STRIP2 | 9.86 | 1.33 | 4.27E-08 |
| TMPRSS3 | 6.63 | 1.33 | 0.000815137 |

| | | | |
|---|---|---|---|
| CHRNA6 | 6.38 | 1.32 | 0.000341705 |
| KCNJ10 | 2.72 | 1.31 | 0.00047695 |
| CBLN3 | 5.38 | 1.31 | 7.22E-05 |
| RASGRP3 | 7.08 | 1.31 | 9.17E-05 |
| DUSP4 | 10.57 | 1.30 | 0.000923268 |
| PTCHD1 | 1.70 | 1.30 | 4.98E-07 |
| GPR87 | 2.47 | 1.30 | 0.000637832 |
| APLP1 | 4.19 | 1.29 | 0.002013388 |
| CTNND1 | 6.72 | 1.29 | 0.000114233 |
| SPEF2 | 6.80 | 1.29 | 3.67E-06 |
| MYO7A | 1.96 | 1.27 | 7.11E-05 |
| FUT7 | 4.80 | 1.27 | 0.002775638 |
| CPM | 6.99 | 1.27 | 0.000163961 |
| EML5 | 5.01 | 1.27 | 0.002240677 |
| IFNL1 | 3.81 | 1.27 | 0.002521307 |
| FHL3 | 6.83 | 1.26 | 1.14E-06 |
| SYP | 5.44 | 1.26 | 0.001365681 |
| THBS1 | 5.54 | 1.26 | 0.003503354 |
| NCEH1 | 6.13 | 1.26 | 4.46E-05 |
| NR4A1 | 6.90 | 1.26 | 4.68E-05 |
| SLC35F2 | 7.04 | 1.25 | 1.11E-08 |
| DMD | 5.16 | 1.25 | 0.002847351 |
| DBH | 2.91 | 1.24 | 0.001756637 |
| COL6A2 | 5.91 | 1.23 | 0.001097686 |
| PRRG4 | 3.78 | 1.22 | 0.005515332 |
| CD83 | 6.50 | 1.21 | 0.004645157 |
| NKD1 | 4.87 | 1.21 | 0.003444565 |
| TNS3 | 3.49 | 1.21 | 0.006246705 |
| RUNX1 | 8.65 | 1.20 | 1.17E-05 |
| ERMN | 4.47 | 1.20 | 0.006067678 |
| CCDC88A | 6.65 | 1.20 | 5.90E-06 |
| KIF1A | 6.45 | 1.20 | 0.001768092 |
| ABCG2 | 4.00 | 1.19 | 0.005753528 |
| BTBD19 | 4.33 | 1.19 | 0.007617773 |
| PLEC | 10.97 | 1.18 | 3.60E-09 |
| CXCR3 | 6.33 | 1.18 | 0.002549726 |
| DMBX1 | 3.05 | 1.18 | 0.007088293 |
| MYO1D | 6.30 | 1.18 | 0.002239403 |
| TNFAIP8L3 | 2.25 | 1.17 | 0.00206138 |
| TMEM110 | 4.73 | 1.17 | 0.007195326 |
| SUOX | 5.43 | 1.16 | 0.004194609 |
| MNDA | 2.12 | 1.16 | 0.000207879 |
| BMPR2 | 7.14 | 1.16 | 3.35E-05 |
| RORC | 5.53 | 1.16 | 0.001823582 |
| CDS1 | 2.95 | 1.15 | 0.00764347 |
| CD101 | 4.71 | 1.14 | 0.007256383 |
| PLEKHA5 | 4.35 | 1.14 | 0.008745299 |
| RHOU | 7.05 | 1.13 | 1.43E-05 |
| RGCC | 8.68 | 1.13 | 0.00085465 |
| DIXDC1 | 8.17 | 1.13 | 0.013403637 |
| ZBTB18 | 6.68 | 1.12 | 0.000637155 |
| ITPR2 | 8.95 | 1.12 | 8.80E-08 |

| | | | |
|---|---|---|---|
| AFDN | 7.94 | 1.12 | 0.001097686 |
| CARMIL3 | 3.63 | 1.11 | 0.014278778 |
| ZFHX3 | 4.57 | 1.11 | 0.011854726 |
| KIFC3 | 2.24 | 1.11 | 0.003154169 |
| NRSN2 | 5.10 | 1.11 | 0.005220396 |
| PLEKHN1 | 4.29 | 1.10 | 0.016183786 |
| RSPH3 | 5.67 | 1.10 | 0.007317014 |
| RASGEF1B | 5.34 | 1.10 | 0.006575772 |
| BMP1 | 5.16 | 1.10 | 0.010226002 |
| APOBEC3H | 7.55 | 1.09 | 0.016712308 |
| THEM5 | 5.38 | 1.09 | 0.011770904 |
| PLXNB1 | 4.16 | 1.08 | 0.016920675 |
| LDLRAD4 | 7.90 | 1.08 | 2.41E-06 |
| KIAA0513 | 6.79 | 1.08 | 0.000233613 |
| CSNK1G3 | 7.61 | 1.08 | 2.39E-06 |
| CFLAR | 10.06 | 1.07 | 3.89E-06 |
| THUMPD2 | 6.68 | 1.07 | 5.23E-05 |
| CFAP57 | 1.59 | 1.06 | 0.000256322 |
| PRR5L | 5.61 | 1.06 | 0.013403637 |
| C1QL1 | 2.64 | 1.06 | 0.006391818 |
| INPP5F | 8.02 | 1.04 | 0.001077172 |
| SLC22A17 | 5.63 | 1.04 | 0.005190745 |
| EGR3 | 7.30 | 1.03 | 0.001364701 |
| MAST4 | 8.81 | 1.03 | 1.77E-05 |
| PLEKHA6 | 3.12 | 1.03 | 0.011687899 |
| PLAGL2 | 9.25 | 1.03 | 2.15E-09 |
| KIAA1671 | 8.18 | 1.03 | 0.000843242 |
| NOTCH1 | 9.24 | 1.03 | 6.62E-05 |
| CD82 | 8.82 | 1.02 | 1.12E-05 |
| FOXO1 | 9.10 | 1.02 | 1.54E-05 |
| RNFT1 | 6.26 | 1.02 | 0.001238295 |
| ADPRH | 5.48 | 1.01 | 0.018113268 |
| PFKFB3 | 10.40 | 1.01 | 0.002621996 |
| GEM | 5.59 | 1.01 | 0.016828788 |
| PLS3 | 3.99 | 1.01 | 0.034335218 |
| C15orf48 | 5.43 | 1.01 | 0.03498595 |
| SEMA4A | 6.45 | 1.01 | 0.030524698 |
| GDPD5 | 6.17 | 1.01 | 0.011481106 |
| KLHL25 | 5.41 | 1.00 | 0.007127081 |
| MELTF | 4.81 | 1.00 | 0.031851784 |
| LAMB3 | 6.16 | 1.00 | 0.023755225 |
| ALPK3 | 2.58 | 1.00 | 0.025294538 |
| KLF2 | 6.39 | -2.62 | 2.77E-15 |
| DPP4 | 10.12 | -2.43 | 1.41E-23 |
| SMAD3 | 9.08 | -2.21 | 2.62E-17 |
| HIC1 | 7.08 | -2.04 | 5.23E-10 |
| MAL | 8.90 | -2.04 | 3.83E-22 |
| SNX18 | 6.98 | -1.85 | 8.50E-10 |
| TRIB2 | 6.75 | -1.80 | 7.65E-08 |
| SDK2 | 6.26 | -1.79 | 1.12E-06 |
| RNF157 | 8.56 | -1.79 | 1.55E-10 |
| ADA2 | 6.59 | -1.78 | 7.71E-07 |

| | | | |
|---|---|---|---|
| KCNA3 | 7.97 | -1.73 | 1.26E-10 |
| ENPP2 | 6.89 | -1.71 | 1.13E-08 |
| MAP3K5 | 7.03 | -1.71 | 9.79E-11 |
| TC2N | 4.52 | -1.62 | 3.00E-05 |
| NCALD | 5.35 | -1.62 | 3.95E-06 |
| HHLA2 | 6.38 | -1.61 | 3.56E-07 |
| HS3ST3B1 | 6.26 | -1.58 | 5.60E-06 |
| MYO1F | 7.53 | -1.57 | 1.19E-07 |
| ABCD2 | 7.48 | -1.57 | 1.63E-10 |
| PRDM1 | 7.65 | -1.55 | 1.87E-06 |
| KCNA2 | 4.89 | -1.53 | 0.000107258 |
| TRPM2 | 5.88 | -1.47 | 2.34E-05 |
| CLMN | 5.63 | -1.41 | 0.000143509 |
| IL32 | 10.98 | -1.33 | 4.45E-18 |
| HDGFL3 | 7.70 | -1.32 | 6.19E-05 |
| NLRP6 | 4.46 | -1.30 | 0.002094263 |
| ST3GAL1 | 9.16 | -1.29 | 4.29E-05 |
| MMP25 | 5.42 | -1.29 | 0.000320214 |
| FGFR1 | 8.22 | -1.27 | 0.000107209 |
| TNFSF8 | 8.06 | -1.23 | 4.30E-06 |
| PIK3AP1 | 6.89 | -1.22 | 4.51E-05 |
| C1orf162 | 6.23 | -1.21 | 0.000145394 |
| EGFL6 | 6.34 | -1.21 | 0.001097686 |
| STX3 | 7.43 | -1.20 | 0.000856736 |
| SYTL2 | 7.15 | -1.19 | 1.43E-05 |
| ANXA1 | 8.76 | -1.19 | 6.62E-05 |
| RPS6KA5 | 7.15 | -1.15 | 3.03E-05 |
| CDHR1 | 5.05 | -1.14 | 0.010726575 |
| GBP5 | 11.05 | -1.14 | 1.66E-08 |
| GIMAP6 | 8.98 | -1.13 | 6.72E-09 |
| AXIN2 | 5.34 | -1.13 | 0.008111524 |
| MB21D2 | 6.80 | -1.11 | 0.003773835 |
| SPNS3 | 6.43 | -1.10 | 0.003154169 |
| NOG | 4.32 | -1.10 | 0.01647488 |
| NFIL3 | 8.95 | -1.10 | 9.33E-07 |
| CST7 | 8.00 | -1.09 | 5.31E-05 |
| VPS37B | 6.47 | -1.09 | 0.001146091 |
| GCSAM | 7.07 | -1.09 | 0.00085465 |
| CSTF2T | 8.80 | -1.07 | 9.56E-07 |
| TGFBR3 | 6.73 | -1.07 | 0.003959614 |
| JAZF1 | 5.48 | -1.07 | 0.006580473 |
| MYBL1 | 6.27 | -1.07 | 0.006190241 |
| RDH10 | 7.67 | -1.06 | 0.006300131 |
| PCSK5 | 4.87 | -1.05 | 0.021883712 |
| LRRN3 | 7.99 | -1.05 | 0.007119445 |
| HBEGF | 7.58 | -1.05 | 0.003773835 |
| CD48 | 9.78 | -1.04 | 3.68E-06 |
| F2R | 6.61 | -1.03 | 0.024724643 |
| CASP9 | 6.74 | -1.02 | 0.004036804 |
| XBP1 | 10.10 | -1.02 | 1.27E-08 |
| PIK3R6 | 6.15 | -1.02 | 0.007317014 |
| NUCB2 | 8.65 | -1.02 | 0.000874722 |

| | | | |
|---|---|---|---|
| RFLNB | 9.27 | -1.02 | 4.92E-05 |
| SELPLG | 9.65 | -1.01 | 5.88E-07 |
| KLF3 | 6.53 | -1.01 | 0.004627405 |
| RASGRP2 | 6.85 | -1.01 | 0.001399694 |
| ELOVL6 | 6.21 | -1.01 | 0.011054493 |
| LGALS14 | 3.81 | -1.00 | 0.039685429 |

**Supplementary table 6** Genes differentially expressed in macrophages after 6 hours of polarisation with IFN-γ (M1). Gene expression was compared to unstimulated macrophages used as control. Genes are ordered by Log2-fold change.

| Gene Name | Log2( Base Mean Count ) | Log2FC | P adjusted |
|---|---|---|---|
| CXCL9 | 10.75 | 6.66 | 3.92E-62 |
| SERPING1 | 7.71 | 5.79 | 1.50E-96 |
| HAPLN3 | 7.42 | 5.76 | 5.44E-49 |
| APOL4 | 8.25 | 5.64 | 1.42E-45 |
| IL31RA | 5.81 | 5.52 | 5.41E-49 |
| P2RY14 | 5.92 | 5.48 | 1.37E-49 |
| RARRES3 | 6.29 | 5.42 | 1.24E-54 |
| ANKRD22 | 4.80 | 4.71 | 1.15E-32 |
| VAMP5 | 5.71 | 4.56 | 4.14E-36 |
| GBP5 | 11.09 | 4.49 | 4.12E-28 |
| KREMEN1 | 6.18 | 4.39 | 1.26E-39 |
| FAM26F | 6.82 | 4.22 | 1.51E-25 |
| GBP1P1 | 4.74 | 4.22 | 1.71E-25 |
| BATF2 | 6.18 | 4.10 | 2.85E-34 |
| GBP4 | 10.05 | 3.90 | 4.26E-21 |
| IRF1 | 10.00 | 3.87 | 3.37E-30 |
| STEAP4 | 4.96 | 3.72 | 6.13E-21 |
| ASCL2 | 5.80 | 3.56 | 3.87E-25 |
| SECTM1 | 8.14 | 3.50 | 2.82E-61 |
| LMNB1 | 7.04 | 3.47 | 1.97E-42 |
| SOCS1 | 7.00 | 3.45 | 1.36E-16 |
| GBP1 | 10.97 | 3.44 | 8.52E-17 |
| MMP25-AS1 | 4.90 | 3.30 | 9.68E-17 |
| STAP1 | 4.74 | 3.30 | 3.15E-16 |
| FCGR1B | 6.38 | 3.27 | 1.26E-26 |
| CD274 | 9.57 | 3.26 | 1.24E-20 |
| TIFA | 6.94 | 3.24 | 1.76E-31 |
| IL27 | 4.18 | 3.23 | 5.00E-15 |
| ENPP2 | 5.33 | 3.06 | 1.47E-15 |
| APOL6 | 10.52 | 3.06 | 1.55E-81 |
| JAK2 | 8.92 | 3.00 | 6.29E-49 |
| TNFSF10 | 7.85 | 2.99 | 1.55E-12 |
| IL15 | 5.43 | 2.91 | 9.67E-16 |
| GBP2 | 8.58 | 2.91 | 1.20E-14 |
| C4orf32 | 5.99 | 2.90 | 1.67E-17 |
| FCGR1CP | 5.11 | 2.86 | 9.41E-14 |
| NFIX | 4.87 | 2.81 | 4.13E-13 |
| WARS | 12.53 | 2.81 | 1.16E-56 |
| APOL1 | 8.18 | 2.81 | 5.94E-51 |
| GCNT1 | 7.52 | 2.79 | 5.19E-36 |
| LAP3 | 10.44 | 2.77 | 3.67E-56 |
| IFI35 | 7.49 | 2.66 | 2.29E-20 |
| FCGR1A | 8.23 | 2.64 | 6.81E-29 |
| IL15RA | 6.46 | 2.63 | 8.49E-10 |
| CD226 | 4.14 | 2.62 | 5.46E-10 |
| XRN1 | 8.97 | 2.61 | 5.65E-52 |

| | | | |
|---|---|---|---|
| ATP10A | 5.42 | 2.60 | 1.16E-11 |
| GK | 8.95 | 2.59 | 1.51E-33 |
| APOBEC3A | 7.85 | 2.59 | 2.76E-20 |
| CFH | 3.56 | 2.57 | 1.24E-09 |
| IL2RA | 4.50 | 2.55 | 2.98E-09 |
| APOL2 | 9.48 | 2.52 | 4.96E-57 |
| STAT1 | 11.43 | 2.48 | 7.89E-15 |
| PSTPIP2 | 9.02 | 2.45 | 6.45E-10 |
| FAM20A | 6.15 | 2.45 | 8.86E-15 |
| GCH1 | 8.51 | 2.44 | 1.43E-08 |
| CYSLTR2 | 4.41 | 2.43 | 1.45E-08 |
| VPS9D1 | 6.65 | 2.43 | 1.29E-19 |
| STAMBPL1 | 4.01 | 2.41 | 1.77E-08 |
| C21orf91 | 5.34 | 2.40 | 2.34E-10 |
| ASPHD2 | 4.55 | 2.39 | 1.35E-08 |
| GRIN3A | 5.55 | 2.38 | 5.88E-12 |
| RHOU | 7.70 | 2.38 | 5.92E-28 |
| PARP14 | 11.16 | 2.38 | 3.14E-11 |
| HIVEP2 | 7.07 | 2.38 | 8.71E-13 |
| SAMD9L | 10.07 | 2.37 | 3.17E-11 |
| C1orf228 | 3.78 | 2.36 | 5.79E-08 |
| JAK3 | 7.04 | 2.35 | 5.29E-08 |
| NLRC5 | 8.52 | 2.33 | 1.55E-39 |
| BATF3 | 4.95 | 2.31 | 9.48E-09 |
| RNF213 | 12.08 | 2.31 | 8.24E-44 |
| PDCD1LG2 | 7.54 | 2.29 | 1.03E-17 |
| CCL13 | 3.87 | 2.24 | 2.98E-07 |
| PPA1 | 7.30 | 2.22 | 2.35E-18 |
| TBX21 | 4.36 | 2.22 | 1.38E-07 |
| SEPT04 | 5.56 | 2.19 | 2.31E-10 |
| IFITM1 | 3.63 | 2.19 | 6.14E-07 |
| CIITA | 10.39 | 2.19 | 6.86E-67 |
| FBXO6 | 7.29 | 2.18 | 5.15E-14 |
| TAGAP | 8.70 | 2.17 | 8.95E-38 |
| FCRL6 | 5.31 | 2.16 | 4.35E-09 |
| IL7 | 4.96 | 2.16 | 2.22E-07 |
| EPSTI1 | 8.18 | 2.16 | 8.28E-07 |
| LIMK2 | 7.00 | 2.16 | 6.24E-17 |
| PARP9 | 9.01 | 2.15 | 6.05E-19 |
| KIAA0040 | 7.62 | 2.15 | 6.39E-24 |
| STX11 | 7.68 | 2.12 | 7.03E-14 |
| TRIM22 | 9.25 | 2.11 | 3.28E-20 |
| CXCL10 | 11.14 | 2.11 | 2.13E-09 |
| AUTS2 | 3.82 | 2.10 | 2.03E-06 |
| BBX | 8.17 | 2.09 | 1.46E-28 |
| FPR2 | 5.04 | 2.08 | 7.61E-07 |
| DDX60 | 7.52 | 2.07 | 9.73E-13 |
| TRAFD1 | 8.45 | 2.07 | 6.36E-22 |
| RNF19B | 8.20 | 2.07 | 2.40E-16 |
| CSF2RB | 9.47 | 2.06 | 3.79E-41 |
| BAZ1A | 9.44 | 2.06 | 3.13E-35 |
| PML | 8.17 | 2.06 | 2.27E-19 |

| | | | |
|---|---|---|---|
| DNMT3B | 3.43 | 2.05 | 4.14E-06 |
| DTX3L | 9.50 | 2.04 | 4.02E-32 |
| GIMAP5 | 4.76 | 2.04 | 5.09E-07 |
| APOL3 | 9.63 | 2.04 | 5.42E-06 |
| GBP3 | 7.16 | 2.03 | 3.39E-15 |
| PLSCR4 | 2.68 | 2.02 | 7.61E-07 |
| CASP4 | 8.94 | 2.01 | 1.36E-31 |
| GCSAM | 3.24 | 2.01 | 6.18E-06 |
| UBE2L6 | 8.91 | 2.01 | 2.18E-27 |
| GUCY1A3 | 2.79 | 2.00 | 1.71E-06 |
| IFIT5 | 6.95 | 2.00 | 1.85E-11 |
| VCAM1 | 6.29 | 1.98 | 1.12E-05 |
| APOBEC3G | 6.53 | 1.98 | 3.88E-11 |
| NOD2 | 6.65 | 1.98 | 4.46E-13 |
| SDC3 | 8.00 | 1.97 | 2.96E-23 |
| IFIT2 | 8.75 | 1.96 | 6.14E-06 |
| DEK | 9.24 | 1.96 | 1.85E-40 |
| SNX10 | 9.89 | 1.95 | 1.11E-22 |
| NEXN | 3.72 | 1.95 | 1.40E-05 |
| CXCL11 | 6.64 | 1.95 | 5.34E-08 |
| CCL7 | 5.74 | 1.94 | 1.81E-08 |
| AFDN | 6.37 | 1.94 | 1.01E-09 |
| CCL2 | 10.17 | 1.93 | 8.42E-08 |
| CERS6 | 8.40 | 1.93 | 6.14E-28 |
| AMER1 | 5.52 | 1.92 | 6.25E-08 |
| EPB41L5 | 3.77 | 1.91 | 2.32E-05 |
| CD69 | 2.54 | 1.91 | 1.51E-06 |
| ARNTL2 | 7.62 | 1.91 | 5.66E-11 |
| MOB3B | 6.15 | 1.90 | 1.20E-09 |
| C5orf56 | 5.34 | 1.90 | 2.42E-06 |
| FAS | 7.29 | 1.90 | 1.52E-12 |
| BRIP1 | 3.76 | 1.89 | 2.96E-05 |
| ENDOD1 | 6.67 | 1.88 | 3.66E-11 |
| BATF | 6.55 | 1.88 | 2.12E-09 |
| MIR503HG | 2.92 | 1.88 | 2.45E-05 |
| IFIT3 | 9.26 | 1.87 | 3.13E-05 |
| CEACAM1 | 2.30 | 1.86 | 1.87E-06 |
| GIMAP7 | 5.95 | 1.86 | 1.13E-07 |
| NMI | 7.81 | 1.85 | 2.13E-19 |
| FGL2 | 10.18 | 1.85 | 6.14E-28 |
| ZFP36 | 8.53 | 1.85 | 1.00E-23 |
| PSME2 | 9.08 | 1.84 | 1.64E-19 |
| SASH1 | 7.93 | 1.84 | 6.86E-12 |
| NUB1 | 8.44 | 1.83 | 2.74E-16 |
| GOLM1 | 5.85 | 1.83 | 2.22E-08 |
| TMEM173 | 5.98 | 1.83 | 8.70E-08 |
| HCAR2 | 4.33 | 1.83 | 5.29E-05 |
| GVINP1 | 7.19 | 1.83 | 7.61E-15 |
| TYMP | 10.13 | 1.82 | 4.96E-19 |
| SOCS3 | 7.33 | 1.81 | 7.44E-05 |
| GLS | 9.46 | 1.79 | 1.05E-32 |
| DENND1B | 7.94 | 1.79 | 3.15E-16 |

| | | | |
|---|---|---|---|
| CASP7 | 7.52 | 1.79 | 7.61E-15 |
| P2RY6 | 7.13 | 1.79 | 9.90E-11 |
| BANK1 | 3.55 | 1.79 | 9.77E-05 |
| CD38 | 6.62 | 1.78 | 8.06E-05 |
| RGS3 | 6.29 | 1.77 | 2.53E-09 |
| CLEC10A | 6.82 | 1.77 | 4.66E-09 |
| GADD45B | 6.89 | 1.75 | 2.70E-08 |
| TNFSF13B | 8.88 | 1.75 | 9.11E-19 |
| B4GALT5 | 10.54 | 1.73 | 2.58E-20 |
| SP110 | 5.95 | 1.72 | 1.81E-06 |
| STAT3 | 9.97 | 1.72 | 1.38E-33 |
| SCIN | 7.87 | 1.72 | 3.71E-10 |
| IFITM3 | 6.85 | 1.72 | 0.000203502 |
| PLSCR1 | 8.32 | 1.72 | 6.00E-05 |
| ICAM1 | 10.31 | 1.72 | 2.48E-06 |
| USP6NL | 7.83 | 1.70 | 7.63E-14 |
| STAT2 | 10.27 | 1.69 | 9.85E-14 |
| XIRP1 | 3.28 | 1.69 | 0.000184552 |
| AIM2 | 2.24 | 1.68 | 2.14E-05 |
| SLC40A1 | 7.55 | 1.68 | 6.94E-05 |
| RCN1 | 8.01 | 1.68 | 1.34E-13 |
| GIMAP4 | 7.45 | 1.68 | 1.76E-12 |
| PDE4B | 7.30 | 1.68 | 0.000269803 |
| JAG1 | 8.03 | 1.68 | 0.000224678 |
| HEG1 | 8.54 | 1.67 | 3.75E-18 |
| TOP1 | 9.36 | 1.67 | 2.88E-25 |
| RTP4 | 3.81 | 1.66 | 0.000325621 |
| MB21D1 | 6.81 | 1.65 | 3.28E-10 |
| SFT2D2 | 9.71 | 1.64 | 1.28E-23 |
| MLLT3 | 4.16 | 1.64 | 0.000263399 |
| SCN9A | 2.73 | 1.63 | 0.000195633 |
| SFMBT2 | 7.93 | 1.63 | 1.83E-15 |
| RHEBL1 | 3.49 | 1.63 | 0.000462236 |
| RMI2 | 3.42 | 1.63 | 0.000506081 |
| PTGES3P1 | 3.64 | 1.62 | 0.000536344 |
| TMEM109 | 8.05 | 1.62 | 2.10E-17 |
| HCAR3 | 4.15 | 1.61 | 0.000546144 |
| RHOBTB3 | 5.24 | 1.61 | 4.93E-05 |
| SLAMF8 | 10.44 | 1.61 | 4.24E-28 |
| IL32 | 5.20 | 1.60 | 0.000510509 |
| LRRK2 | 8.81 | 1.59 | 1.27E-15 |
| MUC1 | 2.62 | 1.59 | 0.000320588 |
| HIVEP3 | 9.25 | 1.59 | 2.33E-11 |
| NAMPT | 9.68 | 1.59 | 0.000510509 |
| MCL1 | 10.10 | 1.59 | 3.14E-21 |
| RUNX3 | 8.06 | 1.58 | 4.01E-14 |
| TSHZ3 | 5.33 | 1.58 | 2.38E-05 |
| DAPP1 | 7.94 | 1.57 | 3.54E-12 |
| RSAD2 | 9.05 | 1.57 | 4.37E-05 |
| ADGRE5 | 9.15 | 1.57 | 2.00E-17 |
| SIPA1L1 | 6.75 | 1.57 | 4.57E-07 |
| ISOC1 | 7.12 | 1.57 | 3.68E-10 |

| | | | |
|---|---|---|---|
| CSRNP1 | 5.72 | 1.56 | 1.03E-05 |
| PARP12 | 9.03 | 1.56 | 1.87E-15 |
| AKAP12 | 2.77 | 1.56 | 0.000427717 |
| ANKRD44 | 7.81 | 1.56 | 8.92E-13 |
| RALA | 8.35 | 1.56 | 8.52E-17 |
| CD40 | 9.02 | 1.55 | 0.000525851 |
| NRP2 | 10.85 | 1.55 | 4.76E-25 |
| ATG3 | 8.68 | 1.55 | 6.55E-21 |
| HELB | 5.93 | 1.55 | 5.55E-06 |
| PDGFRA | 3.73 | 1.54 | 0.001066734 |
| CASP5 | 2.94 | 1.54 | 0.000734111 |
| CASZ1 | 4.46 | 1.53 | 0.000666994 |
| SLC30A4 | 5.49 | 1.53 | 0.000673878 |
| USP30-AS1 | 3.80 | 1.52 | 0.001283654 |
| SMCO4 | 7.20 | 1.52 | 1.80E-09 |
| LINC00996 | 3.79 | 1.52 | 0.001415845 |
| PTGS2 | 5.24 | 1.51 | 0.000497173 |
| LONRF1 | 6.60 | 1.51 | 2.77E-08 |
| HESX1 | 2.88 | 1.51 | 0.000525851 |
| CLEC2B | 7.07 | 1.51 | 5.87E-10 |
| PTPN2 | 7.98 | 1.50 | 1.45E-13 |
| MX1 | 9.48 | 1.50 | 0.001342285 |
| IGF2BP2 | 6.12 | 1.50 | 5.51E-06 |
| ATF5 | 9.02 | 1.49 | 4.93E-05 |
| CCL8 | 7.71 | 1.49 | 7.64E-05 |
| RALB | 9.37 | 1.49 | 1.53E-20 |
| POLR3D | 6.52 | 1.48 | 2.62E-07 |
| SLC2A3 | 8.62 | 1.48 | 1.56E-09 |
| FAM92A | 5.31 | 1.48 | 0.000132647 |
| ARAP2 | 8.43 | 1.48 | 2.40E-14 |
| CMPK2 | 7.33 | 1.48 | 0.001668183 |
| IFIH1 | 8.86 | 1.48 | 0.000118475 |
| XAF1 | 7.00 | 1.47 | 0.002247618 |
| RHBDF2 | 9.29 | 1.47 | 9.34E-11 |
| SCIMP | 8.60 | 1.47 | 5.46E-10 |
| SNX20 | 7.92 | 1.46 | 2.08E-12 |
| CD47 | 9.37 | 1.46 | 1.19E-17 |
| VRK2 | 7.00 | 1.46 | 1.18E-07 |
| INSIG1 | 9.95 | 1.46 | 3.68E-15 |
| RAB39A | 6.60 | 1.45 | 2.98E-07 |
| STOM | 9.41 | 1.45 | 1.17E-17 |
| ANK2 | 5.31 | 1.45 | 0.000252239 |
| CCR5 | 9.98 | 1.45 | 3.03E-11 |
| GALNT3 | 4.68 | 1.44 | 0.000815051 |
| RAPGEF2 | 8.69 | 1.44 | 2.51E-12 |
| PRR5L | 6.42 | 1.44 | 6.48E-06 |
| APOBEC3F | 4.53 | 1.44 | 0.001059776 |
| CDCP1 | 6.80 | 1.44 | 4.27E-08 |
| CASP1 | 9.26 | 1.43 | 1.25E-15 |
| SLC25A28 | 6.39 | 1.43 | 2.18E-06 |
| DYSF | 6.22 | 1.43 | 6.78E-05 |
| CASP10 | 7.13 | 1.43 | 1.40E-08 |

| | | | |
|---|---|---|---|
| MCTP2 | 3.43 | 1.42 | 0.003332239 |
| C19orf12 | 7.27 | 1.42 | 5.46E-10 |
| TRIM21 | 7.51 | 1.41 | 5.87E-10 |
| IFI16 | 9.66 | 1.41 | 3.94E-21 |
| NUDCD1 | 6.26 | 1.41 | 5.39E-06 |
| KPNA5 | 5.31 | 1.41 | 0.000254212 |
| C1QC | 9.27 | 1.40 | 9.34E-11 |
| PARP11 | 6.87 | 1.40 | 1.06E-07 |
| C1QB | 8.28 | 1.40 | 1.76E-07 |
| CASP8 | 7.63 | 1.40 | 7.10E-12 |
| SSTR2 | 7.37 | 1.40 | 7.18E-08 |
| TBC1D31 | 5.37 | 1.40 | 0.000311412 |
| LGALS3BP | 7.47 | 1.40 | 2.08E-09 |
| SRGAP2C | 5.76 | 1.40 | 0.000101118 |
| OAS3 | 9.70 | 1.40 | 0.003607739 |
| GAREM1 | 2.68 | 1.39 | 0.002652242 |
| SCO2 | 5.42 | 1.39 | 0.000237243 |
| MT2A | 3.18 | 1.39 | 0.002717812 |
| OAS2 | 9.11 | 1.39 | 0.004532511 |
| TMTC2 | 4.54 | 1.38 | 0.002112957 |
| DTNB | 5.46 | 1.38 | 0.000267462 |
| SLC6A12 | 7.78 | 1.38 | 1.76E-08 |
| IRF7 | 2.84 | 1.38 | 0.002558134 |
| DYNLT1 | 7.74 | 1.38 | 6.10E-11 |
| TMEM2 | 7.92 | 1.38 | 6.13E-10 |
| WWC3 | 6.70 | 1.38 | 5.88E-07 |
| BIRC3 | 9.02 | 1.38 | 0.000981822 |
| RNF144B | 8.79 | 1.37 | 0.001318616 |
| SLC37A1 | 7.10 | 1.37 | 2.35E-07 |
| IL10RA | 10.19 | 1.37 | 1.81E-10 |
| TFEC | 10.51 | 1.37 | 9.01E-16 |
| RERE | 8.56 | 1.37 | 1.18E-14 |
| P2RX7 | 10.95 | 1.36 | 0.0018682 |
| FYB1 | 10.51 | 1.36 | 2.02E-18 |
| ODF3B | 6.20 | 1.36 | 0.000118458 |
| IFI44L | 7.59 | 1.36 | 0.001138366 |
| PPTC7 | 8.36 | 1.35 | 1.76E-13 |
| GAS6 | 6.51 | 1.35 | 2.26E-05 |
| SRGAP2 | 8.39 | 1.35 | 9.14E-11 |
| PLEK | 12.53 | 1.35 | 9.22E-13 |
| CISH | 7.13 | 1.35 | 1.51E-06 |
| KARS | 9.11 | 1.34 | 1.55E-15 |
| TMEM51 | 7.92 | 1.34 | 1.51E-09 |
| DDX58 | 7.63 | 1.34 | 0.004408931 |
| PRRG4 | 5.77 | 1.34 | 0.000115361 |
| HELZ2 | 7.71 | 1.34 | 0.006591315 |
| BCAR3 | 7.65 | 1.33 | 6.24E-09 |
| CNTLN | 6.80 | 1.33 | 2.60E-07 |
| ZNFX1 | 10.07 | 1.33 | 1.77E-13 |
| PRRT2 | 2.37 | 1.32 | 0.002346497 |
| ST3GAL5 | 8.52 | 1.32 | 2.37E-14 |
| UNC5A | 3.51 | 1.32 | 0.007610186 |

| | | | |
|---|---|---|---|
| TNFAIP8 | 8.51 | 1.32 | 4.57E-07 |
| CDC42SE2 | 8.87 | 1.32 | 1.19E-13 |
| C15orf39 | 6.97 | 1.32 | 1.17E-06 |
| MAP3K7CL | 2.91 | 1.31 | 0.006930568 |
| KDELC2 | 6.57 | 1.31 | 6.14E-06 |
| SWT1 | 5.89 | 1.31 | 9.89E-05 |
| C3orf38 | 7.62 | 1.31 | 1.34E-09 |
| FPR1 | 7.55 | 1.31 | 0.000153166 |
| DSE | 8.84 | 1.31 | 9.34E-11 |
| TMEM236 | 4.29 | 1.31 | 0.006815622 |
| NT5C3A | 6.32 | 1.30 | 5.57E-05 |
| FCER2 | 4.92 | 1.30 | 0.00440233 |
| C5orf15 | 8.00 | 1.30 | 4.51E-08 |
| NECTIN2 | 8.14 | 1.30 | 5.21E-06 |
| SLC30A1 | 8.45 | 1.30 | 2.69E-12 |
| SELENOI | 7.63 | 1.30 | 5.08E-08 |
| PANX1 | 7.11 | 1.29 | 4.57E-07 |
| FARP2 | 7.50 | 1.29 | 8.42E-08 |
| FLVCR2 | 6.75 | 1.28 | 0.000497173 |
| PLA2G4A | 7.02 | 1.28 | 3.41E-07 |
| TCF7L2 | 5.17 | 1.27 | 0.002220157 |
| IFI44 | 7.29 | 1.27 | 0.011270617 |
| LPGAT1 | 9.06 | 1.27 | 1.10E-15 |
| ISG20 | 3.61 | 1.27 | 0.010998713 |
| POLB | 5.64 | 1.26 | 0.000743162 |
| RBMS1 | 9.26 | 1.26 | 5.38E-12 |
| TRABD2A | 4.26 | 1.26 | 0.007610186 |
| SP140L | 7.13 | 1.26 | 6.76E-07 |
| SMCHD1 | 8.75 | 1.25 | 3.69E-14 |
| TGFB1 | 10.49 | 1.25 | 4.83E-23 |
| STK3 | 6.55 | 1.25 | 2.63E-05 |
| INPP4B | 4.06 | 1.25 | 0.012272271 |
| TJP2 | 8.34 | 1.25 | 6.69E-07 |
| CALCOCO2 | 8.78 | 1.24 | 3.54E-14 |
| ZNF618 | 6.26 | 1.24 | 0.000118812 |
| RB1 | 9.09 | 1.24 | 3.25E-15 |
| CBR3 | 3.66 | 1.24 | 0.013950059 |
| EDN1 | 2.35 | 1.24 | 0.004486642 |
| SP140 | 5.21 | 1.24 | 0.004436532 |
| DNAJA1 | 10.05 | 1.24 | 8.84E-18 |
| MRC1 | 10.93 | 1.24 | 5.71E-18 |
| SLC8A1 | 8.00 | 1.23 | 1.68E-09 |
| OPTN | 9.31 | 1.23 | 5.22E-11 |
| TMEM106A | 8.41 | 1.23 | 4.27E-08 |
| ARL5B | 7.22 | 1.23 | 1.19E-05 |
| CARD16 | 5.62 | 1.23 | 0.001216874 |
| TANC1 | 2.71 | 1.22 | 0.011412096 |
| RBCK1 | 7.74 | 1.22 | 7.62E-08 |
| MACF1 | 11.03 | 1.22 | 8.21E-15 |
| SNX16 | 6.09 | 1.22 | 0.000261804 |
| PHF11 | 7.08 | 1.21 | 8.62E-06 |
| MAP3K8 | 6.97 | 1.21 | 0.000206404 |

| | | | |
|---|---|---|---|
| TMEM144 | 8.14 | 1.21 | 5.88E-07 |
| FRMD3 | 5.34 | 1.21 | 0.002489102 |
| GGT5 | 2.70 | 1.21 | 0.010121801 |
| GIMAP6 | 5.81 | 1.20 | 0.000482701 |
| JADE2 | 7.43 | 1.20 | 2.12E-07 |
| OAS1 | 8.05 | 1.20 | 0.012432439 |
| LCP2 | 9.34 | 1.20 | 4.23E-15 |
| ELF4 | 8.58 | 1.20 | 7.23E-11 |
| VCPIP1 | 7.98 | 1.20 | 1.80E-09 |
| SLC38A5 | 3.09 | 1.20 | 0.012337078 |
| GNA13 | 10.04 | 1.19 | 9.12E-18 |
| SMTNL1 | 2.76 | 1.19 | 0.011072112 |
| SLC25A30 | 7.54 | 1.19 | 3.35E-08 |
| EAF1 | 8.59 | 1.19 | 1.39E-08 |
| GPR85 | 3.75 | 1.18 | 0.020974347 |
| NCOA1 | 8.91 | 1.18 | 3.09E-11 |
| RIPK2 | 8.38 | 1.18 | 3.83E-08 |
| PIK3R3 | 4.68 | 1.17 | 0.011270617 |
| ASCC3 | 8.57 | 1.17 | 7.36E-09 |
| PAK1 | 8.54 | 1.17 | 9.36E-11 |
| TXN | 10.33 | 1.17 | 7.51E-07 |
| ATP1B1 | 9.45 | 1.17 | 8.17E-12 |
| TMEM131L | 6.65 | 1.16 | 7.02E-05 |
| LYSMD2 | 5.59 | 1.16 | 0.002270457 |
| KCNJ2 | 6.45 | 1.16 | 0.002506706 |
| PRLR | 6.21 | 1.16 | 0.000459877 |
| GTPBP1 | 7.34 | 1.16 | 1.11E-05 |
| REEP4 | 6.93 | 1.16 | 1.35E-05 |
| MIR155HG | 5.18 | 1.16 | 0.011184968 |
| LYN | 10.58 | 1.15 | 0.003503481 |
| BCL6 | 8.48 | 1.15 | 2.10E-08 |
| C1GALT1 | 6.73 | 1.15 | 9.87E-05 |
| MIIP | 7.02 | 1.15 | 1.62E-05 |
| RNF217 | 6.41 | 1.15 | 0.000257223 |
| LRRC8C | 6.58 | 1.15 | 0.00028248 |
| PPP1R16B | 3.53 | 1.15 | 0.027687338 |
| SAMD4A | 8.70 | 1.14 | 6.31E-09 |
| PRPS2 | 7.11 | 1.14 | 1.16E-05 |
| ATP10D | 7.54 | 1.14 | 4.42E-06 |
| ITPRIPL2 | 8.65 | 1.13 | 1.05E-10 |
| ITGA4 | 7.44 | 1.13 | 5.83E-05 |
| SLC31A2 | 4.70 | 1.13 | 0.013231972 |
| NAMPTP1 | 3.52 | 1.13 | 0.028509454 |
| CYLD | 8.73 | 1.12 | 1.10E-07 |
| BLOC1S6 | 9.04 | 1.12 | 6.60E-13 |
| PSME1 | 8.42 | 1.12 | 2.65E-06 |
| EDEM1 | 10.01 | 1.12 | 5.82E-11 |
| SIGLEC12 | 2.26 | 1.12 | 0.012850694 |
| TMEM229B | 3.58 | 1.12 | 0.033431125 |
| ANKRD29 | 4.91 | 1.12 | 0.011252848 |
| SH3BP4 | 4.90 | 1.12 | 0.011814328 |
| FAM46A | 9.04 | 1.12 | 4.96E-07 |

| | | | |
|---|---|---|---|
| CCNA1 | 5.24 | 1.11 | 0.008287489 |
| LPCAT2 | 8.89 | 1.11 | 5.60E-12 |
| ZFYVE28 | 5.83 | 1.11 | 0.003348 |
| ZNF200 | 6.12 | 1.11 | 0.000734111 |
| MX2 | 8.29 | 1.10 | 0.035383771 |
| SCML1 | 6.61 | 1.10 | 0.000292327 |
| DDX60L | 9.06 | 1.10 | 6.80E-07 |
| AMOTL2 | 3.12 | 1.10 | 0.029924952 |
| IL1RAP | 6.14 | 1.10 | 0.002153857 |
| MSRB1 | 7.07 | 1.10 | 3.43E-05 |
| CD33 | 7.73 | 1.10 | 2.21E-06 |
| AP1AR | 7.37 | 1.10 | 6.58E-05 |
| ADAR | 10.74 | 1.10 | 4.35E-09 |
| MTHFD2 | 9.57 | 1.10 | 1.80E-09 |
| SSB | 8.51 | 1.09 | 1.17E-08 |
| C19orf66 | 6.39 | 1.09 | 0.000413638 |
| GIMAP8 | 7.34 | 1.09 | 8.57E-06 |
| LACTB | 9.76 | 1.09 | 1.82E-14 |
| PDGFA | 2.91 | 1.09 | 0.034663214 |
| SNTB2 | 7.14 | 1.09 | 1.59E-05 |
| BPGM | 6.06 | 1.09 | 0.001427756 |
| LINC00623 | 3.27 | 1.09 | 0.040138337 |
| ZC3H3 | 5.90 | 1.09 | 0.002467696 |
| GTF2F2 | 6.89 | 1.09 | 4.61E-05 |
| CCDC50 | 7.69 | 1.08 | 7.61E-07 |
| DTNBP1 | 6.34 | 1.08 | 0.001075895 |
| AK4 | 7.58 | 1.08 | 0.001211998 |
| SLAMF7 | 11.75 | 1.08 | 0.013421411 |
| MMP25 | 5.54 | 1.08 | 0.007610186 |
| ZHX1 | 8.06 | 1.07 | 2.86E-07 |
| CCR1 | 10.92 | 1.07 | 1.70E-14 |
| PTPRC | 10.94 | 1.07 | 1.38E-13 |
| SREBF1 | 7.70 | 1.07 | 1.17E-06 |
| CETP | 2.22 | 1.07 | 0.025560739 |
| ARID5A | 7.81 | 1.07 | 2.73E-06 |
| SRGAP2B | 4.88 | 1.06 | 0.018244763 |
| SNHG28 | 4.32 | 1.06 | 0.034599559 |
| SNX6 | 8.79 | 1.06 | 2.62E-08 |
| CD209 | 8.02 | 1.06 | 0.000138475 |
| GLUL | 12.88 | 1.06 | 3.66E-07 |
| DHX58 | 6.94 | 1.06 | 0.00503742 |
| FBN2 | 5.69 | 1.06 | 0.003926903 |
| L3MBTL3 | 5.54 | 1.06 | 0.007726869 |
| STAT4 | 5.35 | 1.06 | 0.035097639 |
| F3 | 8.64 | 1.05 | 7.68E-08 |
| COLQ | 4.87 | 1.05 | 0.034400571 |
| GNE | 6.79 | 1.05 | 0.000253638 |
| EXPH5 | 2.25 | 1.05 | 0.028852702 |
| SUCNR1 | 10.05 | 1.05 | 0.00474727 |
| EIF2AK2 | 8.86 | 1.05 | 0.000134538 |
| UBE2F | 6.38 | 1.04 | 0.000933449 |
| ARHGAP17 | 9.29 | 1.04 | 1.93E-12 |

| | | | |
|---|---|---|---|
| SEMA4D | 7.14 | 1.04 | 0.000229094 |
| ZNF276 | 5.91 | 1.04 | 0.005594064 |
| EZH2 | 5.95 | 1.04 | 0.005291699 |
| UBR1 | 7.98 | 1.04 | 2.88E-07 |
| AXL | 5.96 | 1.04 | 0.004486642 |
| RNF138 | 6.42 | 1.04 | 0.001291552 |
| DDX21 | 9.47 | 1.04 | 7.33E-08 |
| PCNX1 | 8.76 | 1.03 | 6.86E-08 |
| KLF10 | 7.97 | 1.03 | 4.14E-07 |
| CR1L | 2.56 | 1.03 | 0.035187253 |
| CNDP2 | 10.58 | 1.03 | 1.14E-15 |
| UBA6 | 8.63 | 1.03 | 3.60E-09 |
| ABCB1 | 2.40 | 1.03 | 0.038541489 |
| SUB1 | 8.49 | 1.03 | 6.57E-07 |
| POMP | 8.85 | 1.03 | 6.61E-10 |
| ARHGAP5 | 8.02 | 1.03 | 1.59E-07 |
| GADD45G | 5.09 | 1.02 | 0.021059355 |
| DSC2 | 7.14 | 1.02 | 0.000453744 |
| PMAIP1 | 4.49 | 1.02 | 0.038432201 |
| GRAMD1B | 6.59 | 1.02 | 0.00182412 |
| DRAM1 | 10.13 | 1.02 | 0.012537881 |
| TRIM5 | 6.89 | 1.02 | 0.000319783 |
| PSMA2 | 4.43 | 1.02 | 0.044847233 |
| ARRDC4 | 7.57 | 1.01 | 0.000142745 |
| PHACTR2 | 7.96 | 1.01 | 5.12E-05 |
| CAMK2D | 7.92 | 1.01 | 2.24E-05 |
| OSBPL6 | 2.41 | 1.01 | 0.04027502 |
| RUNX1 | 8.55 | 1.01 | 2.12E-08 |
| MAX | 8.12 | 1.01 | 1.02E-06 |
| CSRNP2 | 6.96 | 1.01 | 0.000115855 |
| KLF3 | 7.94 | 1.01 | 3.26E-06 |
| CUL1 | 8.44 | 1.01 | 1.76E-07 |
| FAM177A1 | 6.76 | 1.00 | 0.000324205 |
| EML4 | 9.61 | 1.00 | 4.90E-12 |
| GYPC | 7.09 | 1.00 | 0.00025384 |
| TAGLN | 6.43 | 1.00 | 0.000994225 |
| XYLT1 | 7.26 | -2.32 | 2.47E-14 |
| NHSL2 | 7.72 | -2.30 | 1.72E-18 |
| TLR5 | 7.50 | -2.29 | 1.57E-20 |
| CXCR4 | 8.60 | -2.21 | 1.66E-23 |
| RASAL1 | 5.96 | -2.16 | 1.88E-09 |
| GPR183 | 8.16 | -2.10 | 6.03E-18 |
| BMF | 8.32 | -2.05 | 2.60E-23 |
| SRGAP3 | 4.57 | -1.96 | 8.85E-06 |
| ALOX15B | 7.86 | -1.84 | 4.02E-13 |
| PDK4 | 4.85 | -1.78 | 9.42E-05 |
| NHS | 3.74 | -1.78 | 0.000102529 |
| NOTCH3 | 6.91 | -1.78 | 4.96E-07 |
| MERTK | 6.97 | -1.74 | 1.06E-08 |
| IL1R1 | 7.63 | -1.73 | 2.15E-09 |
| OLR1 | 8.35 | -1.72 | 1.47E-10 |
| NAV2 | 5.58 | -1.72 | 6.30E-06 |

| | | | |
|---|---|---|---|
| CDKN2B | 6.16 | -1.71 | 1.20E-06 |
| EEPD1 | 7.06 | -1.71 | 9.80E-09 |
| FAM13A | 5.95 | -1.71 | 3.73E-07 |
| MYCL | 5.15 | -1.70 | 4.38E-05 |
| IFNGR1 | 10.04 | -1.68 | 4.10E-31 |
| ZNF589 | 8.48 | -1.68 | 7.75E-13 |
| TLE3 | 8.41 | -1.67 | 1.77E-16 |
| SLIT3 | 5.66 | -1.62 | 1.36E-05 |
| KCNA2 | 5.77 | -1.62 | 1.51E-05 |
| KANK2 | 5.51 | -1.58 | 6.45E-05 |
| TRIM2 | 5.88 | -1.57 | 3.24E-05 |
| CLMN | 7.64 | -1.57 | 1.81E-10 |
| FBXL20 | 6.50 | -1.55 | 6.86E-07 |
| CABLES1 | 4.70 | -1.53 | 0.000834121 |
| ATG16L2 | 7.90 | -1.52 | 5.18E-11 |
| CACNA2D3 | 2.97 | -1.51 | 0.000745044 |
| RAB3D | 5.73 | -1.51 | 0.000222906 |
| NOL4L | 6.40 | -1.50 | 2.73E-05 |
| SLC25A29 | 7.70 | -1.49 | 1.89E-10 |
| SH3PXD2A | 7.26 | -1.47 | 7.85E-06 |
| SLC24A4 | 4.41 | -1.46 | 0.001974248 |
| AMPD3 | 9.55 | -1.46 | 1.24E-11 |
| BNC2 | 4.87 | -1.45 | 0.001106148 |
| PELI3 | 5.11 | -1.43 | 0.000492313 |
| FOXO3 | 7.34 | -1.43 | 6.81E-09 |
| C15orf52 | 7.17 | -1.42 | 3.69E-07 |
| TNS1 | 9.63 | -1.42 | 9.51E-10 |
| NLRP12 | 5.99 | -1.42 | 3.67E-05 |
| INSR | 6.25 | -1.41 | 3.67E-05 |
| SLC27A1 | 8.06 | -1.40 | 2.78E-09 |
| ABCA1 | 8.17 | -1.39 | 6.17E-09 |
| NAV1 | 6.73 | -1.39 | 3.30E-05 |
| LDLRAD4 | 7.13 | -1.39 | 1.13E-06 |
| CERK | 7.80 | -1.39 | 8.49E-10 |
| ZNF395 | 5.76 | -1.38 | 0.000172052 |
| ZNF704 | 5.12 | -1.36 | 0.003697081 |
| LFNG | 6.56 | -1.36 | 6.14E-06 |
| PLIN2 | 10.72 | -1.35 | 2.43E-13 |
| RDH10 | 6.10 | -1.35 | 0.000174866 |
| YPEL3 | 5.64 | -1.32 | 0.000344703 |
| AMZ1 | 7.17 | -1.32 | 2.46E-05 |
| OLFML2B | 4.81 | -1.32 | 0.004148443 |
| SERINC5 | 9.64 | -1.31 | 1.12E-16 |
| USP54 | 5.62 | -1.31 | 0.000611307 |
| RIN3 | 8.81 | -1.31 | 1.76E-10 |
| SH3PXD2B | 7.87 | -1.31 | 5.14E-05 |
| MMD | 7.19 | -1.30 | 7.09E-06 |
| AATK | 5.26 | -1.30 | 0.002463791 |
| SYNE1 | 7.52 | -1.30 | 5.42E-08 |
| C9orf139 | 5.27 | -1.29 | 0.001668391 |
| FRMD4A | 8.46 | -1.29 | 1.44E-10 |
| SNX21 | 3.69 | -1.29 | 0.009860254 |

| | | | |
|---|---|---|---|
| NT5DC2 | 5.73 | -1.28 | 0.000940408 |
| RGS18 | 5.10 | -1.28 | 0.002829048 |
| PRKCH | 5.80 | -1.28 | 0.000348847 |
| FAM214A | 6.66 | -1.28 | 2.81E-05 |
| ACACB | 5.24 | -1.28 | 0.001747665 |
| AMPD2 | 8.11 | -1.27 | 4.36E-09 |
| ADORA2B | 5.92 | -1.26 | 0.000538084 |
| GAPT | 5.93 | -1.26 | 0.002703925 |
| PTX3 | 6.21 | -1.26 | 0.003157806 |
| KLHL24 | 7.63 | -1.25 | 5.92E-08 |
| HLTF | 6.12 | -1.24 | 0.000569745 |
| ST5 | 6.19 | -1.23 | 0.000550528 |
| AVPI1 | 6.66 | -1.23 | 3.21E-05 |
| DEDD2 | 7.48 | -1.23 | 1.60E-06 |
| EEF1AKMT3 | 5.89 | -1.23 | 0.000847557 |
| TBC1D8 | 7.84 | -1.23 | 1.10E-08 |
| PRAM1 | 8.81 | -1.22 | 4.00E-07 |
| SPATA12 | 4.72 | -1.22 | 0.006675185 |
| FAM212B | 4.93 | -1.22 | 0.005667504 |
| PID1 | 4.04 | -1.22 | 0.01578692 |
| PHACTR1 | 7.74 | -1.22 | 8.72E-08 |
| SLC16A10 | 6.15 | -1.22 | 0.000208637 |
| SLC9A1 | 8.47 | -1.20 | 2.40E-09 |
| SEC31B | 4.90 | -1.20 | 0.006534517 |
| ARRDC3 | 6.96 | -1.20 | 5.30E-05 |
| RTL10 | 6.58 | -1.20 | 0.000374626 |
| RAPGEF3 | 6.35 | -1.20 | 0.000331695 |
| ENC1 | 6.10 | -1.19 | 0.002717812 |
| FHOD1 | 7.68 | -1.19 | 7.14E-08 |
| PTPN13 | 5.10 | -1.19 | 0.008234734 |
| NISCH | 7.57 | -1.19 | 7.19E-06 |
| TFAP4 | 3.86 | -1.18 | 0.020016744 |
| ALK | 5.55 | -1.18 | 0.013031339 |
| EFR3B | 4.07 | -1.18 | 0.020729428 |
| TOM1L2 | 8.40 | -1.17 | 5.42E-08 |
| PADI2 | 6.84 | -1.16 | 0.000336225 |
| PXK | 7.83 | -1.16 | 2.11E-07 |
| STOX2 | 4.26 | -1.16 | 0.022221807 |
| IER5L | 6.49 | -1.15 | 0.00025384 |
| KIAA1456 | 3.87 | -1.14 | 0.026660962 |
| MMP2-AS1 | 6.61 | -1.14 | 0.005842087 |
| PDCD4 | 6.84 | -1.14 | 4.83E-05 |
| BAIAP2-AS1 | 6.89 | -1.14 | 5.57E-05 |
| ABCG1 | 2.60 | -1.13 | 0.023081885 |
| REPS2 | 4.83 | -1.13 | 0.017259151 |
| SLC16A6 | 7.66 | -1.13 | 5.92E-05 |
| KIF21B | 6.36 | -1.13 | 0.000611307 |
| LTB4R | 5.57 | -1.13 | 0.004962631 |
| PLEC | 11.14 | -1.12 | 7.72E-13 |
| TMEM170B | 7.79 | -1.11 | 1.66E-05 |
| SAMD1 | 6.66 | -1.11 | 0.000178697 |
| STK36 | 5.01 | -1.09 | 0.017096637 |

| | | | |
|---|---|---|---|
| SHMT1 | 5.73 | -1.09 | 0.005648987 |
| ASB1 | 6.98 | -1.09 | 0.000112351 |
| PNPLA3 | 4.68 | -1.09 | 0.02376815 |
| YPEL2 | 5.69 | -1.09 | 0.00440233 |
| JMY | 5.38 | -1.09 | 0.01099513 |
| TRIM16 | 4.95 | -1.08 | 0.023479986 |
| LINC00921 | 3.40 | -1.08 | 0.042178953 |
| ABCC5 | 9.19 | -1.08 | 3.40E-05 |
| PPM1H | 6.93 | -1.08 | 0.000112351 |
| FYN | 5.98 | -1.07 | 0.007264166 |
| SLC46A2 | 3.20 | -1.07 | 0.041566292 |
| STMN1 | 6.97 | -1.07 | 0.001133461 |
| TRG-AS1 | 6.37 | -1.07 | 0.001951188 |
| LINC02035 | 5.81 | -1.07 | 0.00495119 |
| CASP2 | 6.68 | -1.07 | 0.000484555 |
| MXD4 | 6.74 | -1.07 | 0.000618973 |
| ADGRD1 | 3.22 | -1.07 | 0.045167218 |
| SH2D3C | 6.42 | -1.07 | 0.002180768 |
| DPEP2 | 7.18 | -1.06 | 0.000211466 |
| ADORA3 | 5.15 | -1.06 | 0.021964755 |
| LINC01094 | 5.53 | -1.05 | 0.011147327 |
| JUP | 5.82 | -1.05 | 0.006475198 |
| GFOD1 | 7.93 | -1.05 | 1.11E-06 |
| ALS2CL | 4.49 | -1.05 | 0.041608831 |
| ARAP3 | 6.02 | -1.04 | 0.004405163 |
| PHLDA3 | 8.05 | -1.04 | 3.63E-05 |
| ULK1 | 6.53 | -1.04 | 0.001137306 |
| IRAK3 | 8.68 | -1.04 | 7.22E-05 |
| KLHDC8B | 6.84 | -1.03 | 0.000689189 |
| DYRK4 | 7.00 | -1.03 | 0.000132647 |
| IQCD | 2.81 | -1.03 | 0.047364472 |
| ZADH2 | 7.13 | -1.03 | 0.000297693 |
| TOM1 | 8.99 | -1.03 | 5.20E-09 |
| UNC119B | 5.54 | -1.02 | 0.012399089 |
| ANKRD36C | 5.93 | -1.02 | 0.012410272 |
| ABCG4 | 2.59 | -1.02 | 0.037559733 |
| KIFC3 | 7.26 | -1.02 | 0.000124331 |
| SLC16A5 | 6.09 | -1.02 | 0.004148443 |
| DTNA | 6.61 | -1.02 | 0.002140742 |
| NLRP1 | 5.76 | -1.02 | 0.008234734 |
| IQGAP3 | 6.68 | -1.02 | 0.00136893 |
| CCDC57 | 6.96 | -1.02 | 0.002112957 |
| UBALD1 | 5.80 | -1.01 | 0.008052809 |
| KCTD7 | 7.51 | -1.01 | 7.22E-05 |
| MYO7A | 6.82 | -1.01 | 0.000767424 |
| MKI67 | 6.45 | -1.01 | 0.005041548 |
| ZMIZ1-AS1 | 8.38 | -1.01 | 7.33E-07 |
| MANSC4 | 2.98 | -1.00 | 0.044532629 |
| GAS2L1 | 6.70 | -1.00 | 0.003313822 |

**Supplementary table 7** Genes differentially expressed in macrophages after 6 hours of polarisation with IL-4 (M2). Gene expression was compared to unstimulated macrophages used as control. Genes are ordered by Log2-fold change.

| Gene Name | Log2( Base Mean Count ) | Log2FC | P adjusted |
|---|---|---|---|
| CD209 | 8.02 | 3.54 | 5.15E-50 |
| CTNNAL1 | 6.21 | 3.48 | 3.25E-24 |
| F13A1 | 6.21 | 3.10 | 1.04E-17 |
| FCER2 | 4.92 | 2.97 | 6.59E-14 |
| MAOA | 6.48 | 2.92 | 7.11E-22 |
| CISH | 7.13 | 2.89 | 7.52E-30 |
| PALLD | 7.45 | 2.85 | 3.88E-34 |
| WNT5B | 3.76 | 2.69 | 1.70E-09 |
| DACT1 | 4.87 | 2.60 | 6.82E-10 |
| PCSK5 | 6.32 | 2.37 | 1.06E-14 |
| CCL13 | 3.87 | 2.25 | 1.41E-06 |
| CLEC4A | 6.88 | 2.24 | 2.98E-19 |
| MRC1 | 10.93 | 2.07 | 5.15E-50 |
| MOB3B | 6.15 | 2.05 | 2.10E-10 |
| BATF3 | 4.95 | 2.02 | 4.92E-06 |
| SOCS1 | 7.00 | 1.98 | 5.61E-05 |
| CTSC | 11.51 | 1.97 | 1.77E-33 |
| CD200R1 | 5.42 | 1.91 | 1.87E-05 |
| AKAP5 | 3.56 | 1.91 | 0.000111139 |
| APOL4 | 8.25 | 1.88 | 0.000125411 |
| CHCHD7 | 6.36 | 1.88 | 1.65E-10 |
| CCL18 | 2.82 | 1.86 | 0.000100657 |
| HOMER2 | 4.35 | 1.80 | 0.000173631 |
| SLA | 8.88 | 1.79 | 9.61E-20 |
| THBD | 5.21 | 1.77 | 4.54E-05 |
| IL17RB | 4.63 | 1.77 | 0.000216725 |
| TMEM236 | 4.29 | 1.76 | 0.000344818 |
| FGL2 | 10.18 | 1.75 | 4.80E-24 |
| PPM1L | 7.30 | 1.75 | 3.59E-11 |
| SCIMP | 8.60 | 1.73 | 5.27E-13 |
| CLEC4G | 2.16 | 1.72 | 8.28E-05 |
| PPP1R3B | 6.00 | 1.72 | 6.13E-07 |
| ENPP2 | 5.33 | 1.72 | 0.000234045 |
| SYT17 | 5.65 | 1.71 | 0.000119425 |
| SPINT2 | 6.73 | 1.69 | 5.56E-10 |
| DCUN1D3 | 5.69 | 1.68 | 5.74E-06 |
| PDP2 | 6.09 | 1.67 | 4.32E-07 |
| PLXNA2 | 6.19 | 1.66 | 3.75E-07 |
| HRH1 | 6.15 | 1.65 | 2.14E-06 |
| NIPAL1 | 4.60 | 1.64 | 0.00049252 |
| FAR2 | 6.93 | 1.63 | 6.82E-10 |
| SNAI3 | 6.98 | 1.60 | 4.08E-08 |
| ARRDC4 | 7.57 | 1.58 | 7.15E-10 |
| CLEC10A | 6.82 | 1.57 | 1.66E-06 |
| RNF19B | 8.20 | 1.55 | 2.07E-08 |
| CHDH | 4.12 | 1.54 | 0.004968513 |

| | | | |
|---|---|---|---|
| GAS6 | 6.51 | 1.54 | 3.48E-06 |
| KREMEN1 | 6.18 | 1.52 | 0.000538524 |
| ARL4C | 8.02 | 1.50 | 4.03E-10 |
| SLC5A3 | 9.42 | 1.49 | 2.20E-18 |
| HR | 5.05 | 1.49 | 0.002750805 |
| FN1 | 7.55 | 1.48 | 7.97E-07 |
| GGT5 | 2.70 | 1.47 | 0.004255567 |
| SUCNR1 | 10.05 | 1.44 | 0.000125411 |
| UST | 4.04 | 1.43 | 0.010797515 |
| DNASE1L3 | 2.98 | 1.43 | 0.010612365 |
| IL1RAP | 6.14 | 1.41 | 0.000111139 |
| PDGFRB | 3.01 | 1.41 | 0.011466664 |
| NUDT16 | 7.70 | 1.39 | 6.82E-10 |
| ARNTL2 | 7.62 | 1.36 | 4.83E-05 |
| ERI1 | 7.30 | 1.36 | 4.81E-08 |
| PTGFRN | 6.96 | 1.36 | 6.40E-06 |
| NOCT | 4.65 | 1.35 | 0.010507465 |
| SLAMF1 | 4.26 | 1.34 | 0.02171794 |
| PTGS1 | 8.43 | 1.34 | 3.54E-13 |
| CARD9 | 6.93 | 1.34 | 7.40E-07 |
| FLVCR2 | 6.75 | 1.31 | 0.00129795 |
| RAMP1 | 2.80 | 1.31 | 0.020639258 |
| SDC4 | 9.27 | 1.31 | 4.54E-08 |
| MTUS1 | 4.93 | 1.30 | 0.011647279 |
| TGFA | 5.35 | 1.29 | 0.00676972 |
| FAM110B | 3.04 | 1.29 | 0.034738266 |
| P2RY12 | 2.10 | 1.29 | 0.006176114 |
| TJP2 | 8.34 | 1.28 | 1.33E-06 |
| PDGFB | 6.98 | 1.27 | 1.38E-05 |
| STK17B | 7.30 | 1.27 | 1.10E-06 |
| LIMA1 | 7.92 | 1.27 | 2.42E-07 |
| BATF | 6.55 | 1.27 | 0.000826352 |
| SLC4A7 | 7.93 | 1.26 | 8.39E-08 |
| AP2A2 | 4.49 | 1.26 | 0.021246471 |
| CRB2 | 1.67 | 1.26 | 0.002862301 |
| PRAG1 | 7.04 | 1.25 | 8.01E-06 |
| P2RY14 | 5.92 | 1.25 | 0.040781147 |
| QSOX1 | 9.33 | 1.24 | 1.53E-15 |
| ACE | 7.02 | 1.24 | 7.54E-05 |
| FCRLB | 4.62 | 1.24 | 0.027814538 |
| SLCO4C1 | 6.01 | 1.23 | 0.002801491 |
| FRMD4A | 8.46 | 1.23 | 2.56E-10 |
| CSRNP1 | 5.72 | 1.19 | 0.007154307 |
| TLE1 | 5.32 | 1.19 | 0.022400693 |
| SEPT3 | 5.70 | 1.17 | 0.007629657 |
| PARM1 | 1.75 | 1.16 | 0.012412151 |
| RGL1 | 10.38 | 1.15 | 1.92E-12 |
| TIFA | 6.94 | 1.15 | 0.00212155 |
| TGM2 | 11.95 | 1.15 | 7.95E-19 |
| CD274 | 9.57 | 1.15 | 0.022636766 |
| SPRED2 | 7.13 | 1.15 | 0.000150214 |
| CDR2 | 6.75 | 1.14 | 0.001270656 |

| | | | |
|---|---|---|---|
| OCSTAMP | 6.47 | 1.14 | 0.000918315 |
| SRGAP1 | 6.46 | 1.13 | 0.000894051 |
| PAPSS2 | 7.69 | 1.13 | 1.86E-05 |
| EMB | 8.00 | 1.13 | 1.87E-05 |
| EPS8 | 6.18 | 1.13 | 0.002360558 |
| C10orf128 | 7.19 | 1.12 | 8.60E-05 |
| CAVIN1 | 5.47 | 1.11 | 0.019566164 |
| AMPD2 | 8.11 | 1.11 | 1.01E-07 |
| SLC7A8 | 8.78 | 1.10 | 7.15E-08 |
| XXYLT1 | 5.27 | 1.10 | 0.027394817 |
| MAT2A | 10.27 | 1.09 | 4.00E-15 |
| PTGER2 | 6.39 | 1.09 | 0.009828833 |
| NR4A3 | 7.25 | 1.09 | 0.001087053 |
| PTPRE | 11.25 | 1.08 | 1.47E-08 |
| MS4A4A | 7.09 | 1.06 | 0.002378264 |
| GGTA1P | 6.43 | 1.06 | 0.007154307 |
| ATXN1 | 9.14 | 1.06 | 1.16E-07 |
| ARHGAP26 | 8.72 | 1.04 | 1.30E-05 |
| IL21R | 6.13 | 1.03 | 0.012617366 |
| CTNS | 8.64 | 1.03 | 2.27E-07 |
| EPB41L2 | 9.12 | 1.03 | 5.93E-09 |
| CCL22 | 10.94 | 1.03 | 1.46E-08 |
| CACNB4 | 1.62 | 1.02 | 0.038643814 |
| FCGR2B | 8.05 | 1.02 | 7.54E-05 |
| NLRP12 | 5.99 | -1.57 | 1.73E-05 |
| CDKN2B | 6.16 | -1.52 | 8.10E-05 |
| TRIM2 | 5.88 | -1.51 | 0.00028429 |
| TLR7 | 8.16 | -1.42 | 2.89E-07 |
| PFKFB3 | 9.92 | -1.39 | 2.41E-13 |
| PRLR | 6.21 | -1.38 | 0.00049252 |
| HGF | 6.61 | -1.35 | 0.000894051 |
| NUPR1 | 8.73 | -1.26 | 2.52E-07 |
| CCDC88C | 6.92 | -1.26 | 7.40E-05 |
| CLEC5A | 5.64 | -1.20 | 0.008654735 |
| ABCA1 | 8.17 | -1.16 | 9.10E-06 |
| RGS1 | 6.55 | -1.16 | 0.002451094 |
| LHFPL2 | 11.09 | -1.13 | 7.36E-11 |
| TESK2 | 5.95 | -1.11 | 0.026801163 |
| SH3RF3 | 7.39 | -1.10 | 0.000254977 |
| ADORA2B | 5.92 | -1.09 | 0.013336603 |
| DENND3 | 7.78 | -1.09 | 0.000217609 |
| TLE3 | 8.41 | -1.09 | 7.97E-07 |
| ARID3B | 5.24 | -1.08 | 0.046379566 |
| C3AR1 | 8.72 | -1.08 | 9.74E-08 |
| FMN1 | 7.21 | -1.07 | 0.000389949 |
| MEFV | 5.70 | -1.06 | 0.049189795 |
| SDS | 10.05 | -1.05 | 1.61E-05 |
| PADI2 | 6.84 | -1.00 | 0.010797515 |

**Supplementary table 8** Genes differentially expressed in macrophages after 6 hours of polarisation with IL-26. Gene expression was compared to unstimulated macrophages used as control. Genes are ordered by Log2-fold change.

| Gene Name | Log2( Base Mean Count ) | Log2FC | P adjusted |
|---|---|---|---|
| ADGRE1 | 5.92 | 3.33 | 3.16E-16 |
| ENPP2 | 5.33 | 2.55 | 1.98E-09 |
| SLAMF1 | 4.26 | 2.40 | 2.06E-07 |
| JAK3 | 7.04 | 2.35 | 5.64E-07 |
| HAPLN3 | 7.42 | 2.29 | 9.08E-07 |
| CXCL9 | 10.75 | 2.25 | 2.32E-06 |
| FPR1 | 7.55 | 2.19 | 8.24E-11 |
| FPR2 | 5.04 | 2.18 | 1.72E-06 |
| TIFAB | 7.59 | 2.01 | 4.63E-10 |
| CYP7B1 | 4.33 | 1.98 | 5.53E-05 |
| IL2RA | 4.50 | 1.95 | 8.30E-05 |
| STEAP4 | 4.96 | 1.93 | 6.74E-05 |
| IL7 | 4.96 | 1.91 | 4.97E-05 |
| THBS1 | 4.44 | 1.89 | 0.000150936 |
| SLC39A8 | 9.05 | 1.84 | 0.000254143 |
| NAMPT | 9.68 | 1.84 | 0.000166773 |
| APOBEC3A | 7.85 | 1.83 | 6.43E-09 |
| MARCKSL1 | 5.70 | 1.80 | 0.000151196 |
| IL32 | 5.20 | 1.78 | 0.000306065 |
| BIRC3 | 9.02 | 1.77 | 4.73E-05 |
| SOCS3 | 7.33 | 1.76 | 0.000585962 |
| BATF | 6.55 | 1.73 | 5.22E-07 |
| BCL3 | 7.86 | 1.70 | 0.0001631 |
| EHD1 | 8.82 | 1.64 | 0.000766203 |
| NEURL3 | 4.63 | 1.63 | 0.001775789 |
| MYO1G | 8.26 | 1.63 | 0.000636641 |
| IL4I1 | 9.32 | 1.63 | 0.000569034 |
| SOD2 | 13.97 | 1.62 | 0.001942074 |
| SGPP2 | 7.47 | 1.62 | 0.001775789 |
| LRG1 | 3.13 | 1.60 | 0.001998455 |
| SLC43A2 | 5.33 | 1.59 | 0.000978303 |
| HIVEP2 | 7.07 | 1.59 | 4.75E-05 |
| VCAN | 6.32 | 1.59 | 3.89E-05 |
| FLVCR2 | 6.75 | 1.58 | 3.62E-05 |
| FAM20A | 6.15 | 1.56 | 3.28E-05 |
| P2RY6 | 7.13 | 1.55 | 4.65E-07 |
| TNFAIP8 | 8.51 | 1.54 | 2.04E-08 |
| APOL3 | 9.63 | 1.54 | 0.003960003 |
| GPR85 | 3.75 | 1.53 | 0.003956175 |
| MCOLN2 | 7.87 | 1.53 | 0.004088297 |
| KREMEN1 | 6.18 | 1.53 | 0.000546116 |
| NFE2L3 | 6.48 | 1.53 | 7.04E-05 |
| TBC1D17 | 8.47 | 1.52 | 0.000826868 |
| NECTIN2 | 8.14 | 1.52 | 4.65E-07 |
| CLEC4D | 4.35 | 1.52 | 0.003972184 |
| LYN | 10.58 | 1.51 | 0.000224058 |

| | | | |
|---|---|---|---|
| DSE | 8.84 | 1.51 | 9.01E-13 |
| CHST2 | 8.04 | 1.50 | 0.004977629 |
| TJP2 | 8.34 | 1.49 | 1.44E-08 |
| ELOVL7 | 4.89 | 1.49 | 0.005264557 |
| GK | 8.95 | 1.48 | 1.60E-09 |
| GPR132 | 6.61 | 1.48 | 0.005117319 |
| ICAM1 | 10.31 | 1.48 | 0.000364895 |
| GADD45B | 6.89 | 1.48 | 3.71E-05 |
| PDCD1LG2 | 7.54 | 1.47 | 2.13E-06 |
| CD38 | 6.62 | 1.47 | 0.005276132 |
| POU2F2 | 8.04 | 1.47 | 0.004615022 |
| S100A8 | 5.05 | 1.46 | 0.000998003 |
| PPA1 | 7.30 | 1.45 | 9.08E-07 |
| MT2A | 3.18 | 1.44 | 0.00508582 |
| CD40 | 9.02 | 1.41 | 0.006195339 |
| CD274 | 9.57 | 1.41 | 0.001349847 |
| ORAI1 | 7.99 | 1.41 | 3.10E-05 |
| TNIP1 | 9.91 | 1.39 | 0.005251679 |
| ZSWIM4 | 6.08 | 1.39 | 0.00239859 |
| ADAMTS14 | 3.44 | 1.39 | 0.009023338 |
| ETV5 | 7.43 | 1.39 | 0.011431695 |
| DOCK4 | 10.48 | 1.37 | 0.001311369 |
| TNIP3 | 4.75 | 1.37 | 0.002058342 |
| SLC2A3 | 8.62 | 1.36 | 4.65E-07 |
| SH3PXD2B | 7.87 | 1.36 | 3.62E-05 |
| VCAM1 | 6.29 | 1.35 | 0.016364314 |
| WTAP | 9.37 | 1.35 | 0.006425896 |
| VNN2 | 5.74 | 1.34 | 0.00174144 |
| HSD11B1 | 5.53 | 1.34 | 0.005177667 |
| PNRC1 | 9.01 | 1.33 | 2.08E-06 |
| CD80 | 6.52 | 1.33 | 0.017698392 |
| RTN1 | 7.06 | 1.33 | 7.90E-05 |
| S100A9 | 9.25 | 1.33 | 5.20E-13 |
| CRIM1 | 8.23 | 1.32 | 0.015942631 |
| PTGIR | 6.95 | 1.32 | 0.018960762 |
| ADM | 5.99 | 1.32 | 0.007615607 |
| ATF5 | 9.02 | 1.31 | 0.001942074 |
| NCF1B | 6.40 | 1.30 | 0.023856634 |
| GJB2 | 7.47 | 1.30 | 0.000434359 |
| PTGER2 | 6.39 | 1.29 | 0.000730977 |
| PELI1 | 7.00 | 1.29 | 0.000276995 |
| NFKB2 | 9.45 | 1.29 | 0.00319909 |
| RNF144B | 8.79 | 1.29 | 0.009004958 |
| PDE4B | 7.30 | 1.28 | 0.024673958 |
| FAM129A | 10.31 | 1.28 | 0.001967249 |
| RELB | 8.05 | 1.27 | 1.17E-05 |
| NFKBIZ | 7.33 | 1.27 | 0.026200971 |
| ARHGAP24 | 5.12 | 1.27 | 0.012636335 |
| HIVEP3 | 9.25 | 1.27 | 2.28E-06 |
| SLCO4A1 | 6.89 | 1.26 | 0.001809799 |
| SLC7A11 | 9.73 | 1.26 | 0.00317531 |
| MIR3142HG | 7.35 | 1.26 | 0.026775027 |

| | | | |
|---|---|---|---|
| TIMP1 | 7.87 | 1.25 | 2.81E-05 |
| PTGER4 | 8.56 | 1.25 | 0.009004958 |
| ZHX2 | 5.75 | 1.24 | 0.010349054 |
| IL7R | 6.69 | 1.24 | 0.035659221 |
| PTPN2 | 7.98 | 1.24 | 4.56E-08 |
| P2RX7 | 10.95 | 1.24 | 0.016425179 |
| ACSL1 | 11.81 | 1.24 | 0.013383811 |
| KYNU | 10.07 | 1.23 | 0.018435127 |
| NFKBIA | 10.33 | 1.23 | 0.01505104 |
| ARNTL2 | 7.62 | 1.23 | 0.000484945 |
| DRAM1 | 10.13 | 1.22 | 0.004977629 |
| PTPRJ | 10.62 | 1.22 | 0.00180762 |
| ETV3 | 8.01 | 1.21 | 1.29E-05 |
| BID | 8.65 | 1.21 | 2.33E-05 |
| TNFRSF4 | 7.46 | 1.21 | 0.027180478 |
| PIM2 | 5.78 | 1.21 | 0.006273297 |
| VNN1 | 5.86 | 1.21 | 0.005424887 |
| NFIX | 4.87 | 1.21 | 0.027637175 |
| ADA | 7.47 | 1.21 | 0.045153895 |
| CD226 | 4.14 | 1.21 | 0.043914411 |
| SLAMF7 | 11.75 | 1.20 | 0.012548475 |
| SLC41A2 | 7.95 | 1.20 | 1.17E-05 |
| HIVEP1 | 8.26 | 1.20 | 7.79E-05 |
| GPR141 | 6.32 | 1.20 | 0.006434773 |
| TCF4 | 8.39 | 1.20 | 2.78E-05 |
| TMEM2 | 7.92 | 1.20 | 1.47E-06 |
| NAMPTP1 | 3.52 | 1.19 | 0.044892269 |
| CCL2 | 10.17 | 1.19 | 0.008259129 |
| CSF2RB | 9.47 | 1.19 | 6.12E-12 |
| B4GALT1 | 9.93 | 1.19 | 2.89E-06 |
| MMP14 | 10.79 | 1.18 | 0.008885852 |
| LINC00926 | 5.47 | 1.18 | 0.022385204 |
| PSTPIP2 | 9.02 | 1.18 | 0.028781305 |
| LINC00937 | 6.06 | 1.18 | 0.018435127 |
| STAT4 | 5.35 | 1.18 | 0.036332006 |
| PFKFB3 | 9.92 | 1.17 | 1.65E-09 |
| CBX6 | 9.01 | 1.16 | 1.81E-05 |
| ACSL5 | 8.56 | 1.15 | 0.000151196 |
| HR | 5.05 | 1.15 | 0.038738284 |
| TNFAIP3 | 9.62 | 1.14 | 0.048742066 |
| MARCKS | 12.14 | 1.14 | 1.29E-08 |
| CD44 | 12.19 | 1.13 | 0.008717488 |
| BCL2 | 7.18 | 1.12 | 0.000166773 |
| IL15 | 5.43 | 1.12 | 0.032998891 |
| NFKB1 | 9.61 | 1.11 | 0.041901802 |
| MAOA | 6.48 | 1.11 | 0.005699492 |
| ZC3H12D | 6.17 | 1.11 | 0.010600013 |
| AHR | 8.98 | 1.10 | 2.26E-06 |
| LAP3 | 10.44 | 1.10 | 1.03E-07 |
| LILRB2 | 4.94 | 1.10 | 0.034243616 |
| CEBPD | 6.85 | 1.09 | 0.001238068 |
| SNHG15 | 5.02 | 1.09 | 0.043796956 |

| | | | |
|---|---|---|---|
| NAB1 | 7.13 | 1.09 | 0.000766203 |
| TFEC | 10.51 | 1.08 | 1.04E-08 |
| KMO | 8.03 | 1.08 | 0.001075683 |
| GPR153 | 6.02 | 1.08 | 0.031005325 |
| LUCAT1 | 5.84 | 1.07 | 0.026423056 |
| RCN1 | 8.01 | 1.06 | 8.74E-05 |
| MTHFD2 | 9.57 | 1.06 | 1.14E-07 |
| CCR5 | 9.98 | 1.05 | 3.27E-05 |
| ARHGAP31 | 10.22 | 1.04 | 3.08E-05 |
| ICOSLG | 6.05 | 1.04 | 0.031639191 |
| CLIC4 | 10.13 | 1.04 | 1.93E-05 |
| PIM3 | 8.82 | 1.03 | 0.000115245 |
| TIFA | 6.94 | 1.03 | 0.008259129 |
| FCGR2A | 9.25 | 1.03 | 3.69E-07 |
| PLEKHM3 | 6.30 | 1.02 | 0.024587628 |
| OGFRL1 | 10.28 | 1.02 | 0.000114396 |
| PRDM1 | 7.58 | 1.02 | 0.002894628 |
| ZC3H12A | 7.25 | 1.02 | 0.022151949 |
| ARHGEF10L | 9.15 | 1.02 | 2.81E-05 |
| TXN | 10.33 | 1.00 | 0.000175587 |

**Supplementary table 9** Genes differentially expressed in macrophages after 6 hours of polarisation with TNF-α. Gene expression was compared to unstimulated macrophages used as control. Genes are ordered by Log2-fold change.

| Gene Name | Log2( Base Mean Count ) | Log2FC | P adjusted |
|---|---|---|---|
| MARCKSL1 | 5.70 | 3.11 | 3.58E-14 |
| ACHE | 3.60 | 2.92 | 2.27E-11 |
| MSC | 7.16 | 2.63 | 1.89E-16 |
| ANO9 | 5.51 | 2.51 | 4.60E-09 |
| LINC00937 | 6.06 | 2.45 | 2.48E-10 |
| GPR153 | 6.02 | 2.42 | 7.06E-11 |
| AP1S3 | 5.41 | 2.37 | 4.60E-09 |
| ARNTL2 | 7.62 | 2.35 | 1.43E-15 |
| VCAM1 | 6.29 | 2.31 | 3.53E-07 |
| BAHCC1 | 5.45 | 2.31 | 6.67E-09 |
| BIRC3 | 9.02 | 2.31 | 4.60E-09 |
| OSM | 5.19 | 2.30 | 7.98E-08 |
| CYP7B1 | 4.33 | 2.29 | 4.18E-07 |
| IRAK2 | 6.88 | 2.28 | 4.50E-07 |
| CHST2 | 8.04 | 2.25 | 6.52E-07 |
| ZSWIM4 | 6.08 | 2.20 | 1.35E-08 |
| TNFRSF9 | 8.67 | 2.20 | 4.80E-07 |
| ZBTB10 | 6.50 | 2.19 | 9.73E-11 |
| FSCN1 | 9.53 | 2.17 | 1.32E-06 |
| GP1BA | 5.90 | 2.17 | 8.69E-07 |
| SDC4 | 9.27 | 2.16 | 3.02E-22 |
| PSTPIP2 | 9.02 | 2.16 | 2.68E-07 |
| SGPP2 | 7.47 | 2.15 | 2.15E-06 |
| HIVEP2 | 7.07 | 2.14 | 1.11E-09 |
| PNRC1 | 9.01 | 2.14 | 3.14E-17 |
| ICAM1 | 10.31 | 2.13 | 6.10E-09 |
| EHD1 | 8.82 | 2.10 | 1.15E-06 |
| JAG1 | 8.03 | 2.10 | 2.86E-06 |
| RASGRP1 | 6.07 | 2.08 | 1.35E-08 |
| NCF1B | 6.40 | 2.05 | 8.06E-06 |
| TNFAIP3 | 9.62 | 2.04 | 3.06E-06 |
| PDE4B | 7.30 | 2.02 | 9.16E-06 |
| NFKB2 | 9.45 | 2.02 | 5.44E-08 |
| HR | 5.05 | 2.01 | 1.81E-06 |
| HS3ST3B1 | 6.16 | 1.99 | 5.86E-06 |
| PHLDB1 | 5.57 | 1.95 | 1.67E-06 |
| GRAMD1A | 9.41 | 1.94 | 2.42E-05 |
| NFKBIA | 10.33 | 1.94 | 2.72E-06 |
| TIFAB | 7.59 | 1.93 | 8.07E-10 |
| TRAF1 | 8.84 | 1.92 | 3.18E-05 |
| NBN | 9.90 | 1.92 | 9.05E-08 |
| RNF144B | 8.79 | 1.91 | 3.28E-06 |
| NEURL3 | 4.63 | 1.90 | 4.66E-05 |
| TNFRSF4 | 7.46 | 1.87 | 1.97E-05 |
| CRIM1 | 8.23 | 1.85 | 4.76E-05 |
| ADM | 5.99 | 1.84 | 9.48E-06 |

| | | | |
|---|---|---|---|
| MCOLN2 | 7.87 | 1.84 | 9.24E-05 |
| CXCL8 | 9.59 | 1.83 | 3.98E-05 |
| IL32 | 5.20 | 1.83 | 6.84E-05 |
| TIFA | 6.94 | 1.82 | 4.85E-09 |
| CD274 | 9.57 | 1.80 | 3.44E-06 |
| APOL3 | 9.63 | 1.80 | 1.47E-04 |
| PLEKHG3 | 6.86 | 1.78 | 1.51E-04 |
| TBC1D9 | 9.21 | 1.78 | 2.46E-06 |
| NFE2L3 | 6.48 | 1.77 | 4.80E-07 |
| RELB | 8.05 | 1.77 | 1.54E-11 |
| KYNU | 10.07 | 1.75 | 5.30E-05 |
| MIR3142HG | 7.35 | 1.74 | 1.67E-04 |
| CLEC4E | 7.80 | 1.74 | 2.49E-04 |
| SLC35F2 | 4.52 | 1.74 | 9.85E-05 |
| ELOVL7 | 4.89 | 1.74 | 2.19E-04 |
| ANKRD33B | 5.13 | 1.73 | 1.24E-04 |
| CDC42EP2 | 3.82 | 1.73 | 2.52E-04 |
| BID | 8.65 | 1.73 | 1.54E-11 |
| TNIP1 | 9.91 | 1.72 | 7.81E-05 |
| FMNL3 | 9.39 | 1.72 | 3.22E-15 |
| SOD2 | 13.97 | 1.72 | 3.29E-04 |
| CLEC6A | 4.21 | 1.72 | 2.49E-04 |
| FAS | 7.29 | 1.70 | 2.62E-09 |
| CLEC4D | 4.35 | 1.69 | 3.29E-04 |
| TNFAIP8 | 8.51 | 1.69 | 1.16E-10 |
| FAM129A | 10.31 | 1.69 | 2.84E-06 |
| CAMKK2 | 8.96 | 1.68 | 1.89E-16 |
| MMP2-AS1 | 6.61 | 1.67 | 5.07E-06 |
| GPR35 | 6.21 | 1.67 | 4.18E-06 |
| IL15RA | 6.46 | 1.67 | 5.11E-04 |
| HIVEP1 | 8.26 | 1.67 | 8.42E-10 |
| STEAP4 | 4.96 | 1.66 | 4.10E-04 |
| FILIP1L | 5.68 | 1.66 | 2.95E-05 |
| NCF1 | 8.35 | 1.66 | 4.20E-04 |
| WTAP | 9.37 | 1.65 | 1.31E-04 |
| SESN3 | 6.46 | 1.64 | 1.32E-06 |
| TRIP10 | 7.61 | 1.63 | 8.64E-09 |
| G0S2 | 7.39 | 1.63 | 1.38E-04 |
| MAGI2-AS3 | 4.67 | 1.63 | 4.64E-04 |
| TJP2 | 8.34 | 1.63 | 7.95E-11 |
| PTGES | 3.31 | 1.62 | 5.20E-04 |
| GJB2 | 7.47 | 1.61 | 1.09E-06 |
| POGLUT1 | 6.60 | 1.60 | 1.42E-06 |
| IRF1 | 10.00 | 1.59 | 4.09E-05 |
| B4GALT1 | 9.93 | 1.59 | 9.08E-12 |
| A4GALT | 3.66 | 1.59 | 1.08E-03 |
| EREG | 3.09 | 1.58 | 5.78E-04 |
| PTGIR | 6.95 | 1.58 | 1.09E-03 |
| NCF1C | 7.24 | 1.58 | 1.19E-03 |
| SLC30A4 | 5.49 | 1.57 | 6.53E-04 |
| NFKB1 | 9.61 | 1.57 | 3.18E-04 |
| ACSL5 | 8.56 | 1.57 | 6.39E-09 |

| | | | |
|---|---|---|---|
| AMPD3 | 9.55 | 1.57 | 9.25E-14 |
| KCNJ2 | 6.45 | 1.56 | 2.35E-05 |
| MMP14 | 10.79 | 1.56 | 4.74E-05 |
| PLEKHM3 | 6.30 | 1.54 | 2.52E-05 |
| IL4I1 | 9.32 | 1.54 | 5.71E-04 |
| TNFAIP2 | 12.48 | 1.53 | 1.24E-04 |
| KMO | 8.03 | 1.53 | 1.20E-07 |
| FPR2 | 5.04 | 1.52 | 1.20E-03 |
| STX11 | 7.68 | 1.52 | 9.38E-07 |
| ARID5B | 7.02 | 1.51 | 4.55E-06 |
| GPR132 | 6.61 | 1.51 | 1.93E-03 |
| JAK3 | 7.04 | 1.51 | 2.11E-03 |
| RUFY3 | 8.41 | 1.50 | 4.05E-09 |
| SLC7A11 | 9.73 | 1.50 | 7.58E-05 |
| PRKAR2B | 5.45 | 1.50 | 2.31E-04 |
| SERPINE1 | 4.98 | 1.49 | 8.81E-04 |
| MYO1G | 8.26 | 1.49 | 1.05E-03 |
| AMZ1 | 7.17 | 1.49 | 1.74E-07 |
| HCAR3 | 4.15 | 1.49 | 2.61E-03 |
| WNT5A | 4.73 | 1.49 | 8.84E-04 |
| HSD11B1 | 5.53 | 1.47 | 6.36E-04 |
| HIP1 | 8.09 | 1.47 | 9.34E-08 |
| MIR155HG | 5.18 | 1.47 | 8.31E-04 |
| TRIM16L | 4.11 | 1.47 | 2.98E-03 |
| USP12 | 9.10 | 1.46 | 2.22E-13 |
| NCK2 | 7.18 | 1.46 | 8.69E-07 |
| PTGER2 | 6.39 | 1.45 | 2.57E-05 |
| NFKBIZ | 7.33 | 1.45 | 3.35E-03 |
| SRC | 10.18 | 1.45 | 1.45E-04 |
| CD40 | 9.02 | 1.44 | 2.24E-03 |
| MCTP1 | 8.60 | 1.44 | 2.03E-10 |
| MSANTD3 | 7.72 | 1.44 | 1.35E-06 |
| DRAM1 | 10.13 | 1.44 | 1.84E-04 |
| SNX10 | 9.89 | 1.43 | 3.11E-11 |
| SAMD14 | 3.19 | 1.42 | 4.52E-03 |
| ADA | 7.47 | 1.42 | 5.04E-03 |
| RTN1 | 7.06 | 1.41 | 5.51E-06 |
| PIM3 | 8.82 | 1.41 | 3.89E-09 |
| DENND5A | 9.09 | 1.40 | 1.53E-08 |
| TBC1D17 | 8.47 | 1.40 | 1.19E-03 |
| IL7 | 4.96 | 1.40 | 3.72E-03 |
| DOCK4 | 10.48 | 1.39 | 3.81E-04 |
| RFTN1 | 9.12 | 1.39 | 1.65E-08 |
| MARCKS | 12.14 | 1.39 | 1.95E-13 |
| DTX4 | 8.48 | 1.38 | 2.19E-06 |
| IFNGR2 | 6.99 | 1.38 | 5.86E-06 |
| CYP27B1 | 6.65 | 1.38 | 3.23E-05 |
| AK4 | 7.58 | 1.37 | 2.52E-05 |
| ACVR2A | 6.28 | 1.37 | 5.06E-05 |
| SLAMF7 | 11.75 | 1.37 | 1.26E-03 |
| SLC43A2 | 5.33 | 1.37 | 3.63E-03 |
| ACSL1 | 11.81 | 1.37 | 1.96E-03 |

| | | | |
|---|---|---|---|
| CCL3L3 | 3.64 | 1.36 | 7.61E-03 |
| ICOSLG | 6.05 | 1.36 | 5.79E-04 |
| MSC-AS1 | 5.77 | 1.36 | 1.11E-03 |
| CD58 | 7.89 | 1.36 | 4.58E-07 |
| N4BP2L1 | 7.25 | 1.35 | 4.98E-07 |
| GBP1 | 10.97 | 1.35 | 7.61E-03 |
| TNIP2 | 7.58 | 1.35 | 1.37E-06 |
| IL7R | 6.69 | 1.35 | 8.61E-03 |
| CERS4 | 5.50 | 1.35 | 9.33E-04 |
| IL1A | 4.91 | 1.35 | 8.33E-03 |
| EBI3 | 6.08 | 1.34 | 1.33E-03 |
| MTF1 | 8.75 | 1.34 | 1.35E-07 |
| BCL2 | 7.18 | 1.34 | 8.08E-07 |
| SLC39A8 | 9.05 | 1.34 | 9.65E-03 |
| ATP2B1 | 9.06 | 1.33 | 9.17E-08 |
| OAF | 5.95 | 1.33 | 5.76E-04 |
| DGKH | 8.02 | 1.33 | 1.78E-06 |
| ARHGAP31 | 10.22 | 1.33 | 4.60E-09 |
| ORAI1 | 7.99 | 1.32 | 3.70E-05 |
| BCL9L | 7.07 | 1.32 | 4.81E-06 |
| CD83 | 10.51 | 1.32 | 3.13E-10 |
| CLINT1 | 9.23 | 1.31 | 7.95E-08 |
| TNFAIP6 | 7.04 | 1.31 | 2.77E-03 |
| CLIC4 | 10.13 | 1.31 | 3.44E-09 |
| TNFSF9 | 3.80 | 1.31 | 1.21E-02 |
| CD44 | 12.19 | 1.30 | 5.93E-04 |
| N4BP3 | 2.18 | 1.29 | 3.00E-03 |
| BCL3 | 7.86 | 1.29 | 4.64E-03 |
| CD80 | 6.52 | 1.29 | 1.28E-02 |
| RHBDF2 | 9.29 | 1.28 | 1.08E-07 |
| SEMA4A | 9.16 | 1.28 | 1.13E-03 |
| NOL4L | 6.40 | 1.27 | 1.57E-04 |
| USP13 | 5.18 | 1.27 | 3.19E-03 |
| ZC3H12A | 7.25 | 1.27 | 7.18E-04 |
| IL1B | 7.50 | 1.27 | 9.11E-03 |
| RILPL2 | 8.40 | 1.26 | 2.97E-09 |
| BTG3 | 5.78 | 1.26 | 1.35E-03 |
| RCN1 | 8.01 | 1.26 | 3.21E-07 |
| TMEM119 | 4.03 | 1.26 | 1.46E-02 |
| PTGS2 | 5.24 | 1.26 | 8.63E-03 |
| EXOC3L4 | 2.34 | 1.25 | 5.97E-03 |
| PDCD1LG2 | 7.54 | 1.25 | 4.19E-05 |
| TSPAN33 | 7.15 | 1.25 | 9.76E-05 |
| TNC | 4.80 | 1.25 | 1.51E-02 |
| GCH1 | 8.51 | 1.25 | 1.74E-02 |
| VILL | 5.07 | 1.25 | 7.26E-03 |
| PDE4DIP | 10.25 | 1.24 | 4.64E-04 |
| PLK3 | 7.50 | 1.24 | 2.75E-05 |
| P2RX7 | 10.95 | 1.24 | 8.12E-03 |
| ESPL1 | 4.49 | 1.24 | 1.43E-02 |
| GRAMD2B | 4.02 | 1.24 | 1.83E-02 |
| BTG1 | 8.38 | 1.23 | 7.19E-03 |

| | | | |
|---|---|---|---|
| NIPAL4 | 6.47 | 1.23 | 1.97E-02 |
| MB21D2 | 5.28 | 1.23 | 7.26E-03 |
| TOR3A | 9.25 | 1.23 | 6.55E-12 |
| PSD3 | 9.78 | 1.23 | 1.19E-08 |
| HCAR2 | 4.33 | 1.23 | 2.03E-02 |
| PTPRJ | 10.62 | 1.23 | 6.62E-04 |
| SRI | 7.63 | 1.23 | 6.06E-05 |
| CXCL2 | 4.75 | 1.23 | 1.98E-02 |
| JUNB | 9.43 | 1.22 | 1.77E-07 |
| ADAMTS14 | 3.44 | 1.22 | 1.76E-02 |
| SYT17 | 5.65 | 1.22 | 8.85E-03 |
| NFE2L2 | 10.19 | 1.22 | 7.26E-14 |
| ETV3 | 8.01 | 1.21 | 3.28E-06 |
| RIPK2 | 8.38 | 1.21 | 5.44E-08 |
| PLAGL2 | 7.37 | 1.21 | 1.02E-05 |
| GADD45B | 6.89 | 1.21 | 6.52E-04 |
| C15orf48 | 9.23 | 1.20 | 2.56E-02 |
| SNHG15 | 5.02 | 1.20 | 9.84E-03 |
| NBPF19 | 7.88 | 1.20 | 1.67E-07 |
| DLC1 | 4.82 | 1.20 | 1.06E-02 |
| SLC7A11-AS1 | 3.35 | 1.19 | 2.66E-02 |
| CKB | 3.64 | 1.19 | 2.47E-02 |
| BMT2 | 6.46 | 1.19 | 3.44E-04 |
| OGFRL1 | 10.28 | 1.19 | 9.30E-07 |
| NINJ1 | 10.06 | 1.19 | 2.15E-03 |
| ENTHD1 | 4.14 | 1.18 | 2.51E-02 |
| TFEC | 10.51 | 1.18 | 5.93E-11 |
| GPR84 | 6.92 | 1.18 | 2.88E-02 |
| NUB1 | 8.44 | 1.18 | 1.93E-06 |
| PTX3 | 6.21 | 1.18 | 5.73E-03 |
| GBP2 | 8.58 | 1.17 | 1.24E-02 |
| MN1 | 3.16 | 1.17 | 2.25E-02 |
| TXN | 10.33 | 1.17 | 1.70E-06 |
| PSME2 | 9.08 | 1.17 | 1.85E-07 |
| ITGB8 | 4.16 | 1.16 | 3.24E-02 |
| RNF19B | 8.20 | 1.16 | 4.54E-05 |
| C3 | 9.71 | 1.16 | 1.87E-06 |
| ST3GAL2 | 8.43 | 1.16 | 2.76E-06 |
| RDX | 10.13 | 1.16 | 2.97E-09 |
| SLC41A2 | 7.95 | 1.15 | 9.16E-06 |
| LINC01268 | 3.52 | 1.15 | 3.09E-02 |
| IKBKE | 7.67 | 1.15 | 1.99E-05 |
| FZD7 | 4.59 | 1.14 | 2.80E-02 |
| DAPP1 | 7.94 | 1.14 | 3.61E-06 |
| SRGN | 9.74 | 1.14 | 6.09E-07 |
| THBS1 | 4.44 | 1.14 | 3.90E-02 |
| PKD2 | 7.01 | 1.14 | 9.18E-05 |
| CBX6 | 9.01 | 1.13 | 8.87E-06 |
| C17orf58 | 5.34 | 1.13 | 1.51E-02 |
| PVR | 6.98 | 1.13 | 1.04E-04 |
| LRRFIP2 | 7.92 | 1.13 | 7.14E-07 |
| TCF4 | 8.39 | 1.13 | 3.27E-05 |

| | | | |
|---|---|---|---|
| LUCAT1 | 5.84 | 1.13 | 8.52E-03 |
| IRAK3 | 8.68 | 1.12 | 9.14E-06 |
| ASS1 | 2.81 | 1.12 | 2.86E-02 |
| LYRM4 | 5.71 | 1.12 | 1.01E-02 |
| TRIM2 | 5.88 | 1.12 | 3.19E-03 |
| ATF5 | 9.02 | 1.12 | 6.69E-03 |
| GCLM | 7.55 | 1.12 | 3.63E-05 |
| MOB3C | 7.98 | 1.12 | 2.09E-06 |
| RAPGEF2 | 8.69 | 1.12 | 4.93E-07 |
| KDM6B | 8.05 | 1.11 | 1.77E-06 |
| TNFRSF18 | 4.07 | 1.11 | 1.02E-02 |
| KANK1 | 6.34 | 1.11 | 2.38E-03 |
| CCR7 | 5.42 | 1.11 | 3.23E-02 |
| HCK | 10.44 | 1.10 | 1.19E-06 |
| TTYH2 | 7.53 | 1.10 | 6.97E-05 |
| ARAP2 | 8.43 | 1.09 | 2.56E-07 |
| STAP2 | 2.88 | 1.09 | 4.33E-02 |
| UXS1 | 8.21 | 1.09 | 4.29E-07 |
| PLXNA1 | 10.65 | 1.08 | 7.45E-09 |
| TBC1D2B | 9.10 | 1.08 | 1.67E-06 |
| UBTD2 | 7.77 | 1.08 | 7.50E-05 |
| CSF2RB | 9.47 | 1.07 | 3.46E-10 |
| ST3GAL4 | 6.13 | 1.07 | 2.34E-03 |
| CFP | 6.00 | 1.07 | 1.95E-02 |
| SCN1B | 4.78 | 1.07 | 4.36E-02 |
| TMEM237 | 4.34 | 1.07 | 4.53E-02 |
| PTGER4 | 8.56 | 1.07 | 2.21E-02 |
| ITGAV | 8.96 | 1.07 | 3.00E-06 |
| RAP1B | 9.52 | 1.07 | 1.06E-06 |
| ZMIZ2 | 9.24 | 1.06 | 1.55E-07 |
| VOPP1 | 9.31 | 1.06 | 9.76E-07 |
| LPAR1 | 6.87 | 1.06 | 7.82E-04 |
| MREG | 10.03 | 1.05 | 2.44E-10 |
| CCR5 | 9.98 | 1.05 | 7.73E-06 |
| CFLAR | 10.36 | 1.05 | 6.66E-08 |
| DPYSL2 | 9.91 | 1.05 | 3.13E-06 |
| RASSF5 | 8.64 | 1.05 | 1.28E-04 |
| BTBD19 | 5.91 | 1.04 | 6.23E-03 |
| TNIK | 7.80 | 1.04 | 7.82E-04 |
| UNC13A | 3.93 | 1.04 | 7.93E-03 |
| ARHGEF10L | 9.15 | 1.03 | 5.05E-06 |
| DAPK1 | 10.67 | 1.03 | 4.60E-09 |
| TSC22D1 | 7.88 | 1.03 | 6.57E-05 |
| CYLD | 8.73 | 1.03 | 3.29E-06 |
| MAOA | 6.48 | 1.03 | 7.57E-03 |
| IL15 | 5.43 | 1.03 | 3.84E-02 |
| TANK | 8.78 | 1.02 | 4.28E-06 |
| SQSTM1 | 11.52 | 1.02 | 1.05E-06 |
| RHOQ | 10.19 | 1.02 | 1.67E-06 |
| EOGT | 8.49 | 1.02 | 4.83E-05 |
| PLEK | 12.53 | 1.02 | 6.09E-07 |
| ALCAM | 9.90 | 1.01 | 7.73E-06 |

| | | | |
|---|---|---|---|
| ZC3H12C | 8.80 | 1.01 | 5.86E-06 |
| PDK4 | 4.85 | -2.15 | 2.29E-06 |
| HGF | 6.61 | -2.10 | 6.67E-09 |
| ADORA3 | 5.15 | -2.05 | 1.26E-06 |
| CABLES1 | 4.70 | -1.98 | 1.08E-05 |
| FAM46A | 9.04 | -1.96 | 3.14E-17 |
| ALK | 5.55 | -1.87 | 2.37E-05 |
| MS4A6A | 9.41 | -1.86 | 1.25E-16 |
| TMEM37 | 6.47 | -1.83 | 9.76E-05 |
| SLC40A1 | 7.55 | -1.83 | 2.90E-05 |
| ZNF704 | 5.12 | -1.82 | 6.52E-05 |
| SLC45A4 | 7.52 | -1.79 | 1.19E-08 |
| SLC46A1 | 5.78 | -1.76 | 4.81E-06 |
| PMP22 | 6.99 | -1.74 | 1.55E-07 |
| SECTM1 | 8.14 | -1.72 | 2.99E-09 |
| AXL | 5.96 | -1.65 | 1.66E-05 |
| GPRC5B | 4.27 | -1.65 | 5.29E-04 |
| MERTK | 6.97 | -1.65 | 2.08E-07 |
| MGAT4A | 9.07 | -1.65 | 4.32E-12 |
| FES | 6.82 | -1.63 | 3.00E-06 |
| FCGR2C | 6.76 | -1.62 | 6.06E-05 |
| RDH10 | 6.10 | -1.61 | 9.14E-06 |
| GCNT1 | 7.52 | -1.60 | 9.34E-08 |
| NREP | 6.92 | -1.60 | 6.96E-04 |
| RHOBTB1 | 5.03 | -1.60 | 3.23E-04 |
| ABCC5 | 9.19 | -1.58 | 8.45E-10 |
| BNC2 | 4.87 | -1.57 | 5.44E-04 |
| HSPA7 | 5.42 | -1.57 | 7.14E-04 |
| KLF4 | 6.25 | -1.56 | 4.41E-05 |
| CACNA2D3 | 2.97 | -1.56 | 6.20E-04 |
| HPSE | 7.86 | -1.56 | 6.39E-09 |
| TESK2 | 5.95 | -1.54 | 1.07E-04 |
| CORO1A | 7.37 | -1.53 | 1.81E-07 |
| LTB4R | 5.57 | -1.52 | 1.11E-04 |
| GPR34 | 6.60 | -1.51 | 1.40E-04 |
| C11orf21 | 5.60 | -1.50 | 1.28E-04 |
| CD180 | 8.06 | -1.48 | 3.03E-07 |
| FAM13A | 5.95 | -1.48 | 2.80E-05 |
| LYL1 | 6.44 | -1.47 | 2.29E-06 |
| RGS18 | 5.10 | -1.45 | 8.57E-04 |
| RGS14 | 5.29 | -1.44 | 8.31E-04 |
| FOS | 6.73 | -1.44 | 3.07E-06 |
| GLUL | 12.88 | -1.44 | 9.47E-12 |
| SCIMP | 8.60 | -1.43 | 8.35E-08 |
| PRR5L | 6.42 | -1.43 | 9.76E-05 |
| RNF125 | 6.27 | -1.42 | 2.45E-04 |
| COBLL1 | 4.23 | -1.41 | 4.70E-03 |
| KANK2 | 5.51 | -1.41 | 7.18E-04 |
| JAML | 8.48 | -1.39 | 6.05E-09 |
| SCAMP5 | 3.83 | -1.39 | 6.29E-03 |
| DPEP2 | 7.18 | -1.39 | 1.42E-06 |
| ZNF331 | 6.93 | -1.39 | 8.06E-06 |

| | | | |
|---|---|---|---|
| SPTBN4 | 6.04 | -1.38 | 9.09E-05 |
| APLN | 4.28 | -1.38 | 5.36E-03 |
| LINC02035 | 5.81 | -1.37 | 2.75E-04 |
| IL10 | 5.43 | -1.36 | 1.29E-03 |
| PTPN22 | 6.82 | -1.35 | 6.51E-05 |
| FAM117B | 4.50 | -1.35 | 4.64E-03 |
| SDS | 10.05 | -1.35 | 2.97E-09 |
| DOK2 | 7.08 | -1.35 | 1.30E-06 |
| CDCA7L | 5.75 | -1.34 | 8.17E-04 |
| HHEX | 5.44 | -1.34 | 2.47E-03 |
| C1orf127 | 3.89 | -1.33 | 9.80E-03 |
| MYO7A | 6.82 | -1.33 | 9.05E-06 |
| LRRC25 | 8.23 | -1.33 | 2.99E-09 |
| DIRAS1 | 5.21 | -1.33 | 2.49E-03 |
| SELENOP | 7.82 | -1.33 | 4.75E-06 |
| ITSN1 | 7.19 | -1.32 | 1.06E-04 |
| DHRS3 | 6.83 | -1.31 | 8.06E-05 |
| ABI3 | 6.45 | -1.31 | 1.46E-04 |
| STARD4-AS1 | 3.99 | -1.30 | 1.20E-02 |
| GAS6 | 6.51 | -1.30 | 5.94E-04 |
| DISC1 | 6.04 | -1.30 | 2.44E-03 |
| FRAT2 | 5.71 | -1.30 | 1.57E-03 |
| CHST13 | 5.33 | -1.29 | 2.61E-03 |
| CYSLTR1 | 4.70 | -1.29 | 1.09E-02 |
| GPR155 | 5.25 | -1.29 | 3.16E-03 |
| PTGFRN | 6.96 | -1.29 | 6.51E-05 |
| TAGLN | 6.43 | -1.28 | 1.20E-04 |
| DBP | 6.35 | -1.27 | 2.40E-04 |
| SLA | 8.88 | -1.26 | 1.40E-08 |
| TNS1 | 9.63 | -1.26 | 2.68E-07 |
| GGA2 | 9.69 | -1.25 | 1.58E-09 |
| TRIM25 | 8.91 | -1.25 | 2.24E-10 |
| FOXRED2 | 6.28 | -1.25 | 9.50E-04 |
| TRIM58 | 4.25 | -1.25 | 1.54E-02 |
| GAL3ST4 | 3.86 | -1.24 | 1.92E-02 |
| SLC46A3 | 7.40 | -1.23 | 3.93E-05 |
| GRAMD1B | 6.59 | -1.23 | 4.70E-04 |
| RNF166 | 7.67 | -1.23 | 1.29E-06 |
| SHMT1 | 5.73 | -1.23 | 2.20E-03 |
| SSBP2 | 4.13 | -1.22 | 2.00E-02 |
| ASRGL1 | 5.94 | -1.22 | 1.77E-03 |
| SRGAP3 | 4.57 | -1.22 | 1.86E-02 |
| HS3ST2 | 8.17 | -1.21 | 2.29E-06 |
| SKI | 7.08 | -1.21 | 3.27E-05 |
| C15orf52 | 7.17 | -1.21 | 4.56E-05 |
| TRIM14 | 8.72 | -1.20 | 3.06E-08 |
| METTL7A | 7.36 | -1.20 | 2.26E-05 |
| GIMAP1 | 5.59 | -1.19 | 6.14E-03 |
| KLHDC8B | 6.84 | -1.19 | 1.07E-04 |
| SLC36A1 | 9.41 | -1.19 | 1.54E-08 |
| RAB42 | 8.67 | -1.18 | 2.73E-07 |
| SH3PXD2A | 7.26 | -1.18 | 8.36E-04 |

| | | | |
|---|---|---|---|
| CD14 | 10.12 | -1.18 | 1.25E-16 |
| MAF | 8.95 | -1.17 | 1.51E-02 |
| TSHZ1 | 5.72 | -1.17 | 3.80E-03 |
| PITHD1 | 7.91 | -1.17 | 1.63E-05 |
| PRAM1 | 8.81 | -1.17 | 3.41E-06 |
| ZNF703 | 6.16 | -1.16 | 1.34E-03 |
| SPATA12 | 4.72 | -1.16 | 1.59E-02 |
| FCGR1A | 8.23 | -1.16 | 8.93E-05 |
| CD93 | 4.33 | -1.15 | 2.85E-02 |
| MXI1 | 6.83 | -1.15 | 7.31E-05 |
| PRMT7 | 5.56 | -1.14 | 5.06E-03 |
| CEBPD | 6.85 | -1.14 | 9.33E-04 |
| ATP8B4 | 6.51 | -1.14 | 3.63E-03 |
| MNDA | 9.29 | -1.13 | 8.42E-10 |
| MEF2C | 6.69 | -1.13 | 2.93E-03 |
| ZCCHC24 | 5.12 | -1.13 | 1.57E-02 |
| FAM212B | 4.93 | -1.12 | 1.89E-02 |
| GRIN3A | 5.55 | -1.12 | 2.00E-02 |
| CORO2A | 7.46 | -1.12 | 1.04E-04 |
| ABCG1 | 2.60 | -1.12 | 3.47E-02 |
| C19orf35 | 4.36 | -1.12 | 3.47E-02 |
| RTL10 | 6.58 | -1.11 | 1.74E-03 |
| PXMP4 | 4.55 | -1.11 | 2.88E-02 |
| FAM53B | 7.17 | -1.11 | 4.15E-05 |
| PPM1L | 7.30 | -1.11 | 3.45E-04 |
| ST5 | 6.19 | -1.10 | 3.76E-03 |
| MANSC4 | 2.98 | -1.10 | 2.91E-02 |
| BLNK | 7.06 | -1.10 | 3.22E-04 |
| KLHL30 | 3.18 | -1.10 | 4.84E-02 |
| ADAMTSL4 | 7.40 | -1.10 | 7.33E-05 |
| PIK3IP1 | 6.68 | -1.10 | 9.90E-04 |
| THBD | 5.21 | -1.09 | 3.41E-02 |
| MAML3 | 4.52 | -1.09 | 4.64E-02 |
| ARPIN | 8.49 | -1.09 | 2.43E-05 |
| ITGA4 | 7.44 | -1.09 | 5.08E-04 |
| ID2 | 9.01 | -1.09 | 3.65E-09 |
| ZNF395 | 5.76 | -1.09 | 7.18E-03 |
| MBP | 10.08 | -1.08 | 1.75E-07 |
| GTPBP3 | 4.48 | -1.08 | 4.17E-02 |
| TMEM71 | 4.68 | -1.07 | 4.82E-02 |
| SIDT2 | 9.73 | -1.07 | 1.42E-09 |
| REPS2 | 4.83 | -1.07 | 3.78E-02 |
| NLRC4 | 7.43 | -1.07 | 1.64E-05 |
| CD200R1 | 5.42 | -1.07 | 4.94E-02 |
| ASGR1 | 5.11 | -1.07 | 2.86E-02 |
| HMOX1 | 9.89 | -1.07 | 1.95E-10 |
| SNX29 | 8.79 | -1.06 | 2.82E-06 |
| SLFN11 | 9.35 | -1.06 | 1.98E-05 |
| STARD13 | 7.02 | -1.06 | 4.39E-04 |
| SLC37A2 | 10.53 | -1.06 | 6.10E-09 |
| TRIM32 | 5.63 | -1.06 | 1.85E-02 |
| RNASE6 | 8.80 | -1.05 | 6.80E-08 |

| | | | |
|---|---|---|---|
| SIGLEC1 | 10.01 | -1.05 | 8.78E-03 |
| TMEM65 | 6.23 | -1.05 | 8.08E-03 |
| TK2 | 6.71 | -1.05 | 1.40E-03 |
| PADI2 | 6.84 | -1.05 | 2.34E-03 |
| SDCCAG3 | 6.87 | -1.05 | 1.09E-03 |
| APBB1IP | 8.69 | -1.05 | 8.95E-07 |
| RASGRP4 | 5.91 | -1.04 | 1.31E-02 |
| LMO2 | 6.91 | -1.04 | 5.04E-04 |
| PLA2G15 | 8.49 | -1.04 | 6.48E-05 |
| NAPSB | 6.17 | -1.04 | 8.78E-03 |
| NUPR1 | 8.73 | -1.03 | 2.42E-05 |
| ZNF467 | 5.13 | -1.03 | 3.03E-02 |
| QPRT | 6.13 | -1.03 | 8.86E-03 |
| LPAR6 | 7.80 | -1.03 | 4.59E-04 |
| TMEM170B | 7.79 | -1.03 | 1.34E-04 |
| ZBTB4 | 8.71 | -1.03 | 4.77E-07 |
| HLTF | 6.12 | -1.03 | 8.45E-03 |
| GIMAP6 | 5.81 | -1.03 | 1.43E-02 |
| MAFB | 10.21 | -1.02 | 4.25E-11 |
| LGR4 | 6.84 | -1.02 | 3.19E-03 |
| SLC16A7 | 6.68 | -1.02 | 5.22E-03 |
| PFKFB4 | 6.30 | -1.02 | 2.71E-03 |
| TTC7A | 8.25 | -1.01 | 1.11E-04 |
| SLC18B1 | 7.25 | -1.01 | 7.91E-04 |
| ENC1 | 6.10 | -1.01 | 2.17E-02 |
| SLC12A9 | 7.64 | -1.00 | 3.62E-05 |
| RCBTB2 | 8.58 | -1.00 | 9.82E-05 |
| XYLT1 | 7.26 | -1.00 | 3.68E-03 |